

THE ROLE OF THE ACTIN CYTOSKELETON
DURING MUSCLE DEVELOPMENT IN *DROSOPHILA* AND MOUSE

by

Shannon Faye Yu

A Dissertation

Presented to the Faculty of the Louis V. Gerstner, Jr.

Graduate School of the Biomedical Sciences

in Partial Fulfillment of the Requirements of the Degree of

Doctor of Philosophy

New York, NY

Oct, 2013

Mary K. Baylies, PhD
Dissertation Mentor

Date

Copyright by Shannon F. Yu 2013

ABSTRACT

The actin cytoskeleton is essential for many processes within a developing organism. Unsurprisingly, actin and its regulators underpin many of the critical steps in the formation and function of muscle tissue. These include cell division during the specification of muscle progenitors, myoblast fusion, muscle elongation and attachment, and muscle maturation, including sarcomere assembly. Analysis in *Drosophila* has focused on regulators of actin polymerization particularly during myoblast fusion, and the conservation of many of the actin regulators required for muscle development has not yet been tested. In addition, dynamic actin processes also require the depolymerization of existing actin fibers to replenish the pool of actin monomers available for polymerization. Despite this, the role of actin depolymerization has not been described in depth in *Drosophila* or mammalian muscle development.

Here, we first examine the role of the actin depolymerization factor Twinstar (Tsr) in muscle development in *Drosophila*. We show that Twinstar, the sole *Drosophila* member of the ADF/cofilin family of actin depolymerization proteins, is expressed in muscle where it is essential for development. *tsr* mutant embryos displayed a number of muscle defects, including muscle loss and muscle misattachment. Further, regulators of Tsr, including a Tsr-inactivating kinase, Center divider, a Tsr-activating phosphatase, Slingshot and a synergistic partner in depolymerization, Flare, are also required for embryonic muscle development. Muscle-specific depletion of *tsr* resulted in progressive loss of

sarcomeric organization, overall growth defects and locomotor deficiencies. These data are the first to demonstrate a role for the ADF/cofilin family of actin depolymerizing proteins in muscle development and function in *Drosophila*.

To elucidate the conservation of myoblast fusion proteins in mammalian cells, we analyzed the role of the actin regulators Dock1 and IQSec1 in C2C12 myoblasts. We demonstrate that the actin regulators, Dock1 and IQSec1, homologs of the respective fusion proteins Myoblast city and Loner, play a conserved role in mammalian myoblast fusion. Depletion of Dock1 or IQSec1 in C2C12 myoblasts, an *in vitro* mouse myoblast cell line, resulted in a severe fusion block. Further, we show that Dock1 is not required for myoblast differentiation, migration and alignment or adhesion and likely plays a role at the site of myoblast fusion, similar to *Drosophila* Myoblast city. Finally, we identify the site of fusion in mammals using an indirect reporter for the actin cytoskeleton, suggesting that actin regulation at the site of myoblast-myoblast contact is essential for the fusion process.

Together, this work significantly extends the growing body of research indicating that myoblast fusion employs a conserved set of proteins and processes from *Drosophila* to mammals and underscores the importance of the actin cytoskeleton to both muscle development and maintenance. Importantly, the recent identification of mutations in Cofilin 2, the mammalian homolog of Twinstar, in patients affected with nemaline myopathy suggests that actin depolymerization is also an essential mechanism to maintain proper muscle function in humans.

BIOGRAPHICAL SKETCH

Shannon Faye Yu was born on July 5, 1985 in Augusta, Georgia, home of the Masters Tournament and twice the Georgia capital. She is the favorite daughter of Chin U and Robin Jan Yu and the older sister of Brantley Chin Yu. While growing up in Augusta, Shannon learned how to be a polite and proper Southern lady but also how to drive a manual transmission. In high school, she made good grades and made the cheerleading squad. Most importantly, however, she discovered that biology was her “thing.”

She matriculated at the University of Georgia (UGA) in 2003 as a “pre-med” major and traded her hoop skirts for the red and black. At UGA, she developed a passion for Georgia football (Go Dawgs!) and found a group of friends (henceforth referred to as 2North) that love the Sound of Music, dance parties and 5 Star Day (R.I.P.) as much as she does. Shannon did her undergraduate thesis research with Dr. Nancy Manley studying parathyroid development in the mouse. Her experience working in the lab coupled with the fact that blood made her queasy, Shannon decided to apply to graduate programs and become a scientist. Despite her love of the South, Shannon knew in her heart that there were other, better places to live. Thus, she applied to graduate programs exclusively in New York City (NYC) and matriculated at the Louis V. Gerstner, Jr. Graduate School of the Biomedical Sciences (GSK) in July 2007.

In graduate school, Shannon joined the lab of Dr. Mary K. Baylies, where she studied many aspects of muscle development in mouse and *Drosophila* that she will tell you about shortly. She has never once regretted her choice of program or laboratory (though she may have regretted coming to graduate school at all at some points #haventweall).

While in graduate school, Shannon met a real-life New Yorker. He taught her how to “properly” cross the street and how to do a Western blot. She taught him how to use a plate and utensils and how to make ramen from a bag. Together, they play tennis badly, enjoy visiting ballparks during their travels and turn their noses up at non-NYC bagels and pizza. In her spare time, Shannon climbs on “curtains,” reads cookbooks and Murakami novels and surfs the Internet. In addition, Shannon enjoys watching HBO every Sunday night, eating candy and reading the 2North listserv. After graduation, she is looking forward to joining the circus.

ACKNOWLEDGEMENTS

Without the love, friendship and support of a large number of individuals, I would not have started, stayed or completed graduate school. Foremost, I am grateful to my family for their unwavering belief in me and for raising me to have the same. I am also fortunate to have a second family nearby — John's family — which has warmly welcomed me into their homes and lives for the last six years. 2North (my third family) has sustained, entertained and inspired me since we met so many years ago. To them: Thank you for being a friend. Traveled down the road and back again. Your heart is true. You're a pal and a confidant.

I would never have gotten into science without Mr. Campbell, my high school biology teacher, or into graduate school without Dr. Nancy Manley, my undergraduate thesis mentor. I am grateful that Drs. Kathryn Anderson and Lorenz Studer agreed to be a part of my Special Committee. Their comments were crucial to developing this work. I would also like to recognize the generosity of the fly community in sharing stocks, reagents and, in the case of Dr. Eric Lai, his confocal.

Every member of my lab has provided essential comments, advice and technical assistance for many aspects of this work. For that I am incredibly appreciative. In particular, Dr. Krista Dobi taught me everything I know about basic fly husbandry during my rotation and then taught me again when I transitioned to a fly project three years into my thesis research. Her screen provided the initial impetus for studying Coronin and resulted in the work

presented in Chapter 3 of this thesis. She has also read almost every piece of my writing (including this thesis), and her insights have improved each one tremendously. Dr. Ingo Bothe generated a library of useful stocks, which made my fly work incredibly efficient. In addition, his analysis of the requirement for PIP₂ during *Drosophila* myoblast fusion was invaluable to my own work in C2C12 myoblasts, and his focus on myoblast fusion in the embryo was indispensable when I discovered my own fusion phenotype. Victoria Schulman has kept me company during the early morning and weekend hours for the last few years, and her strong work ethic has been an example to us all. Throughout the years, my bay mate, Kate Rochlin, has provided valuable advice on scientific (and often, not so scientific matters) and has played one of the largest roles in shaping my graduate school experience. In the future, when I reminisce on my time here, she will undoubtedly be featured in many of the happy memories. Lastly, I will be forever grateful to Dr. Mary Baylies for allowing me to join her lab and for giving me the freedom (and the confidence) to define my own space within this field and to go beyond the embryo to pursue interesting phenotypes.

But no one compares to John. John has been my closest friend, greatest supporter and easily my most important discovery in graduate school.

TABLE OF CONTENTS

LIST OF FIGURES	xv
LIST OF TABLES	xxi
LIST OF ABBREVIATIONS	xxii
CHAPTER ONE: INTRODUCTION	1
Chapter Overview	2
Muscle development in <i>Drosophila</i>	3
Myoblast specification.....	3
Myoblast fusion and myotube formation	10
Sarcomerogenesis.....	45
Larval muscle growth.....	56
Metamorphosis and adult myogenesis	57
Mesoderm and Muscle Development in Mammals.....	62
Myoblast specification.....	64
Myoblast fusion and myotube formation	67
Muscle repair	81
C2C12 satellite cell-derived myoblasts.....	82
The actin cytoskeleton and its regulators	83
Actin structure and polymerization.....	83

Branched actin polymerization.....	87
Arp2/3.....	87
Nucleation-promoting factors (NPFs).....	88
Unbranched actin polymerization.....	90
Formins	90
Spire	93
Leiomodin.....	95
Actin depolymerization.....	96
Gelsolin/vilin	96
The ADF/cofilin family of proteins.....	99
Structure.....	99
ADF/cofilin-actin interface	102
ADF/cofilin enhance the dynamics of actin assembly	104
Regulation of ADF/cofilin activity	106
In vivo functions of ADF/cofilin: evidence from genetic model organisms	110
The coronin family of proteins	116
Structure	117
Type I, II, III coronins	118
F-actin-binding	121
Interactions with ADF/cofilin	123
Interactions with Arp2/3	125
In vivo functions of coronin: evidence from genetic model organisms	126

Summary	130
CHAPTER TWO: Twinstar is required for muscle development, maintenance and function in Drosophila.....	131
Chapter Overview	132
Results.....	133
Tsr is expressed in Drosophila body wall muscle	133
Tsr is required for muscle development in the Drosophila embryo	139
Tsr plays an essential, muscle-autonomous role in Drosophila	140
Founder cells (FC) and adult progenitors (APs) appear to be specified correctly in tsr mutant embryos	144
Tsr plays a role in generating proper muscle-tendon attachments	145
Regulators of Tsr are also required for embryonic muscle development ...	149
Muscle-specific depletion of Tsr regulators does not affect embryonic muscle development	155
Tsr is required for myoblast fusion	157
Tsr is localized to the larval sarcomere	162
Tsr is required for sarcomere organization and maintenance	165
Muscle-specific depletion of tsr results in excessively polymerized actin ..	170
Tsr is required for muscle-dependent events in metamorphosis.....	172
Drosophila as a disease model for Nemaline myopathy	176
Discussion.....	180

CHAPTER THREE: Coro is required for muscle development and function in Drosophila	190
Chapter Overview	191
Results.....	192
Coro is expressed in the body wall muscle of the Drosophila embryo	192
Coro is required for the proper development of the embryonic body wall muscle	196
Coro is required for muscle function	201
Verifying coro is disrupted in coroeX alleles	207
Muscle-specific knockdown of coro does not affect embryonic muscle development.....	214
Sequencing coro alleles.....	216
Coro is expressed in the Drosophila larval muscle where it is required for muscle activity	222
Discussion.....	225
CHAPTER FOUR: Dock1 and IQSec1, homologs of the fusion proteins Myoblast city and Loner, respectively, play a conserved role in mammalian myoblast fusion	235
Chapter Overview	236
Results.....	239
Generation of stable clones expressing shRNAs against Dock1 and IQSec1	239

Knockdown of Dock1 and IQSec1 blocks fusion but not differentiation.....	241
Dock1 is reduced in a subset of cell lines	243
Dock1 is not required for myoblast shape changes	246
Dock1 is not required for myoblast migration in vitro	246
Dock1 is not required for myoblast-myoblast alignment and adhesion.....	253
IQSec1 is not required for myoblast migration in vitro	255
IQSec1 is not required for myoblast-myoblast adhesion.....	255
Discussion.....	257
CHAPTER FIVE: Identification of the site of myoblast fusion in mammals:	
PI(4,5)P2 accumulates at the site of myoblast-myoblast adhesion and fusion in vitro	265
Chapter Overview	266
Results.....	267
Lentivirus-mediated expression of fluorophores allows for long-term expression in C2C12 myoblasts.....	267
Live imaging of fusion	270
Identification of actin reporters.....	272
Stable expression of Lifeact or UtrCH reporters is toxic to C2C12 myoblasts	276
Transient expression of phospholipid markers does not affect myoblast differentiation.....	278

Live imaging of PLC δ PH::eGFP reveals accumulation of PIP2 that precedes the fusion event.....	280
Stable expression of phospholipid markers blocks myoblast fusion but does not affect differentiation or cell-cell adhesion	284
Live imaging of lentivirus lines shows PLC δ PH::eGFP accumulations perdure and myoblasts maintain contact with one another	286
Discussion.....	287
CHAPTER SIX: CONCLUSIONS	294
CHAPTER SEVEN: MATERIALS AND METHODS	318
Drosophila.....	319
Satellite cell-derived C2C12 myoblasts	325
APPENDIX.....	330
BIBLIOGRAPHY	335

LIST OF FIGURES

1.1. Drosophila life cycle	4
1.2. Drosophila embryonic body wall muscle pattern.....	7
1.3. Mesoderm and muscle specification in Drosophila.....	9
1.4. Identity genes are expressed in incompletely overlapping subsets of Drosophila muscles.....	11
1.5. Cell-cell fusion utilizes a conserved set of cellular behaviors	14
1.6. Founder cells form four characteristic groups.....	16
1.7. Overview of proteins required for myoblast fusion in Drosophila.....	22
1.8. F-actin foci and PIP2 accumulations mark the site of fusion in Drosophila ..	25
1.9. Roles of fusion proteins in actin and PIP2 foci dynamics	33
1.10. Drosophila muscle-tendon interactions.....	38
1.11. The mature myotendinous junction	43
1.12. The structure of the sarcomere.....	46
1.13. An overview of myotendinous junctions and costameres	52
1.14. Change in muscle size during Drosophila larval development	55
1.15. The Drosophila adult dorsal longitudinal muscles are formed from persistent larval scaffolds.....	59
1.16. Vertebrate muscle is composed of bundles of myofibrils.....	63

1.17. Overview of Pax3/7 function during mammalian skeletal muscle formation	65
1.18. Two phases of mammalian myoblast fusion	68
1.19. Overview of proteins required for mammalian myoblast fusion	72
1.20. Adult muscle repair by satellite cells	80
1.21. An overview of branched actin polymerization mediated by Arp2/3 and its NPFs	85
1.22. Overview of formin actin nucleators.....	91
1.23. Models for actin nucleation and polymerization by Spire and Leiomodin ...	94
1.24. Model for actin severing by gelsolin.....	97
1.25. Alignment of cofilin homologs.....	100
1.26. Effect of cofilin-binding on F-actin structure	103
1.27. Regulation of cofilin by kinases and phosphatases	108
1.28. Defects in adult myofibril organization in unc-60 mutants.....	111
1.29. Progressive muscle defects in Cfl2 ^{-/-} mice	115
1.30. Coronin family of proteins	119
1.31. Model of type I coronin function	124
1.32. Muscle-specific depletion of coronin results in frayed myofibrils in adult indirect flight muscles	128
2.1. Tsr is expressed throughout development and in the somatic body wall muscles of the <i>Drosophila</i> embryo	134

2.2. Mutation of <i>tsr</i> results in defects in embryonic muscle patterning	137
2.3. <i>Tsr</i> is required specifically in the muscle	141
2.4. Founder cell (FC) and adult progenitor (AP) specification is unaffected in <i>tsr</i> mutant embryos	146
2.5. Tendon specification and differentiation are unaffected in <i>tsr</i> mutant embryos	148
2.6. <i>Tsr</i> -interacting proteins are required for proper muscle development.....	150
2.7. Muscle-specific depletion of <i>Tsr</i> -interacting proteins does not result in any embryonic muscle phenotypes.....	153
2.8. <i>Tsr</i> genetically interacts with <i>Cdi</i> , <i>Ssh</i> and <i>Flr</i> in the <i>Drosophila</i> body wall muscle	156
2.9. <i>tsr</i> ; <i>ssh</i> double mutant myoblast are capable of making contact with one another but do not form an actin focus.....	158
2.10. <i>Tsr</i> is localized to the Z-disc and H-zone in <i>Drosophila</i> larval muscle	161
2.11. Muscle-specific depletion of <i>Tsr</i> results in severe and progressive loss of sarcomere organization.....	163
2.12. Muscle-specific overexpression of <i>Tsr</i> does not affect larval muscle function but does cause flightlessness in adults	166
2.13. Depletion of <i>tsr</i> results in hyperpolymerization of actin and severe defects in sarcomere organization	168
2.14. Expression of UAS- <i>tsr</i> RNAi in a single muscle causes a severe defect in sarcomere organization.....	171

2.15. Tsr is required for muscle-dependent events during Drosophila metamorphosis.....	173
2.16. Accumulations resembling nemaline bodies are present in muscle in which tsr is reduced.....	175
2.17. UAS-tsr(G19A)::mCherry is properly localized to Z-discs in larval muscle	177
2.18. UAS-tsr(G19A)::mCherry is unable to rescue tsr depletion.....	179
3.1. coro is highly expressed throughout Drosophila development.....	193
3.2. Coro is expressed in the embryonic body wall muscle of Drosophila	195
3.3. P-element insertions in coro do not disrupt the embryonic muscle	197
3.4. Deficiencies which remove coro do not cause an embryonic muscle phenotype	199
3.5. coro excision allele mutants have embryonic muscle defects	203
3.6. The lateral transverse (LT) muscles are specifically affected in coro mutants	206
3.7. Coro is required for larval locomotion	212
3.8. Coro mutant adults have defects in walking, jumping and flying	213
3.9. Coro mutant adults have aberrant DLMS	215
3.10. Transheterozygous embryos phenocopy single allele mutants	218
3.11. coro excision alleles complement deficiencies which completely remove coro	220

3.12. Muscle-specific depletion of coro does not result in embryonic phenotypes.	223
3.13. Muscle-specific depletion of coro using RNAi in coro(ex6) mutant embryos	226
3.14. Graphical representation of coro allele sequencing data.....	228
3.15. Coro is expressed in the Drosophila larval muscles	230
3.16. Coro is required for muscle function in the larvae and adult.....	232
4.1. C2C12 satellite cell-derived myoblasts fuse in vitro	238
4.2. Screening cell lines with putative reduction of Dock1 and IQSec1	240
4.3. Reduction of Dock1 and IQSec1 result in myoblast fusion defects in vitro.	242
4.4. Dock1 is expressed throughout myoblast fusion in vitro	244
4.5. Dock1 is depleted in a subset of the presumptive Dock1 knockdown myoblast lines	245
4.6. Dock1 knockdown myoblasts are able to remodel into spindle-shaped cells	247
4.7. Dock1 knockdown myoblasts are capable of migrating	249
4.8. Cell spreading is affected in some Dock1 knockdown myoblasts.....	251
4.9. Components of focal adhesions are properly localized in Dock1 knockdown myoblasts	252
4.10. Dock1 is not required for myoblast-myoblast adhesion.....	254
4.11. Knockdown of IQSec1 does not affect migration	256

4.12. Knockdown of IQSec1 does not affect the localization of adhesion proteins	258
5.1. Lentivirus-mediated expression of cytoplasmic eGFP and mCherry does not affect the differentiation or fusion of C2C12 myoblasts.....	268
5.2. Live imaging of differentially labeled C2C12 myoblasts.....	271
5.3. Localization of actin-binding reporters in C2C12 myoblasts during differentiation.....	275
5.4. Expression of actin-binding reporters is toxic.....	277
5.5. Transient expression of phospholipid reporters does not affect differentiation	279
5.6. Live imaging suggests PIP2 accumulates asymmetrically during myoblast fusion.....	281
5.7. Overexpression of PH domain reporters blocks fusion but not differentiation or adhesion.....	283
5.8. Live imaging of myoblasts overexpressing PLC δ PH::eGFP and BTKPH::eGFP	285

LIST OF TABLES

1.1. A partial list of proteins required for myoblast fusion in Drosophila and mouse	18
3.1. A list of unique and overlapping genes deleted in two deficiencies that remove coro	200
3.2. Summary of phenotypes observed in homozygous embryos	202
3.3 Summary of defects observed with coro excision alleles.....	208
3.4. Summary and comparison of phenotypes observed in animals homozygous for coro alleles used in this study and in Bharathi et al., 2004.....	210
3.5. Viability and fertility of coro transheterozygotes.....	217
5.1. Summary of efficiency of lentivirus infection	269
5.2. Summary of actin-binding plasmids	274

LIST OF ABBREVIATIONS

A	anterior
ADF	Actin depolymerizing factor
ADF-H	actin depolymerizing factor homology domain
AEL	after egg laying
AP	adult muscle precursor
Ap	Apterous
APF	after puparium formation
Arf	ADP ribosylation factor
BDGP	Berkeley <i>Drosophila</i> Genome Project
bHLH	basic helix-loop-helix
Blow	Blown fuse
C2	calcium-binding domain
Cdi	Center divider
CIN	Chronophin
CNS	central nervous system
Coro	Coronin
Crk	CT10 regulator of kinase
D	dorsal
DA	dorsal
D.C.	District of Columbia
Dei	Delilah (also Taxi, Tx)
DGrip	<i>Drosophila</i> Glutamate receptor-interacting protein
DHR	Dock Homology Region
DLM	dorsal longitudinal muscle
Dmef2	<i>Drosophila</i> Myocyte enhancer factor 2
DO	dorsal oblique
Dock	Dreadlock
DOCK	Dedicator of cytokinesis
Dpp	Decapentaplegic

Drl	Derailed
Duf	Dumbfounded/Kirre
D-WIP	<i>Drosophila</i> WASp interaction partner (also Vrp1/Sltr)
DVM	dorso-ventral muscle
ECM	extracellular matrix
Ed	Echinoid
Egfr	Epidermal growth factor receptor
Elmo	Engulfment and cell motility
Eve	Even-skipped
FC	founder cell
FCM	fusion-competent myoblast
Flr	Flare
FuRMAS	fusion-restricted myogenic-adhesive structure
GEF	Guanine nucleotide exchange factor
GFP	green fluorescent protein
GSK	Gerstner Sloan-Kettering
Hbs	Hibris
Hh	Hedgehog
How	Held out wings
If	Inflated
IFM	indirect flight muscle
Ig	Immunoglobulin
ILK	Integrin-linked kinase
Insc	Inscutable
IQSec	IQ motif and SEC7 domain-containing protein
Kak	Kakapo
Kon	Kon-tiki
Kr	Krüppel
L1	first-instar larvae
L2	second-instar larvae
L3	third-instar larvae

Lam	Laminin
LIMK	LIM domain kinase
Lmd	Lameduck (Myoblasts Incompentent/Gleeful)
LOM	larval oblique muscle
Lrt	Leucine-rich tendon-specific protein
L'sc	Lethal of scute
LT	lateral transverse
Mbc	Myoblast city
Mew	Multiple edematous wings
MHC	Myosin heavy chain
MPC	mesodermal precursor cell
MRF	myogenic regulatory factor
MTJ	myotendinous junction
Myf4	myogenic factor 4
Myf5	myogenic factor 5
MyoD	Myoblast determining protein
Mys	Myospheroid
N	Notch
Nb	Numb
NPF	Nucleation promoting factor
NYC	New York City
P	posterior
PH	Pleckstrin homology
PhD	Doctor of Philosophy
PIP₂	Phosphatidylinositol 4,5-bisphosphate
PIP₃	Phosphatidylinositol 3,4,5-triphosphate
RING	Really Interesting New Gene
RNAi	RNA interference
Rols	Rolling pebbles/Antisocial
Rst	Roughest/IrreC
SCAR	suppressor of cAMP receptor

Slou	Slouch
Sns	Sticks and stones
Ssh	Slingshot
TDT	tergal depressor of the trochanter (jump muscle)
TEM	transmission electron microscopy
TPR	tetratricopeptide repeat
TRiP	Transgenic RNAi Project
Tsr	Twinstar
Tw	Twist
UGA	University of Georgia
V	ventral
VDRC	Vienna <i>Drosophila</i> RNAi Center
Vg	Vestigal
WAVE	WASp family Verprolin-homologous protein
WASp	Wiskott-Aldrich syndrome protein

CHAPTER ONE: INTRODUCTION

Chapter Overview

Actin and its regulators are critical components for the formation and function of muscle tissue, including myoblast fusion, myotendinous junction formation and maintenance and muscle contraction. To date, the majority of studies have been conducted in *Drosophila* and the conservation of many of the actin-based processes and actin regulators required for *Drosophila* myoblast fusion has not yet been tested. Furthermore, the role of actin depolymerization, required to maintain dynamic actin processes, has not been fully described in *Drosophila* or mammals.

During my thesis work, I showed a novel role for actin depolymerization in muscle development and function in *Drosophila*. I also demonstrated that two orthologs of *Drosophila* fusion proteins play a conserved role in mammalian myoblast fusion and that the site of myoblast fusion in mammals can be identified by a local, dynamic accumulation of a membrane phospholipid. Together, my thesis research indicated that muscle development and function employs a conserved set of actin regulators and actin-dependent processes from *Drosophila* to mammals.

To place my work into context, I begin by describing the development of the body wall muscles of *Drosophila* throughout development, followed by a comparison to muscle development in mammals, highlighting the most relevant aspects for this work. Next, I will introduce the actin cytoskeleton and describe the proteins required for branched and non-branched actin polymerization.

Finally, I will discuss the role of and the importance of proteins that depolymerize actin filaments in order to maintain a dynamic actin cytoskeleton.

Muscle development in *Drosophila*

Drosophila is a holometabolous insect, meaning its development occurs over four distinct developmental stages: embryo, larva, pupa and adult (Figure 1.1). Each stage also has different requirements for muscle activity. For example, the musculature of the larvae, specialized for crawling and feeding, is patterned and formed in the stationary embryo. Likewise, the adult musculature, which is designed for walking, jumping and flying, must be completely remodeled from the embryonic/larval muscle pattern and is formed during the immobile pupal stage.

Myoblast specification

Drosophila body wall muscles are derived from the embryonic mesoderm (Figure 1.2) (Bate, 1990). The basic helix-loop-helix (bHLH) transcription factor Twist (Twi) is highly conserved from *Drosophila* to vertebrates and plays a critical role in mesoderm specification in *Drosophila* (Thisse et al., 1987; 1988). Through Wingless (Wg), Decapentaplegic (Dpp) and Hedgehog (Hh) signaling between the ectoderm and mesoderm, Twi levels are modulated into high and low expression domains (Figure 1.3A).

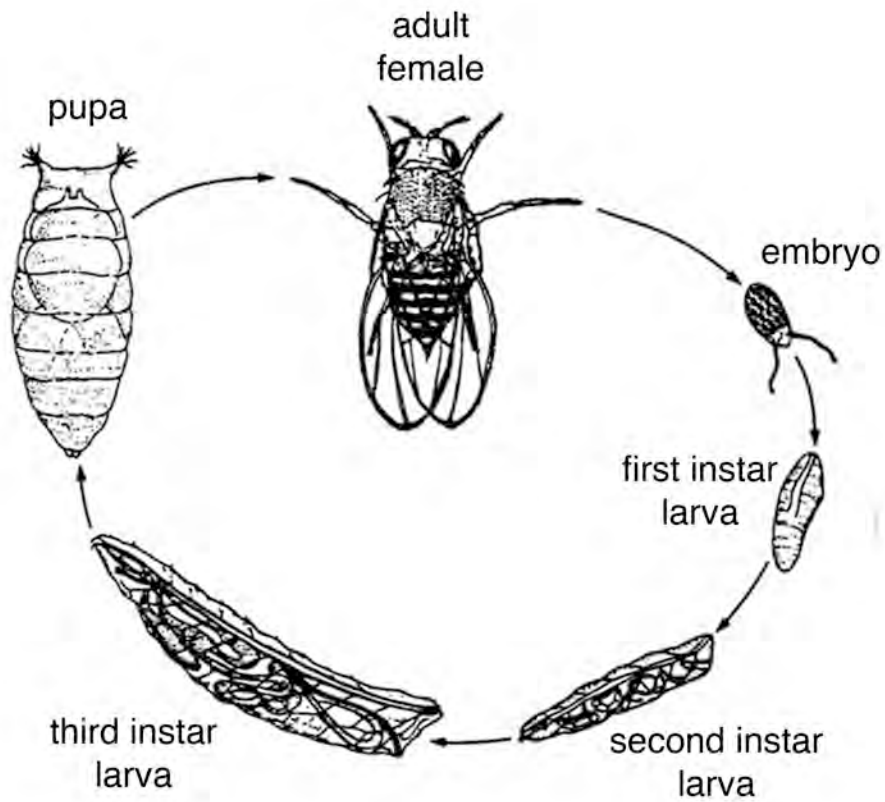


Figure 1.1. *Drosophila* life cycle. *Drosophila* is a holometabolous insect, developing over the course of ten days and transitioning through four distinct stages: embryonic, larval (which is divided into first, second and third instar), pupal and adult.

Mesodermal cells expressing high levels of *Tw* become somatic mesoderm, while mesodermal cells expressing lower levels of *Tw* become other mesodermal cell types, including visceral mesoderm (Baylies et al., 1998).

Once the somatic mesoderm has been properly specified, a wave of cell division occurs, and a subset of cells are specified as muscle progenitor cells (Bate, 1990; Carmena et al., 1995). The selection of muscle progenitor cells is similar to neuroblast specification in the central nervous system (Bate, 1990; Corbin et al., 1991). The gene *lethal of scute* (*l'sc*) is expressed in clusters, known as equivalence groups, in the somatic mesoderm, conferring the ability of these cells to form muscle progenitors (Figure 1.3B) (Carmena et al., 1995). Over time, lateral inhibition mediated by neurogenic genes, including Notch (N), localizes *l'sc* expression to single cell from each group. This cell, the muscle progenitor cell, moves in close contact with the ectoderm and begins to express a specific combination of transcription factors, including Even-skipped (Eve), Slouch (Slou) and Krüppel (Kr). Somatic mesoderm cells that are not specified as muscle progenitors differentiate into fusion-competent myoblasts (FCMs) (Baylies et al., 1998).

Subsequently, muscle progenitor cells undergo asymmetric division to form two sibling muscle founder cells (FCs) or a single muscle FC and an adult muscle precursor cell (AP) (Figure 1.3B). Thirty FCs and six APs are specified per abdominal hemisegment (Bate et al., 1991; Currie and Bate, 1991; Nose et al., 1998). As with muscle progenitor specification, this process contains parallels to the development of the central nervous system. For example, both the

asymmetric division of neuroblasts and muscle progenitor cells require Notch (N), Numb (Nb) — a membrane-associated inhibitor of Notch signaling, and Inscuteable (Insc) — a cytoplasmic adaptor protein (Carmena et al., 1998; Guo et al., 1996; Kraut and Campos-Ortega, 1996; Ruiz-Gomez and Bate, 1997). Insc controls the localization of proteins, including Nb, directing Nb to accumulate on the opposite side of the cell. Subsequent cell division results in the asymmetric inheritance of Insc and Nb (Carmena et al., 1998; Kraut and Campos-Ortega, 1996; Ruiz-Gomez and Bate, 1997). The daughter cell that inherits Nb (thus, inhibits Notch signaling) becomes an FC and maintains expression of its specific combination of muscle progenitor transcription factors (such as Kr, Eve or Slou). The daughter cell that inherits Insc (thus, can receive Notch signaling) can become either an FC or an AP and represses the expression of progenitor cell genes. Additionally, APs maintain Twist expression and will not differentiate until later in development (see below) (Bate et al., 1991; Currie and Bate, 1991).

Founder cells are a diverse population of myoblasts: each FC has a unique identity that is characterized by the combinatorial expression of transcription factors, such as Kr, Slou, Eve, Apterous (Ap) and Vestigial (Vg) (Bourgouin et al., 1992; Dohrmann et al., 1990; Frasch et al., 1987; Gaul et al., 1987; Ruiz-Gomez et al., 1997; Williams et al., 1991). For example, all four lateral transverse (LT) muscles simultaneously express Ap but only two LTs express Kr (Bourgouin et al., 1992; Gaul et al., 1987; Ruiz-Gomez et al., 1997) (Figure 1.4). Underscoring the importance of the FC identity program in determining the final morphological characteristics of each muscle is the

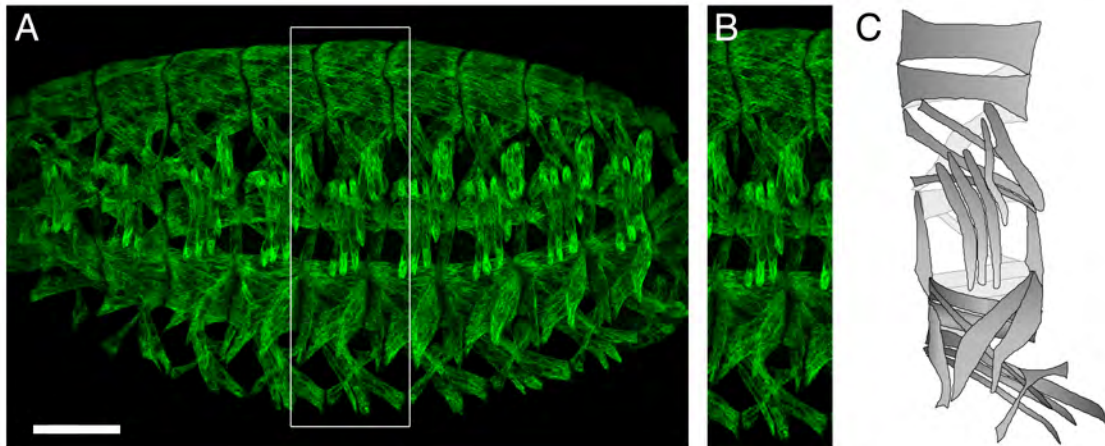


Figure 1.2. *Drosophila* embryonic body wall muscle pattern. The body wall muscles of the *Drosophila* embryo are segmentally repeating, and each abdominal hemisegment contains 30 unique muscles. (A-B) Maximum intensity projection of a whole-mount embryo (A) or a single hemisegment (B) of an embryo stained with an antibody against Myosin heavy chain (green). (C) Cartoon of the 30 muscles in a single abdominal hemisegment. Bar, 50 μ m.

formation of attached and innervated mononucleate muscle fibers of the correct position in the absence of fusion (Rushton et al., 1995). Furthermore, alteration of identity gene expression either by loss or ectopic expression can result in changes to muscle identity (Bourgouin et al., 1992; Ruiz-Gomez et al., 1997). More often, however, ectopic expression of a single identity gene is not sufficient to completely transform muscle identity (Croizatier and Vincent, 1999; Jagla et al., 1998; Knirr et al., 1999).

In contrast, fusion competent myoblasts (FCMs) are often considered a more uniform and naïve population of myoblasts: all FCMs express *Lmd* (also known as *Myoblasts Incompetent/Gleeful*), which is required for their differentiation (Duan et al., 2001; Furlong et al., 2001; Ruiz-Gómez et al., 2002). Upon fusion with an FC/myotube, the nucleus of the newly incorporated FCM loses expression of *Lmd* and expresses the identity program of the FC to which it has fused. Recent evidence, however, has identified gene expression patterns and cell behaviors unique to subsets of FCMs, suggesting that they have more diversity than first appreciated (Artero, 2003; Beckett and Baylies, 2007; Estrada et al., 2006). For example, only a subset of FCMs express the FCM-specific gene *hibris* (Artero et al., 2001). Three-dimensional analysis of FCMs organization further supports the idea that FCMs are not uniform (Beckett and Baylies, 2007). At the time of FCM specification, FCMs comprise several cell layers: the most external FCMs contact FCs and the more internal FCMs contact primarily other FCMs. After FCM specification, a subset of FCMs undergo cell division. Though the significance of these divisions is unknown, it is likely that they are required to

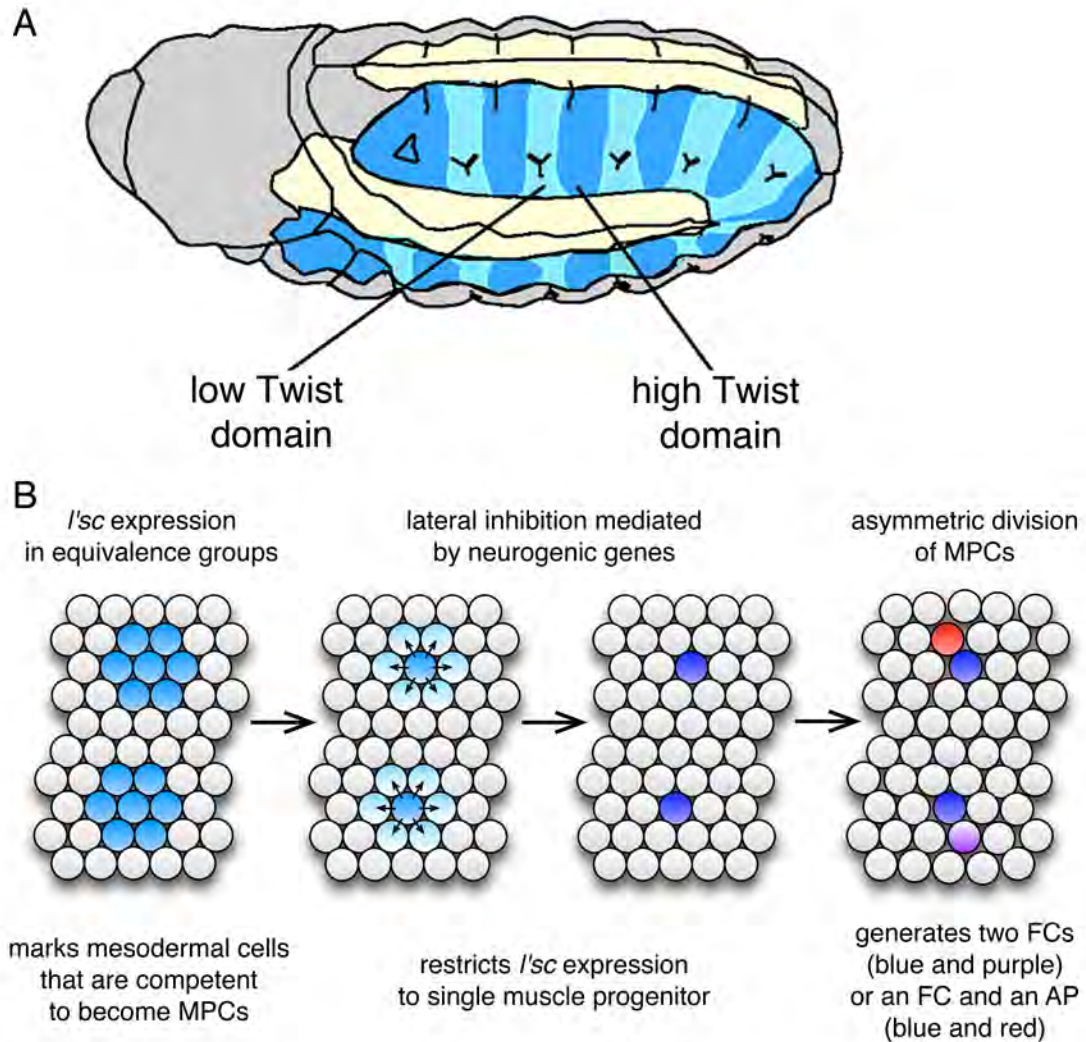


Figure 1.3. Mesoderm and muscle specification in *Drosophila*. (A) Cartoon of a stage 10 embryo showing Twist expression modulated into high (dark blue) and low (light blue) Twist domains. Cells of the high Twist domain give rise to all somatic muscles. (B) Expression of *lethal of scute* (*l'sc*) in cells of the high Twist domain marks groups of mesodermal cells (dark blue) that are competent to become muscle progenitor cells (MPCs). Lateral inhibition restricts *l'sc* expression to a single MPC. The remaining mesodermal cells (grey) become fusion competent myoblasts. Asymmetric division of MPCs generates two founder cells (FCs, blue and purple) or an FC and an adult muscle precursor (AP, blue and red, respectively). Modified with permission from Baylies et al., 1998).

generate a sufficient number of FCMs to complete fusion. Thus, FCMs, like FCs, contain positional and identity information, and this diversity could impact muscle development.

The adult muscle precursors (APs), which are formed during the asymmetric division of muscle progenitor cells, continue to express *Tw* until the onset of adult muscle differentiation later in development (Bate et al., 1991; Currie and Bate, 1991). The thoracic APs are associated with the imaginal discs (Bate et al., 1991). In the abdominal hemisegments of the embryo, APs are associated with the embryonic peripheral nervous system, and these six persistent *Tw*-expressing cells can be found in three locations, one ventral, two lateral and three dorsal. APs proliferate during larval development, producing six clusters of *Tw*-expressing cells, and remain closely associated with the nervous system (Bate et al., 1991; Currie and Bate, 1991). As adult muscle development begins (discussed in more detail below), these cells further proliferate and spread out along the nerves to seed muscles throughout the adult (Currie and Bate, 1991). *Tw* expression declines as the adult myoblasts begin to fuse and form the adult musculature during metamorphosis.

Myoblast fusion and myotube formation

In the *Drosophila* embryo, a repeated pattern of 30 distinct muscle fibers, seeded by the 30 FCs, is present in each abdominal hemisegment (Figures 1.2, 1.4). Though each muscle fiber can be distinguished by its size, shape, orientation,

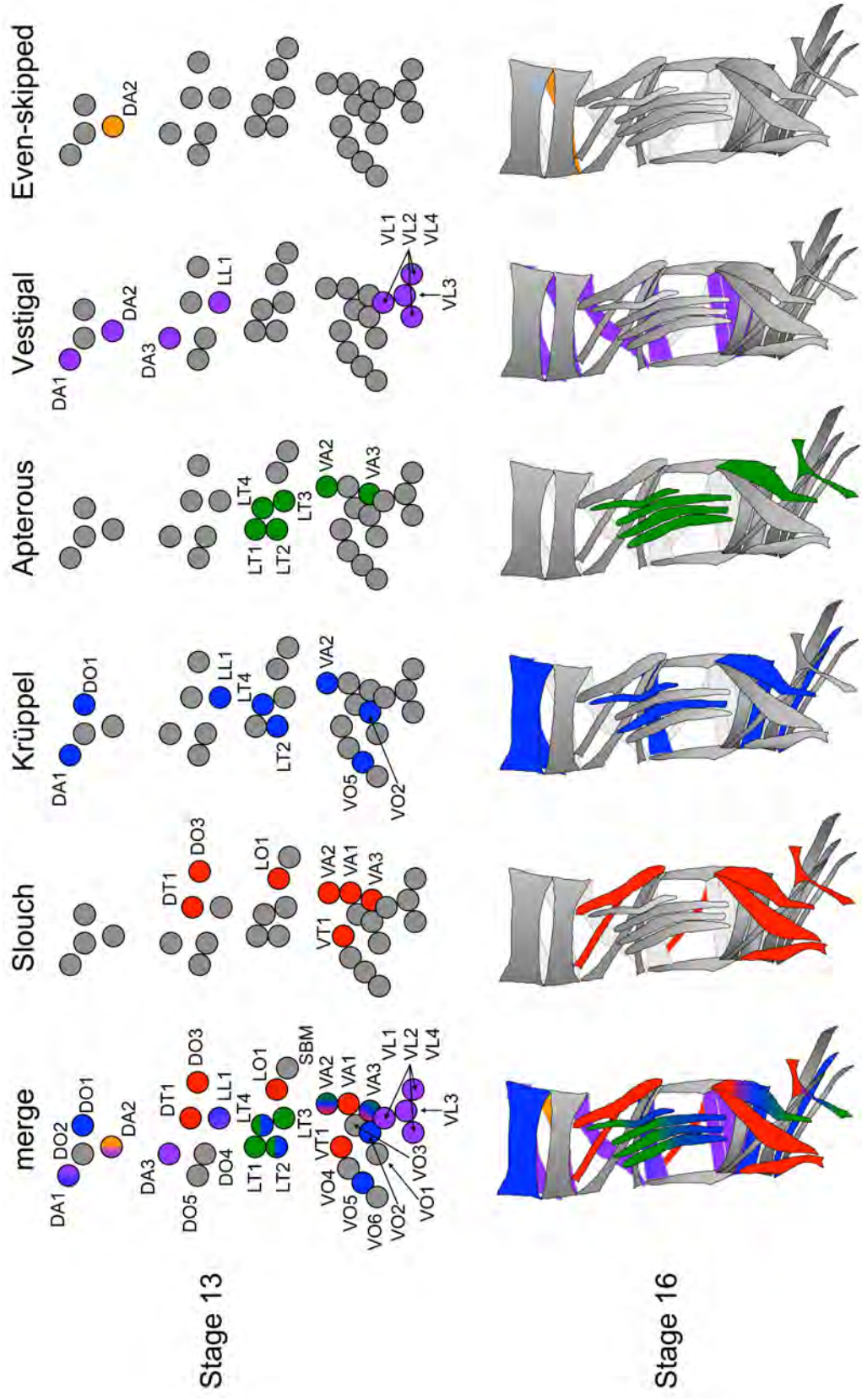


Figure 1.4. Identity genes are expressed in incompletely overlapping subsets of *Drosophila* muscles. Cartoon of founder cell organization at stage 13, prior to fusion (top row) and the final muscle pattern at stage 16, after fusion is complete (bottom row). Expression patterns of indicated identity genes at stage 13 (top) and the muscles they give rise to at stage 16 (bottom) indicate that identity genes are expressed in incompletely overlapping subsets of FCs/muscles (merge). Thus, the expression of a single identity gene does not determine muscle identity. Note that some identity genes, like *apterous*, are expressed in FCs at stage 13 but not in the final muscle at stage 16. Dorsal is top, anterior is left.

number of nuclei, innervation and tendon attachment sites, all muscle fibers form from the fusion of mononucleate myoblasts to generate a syncytial muscle (Baylies et al., 1998; Frasch, 1999). Like other examples of cell-cell fusion, myoblast fusion undergoes a set of conserved cellular behaviors: cell migration, cell-cell recognition and adhesion, close apposition of plasma membranes and bilayer mixing resulting in membrane fusion (Figure 1.5) (Chen, 2010; Chen et al., 2007).

Myoblast fusion in the *Drosophila* embryo occurs over a 5-6 hour period during late embryogenesis (stages 12-15; 7.5-13 hours after egg laying [AEL]). The size of each muscle is partially determined by the number of fusion events, ranging from as few as 2 to as many as 24 in an individual muscle (Bate, 1990; Beckett and Baylies, 2007; Folker et al., 2012). While there is some variation in the final size of individual muscles, a characteristic mean number of nuclei has been determined in several muscles (Beckett and Baylies, 2007).

During the stages when fusion is occurring (stages 12-14), founder cells have a stereotypic organization within the somatic mesoderm that prefigures the final muscle pattern (Figure 1.6A-C) (Beckett and Baylies, 2007). FCs form four characteristic groupings at each stage: the dorsal group comprises 4 FCs (DO1, DO2, DA1 and DA2), the dorsal-lateral group includes 6 FCs (DO3-5, DA3, DT1 and LL1), the lateral group consists of 6 FCs (LT1-4, SBM and LO1) and the ventral group is made of 14 FCs (VT1, VA1-3, VL1-4 and VO1-6) (Figure 1.6D). Despite the consistency in the final muscle pattern, however, FCs themselves are less precisely positioned. Instead, within each group, FCs maintain a characteristic spatial relationship with respect to one another.

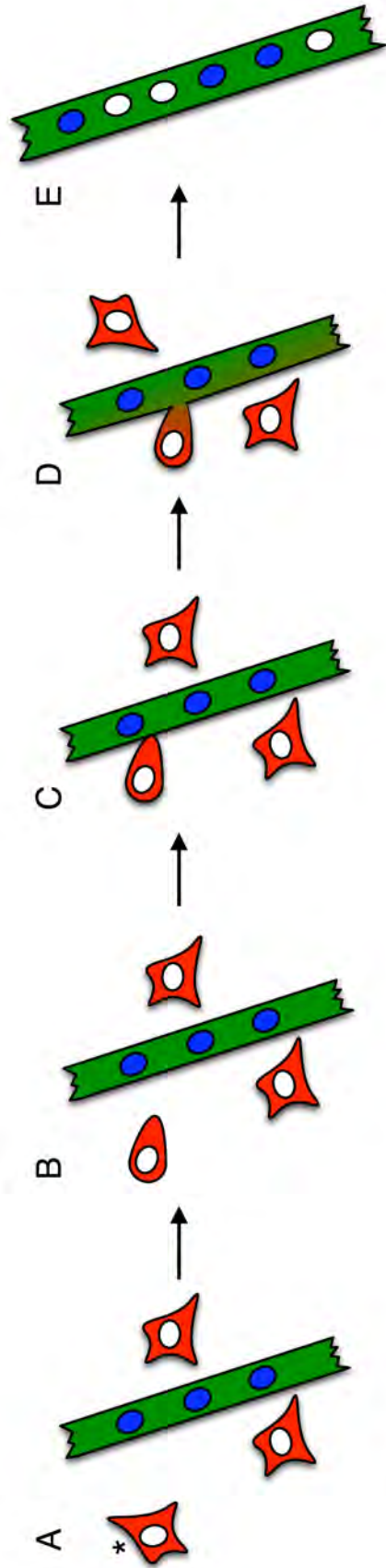


Figure 1.5. Cell-cell fusion utilizes a conserved set of cellular behaviors. Myoblast fusion (shown as an example), like other examples of cell-cell fusion, undergoes a set of conserved cellular behaviors. The indicated myoblast (asterisk) undergoes dramatic cell shape changes (A-B) and migrates towards its fusion partner (B-C). (C) The myoblast and myotube recognize and adhere to one another. Close apposition of their plasma membranes and bilayer mixing results in membrane fusion (D) and the incorporation of the new nucleus into the growing myotube. (E) This process repeats until a myotube of the desired nuclear number is attained.

Within the dorsal group, for example, the most dorsal and most ventral FCs mark DA1 and DA2, respectively. Of the remaining two FCs, the most anterior FC is DO2 and the remaining FC specifies DO1.

Transmission electron microscopy (TEM) has been used to examine myoblast fusion at the ultrastructural level to identify different stages of fusion and to order them into a sequential process based on the prevalence of a structure at a particular developmental stage (Berger et al., 2008; Doberstein et al., 1997; Massarwa et al., 2007; Sens et al., 2010). One model, based on traditional chemical fixation, proposes that following FC/FCM contact, paired electron-dense vesicles, or pre-fusion complexes, form and align along apposed membranes of fusing myoblasts. Electron-dense plaques subsequently form, presumably from the contents of the earlier pre-fusion complexes. Finally, multiple fusion pores at the fusion site expand, and the vesiculating membrane from the site is removed. These events lead to membrane breakdown, resulting in cytoplasmic continuity and ultimately the addition of another nucleus to the growing myotube (Berger et al., 2008; Doberstein et al., 1997; Massarwa et al., 2007). In contrast, a more recent TEM analysis using high-pressure freezing, indicates that only a single, large fusion pore forms between FC/myotubes and FCMs, and evidence for membrane vesiculation was not observed, suggesting that this is not required for fusion pore expansion (Sens et al., 2010). Similarly, single-channel pores are found in other fusing systems, and membrane vesiculation does not appear to play a role in pore expansion (Chen et al., 2008; Gammie et al., 1998; Mohler et al., 1998).

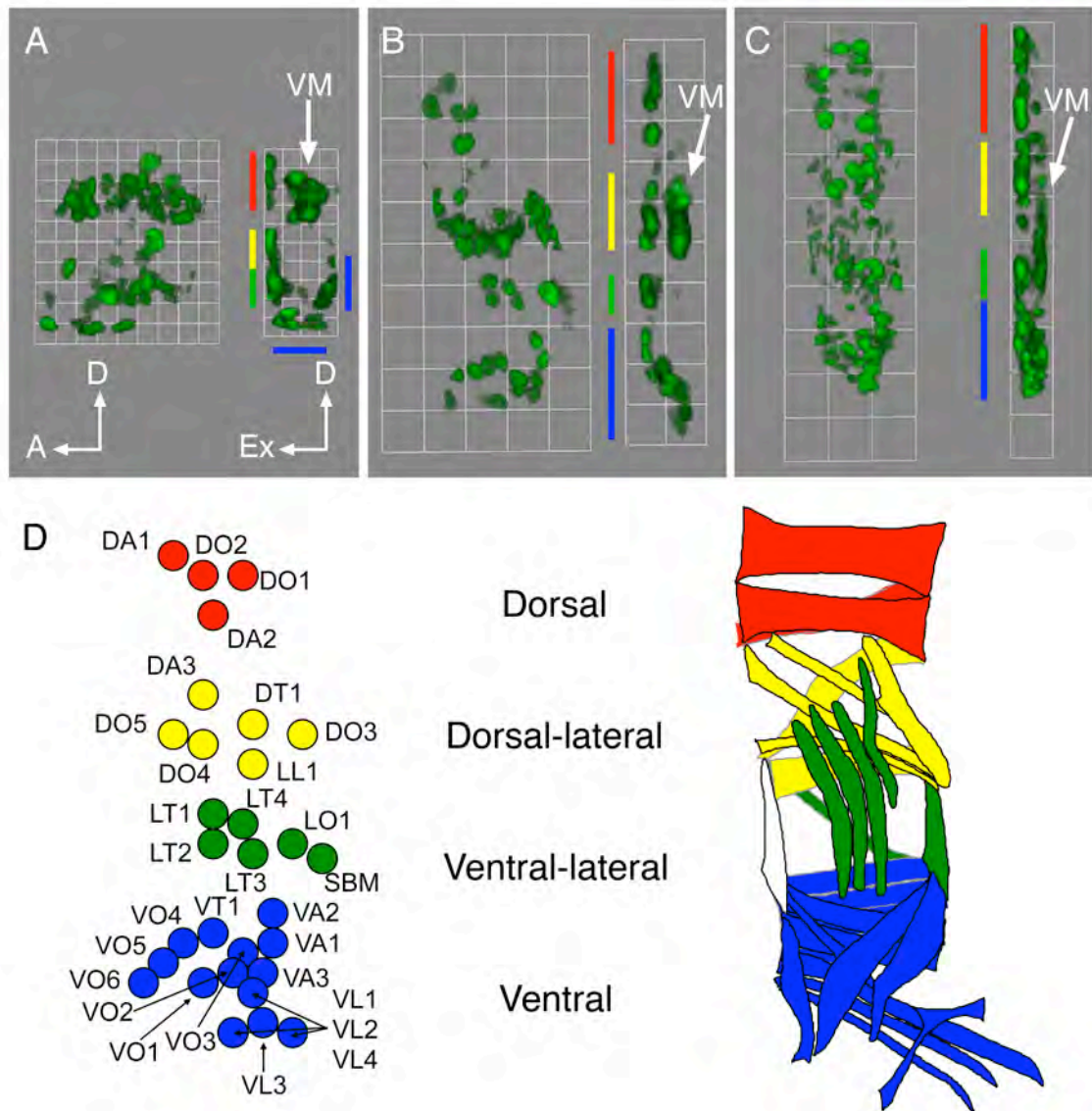


Figure 1.6. Founder cells form four characteristic groups. (A-C) Three-dimensional renderings of a single mesodermal hemisegment of an *rp298-lacZ* embryo stained with an antibody against β -gal to label FC/myotube nuclei (green). Each panel shows an external view (left) and a side view rotated 90° clockwise (right). A, anterior. D, dorsal. Ex, exterior. SM, somatic muscle. VM, visceral muscle. (A) At stage 12 (1 grid unit = 5.7 μ m), the most ventral FCs (blue) are located internally. (B-C) At stages 13 (B, 1 grid unit = 10.9 μ m) and 14 (C, 1 grid unit = 14.1 μ m), after germband retraction, these cells move externally. (D) A map of FC organization at stage 13 (left) and the final muscles they generate at stage 16 (right). (A-D) During these stages, FCs are organized into four groups: dorsal (red), dorsal-lateral (yellow), lateral (green) and ventral (blue). Modified from (Beckett et al., 2007).

Thus, the number of fusions pores that form during *Drosophila* myoblast fusion requires further clarification.

A number of genetic studies have identified gene products required for myoblast fusion in *Drosophila* (Table 1.1, Figure 1.7) (Rochlin et al., 2009). These gene products fall into several categories based on their predicted functions, including proteins that mediate recognition and adhesion, proteins that regulate the actin cytoskeleton, adaptor proteins that link those two categories of proteins together and proteins that currently have an unknown function.

Recognition and adhesion of myoblasts

Four Immunoglobulin (Ig) domain-containing single pass transmembrane proteins, Dumfounded/Kin-of-Irre (Duf/Kirre), Roughest/Irregular-optic-chiasma-C (Rst/Irre), Sticks and stones (Sns) and Hibris (Hbs), function in the attraction, migration, recognition and adhesion of myoblasts, indicating that these steps, often considered functionally distinct, are mechanistically and genetically linked during myoblast fusion (Table 1.1, Figure 1.7) (Artero et al., 2001; Bour et al., 2000; Dworak et al., 2001; Ruiz-Gomez et al., 2000; Shelton et al., 2009; Strünelberg et al., 2001). Duf is expressed specifically in FCs, while Sns and Hbs are expressed exclusively in FCMs. Rst is expressed in both cell types, but functions specifically in FCs.

Duf and Rst perform redundant functions in the attraction, recognition and adhesion of FCs with FCMs. Both serve as attractants for FCMs;

Table 1.1. A partial list of proteins required for myoblast fusion in *Drosophila* and mouse.

<i>Drosophila</i> (mouse)	Protein class	Actin focus class	PIP ₂ accumulation	TEM	References
cell recognition and adhesion:					
Duf/Kirre (Kirrel)	Ig superfamily	no focus			(Ruiz-Gomez et al., 2000; Strunkelberg et al., 2001; Richardson et al., 2007; Sohn et al., 2009)
Rst/Irre C	Ig superfamily	no focus			(Strunkelberg et al., 2001; Richardson et al., 2007)
Sns (Nephrin)	Ig superfamily	no focus	absent		(Bour et al., 2000; Richardson et al., 2007; Sohn et al., 2009)
Hbs	Ig superfamily		absent		Artero et al., 2001; Dworak et al., 2001; Shelton et al., 2009)
cell signaling:					
Rols (Tanc1/2)	multi-protein interaction domain-containing	reduced number; normal size	reduced number		(Chen and Olson, 2001; Menon and Chia, 2001; Rau et al., 2001; Richardson et al., 2007; Avirneni-Vadlamudi et al., 2012)
Arf6 (Arf6)	GTPase				(Chen et al., 2003)
Blow (unknown)	PH-domain-containing	increased number; enlarged size	form	absence of electron-dense plaques	(Doberstein et al., 1997; Schröter et al., 2004; Jin et al., 2011; Richardson et al., 2007)
D-Nck	SH2 and SH3 domain-containing adaptor				(Kaipa et al., 2013)
Crk	SH2 and SH3 domain-containing adaptor				(Kim et al., 2007)

Table 1.1. Con't.

Mbc (Dock1/5)	Rac GEF	increased number; enlarged size	form	nearly complete absence of prefusion complexes	(Rushton et al., 1995; Doberstein et al., 1997; Erickson et al., 1997; Richardson et al., 2007; Laurin et al., 2008; Pajcini et al., 2008)
Rac1/2 (Rac1)	GTPase	increased number; enlarged size		absence of fusion pores (<i>Drac^{G12V}</i>)	(Luo et al., 1994; Doberstein et al., 1997; Hakeda-Suzuki et al., 2002; Vasyutina et al., 2005; Charrasse et al., 2007; Richardson et al., 2007)
Loner (IQSec1)	putative Arf6 GEF	increased number; normal size	form		(Chen et al., 2003; Richardson et al., 2007; Pajcini et al., 2008)
ArpC1	Arp2/3 complex	normal size			(Massarwa et al., 2007)
Arp3	Arp2/3 complex	normal size			(Richardson et al., 2007; Berger et al., 2008)
Kette (Nap1)	SCAR/WAVE complex	increased number; enlarged size	form	increased size of electron-dense plaques	(Schröter et al., 2004; Richardson et al., 2007; Nowak et al., 2009)
SCAR	NPF for Arp2/3	enlarged (M/Z)	form		(Richardson et al., 2007; Berger et al., 2008; Gildor et al., 2009)
D-Wip	Wip/WASp complex	normal size	form	persistent electron dense vesicles and the absence of fusion pores ¹ , or formation of fusion pores ²	(¹ Kim et al., 2007; ² Massarwa et al., 2007; Richardson et al., 2007; ² Gildor et al., 2009; ¹ Sens et al., 2010)
WASp	NPF for Arp2/3		form	formation of small fusion pores	(Kim et al., 2007; Schäfer et al., 2007; Gildor et al., 2009)

ectopic expression of these proteins is sufficient to alter the migratory path of FCMs (Ruiz-Gomez et al., 2000; Strünkelberg et al., 2001). Duf and Rst can also both adhere directly to Sns which, in conjunction with Hbs, mediates recognition and adhesion in FCMs (Dworak et al., 2001; Galletta et al., 2004). Duf and/or Rst-mediated processes are essential for myoblast fusion. Removal of both Duf and Rst is required to generate a complete fusion defect, while the expression of either gene is sufficient to rescue this defect (Strünkelberg et al., 2001).

Similarly, Sns is required in the FCM to recognize and adhere to FCs in a Duf/Rst-dependent manner (Figure 1.7) (Bour et al., 2000; Galletta et al., 2004; Kocherlakota et al., 2008). Loss of *sns* causes a severe fusion defect, though the occasional fusion event has been reported (Beckett and Baylies, 2007; Bour et al., 2000). In contrast to the redundant relationship between Duf and Rst, Hbs and Sns play only partially redundant functions during myoblast fusion (Artero et al., 2001; Dworak et al., 2001; Menon, 2005; Shelton et al., 2009). *hbs* mutants appear largely wild-type and Hbs can only direct a small amount of fusion in *sns* mutants (Shelton et al., 2009).

Interestingly, these four transmembrane proteins are the only molecules that appear to mediate FC-FCM adhesion and fusion in *Drosophila*. Mutation of the *Drosophila* homologs of integrin and cadherin family members, proteins for which a role in mammalian myoblast fusion is well-documented (discussed below in “Mesoderm and muscle development in mammals”), does not cause any

defects in myoblast fusion (Iwai et al., 1997; Prakash et al., 2005; Prokop et al., 1998a; Roote and Zusman, 1995; Zusman et al., 1993).

Adaptor proteins link recognition and adhesion to actin cytoskeleton regulation

Myoblast recognition and subsequent adhesion results in the organization of Duf and Sns into a ring-like structure termed the FuRMAS (fusion-restricted myogenic-adhesive structure) (Figure 1.7) (Haralalka et al., 2011; Kesper et al., 2007; Sens et al., 2010). This structure is believed to serve as a signaling center, triggering signaling cascades from the membrane to intracellular proteins, leading to the recruitment of the fusion machinery to this site (Kesper et al., 2007). Following adhesion/organization of the FuRMAS, Duf, via its intracellular region, recruits the FC-specific adaptor protein Rolling Pebbles/Antisocial (Rols) to the fusion site (Bulchand et al., 2010; Chen and Olson, 2001; Menon and Chia, 2001; Rau et al., 2001). Rols functions in a positive-feedback loop to ensure that Duf is recycled back to the myotube membrane for subsequent rounds of fusion (Menon, 2005). Rols also contains a number of protein-protein interaction motifs, including nine ankyrin repeats, three tetratricopeptide repeats (TPRs), a RING finger and a coiled-coil domain. Rols likely interacts with and recruits downstream proteins to the fusion site (Chen and Olson, 2001; Menon and Chia, 2001; Rau et al., 2001). The giant cytoskeletal protein D-Titin is recruited to sites of fusion in a Rols-dependent manner (Menon and Chia, 2001).

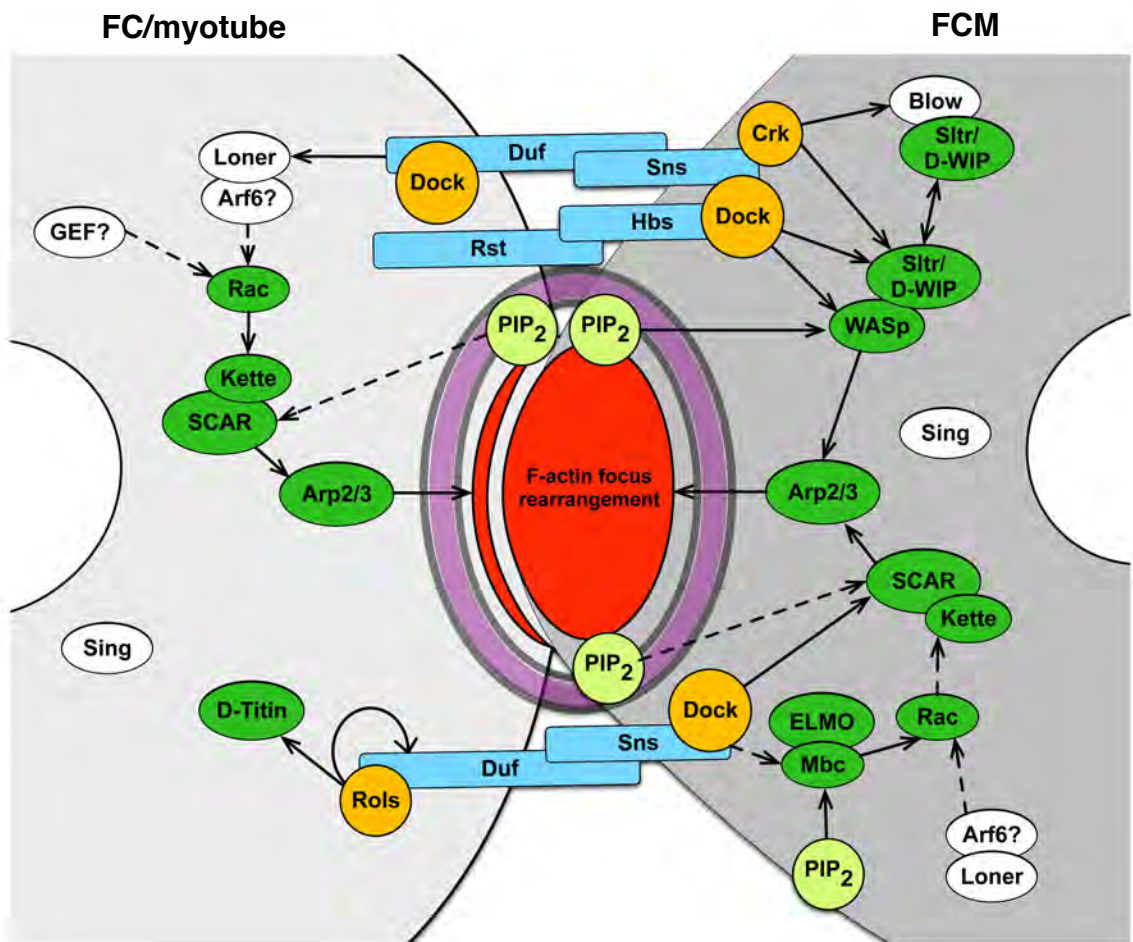


Figure 1.7. Overview of proteins required for myoblast fusion in *Drosophila*.

The indicated proteins and pathways correspond to those that will be discussed in more detail in the text. The represented proteins generally include those for which a role in fusion has been demonstrated with loss of function analysis. Protein-protein relationships linked with dashed arrows are based on protein functions in other tissues. Proteins involved in the recognition and adhesion of FC/myotube and FCM are blue. Proteins that regulate the actin cytoskeleton are green. Adaptor proteins that link the transmembrane receptors to the actin regulators are orange. Proteins with unknown or unclear roles are white. Solid arrows from PIP₂ indicate that the interaction is via a pleckstrin homology (PH) domain; dashed arrows indicate that the interaction is via a calcium-binding (C2) domain. Nuclei, white. FC/myotube, light grey. FCM, dark grey. F-actin focus, red oval. FuRMAS, purple ring.

D-Titin is essential for myoblast fusion, but also plays a later role in sarcomere development (Machado and Andrew, 2000; Zhang et al., 2000). Duf also recruits the putative Arf6 guanine nucleotide exchange factor (GEF) Loner (also known as Schizo) to membranes in S2 cells, and the two proteins physically interact *in vitro*, though the domain responsible for this interaction does not appear to be completely necessary for fusion (Bulchand et al., 2010). Further, Loner has never been observed at the fusion site, suggesting that this interaction does not occur during myoblast fusion.

Similarly, the Sns cytodomain contains essential phospho-tyrosine residues and several redundant functional domains that direct myoblast fusion (Kocherlakota et al., 2008). Thus, like Duf, Sns may interact with an array of proteins to transduce downstream signaling cascades. One putative interaction is with CT10 regulator of kinase (Crk), which can subsequently recruit actin regulators, including Blown fuse (Blow) and *Drosophila* WASp Interacting Protein (D-WIP) [also known as Solitary (Sltr)/Verprolin 1 (Vrp1)], to the fusion site (discussed in more detail below) (Berger et al., 2008; Jin et al., 2011; Kim et al., 2007; Massarwa et al., 2007).

The adaptor protein D-Nck [also known as Dreadlock (Dock)], also colocalizes with Duf and Sns at the site of myoblast fusion and physically interacts with all four cell adhesion proteins (Table 1.1, Figure 1.7) (Kaipa et al., 2013). D-Nck also interacts genetically with Duf, Sns and Hbs; double mutants have enhanced myoblast fusion defects. Downstream, D-Nck biochemically and genetically interacts with SCAR, D-WIP and WASp, regulators of actin

polymerization that are essential for myoblast fusion in *Drosophila* (discussed in more detail below) (Berger et al., 2008; Gildor et al., 2009; Kaipa et al., 2013; Massarwa et al., 2007; Richardson et al., 2007; Schäfer et al., 2007; Sens et al., 2010). D-Nck and Crk fulfill a similar function and may play a redundant role in linking the the FCM-specific receptors to WASp/D-WIP (Kaipa et al., 2013; Kim et al., 2007). Taken together, the FuRMAS links the first class of fusion proteins, those that are responsible for the attraction, recognition and adhesion of FCs and FCMs, to a second class of fusion proteins, those that regulate the actin cytoskeleton, through adaptor proteins such as Rols, Crk and D-Nck.

Actin regulation during myoblast fusion

A number of studies have established the fundamental role that the actin cytoskeleton and its regulators play in myoblast fusion (Abmayr and Pavlath, 2012; Rochlin et al., 2009). A specific actin structure, termed the F-actin focus, marks the fusion site (Figures 1.7, 1.8) (Richardson et al., 2007). The formation and the dissolution of the actin focus directly precedes membrane dissolution and cytoplasmic continuity and depends on the Arp2/3 complex and its regulation, which nucleates branched actin polymerization (Figure 1.8) (Berger et al., 2008; Massarwa et al., 2007; Richardson et al., 2007). In wild-type embryos, the average focus size is 1.9 μm (ranging from 0.7-4.5 μm) and the average duration of the focus is 11.9 minutes (ranging from 5.7 – 29.5 minutes). The FuRMAS (Figure 1.7) surrounds the actin foci and is speculated to limit the size of the fusion site;

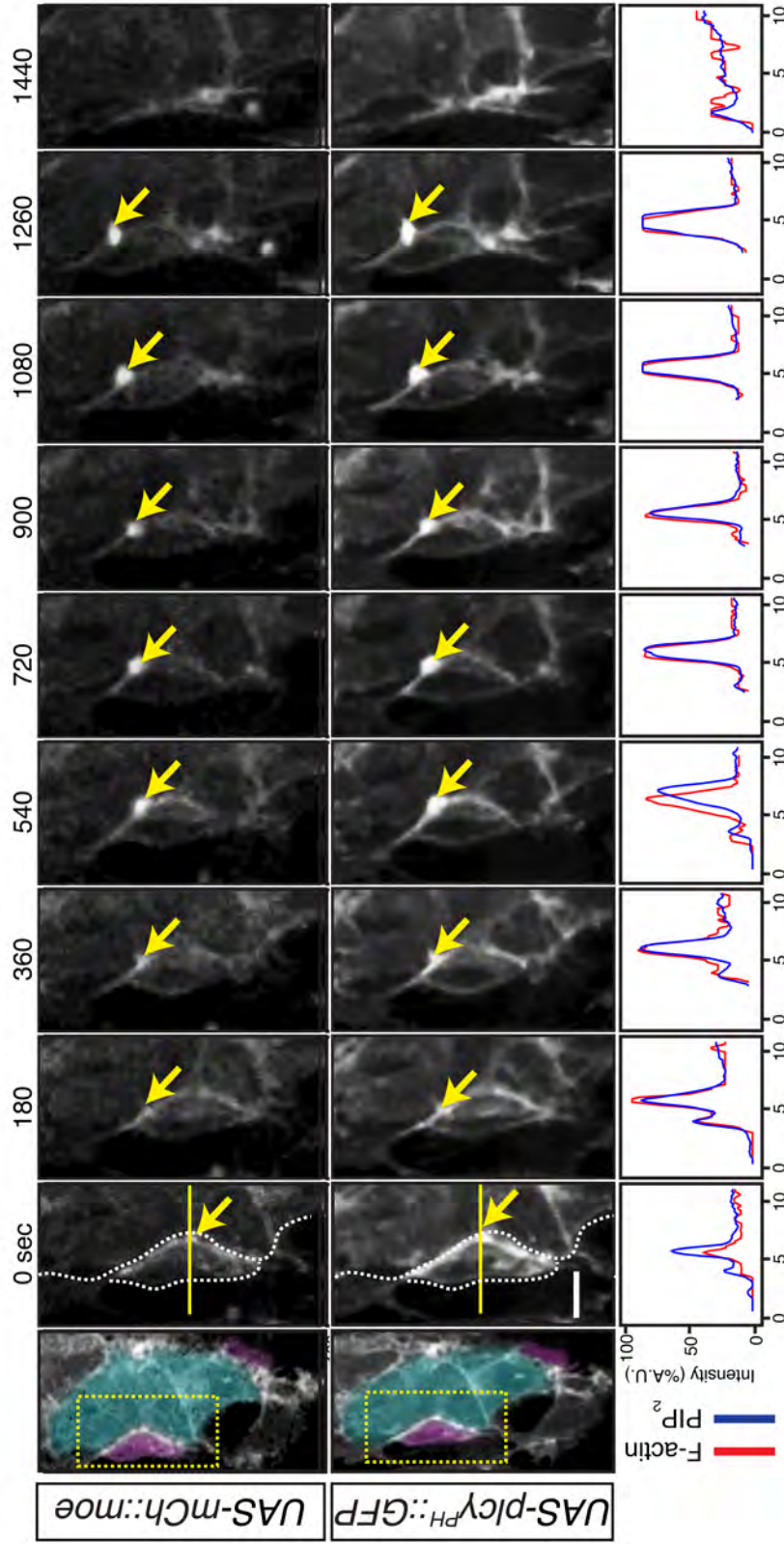


Figure 1.8. F-actin foci and PIP₂ accumulations mark the site of fusion in *Drosophila*. Time-lapse imaging of the VA1 muscle (turquoise) with an attached FCM (magenta) in a stage 14 embryo (11.5 hours AEL) expressing *mCherry::moesin* (*moe*, top) and *plcy^{PH}::GFP* (bottom) under *Dmef2-Gal4* control. The area shown in the adjacent stills are boxed in yellow. 0 sec shows the initial membrane alignment, and discrete enrichments of both signals (indicated by arrows) overlap spatially and temporally during myoblast fusion. This is highlighted further in the accompanying line scans. Bar, 5 μ m. (M. Baylies and I. Bothe, personal communication).

consistent with this, the FuRMAS has been reported to range in size from 1-5 μm in fixed samples (Kesper et al., 2007; Sens et al., 2010). Recent data indicate that the F-actin focus is asymmetric: the majority of F-actin is found in the FCM within invasive, podosome-like “fingers” termed the PLS (podosome-like structure, discussed in more detail below), while only a thin sheath of actin is in the FC (Figure 1.7) (Haralalka et al., 2011; Sens et al., 2010). During myoblast fusion, Arp2/3 can be activated by two families of nucleation-promoting factors (NPFs), SCAR/WAVE and WASp (Berger et al., 2008; Gildor et al., 2009; Massarwa et al., 2007; Richardson et al., 2007; Schäfer et al., 2007; Sens et al., 2010). In FCMs, the F-actin focus is formed by the activities of both SCAR/WAVE and WASp; while the sheath of actin in the FC is proposed to be formed by the action of SCAR/WAVE alone.

The SCAR/WAVE complex activates Arp2/3 to mediate actin polymerization (Pollard, 2007). SCAR is required in both FCs and FCMS and is necessary for their migration and fusion (Table 1.1, Figure 1.7) (Berger et al., 2008; Gildor et al., 2009; Richardson et al., 2007; Schroter, 2004; Sens et al., 2010). In support of this, SCAR is uniformly cytoplasmic in pre-migratory myoblasts, but becomes asymmetrically localized to lamellipodia during migration (Gildor et al., 2009). *Kette*, the *Drosophila* homolog of Nap1 and a conserved member of the SCAR/WAVE regulatory complex, is also required for myoblast fusion (Schroter, 2004). *Kette* regulates myoblast fusion through stabilization of SCAR and appears to be required for proper SCAR localization (Richardson et al., 2007). In *kette* mutants, SCAR protein levels are reduced and residual

protein is mislocalized. In the FCM, Kette also interacts genetically with the FCM-specific protein Blow (Artero et al., 2001; Schroter, 2004).

The SCAR/WAVE complex is activated by the small GTPase, Rac (Table 1.1, Figure 1.7) (Pollard, 2007). *Drosophila rac1 rac2 mtl* mutant embryos or embryos in which constitutively active or dominant negative Rac1 is expressed display defects in myoblast fusion, dorsal closure, organization of the actin cytoskeleton and axon guidance (Hakeda-Suzuki et al., 2002; Luo et al., 1994; Richardson et al., 2007). In addition, Rac triple mutant FCMs remain rounded, suggesting that they are incapable of migrating. SCAR is also mislocalized in migrating and fusing *rac1 rac2 mtl* mutant myoblasts, further supporting a role for Rac and SCAR in the migration of myoblasts prior to fusion (Gildor et al., 2009). Rac is found in both FCs and FCMs; however, recent data suggest that active Rac1 is asymmetrically localized to FCMs where the majority of the F-actin focus is located (Figure 1.7) (Haralalka et al., 2011; Richardson et al., 2007). Though some rescue was observed when Rac was expressed in the FCs of *rac1 rac2* mutants, fusion is nearly completely rescued by expression of wild-type Rac in FCMs. Due to maternal loading, limited fusion does occur in *rac1 rac2* mutants. Thus, it is impossible to rule out a role for Rac in FC/myotubes.

During *Drosophila* myoblast fusion, Rac is (presumably) activated by the GEF Myoblast city (Mbc) (Table 1.1) (Kiyokawa et al., 1998; Nolan et al., 1997). Consistent with this, *mbc* mutant embryos have a similar phenotype to *rac1 rac2 mtl* mutant embryos, exhibiting a severe fusion deficiency, defects in dorsal closure and a decrease in cytoskeletal organization in the epidermis (Luo et al.,

1994; Nolan et al., 1997; Rushton et al., 1995). Interestingly, Mbc is asymmetrically required during the fusion process: Mbc is localized to the fusion site specifically in FCMs, suggesting that this is the location of its activity (Figure 1.7) (Haralalka et al., 2011; Richardson et al., 2007). In support of this, the myoblast fusion defect observed in *mbc* mutant embryos can be rescued by expression of Mbc only in FCMs (Haralalka et al., 2011). Thus, Mbc is required only in the FCM to activate Rac and another GEF(s) must be responsible for activating Rac in FCs for the first fusion event. Further, the role of Rols (an FC-specific protein) cannot be to recruit Mbc to Duf as previously suggested (Chen and Olson, 2001).

Mbc derives its GEF activity from the Dock Homology Region-2 (DHR-2) domain (Cote, 2002; Côté and Vuori, 2007; Kiyokawa et al., 1998; Meller, 2005). A single point mutation within the catalytic DHR-2 domain in Mbc has a fusion defect as severe as null alleles, indicating that this activity is required for myoblast fusion (Erickson et al., 1997; Nolan et al., 1997; Rushton et al., 1995). *mbc* also encodes an internal DHR-1 domain and proline-rich sites in the C-terminus (Balagopalan et al., 2006; Brugnera et al., 2002; Côté et al., 2005; Erickson et al., 1997). The DHR-1 domain has been shown to interact directly and specifically with phosphatidylinositol (3,4,5)-trisphosphate (PIP₃) and is essential for fusion (Balagopalan et al., 2006; Côté et al., 2005). Recent data also suggest that this domain can interact with singly and doubly phosphorylated phosphoinositides (Bothe et al., in revision). The proline-rich C-terminus is important to facilitate interaction with the adaptor protein Crk (Hasegawa et al.,

1996; Matsuda et al., 1996). The primary role of this interaction is suggested to be in recruiting Mbc to target sites at the plasma membrane, though this activity appears to be dispensable for fusion (Balagopalan et al., 2006; Hasegawa et al., 1996). No loss of function mutants are available for Crk, but overexpression of a membrane-targeted Crk causes myoblast fusion defects (Abmayr et al., 2003).

The N-terminal SH3 domain of Mbc is essential for its interaction with Elmo (Engulfment and cell motility), a scaffolding protein that forms a conserved complex with Mbc and Rac (Table 1.1, Figure 1.7) (Brugnera et al., 2002; Côté et al., 2005). The Mbc/Elmo complex has been suggested to act as a novel bipartite GEF wherein the binding of Elmo to Mbc increases the affinity of the GEF for nucleotide-free Rac to enhance the exchange of GDP for GTP. Mbc and Elmo biochemically interact in *Drosophila* muscle (Geisbrecht et al., 2008). Further, mutation of *elmo* resulted in muscle defects in the embryo, and overexpression of *mbc* and *elmo* together in the muscle caused a defect in myoblast fusion, indicating that Elmo is required for myoblast fusion in *Drosophila*.

A second GEF, Loner/Schizo was isolated in a genetic screen designed to identify additional genes involved in skeletal muscle development in *Drosophila* (Table 1.1) (Chen et al., 2003). *loner* mutants exhibit a strong defect in myoblast fusion. Loner is a cytoplasmic protein that localizes to discrete puncta within myoblasts, and like Mbc, Loner activity converges on Rac, although indirectly (Figure 1.7) (Chen et al., 2003). Further, Loner is localized near the site of fusion, adjacent to the actin focus and does not appear to play a role in actin regulation at the fusion site (Richardson et al., 2007). What role Loner is playing in myoblast

fusion has been unclear. Loner contains a central catalytic domain with significant homology to the yeast Sec7 domain (Chen et al., 2003; Someya et al., 2001). Sec7 domain-containing proteins are GEFs with activity on ADP ribosylation factors (Arfs), a family of small GTPases belonging to the Ras superfamily (Donaldson and Jackson, 2000; Jackson and Casanova, 2000). Data in *Drosophila* suggest that the Sec7 domain of Loner has specific activity towards Arf6 *in vitro* (Chen et al., 2003). Thus, Loner may be involved in Arf-dependent processes, such as trafficking and actin cytoskeletal reorganization (D'Souza-Schorey and Chavrier, 2006). Recent data also suggest mammalian Arf6 is required for the spatial restriction of Rac activation, suggesting that Loner might indirectly localize Rac (Palamidessi et al., 2008). The activity of the Loner Sec7 domain is required for muscle fusion. Mutants in which the Sec7 domain is deleted or is catalytically inactive cannot rescue the fusion defect; however, its targets *in vivo* remain unclear as *Arf6* null flies are viable and myogenesis is not perturbed (Chen et al., 2003; Dyer et al., 2007). It is possible that a second Arf fulfills the roles of Arf6 in its absence or that Loner activates another Arf *in vivo*.

In a second NPF pathway, *Drosophila* WASp and WASp Interacting Protein promote actin polymerization in FCMs by activating Arp2/3 (Table 1.1, Figure 1.7) (Kim et al., 2007; Massarwa et al., 2007; Schäfer et al., 2007). D-WIP interacts with WASp via its WASp-binding domain (WBD), and D-WIP (and consequently WASp) is recruited to the fusion site via Sns-dependent localization of Crk (Kim et al., 2007). Loss of either D-WIP or WASp causes a severe fusion defect. In addition, Crk also recruits the FCM-specific protein Blow to sites of

fusion (Jin et al., 2011). Blow affects the stability of WASp by competing for D-WIP-binding. Thus, mutation in *blow* causes an accumulation of D-WIP/WASp at the fusion site and a block in fusion (Doberstein et al., 1997; Jin et al., 2011; Richardson et al., 2007)

In addition to the F-actin focus, a local accumulation of the membrane phospholipid phosphoinositol 4,5-bisphosphate (PIP₂), a known regulator of actin dynamics and activator of Arp2/3, marks the site of fusion in *Drosophila* (Figure 1.8) (Miki et al., 1996; Papayannopoulos et al., 2005; Shewan et al., 2011, Bothe et al., in revision). Live imaging of two PIP₂ reporters, *plcy^{PH}::GFP* and *plcδ^{PH}::GFP*, reveals an accumulation at the site of myoblast-myoblast contact, reminiscent of the actin focus. The duration of the PIP₂ accumulation is similar to that of the actin focus [average of 12 minutes, in agreement with published data (Richardson et al., 2007)] during myoblast fusion (Bothe et al., in revision). Co-expression of the F-actin and PIP₂ reporters, *mCherry::moesin* and *plcy^{PH}::GFP*, respectively, indicates that the F-actin and PIP₂ accumulations indeed overlap spatially and temporally (Figure 1.8). PIP₂ accumulates in both the FC/myotube and FCM, in contrast to the F-actin focus which is found mainly in the FCM (Haralalka et al., 2011; Sens et al., 2010, Bothe et al., in revision). Furthermore, PIP₂ accumulation and downstream signaling are essential for myoblast fusion. PIP₂ and other phosphoinositides interact with downstream proteins through their pleckstrin homology (PH) or calcium-binding (C2) domains (Lemmon, 2008). A number of fusion proteins, including Mbc, Loner, Blow, WASp and SCAR, contain PH or C2 domains, which bind to PIP₂ in addition to other phosphoinositides

(Bothe et al., in revision). “Masking” PIP₂ through the overexpression of the PIP₂-reporter resulted in the mislocalization of the actin regulators, Mbc and WASp, two proteins that contain PH domains that bind PIP₂. SCAR is also mislocalized, indicating that PIP₂ affects both arms of Arp2/3 activation. Further, “masking” PIP₂ resulted in a severe fusion block and in the formation of a small actin focus, consistent with a role for PIP₂ in regulating Arp2/3 activity. Additionally, modulation of PIP₂ levels by overexpression of kinase-dead Skittles (Sktl), the PI-5-Kinase that phosphorylates PIP to generate PIP₂ also caused a fusion defect and tagged-kinase-dead Sktl remained at the fusion site where it colocalized with *plcy^{PH}::GFP*. Using a similar approach, enrichment of PIP₃ was never observed, suggesting that it is not required for fusion. Together, the data suggest a model in which PIP₂ accumulation at the fusion site activates Arp2/3 via the correct localization and activation of members of the WASp and SCAR NPF pathways.

In addition to providing physical markers for the fusion site, the actin and PIP₂ foci have also proven to be a valuable tool for classifying fusion mutants (Table 1.1, Figure 1.9). Previous studies of essential fusion genes were hindered due to the similarities between mutant phenotypes, which consist of small muscles with one or few nuclei and numerous unfused myoblasts. These phenotypes, as a result of their similarity to one another, often gave little mechanistic insight to the role of a protein during fusion. Analysis of the actin and/or PIP₂ foci in fusion mutants, however, has informed the role of these proteins during fusion.

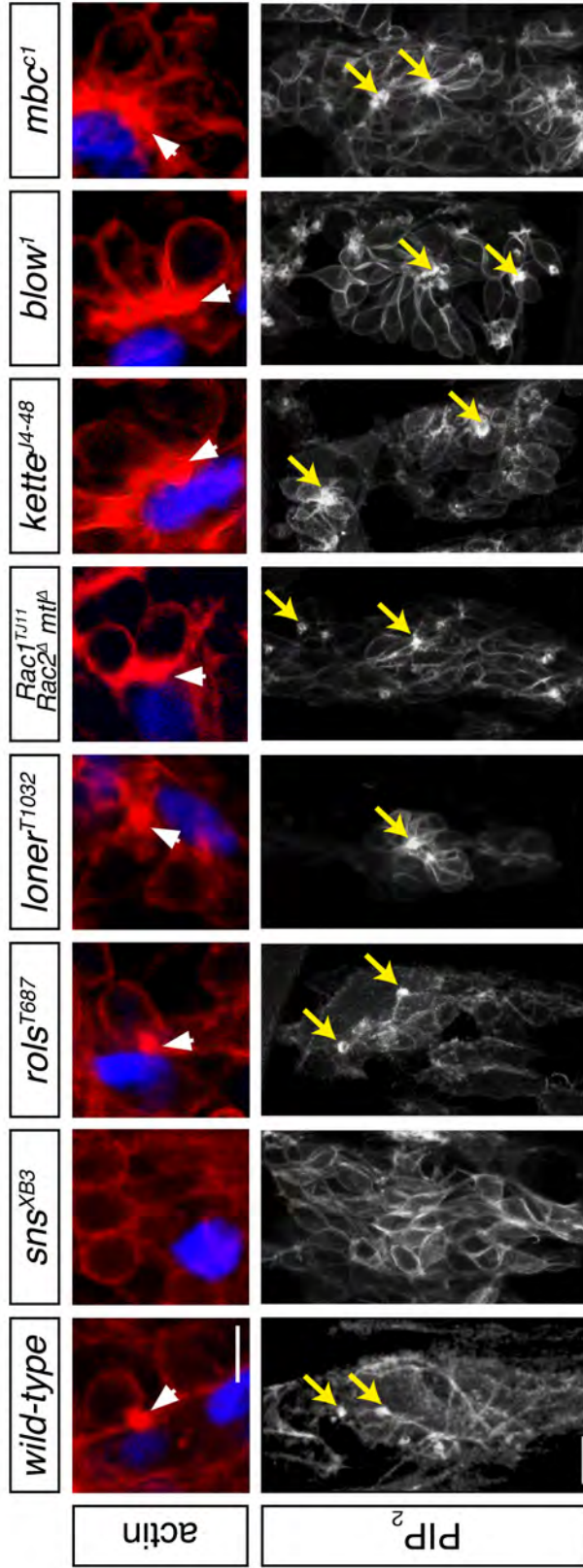


Figure 1.9. Roles of fusion proteins in actin and PIP₂ foci dynamics. (Top) Stage 14 *rp298-lacZ* embryos stained with phalloidin to label F-actin (red) and an antibody against β-gal to label FCs/myotube (blue). Actin foci are indicated by arrowheads. Foci fail to form in *sns^{XB3}* and *rols^{T627}* mutant embryos (class 1), though an occasional focus of wild-type size is observed. Wild-type foci form in *loner^{T1032}* mutant embryos (class 2), while enlarged foci form in *Rac1^{TJ11}*, *Rac2^Δ*, *mtl^Δ* embryos, *kette^{l4-48}* embryos, *blow¹* embryos and *mbc^{C1}* mutant embryos (class 3). Bar, 5 μm. Used with permission from (Richardson et al., 2007). (Bottom) Still images of time lapse from stage 14 embryos expressing the *plcy^{PH}::GFP* reporter (greyscale). PIP₂ enrichments are indicated by arrowheads. Foci fail to form in *sns^{XB3}* and *rols^{T627}* mutant embryos, though an occasional PIP₂ enrichment is observed. PIP₂ enrichments form in *loner^{T1032}* mutant embryos. Similarly, PIP₂ enrichments are observed in *Rac1^{TJ11}*, *Rac2^Δ*, *mtl^Δ* embryos, *kette^{l4-48}* embryos, *blow¹* embryos and *mbc^{C1}* embryos. Bar, 10 μm. (M. Baylies and I. Bothe, personal communication.)

Mutants distributed into three classes based on actin focus size and number (Table 1.1, Figure 1.9). Interestingly, these three classes also grouped mutants based on the process that they affect during fusion. In the first class of fusion mutants, which includes the four known transmembrane proteins required for myoblast recognition and adhesion, foci number is greatly reduced, consistent with a requirement for FC/myotube-FCM adhesion in F-actin focus formation. In the second class, which contains the majority of known fusion genes that impinge on actin cytoskeletal regulation, foci are enlarged, suggesting that these genes are required for actin organization at the fusion site. The proteins in this class, including Rac, Mbc and Kette, are localized to the actin focus, further indicating that the actin focus is the site of their activity (Richardson et al., 2007). In addition, the reduction or complete absence of foci in double mutants that affect both actin pathways (SCAR/WAVE and WASp) indicate that these two pathways are responsible for the formation of the actin focus (Sens et al., 2010, Bothe et al., in revision). Finally, the third class of mutants, which currently consists of only two known genes, contains normal sized foci, implying that these genes may play other roles during fusion.

Like the actin focus, PIP₂ foci formation requires myoblast adhesion (Richardson et al., 2007). PIP₂ accumulations were absent in embryos mutant for the adhesion molecules Sns and Hbs (Table 1.1, Figure 1.9) (Bothe et al., in revision). In mutants of actin regulators (*mbc*, *kette*, *loner*, *blow*, *Dwip*, *Scar* and *WASp*), PIP₂ accumulated at the contact site. Thus, PIP₂ enrichment does not

depend upon Arp2/3-mediated actin polymerization for its accumulation and its accumulation is upstream or parallel to Arp2/3 activity.

Similarly, TEM analysis of a number of fusion mutants has revealed distinct blocks in fusion, providing additional insight into the order of events as well as into the mechanism of several fusion genes (Table 1.1). Recent TEM using high-pressure freezing has also increased our understanding of the organization and composition of the fusion site from actin focus formation to fusion pore formation, revealing the presence of finger-like projections, called the podosome-like structure, or PLS, which protrude from the FCM and into the associated myotube (Sens et al., 2010). These projections appear to be filled with actin filaments and therefore may represent the actin foci that are observed in live and fixed embryos (Haralalka et al., 2011; Kesper et al., 2007; Richardson et al., 2007; Sens et al., 2010). The PLS is observed prior to the formation of the fusion pore and though multiple finger-like projections are present, a single fusion pore forms at the tip of one projection (Sens et al., 2010).

Muscle attachment

To transmit force, muscles must physically connect to the skeletal system via tendons or tendon-like cells. In *Drosophila*, which lacks an internal skeleton, muscles are connected to the exoskeleton through tendon-like cells of ectodermal origin. The tendon cells, along with the other epidermal cells, secrete cuticle and together, comprise the exoskeleton (Volk, 1999). The differentiation of

tendon cells is biphasic. The initial patterning of tendon precursor cells and muscle founder cells (FCs) emerge in parallel and are independent of one another; in *twist* mutant embryos, which completely lack mesoderm, early tendon patterning is normal (Becker et al., 1997). Terminal differentiation of tendon cells, as well as the proper attachment of embryonic muscles, however, is dependent on the communication of tendon precursors with myotubes and requires muscle cell polarity, signal exchange and recognition between myotube and tendon. In mutant embryos which lack a key regulator of tendon cell differentiation, muscles extend to aberrant positions and adhere to one another (Frommer et al., 1996). Thus, the early tendon field is broad, with many ectodermal cells being competent to differentiate into tendons. Subsequent signaling to muscles narrows this domain and a stereotypical, repeating pattern of tendon cells emerges, complementary to the pattern of muscles in the embryo.

Initial tendon precursor determination is regulated by signaling pathways that pattern the embryonic ectoderm, including positive signals from the Hedgehog (Hh) and epidermal growth factor receptor (Egfr) pathways and negative signals from the Wingless (Wg) pathway (Figure 1.10A) (Hatini and DiNardo, 2001; Volk and VijayRaghavan, 1994). For example, Hh and Wg signaling promote the expression of StripeB (SrB), an early growth response (Egr)-like transcription factor encoded by the *stripe* gene and a key regulator of early tendon cell differentiation (Volk et al., 1994; Frommer et al., 1996; Becker et al., 1997; Piepenburg et al., 2000). In *stripe* mutant embryos, the expression of the majority of tendon-specific genes is reduced, though not absent, suggesting

that Stripe is required for enhancing their transcription (Frommer et al., 1996). Overexpression of Stripe is also sufficient to induce the transcription of these genes (Becker et al., 1997; Vorbruggen et al., 1997). The onset of SrB activation delineates ectodermal cells from tendon precursor cells. SrB positively regulates its own transcription as well as the transcription of several genes implicated in muscle targeting to tendon cells, including *slit*, *Thrombospondin (Tsp)*, *Leucine-rich tendon-specific protein (Lrt)* and *slowdown (slow)* (Becker et al., 1997; Kramer et al., 2001; Subramanian et al., 2007; Chanana et al., 2009; Wayburn et al., 2009; Gilsohn et al., 2010). SrB levels are maintained at a low level in tendon precursor cells to prevent their differentiation into mature tendon cells. This is achieved post-transcriptionally by the long isoform of Held out wings [How(L)], an RNA-binding protein, which binds to the 3' untranslated region (UTR) of *stripe*. How(L) is a transcriptional target of SrB; thus, SrB levels are regulated by a negative feedback loop (Nabel-Rosen et al., 1999, 2002). In *how* mutants, SrB levels are high, and many tendon precursor cells prematurely differentiate in the absence of muscle contact.

To achieve final differentiation, tendon precursors must interact with muscles. As they are growing via fusion, myotubes become polarized and extend growth cone-like filopodia from each muscle end (Schnorrer et al., 2004). Myotube extension does not seem to require Stripe expression in tendon precursors initially, but at later stages, tendon cells are critical in guiding this process (Bate et al., 1990; Frommer et al., 1996; Becker et al., 1997; Vorbruggen et al., 1997).

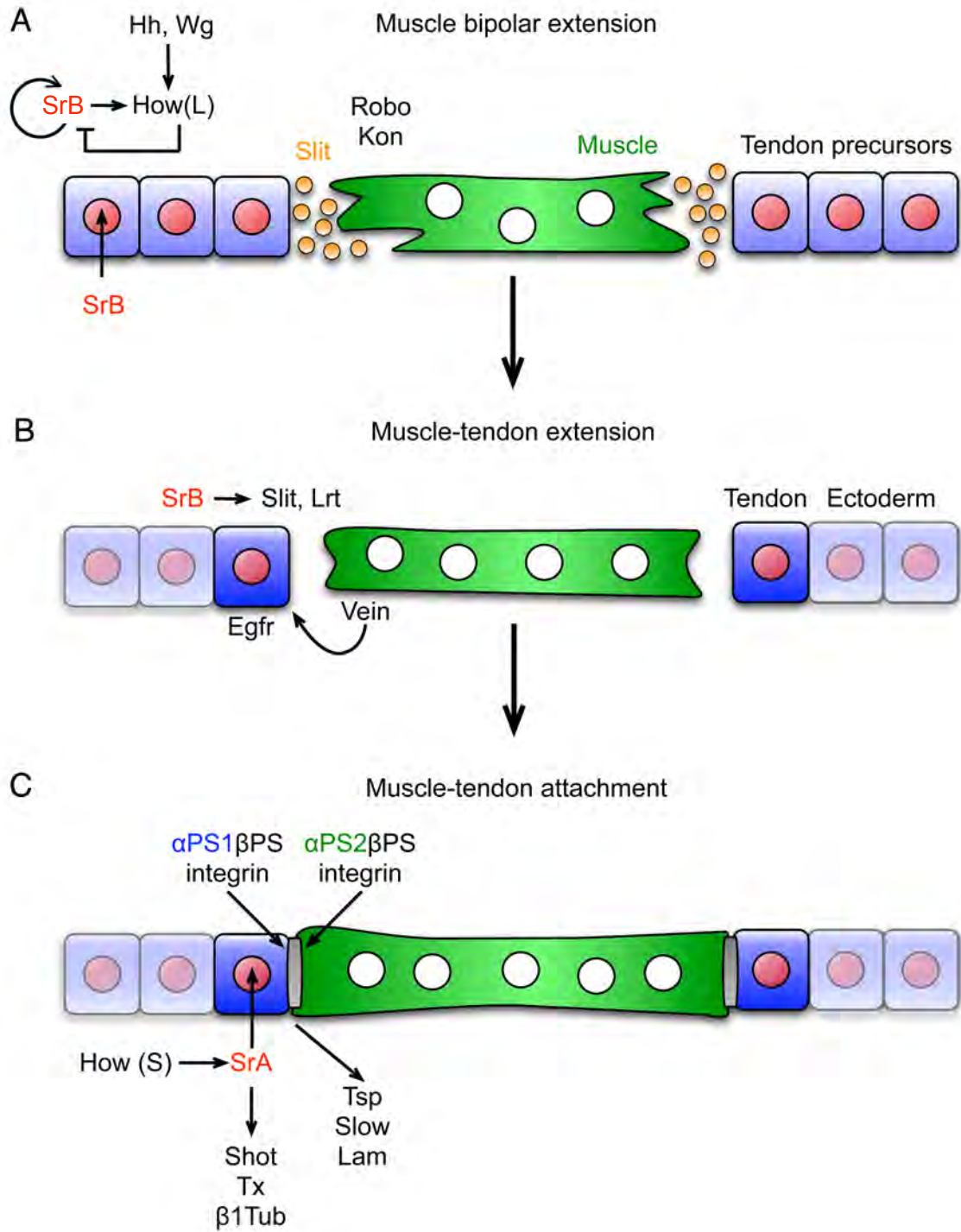


Figure 1.10. *Drosophila* muscle-tendon interactions. (A) StripeB (SrB) expression is induced in tendon progenitors by Hedgehog (Hh) and Wingless (Wg). SrB expression is maintained at a low level by post-transcriptional repression by the long isoform of the RNA-binding protein Held out wings [How(L)]. Tendon progenitors (segment border tendons) secrete Slit, which binds to the muscle-specific Robo receptor (VL muscles) to provide the initial cue for directing muscle bipolar extension. Kon-tiki (VL muscles) also contributes to muscle extension. (B) Secretion of Vein, a neuregulin-like ligand for the epidermal growth factor receptor (Egfr), initiates tendon differentiation and elevate SrB expression. SrB further induces the expression of Slit and Lrt. Tendon precursors that do not bind muscles lose SrB expression and become ectoderm cells. (C) The short isoform of How, How(S), is elevated and promotes the expression of StripeA (SrA). SrA induces terminal differentiation by induction of Short stop (Shot), Taxi (Tx, also Delilah) and β 1 Tubulin (β 1Tub). At this time, the myotendinous junction forms through the interaction of heterodimeric integrins expressed in tendons and muscles and their association with extracellular matrix components including Thrombospondin (Tsp), Slow and Laminin (Lam). Modified with permission from (Schweitzer et al., 2010).

Myotubes in *stripe* mutant embryos begin to extend but eventually mistarget and fail to attach to tendon cells, causing a severe disruption in the muscle pattern (Frommer et al., 1996). Moreover, ectopic expression of StripeB causes ectopic elongation (Vorbruggen et al., 1997; Beckett et al., 2007). Taken together, myotube extension requires intrinsic and extrinsic factors.

A single tendon-derived guidance signal has been described for the ventral longitudinal (VL) muscles (Figure 1.10A-B). These tendons (segment border tendons) secrete Slit, while the tendons that bind the lateral transverse muscles (intrasegmental tendons), for example, do not (Kramer et al., 2001; Volohonsky et al., 2007). Slit binds to the muscle-specific receptor Roundabout (Robo) and Robo2. Robo and Robo2 are expressed in the VL muscles (Figure 1.10A) (Kramer et al., 2001). The Slit/Robo guidance system is employed in axon guidance where Slit acts to repulse axons from the midline (Kidd et al., 1999; Dickson et al., 2006). This system is also responsible for the early repulsion of mesodermal cells from the midline. Later during muscle development, however, Slit functions as an attractive cue to guide muscles towards the proper attachment site (Kramer et al., 2001). In *slit* mutants and *robo*, *robo2* double mutants, muscles can improperly cross the midline. Loss of *slit* also results in aberrant attachment site formation within the normal muscle domain. Further, overexpression of Robo in the lateral transverse muscles, which attach to non-Slit secreting intrasegmental tendons, results in their misattachment to segment border tendons (Kramer et al., 2001). Robo also binds to Lrt, a novel leucine-rich repeat transmembrane protein expressed in tendon cells (Wayburn et al., 2009).

Muscles in *lrt* mutants occasionally formed improper muscle-tendon attachments; however, many muscles continued to extend filopodia after arriving at the tendon cell, suggesting that *Lrt* may play act as a migration stop signal.

Like Robo, Derailed (*Drl*), a receptor related to tyrosine kinases (RYK), also acts as a guidance receptor for axons and myotubes (Fradkin et al., 2010). *Drl* is expressed in lateral transverse muscles 1-3 (LT1-3) and the tendon progenitors for those muscles (Hovens et al., 1992; Stacker et al., 1993; Callahan et al., 1996). *Drl* levels increase during attachment site selection, and *Drl* is enriched at the ends of LT1-3. Mutation of *drl* results in ventral attachment defects. Importantly, however, tendon differentiation is unaffected, and the attachment defects can be rescued by expressing *Drl* in the muscle, suggesting that *Drl* is required specifically there. *Dnt*, a *Drl* ortholog, is also required for muscle attachment site selection; LTs in *dnt* mutants overshoot their normal attachments (Lahaye et al., 2012). The third ortholog, *Drl-2*, however, does not appear to be required for this process. The ligand for *Drl* during axon guidance is *Wnt5* (Fradkin et al., 2004). *Wnt5* also appears to act as a ligand for *Drl* and *Dnt* during attachment site selection in LTs 1-3 (Lahaye et al., 2012). Similar to the phenotypes observed in *drl* and *dnt* mutants, LT muscles in *wnt5* mutants bypass their normal contacts and make ectopic attachment sites. Further, *Wnt5* is expressed in tendons and LTs, but expression in either cell type is sufficient to rescue the misattachment phenotype.

A number of additional muscle-specific receptors and transmembrane proteins have been implicated in VL muscle attachment, though their ligand has

not been identified. *Drosophila* Grip (DGrip, Glutamate receptor-interacting protein), an adaptor protein containing multiple PDZ domains, interacts with the transmembrane proteins Kon-tiki (Kon, also Perdido) and Echinoid (Ed) (Figures 1.10A, 1.11) (Swan et al., 2004, 2006; Schnorrer et al., 2007; Estrada et al., 2007). DGrip, Kon and Ed are specifically expressed in the VL muscles, localize to muscle ends and mediate VL targeting to tendons. Mutation of *dgrip*, *kon* or *ed* results in VL misattachment. In addition, overexpression of DGrip in the LT muscles results in their misattachment to segment border tendons, suggesting that a DGrip ligand is present in those tendons, similarly to the Slit/Robo guidance system (Swan et al., 2004; Kramer et al., 2001).

To properly mature, tendon precursors require a signal derived from the approaching myotubes. These myotubes secrete the Egfr neuregulin-like ligand, Vein (Figures 1.10B, 1.11) (Yarnitzky et al., 1997). In embryos mutant for *vein*, tendons fail to upregulate markers of terminal differentiation, and myotubes are “blind” to the location of tendon cells. Vein becomes enriched between the myotube and a single tendon precursor (Yarnitzky et al., 1997; Nabel-Rosen et al., 1999, 2002). Vein signal is likely restricted to a single tendon progenitor by Kakapo (Kak), a large cytoplasmic cytoskeletal protein with homology to the plakin and dystrophin families (Strumpf et al., 1998; Gregory et al., 1998). Kak is expressed in tendon progenitors and is upregulated in muscle-bound tendons. In *kak* mutants, multiple tendon progenitors express markers of fully differentiated tendons (Strumpf et al., 1998). Further, Vein localization is more diffuse, suggesting that Kak may be part of a mechanism to restrict the domain of Vein to a single muscle-tendon junction.

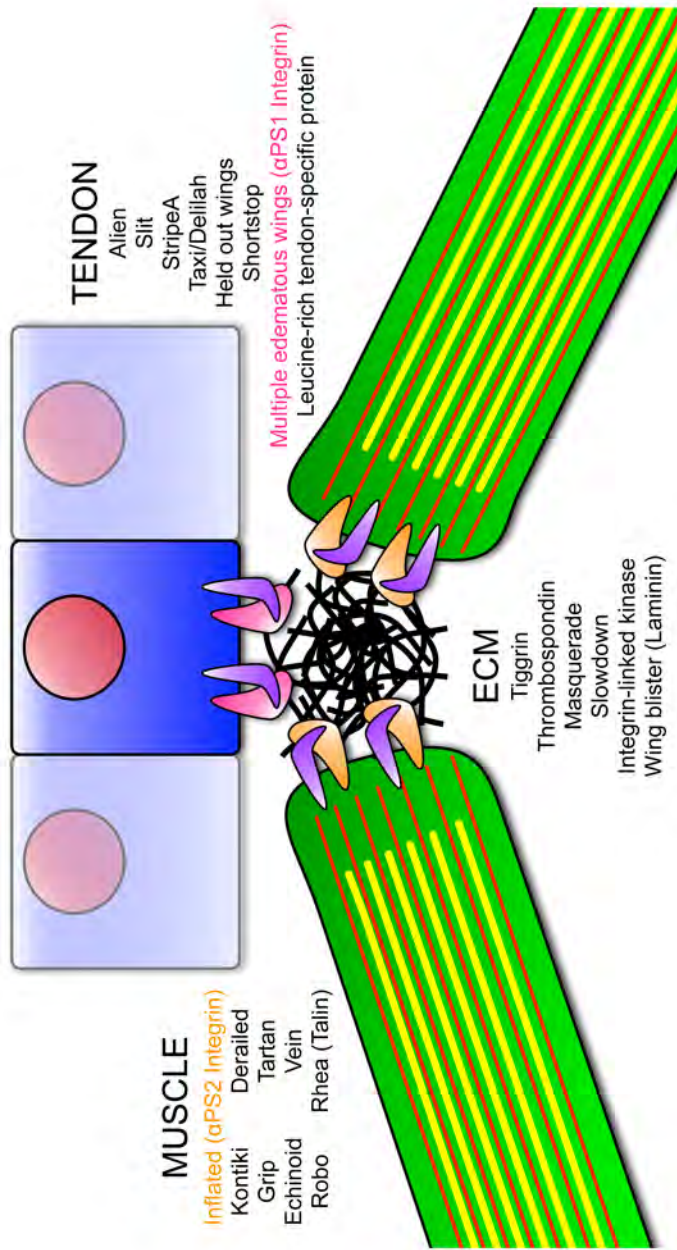


Figure 1.1).he mature myotendinous junction. A schematic of a mature muscle attachment site is shown with the muscles (green) linked to tendon cell (blue) by integrin–extracellular matrix (ECM) linkage. Tendon- and muscle-specific heterodimeric integrin complexes (purple and pink or purple and orange, respectively) connect to the ECM deposited by either the tendon or muscle cell. Tendon-specific and muscle-specific components are listed, as are components of the ECM (black). Used with permission from (Gregory et al., 1999).

The mechanism by which Kak achieves this is unclear, however, Kak is required to localize transmembrane adhesion proteins in neurons, suggesting that it is indirect (Prokop et al., 1998). Vein induces the expression of the short isoform of How, How(S), presumably via EGFR activation, in a single tendon precursor cell (now a mature tendon cell) (Figure 1.10C) (Yarnitzky et al., 1997; Nabel-Rosen et al., 1999, 2002). How(S) antagonizes How(L) to overcome its repression of Stripe and promotes the expression of StripeA, the more active isoform of *stripe* (Vолоhonsky et al., 2007). In turn, StripeA induces the expression of markers of terminal tendon cells, including *short stop (shot)*, *delilah (dei)* and $\beta 1$ -*tubulin* while the other tendon progenitor cells dedifferentiate (Figures 1.10C, 1.11) (Armand et al., 1994; Buttgereit et al., 1996; Becker et al., 1997; Strumpf et al., 1998; Subramanian et al., 2003; Volohonsky et al., 2007).

Once the muscle end approaches the correct tendon, the construction of the myotendinous junction begins. The myotendinous junction (MTJ) is a hemi-adherens junction and is critical for transmitting and countering muscle contraction (Figures 1.10C and 1.11). The MTJ is composed of interactions between integrin heterodimers expressed in muscle and tendon cells and the extracellular matrix proteins secreted by each cell (Brown et al., 2000). Tendon cells express the heterodimer α PS1 β PS (α PS1, also Multiple edematous wings [Mew]; β PS, also Myospheroid [Mys]), which interacts with laminin (Lam) secreted by the tendon (MacKrell et al., 1988; Gotwals et al., 1994; Brown et al., 2000; Bokel et al., 2002). Muscles express α PS2 β PS (α PS2, also Inflated [If]) which binds to Tsp secreted by the tendon and Tiggrin (Tig) secreted by the

muscle (Fogerty et al., 1994; Gotwals et al., 1994; Brown et al., 2000; Bokel et al., 2002; Subramanian et al., 2007; Chanana et al., 2007). Mutation of *mys*, *if* or *tsp* result in non-functional myotendinous junctions and the detachment of muscle from tendon (Newman et al., 1981; Leptin et al., 1989; Brown et al., 1994; Subramanian et al., 2007).

Tsp is secreted by the tendon prior to the arrival of the muscle to the future site of the MTJ; however, the muscle does not begin to accumulate PS2 integrin on its surface until it approaches the tendon cell, suggesting a spatial and temporal regulation of integrin-ECM interaction (Subramanian et al., 2007; Gilsohn et al., 2010). Slowdown (*Slow*), a tendon-secreted protein that accumulates at the MTJ, appears to regulate the timing of the Tsp- α PS2 β PS interaction (Gilsohn et al., 2010). In *slow* mutants, Tsp and integrins prematurely accumulate at muscle ends and tendons, and muscles rupture upon muscle contraction in the larvae. In addition, muscle ends fail to “spread” along the correct attachment site and remain narrow, likely due to the premature accumulation (and likely premature interaction) of Tsp and integrins. In support of this, *Slow* biochemically interacts with Tsp, which hinders the Tsp-integrin interaction, suggesting that *Slow* may modulate integrin responsiveness to Tsp.

Sarcomerogenesis

After myotendinous junction formation, striated muscles begin to assemble myofibrils. In *Drosophila*, this process begins at stage 17, just prior to hatching.

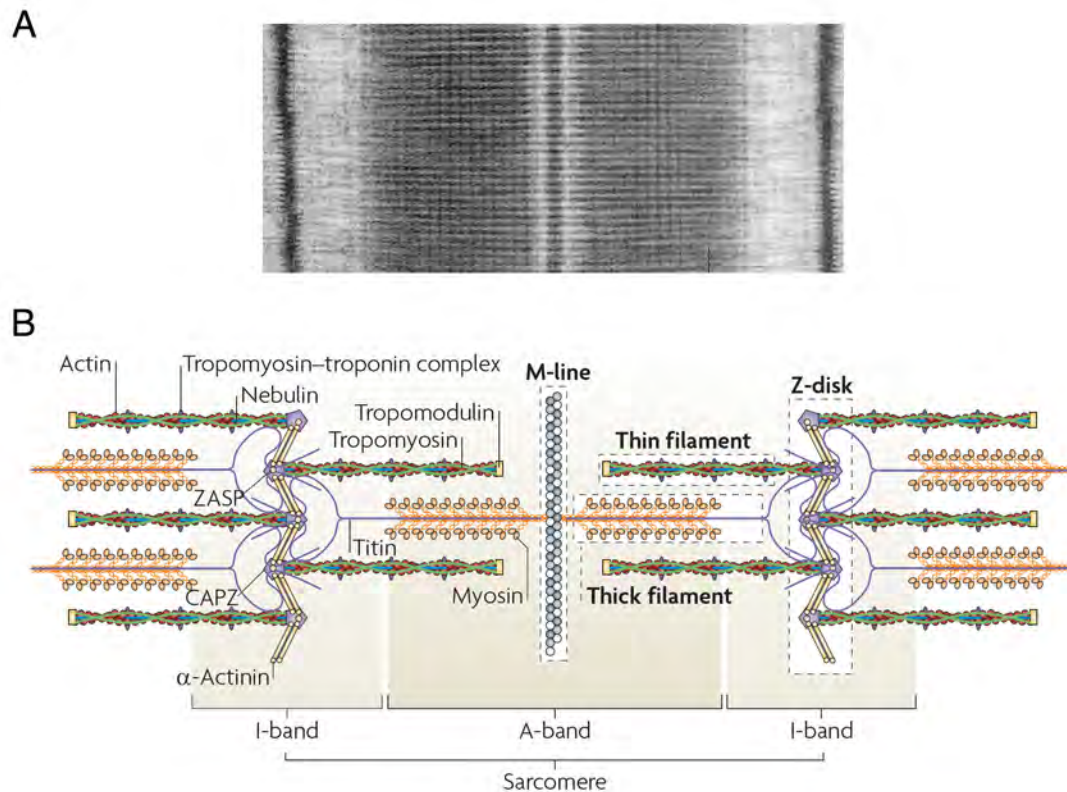


Figure 1.12. The structure of the sarcomere. (A-B) A single sarcomere, the smallest functional contractile unit of muscle, spans Z-disc to Z-disc. (A) Electron micrograph of a longitudinal section of striated muscle depicting a single sarcomere. Used with the permission of Dr. Pradeep Luther, Imperial College London (Luther et al., 2011). (B) Thin filaments, composed of F-actin and the tropomyosin-troponin complex, are cross-linked by α -actinin and anchored to the Z-disc, which forms the sarcomere boundaries. Thin filaments also contain the vertebrate-specific protein nebulin, which regulates thin filament length. Thin filaments are capped by CAPZ (barbed-end) and tropomodulin (pointed-end). ZASP, a PDZ-LIM domain protein, organizes the Z-disc. Thick filaments, composed of muscle myosin, are anchored to the M-line. A-band, area spanned by the thick filament. I-band, area spanned by thin filaments that do not overlap with thick filaments. Vertebrate Titin (depicted) extends from the M-line to Z-disc and provides elastic support. *Drosophila* Titin (D-Titin) extends from the Z-disc to the distal region of the thick filament. Reproduced with permission from (Sparrow et al., 2009).

Each muscle contains dozens of myofibrils and each myofibril consists of numerous sarcomeres (Figure 1.12A-B). Sarcomeres, the smallest functional contractile unit in striated muscle, are highly organized macromolecular complexes consisting of regular arrays of F-actin-containing thin filaments and myosin II-containing thick filaments bracketed by Z-discs, which demarcate the sarcomere boundary (Figure 1.12B) (Clark et al., 2002). The thick filaments compose the sarcomeric A-band. The region of the thin filament that does not overlap with the thick filament is termed the I-band.

Actin, the main component of the thin filament and the most abundant protein in striated muscle, is precisely regulated by template proteins, capping proteins and proteins that regulate actin polymerization to generate consistent thin filaments lengths in muscle. Due to the natural polarity of F-actin filaments, the thin filament is also polar and is capped at the barbed-end by CapZ [*Drosophila* Capping protein beta (Czb)] and at the pointed-end by tropomodulin [*Drosophila* Sanpodo (Spdo)] (Figure 1.12B). Unlike actin polymerization in other cellular contexts, sarcomeric F-actin in muscle is primarily polymerized at the pointed-end (Pollard et al., 2000; Fischer et al., 2003). (The dynamics and regulation of actin polymerization are discussed in more detail below.) Overexpression of Spdo results in the arrest of thin filament elongation in adult muscle and affects flight ability (Mardahl-Dumesnil et al., 2001). Spdo activity is likely antagonized by SALS (Sarcomere length short), a novel actin-binding protein localized to thin filament pointed-ends (Bai et al., 2007). Loss of *sals* causes thin filament shortening upon its loss and the failure of labeled actin to

incorporate into thin filaments. Further, overexpression of SALS, in contrast to Spdo, results in elongation of thin filaments.

Z-discs, the markers of sarcomere boundaries, are also the anchoring site for the plus end of sarcomere thin filaments (Figure 1.12A-B). Interestingly, precursor Z-discs called Z-bodies or I-Z-I structures are the first identifiable structures during sarcomere assembly, suggesting that they provide the initial organizational cue (Clark et al., 2002). The major Z-disc protein, α -actinin, crosslinks actin to titin, a giant cytoskeletal protein. Despite its prevalence in the Z-disc, α -actinin is not essential for sarcomerogenesis in *Drosophila* (Fyrberg et al., 1998; Dubreuil et al., 2000). Mutant larvae die soon after hatching and Z-disc organization is defective though normal striations appear initially, suggesting that α -actinin is required for stabilizing the muscle cytoskeleton upon contraction.

Proteins from the Alp/Enigma family cooperate with α -actinin in Z-disc maintenance. Vertebrate ZASP (Alp and Cypher/Z band alternatively spliced PDZ-motif protein), the best characterized member of the family, binds to and colocalizes with α -actinin at Z-discs (Xia et al., 1997; Faulkner et al., 1999; Pomies et al., 1999). *Drosophila* encodes three Alp/Enigma proteins, Zasp52, Zasp66 and Zasp67 (Jani et al., 2007; Katzemich et al., 2013). All 13 identified isoforms of Zasp52 contain a PDZ domain, Zasp-like motif and some combination of LIM domains. Live and fixed imaging of sarcomerogenesis in the embryonic body wall and adult flight muscles respectively indicates that Zasp52 assembles into Z-body-like clusters in the embryo and is one of the first repetitively-spaced Z-disc markers in the adult flight muscles, suggesting that it is

required early in sarcomere organization (Katzemich et al., 2013). Zasp52 localizes to Z-discs in all *Drosophila* muscle types where it colocalizes with α -actinin and plays a role in Z-disc assembly in the embryo (Jani et al., 2007). Though data from other groups suggest that Zasp52 may only be required for Z-disc maintenance, similarly to α -actinin, *zasp* mutant embryos have a severe phenotype, while *actn* mutant embryos appear wild-type (Rui et al., 2010; Fyrberg et al., 1998; Dubreuil et al., 2000). Further, the Z-disc localization of α -actinin is lost in *zasp* mutants, while Zasp52 properly localizes in *actn* mutants. Thus, Zasp52 is more upstream than α -actinin in Z-disc organization. Zasp66 and Zasp67, which also localize to Z-discs and contribute to Z-disc organization in the pupae and the adult, feature a similar PDZ and Zasp-like region to Zasp52, but lack LIM domains (Katzemich et al., 2013). In addition, Zasp66 physically interacts with α -actinin.

In addition to F-actin, sarcomere thin filaments also include the conserved tropomyosin-troponin complex [in *Drosophila*: Tropomyosin 1/2 (Tm1/2); Troponin I, Wings up A (WupA); Troponin T, Upheld (Up); Troponin C (multiple TpnC genes)] (Figure 1.12B). Mutations in *Drosophila Tm1* result in adult flies with abnormally shortened sarcomeres that are incapable of flight (Kreuz et al., 1996). Similarly, mutations in *wupA* or *up*, affect adult flight muscle myofibril organization, and consequently, mutant adults cannot fly (Beall et al., 1991; Nongthomba et al., 2007). The primary function of this complex is to regulate the interaction of the thin and thick filaments during contraction. Tropomyosin also

stabilizes the thin filament by slowing polymerization and depolymerization at the pointed-end (Clark et al., 2002).

Thick filaments, composed of the motor protein myosin II, are anchored and crosslinked by proteins at the M-line in the middle of the sarcomere (Figure 1.12B) (Clark et al., 2002). Interactions between the myosin II head, the catalytic domain of muscle myosin composed of the N-terminal region of muscle Myosin heavy chain (MHC) and two light chains, and F-actin in the thin filaments generate contractile force which shortens sarcomere length. ATP hydrolysis is coupled to the interaction of the head domain and actin and drives the angular rotation of the myosin head, resulting in sarcomere shortening in a process called the power stroke. ADP is released and the sarcomere returns to a relaxed state. This process likely repeats several times in a single muscle contraction. The power stroke is fine-tuned for the contractile requirements of each muscle, and in *Drosophila*, this is achieved through the generation of tissue- and stage-specific isoforms of the single *Mhc* gene (Swank et al., 2000; Clark et al., 2002).

The elasticity of the sarcomere is determined by proteins that connect the Z-disc to the thick filament (Clark et al., 2002). In *Drosophila*, the *sallimus (sls)* locus encodes a number of related splice isoforms that play this role, including D-Titin, Kettin and Zormin (Figure 1.12B) (Burkart et al., 2007). D-Titin, the largest isoform, encodes a giant cytoskeletal protein that is required for myoblast fusion and sarcomere assembly in the embryo and stretches from the Z-disc to the distal region of the thick filaments (Zhang et al., 2000; Machado et al., 2000; Burkart et al., 2007). In contrast, vertebrate Titin is larger and extends all the way

to the M-line. D-Titin encodes some, but not all of the domains found in vertebrate Titin (Machado et al., 2000). For example, the most N-terminal domains of vertebrate Titin, which localize to the Z-disc and interact with α -actinin, are present in D-Titin, as are the domains that localize to the I-band; however, the domains found in the A-band and M-line of vertebrate Titin are absent in D-Titin. Thus, all Titin proteins are able to act as sarcomeric templates and as elastic I-band elements but only vertebrate Titin is able to function as a thick filament ruler. Projectin, encoded by a separate locus, interacts with the thick filaments and localizes to the I-band or A-band in *Drosophila*, and data suggest that Projectin and D-titin (or Kettin) may interact to function as a single vertebrate Titin (Machado et al., 2000; Clark et al., 2002). Further, Titin, which is anchored to Z-discs by its binding to α -actinin, is absent in *Actn* mutants, suggesting that it is downstream of α -actinin and Zasp52 (Jani et al., 2007).

The ends of myofibrils are anchored to the exoskeleton via the same integrin and ECM interactions that form the MTJ (Figure 1.13) (Clark et al., 2002; Sparrow et al., 2009). Integrins are linked to the internal actin cytoskeleton of the muscle (i.e. sarcomere thin filaments) and are necessary for subsequent muscle differentiation after MTJ formation. Z-discs in *myospheroid* mutants fail to form *in vivo* and *in vitro*, highlighting the essential role MTJ formation plays in sarcomerogenesis (Volk et al., 1990). A number of additional proteins that link integrins to the internal actin cytoskeleton are required for muscle attachment and sarcomerogenesis. For example, Zasp52, a component

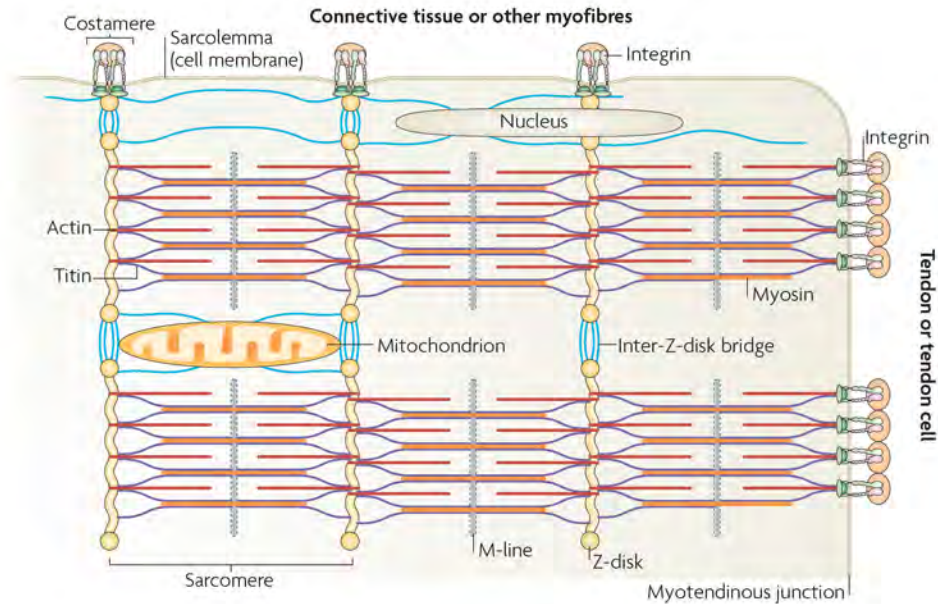


Figure 1.13. An overview of myotendinous junctions and costameres. Two myofibrils, their connections to each other and to the sarcolemma are shown. Myofibrils are aligned laterally via Z-discs and connected to each other and to costameres by cytoskeletal proteins (yellow) and intermediate filament proteins (blue). At the MTJ (right end of myofibril), integrins connect myofibrils to the tendon matrix. At the costamere, integrins connect Z-discs to the surrounding connective tissue or to other myofibrils. Figure reproduced with permission from (Sparrow et al., 2009).

of the Z-disc, acts as a cytoskeletal adaptor downstream of integrins and genetically interacts with integrins in the assembly of focal adhesions and the MTJ (Jani et al., 2007). In *zasp* mutant embryos, muscles detach even though β PS-integrin is localized to MTJs. In addition, the cytoskeletal protein Rhea (Talin) is essential for mediating integrin-based adhesion, linking ECM-bound integrins to the actin cytoskeleton and clustering integrins (Figure 1.11) (Brown et al., 2000; 2002). Integrin clustering recruits additional cytoskeletal adapter proteins necessary to form a strong link to the cytoskeleton (Brown et al., 2002). *rhea* mutant embryos exhibit muscle attachment defects similar to *mys* mutants (Newman et al., 1981; Leptin et al., 1989; Brown et al., 1994; 2002). Mutation of *Drosophila integrin-linked kinase (ilk)*, which binds to the cytoplasmic tail of integrins, causes defects that are similar to those observed when integrin adhesion is lost, including defects in muscle attachment (Figure 1.11) (Brown et al., 2000; Bokel et al., 2002; Zervas et al., 2001). However, the muscle detachment phenotype is associated with the detachment of actin filaments from muscle ends rather than muscle detachment from tendons. Interestingly, the kinase activity of ILK (Integrin-linked kinase) does not seem to be required for its function in this context and is likely a pseudo-kinase with protein adaptor functions. ILK binds PINCH (Particularly Interesting New Cysteine Histidine protein), a scaffolding protein containing five tandem LIM domains that is responsible for supporting protein complexes at sites of integrin adhesion (Rearden et al., 1994; Clark et al., 2003). Mutation of *pinch* (also known as *steamer duck*, *stck*) results in muscle misattachment and loss of actin

cytoskeletal organization within the muscle (Brown et al., 2000; Bokel et al., 2002; Clark et al., 2003). ILK localization is not affected in *pinch* mutants, indicating that although PINCH and ILK are colocalized at MTJs and bind one another, ILK localization is not dependent on PINCH and the *pinch* mutant phenotype is not a result of ILK mislocalization. Further, PINCH and Rhea depend on the presence of integrins for their accumulation at MTJs, while ILK depends on integrin presence to a lesser degree (Zervas et al., 2001; Brown et al., 2002; Clark et al., 2003). Thus, integrins are the most upstream organizer of MTJs and muscle cytoarchitecture and link the formation of a stable MTJ to subsequent muscle differentiation.

Myofibrils are also connected laterally to the ECM by costameres, sites of protein complex formation that link muscle Z-discs to the ECM (Figure 1.13) (Danowski et al., 1992). Like the MTJ, costameres transmit contractile force (from the Z-line to the basement membrane and then to the myofibril ends) and serve as organizational centers for the cytoskeleton. Three cytoskeletal networks act together to maintain the structural integrity of the membrane during contraction and to promote the stable linkage of the myofibril to the muscle membrane: integrins/focal adhesion complexes, the dystroglycan complex and the spectrin-based cytoskeleton. Thus, integrins also accumulate at costameres in *Drosophila* (Figure 1.13) (Volk et al., 1990). This localization is secondary to the appearance of integrin at the MTJ, indicating that muscles do not begin to organize their costameres until after a stable MTJ has formed.

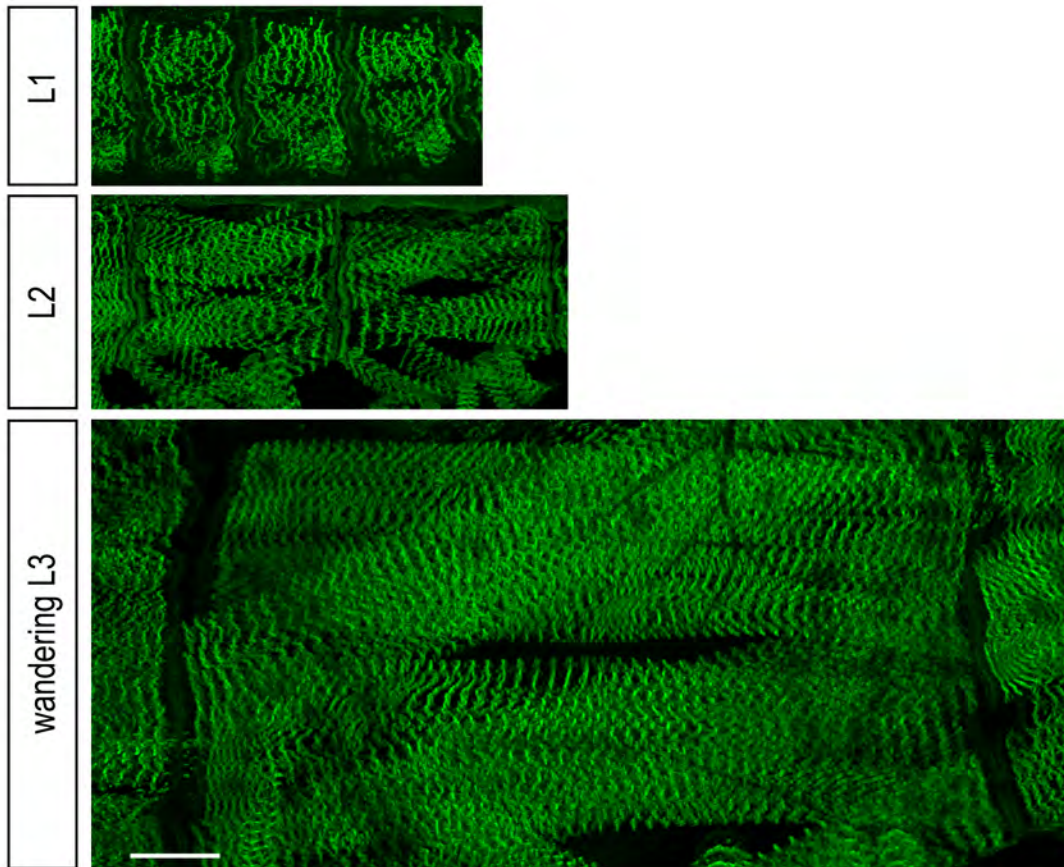


Figure 1.14. Change in muscle size during *Drosophila* larval development. The dorsal muscles in *GFP::Zasp66* larvae at the indicated stages. *GFP::Zasp66* labels the Z-discs of the sarcomere. Three hemisegments are depicted at the first-instar (L1) stage; two hemisegments are depicted at the second-instar (L2) stage and a single hemisegment is shown at the end of third-instar (wandering L3) stage. In addition to overall muscle growth, the number of Z-discs increases. Bar, 50 μm .

Larval muscle growth

At the end of embryogenesis (22-24 hours AEL at 25°C), embryos hatch from the egg shell as larvae (Figure 1.1). Larval development comprises five days and transitions through three progressively larger larval instar stages: first instar (L1), second instar (L2) and third instar (L3). The three larval instars can be distinguished by two characteristics: spiracles, external tracheal openings that allow for gas exchange, and mouthparts (Bodenstein et al., 1950). First instar larvae lack prominent anterior spiracles. The anterior spiracles are closed in second instar larvae, and in third instar larvae, they are fully developed and contain protruding finger-like processes. Posterior spiracles are present and apparent at all larval instars. In addition, mouthparts from larvae of each stage contain a typical number of mouth hooks. First instar larvae usually have one tooth, second instar larvae have two to three teeth and third instar larvae have nine to twelve teeth.

Larvae eat 3-5 times their weight during development (Chiang and Hodson, 1950). Unsurprisingly, this period is characterized by dramatic growth of the whole animal as well as proportional growth of the muscles (Figure 1.14). During larval development, the surface area of the muscle increases 100-fold (Johansen et al., 1989). The number of sarcomeres per muscle also increases, while the length of the unit sarcomere remains relatively constant, suggesting that additional sarcomeres are added to growing muscles (Haas et al., 1950). Indeed, analysis of sarcomere organization and number from the stage 17

embryo until wandering L3 larvae indicates that sarcomere number increases throughout development (Haas et al., 1950; this study}. Muscle growth at this stage is not due to additional fusion during larval development, but to an increase in nuclear size as a result of endoreplication during this period (Demontis et al., 2009; Haas et al., 1950). Endoreplication is necessary but not sufficient for larval muscle growth, and this process is regulated by Insulin-like receptor/Target of Rapamycin (InR/Tor) signaling and Forkhead box O (FoxO) and dMyc activity (Demontis et al., 2009).

Metamorphosis and adult myogenesis

After reaching a critical mass, wandering third instar larvae cease crawling and begin to form a puparium in a process known as pupariation (Figure 1.1) (Robertson et al., 1936). Pupariation includes shortening of the larval body, eversion of the anterior spiracles and tanning of the larval cuticle. Shortening of the larval body requires the contraction of the body wall muscle (Fraenkel et al., 1940). Thus, defects in abdominal muscle contraction at the onset of pupariation, caused by mutation of *D-titin* or other components of the sarcomere, result in aberrantly long, thin puparia (Ball et al., 1985; Clark et al., 2007; LaBeau-DiMenna et al., 2012).

The onset of larval-pupal apolysis (separation of the cuticle from the epidermis) [4-6 hours APF (after puparium formation)] is characterized by the appearance of a gas bubble in abdomen. The gas bubble is subsequently

dispersed posteriorly (moving the pupa anteriorly), then anteriorly (which places pupa in the posterior of pupal case). Gas bubble translocation requires coordinated abdominal muscle contractions. Head eversion (12 hrs APF) is also driven by the increase in hydrostatic pressure due to the orchestrated contractions of the abdominal muscles and the pharyngeal dilator muscles (Robertson et al., 1936; Fristrom et al., 1965). In addition to affecting puparium size, mutation of sarcomeric proteins also causes defects in gas bubble translocation and head eversion (Clark et al., 2007). In Chapter 2, we will present data demonstrating that muscle-specific depletion of *twinstar*, the *Drosophila* homolog of cofilin, results in defects in larval contraction at pupariation and gas bubble translocation and head eversion during metamorphosis.

During metamorphosis, which comprises four days, the majority of larval tissues, including muscle, are histolyzed and replaced with newly formed tissues from cells set aside during embryonic development (Robertson et al., 1936; Crossley et al., 1978). Adult muscles are formed from the adult precursor cells (APs) that were generated during the specification of embryonic FCs earlier in development. Adult muscles, like embryonic muscles, are syncytial and are formed from the fusion of mononucleated myoblasts. Though adult muscles also undergo fusion, the proteins and cellular behaviors that underlie this process are less well understood compared to those that regulate fusion during embryonic myogenesis. This is due, in part, to functional requirements earlier in development. However, many of the same regulators have been implicated in adult myoblast fusion, including WASp, SCAR/WAVE, D-WIP, Kette and Arp2/3.

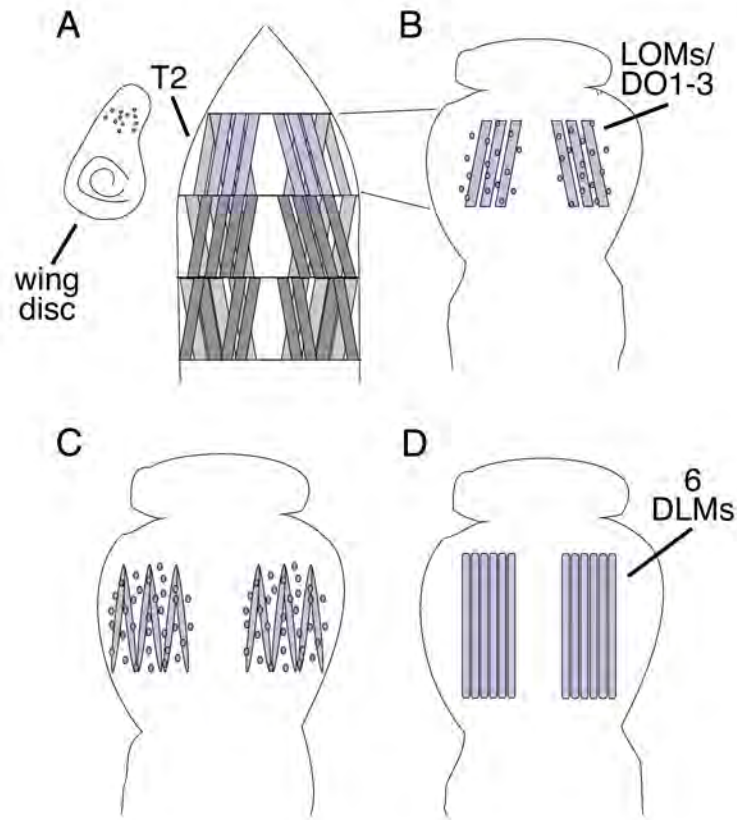


Figure 1.15. The *Drosophila* adult dorsal longitudinal muscles are formed from persistent larval scaffolds. (A) Three muscles (blue) in the second thoracic hemisegment (T2) persist into metamorphosis and serve as scaffolds for the development of the dorsal longitudinal muscles (DLMs). Myoblasts are associated with the wing imaginal disc. (0 hrs after puparium formation, APF) (B) A wave of histolysis destroys the other larval muscles early in pupal development. The persistent muscles are surrounded by myoblasts (6-8 hrs APF). (C) The myoblasts begin to fuse and the larval muscles split to give rise to the six DLM fibers (14-18 hrs APF). (D) The six DLMs grow to fill the thoracic space and are one-third their adult size at 36 hrs APF. Adapted with permission from (Fernandes et al., 1996).

Further, transient F-actin structures reminiscent of the F-actin focus described in embryonic muscle development have been observed, suggesting that embryonic and adult myoblast fusion employ a conserved set of proteins and cellular processes (Mukherjee et al., 2011).

The largest group of adult thoracic muscles are the indirect flight muscles (IFMs). In all, there are 26 IFMs: seven pairs of dorsal-ventral muscles (DVMs), which are responsible for wing elevation, and six pairs of dorsal longitudinal muscles (DLMs), which antagonize the action of DVMs by depressing wings (Crossley et al., 1978). IFMs form a group of muscles distinct from all other muscles. In contrast to other thoracic muscles, like the tergal depressor of the trochanter (TDT, or “jump muscle”), IFMs are fibrillar, express a unique set of muscle proteins and are asynchronous (Tiegs et al., 1955; Ikeda et al., 1981). Despite these shared properties that set them apart from other thoracic muscles, DVMs and DLMs follow different developmental programs: DVMs develop *de novo*, as is the case for the majority of muscle groups, including the TDT. DLMs, however, develop from three pairs of larval muscles in the second thoracic hemisegment (T2) (Figure 1.15A). In T2, histolysis is completed 8 hours APF and the remaining larval muscles, known as the larval oblique muscles (LOMs, also dorsal oblique muscles [DO1-3]), are used as templates on which the adult dorsal longitudinal muscles are assembled (Figure 1.15B) (Robertson et al., 1936; Crossley et al., 1978; Fernandes et al., 1991). Importantly, the pharyngeal dilator muscles, which are required for head eversion, are also not histolyzed, suggesting that such residual muscles are crucial for early events of metamorphosis.

The LOMs are surrounded by myoblasts (6-8 hours APF) and begin to dedifferentiate (10-12 hours APF), which includes the disassembly of myofibrils, appearance of vacuoles and the loss of birefringence, before elongating along the length of the thorax (12 hours APF) (Figure 1.17B) (Robertson et al., 1936; Fernandes et al., 1991) As fusion proceeds (14-16 hours APF), these muscles begin to split longitudinally to give rise to the six bilaterally symmetric DLM fibers in the final adult muscle pattern (Figure 1.15C-D). Fusion is completed a few hours later (28 hours APF) and the fibers continue to grow to fill the thoracic space. At 36 hours APF, DLMs are only one-third their adult size.

When larval scaffolds are lost or ablated, myoblasts are able to fuse *de novo* to form DLMs, similarly to the formation of DVMs, indicating that larval scaffolds are dispensable for DLM formation (Farrell et al., 1996; Fernandes et al., 1996). In the absence of larval scaffolds, however, the number of DLM fibers can vary from 2-12, suggesting that the function of the larval scaffold is to properly partition the forming adult muscles into the proper number of DLMs. In contrast, variability in DVM number is common, suggesting that their absolute number is less important for their function (de la Pompa et al., 1989). In Chapter 3, we will present data showing that overall DLM organization is occasionally perturbed in *coro* mutant adults.

Mesoderm and Muscle Development in Mammals

As in *Drosophila*, skeletal muscle in mammals (the equivalent of body wall muscle in *Drosophila*) is composed of multinucleate cells that develop from the fusion of mononucleate myoblasts to form a syncytial cell. Each muscle also adapts a shape specific to its function. Despite the similarities underlying the fusion process between them, the molecular steps leading to the generation of differentiated, mononucleated myoblasts are somewhat different in mammals compared to *Drosophila*. For example, *Drosophila* Twist is necessary for gastrulation and the formation of mesoderm and muscle, while mouse embryos correctly specify mesoderm in the absence of Twist (Chen et al., 1995; Baylies et al., 1996). In addition, mouse Twist is not expressed in the myotome and may actually function to repress premature myogenesis (Castanon et al., 2002).

Vertebrate systems also have additional layers of complexity factored in by evolution: notably, the duration of fusion during embryonic development, which is measured in days for the mouse and not hours as in *Drosophila*, gene duplications, and the sheer numbers of fusion events that can number in the thousands in a mouse or human fiber. Further, mammalian skeletal muscle is comprised of bundles of muscle fibers, increasing the difficulty of studying this process in mammals *in vivo* (Figure 1.16).

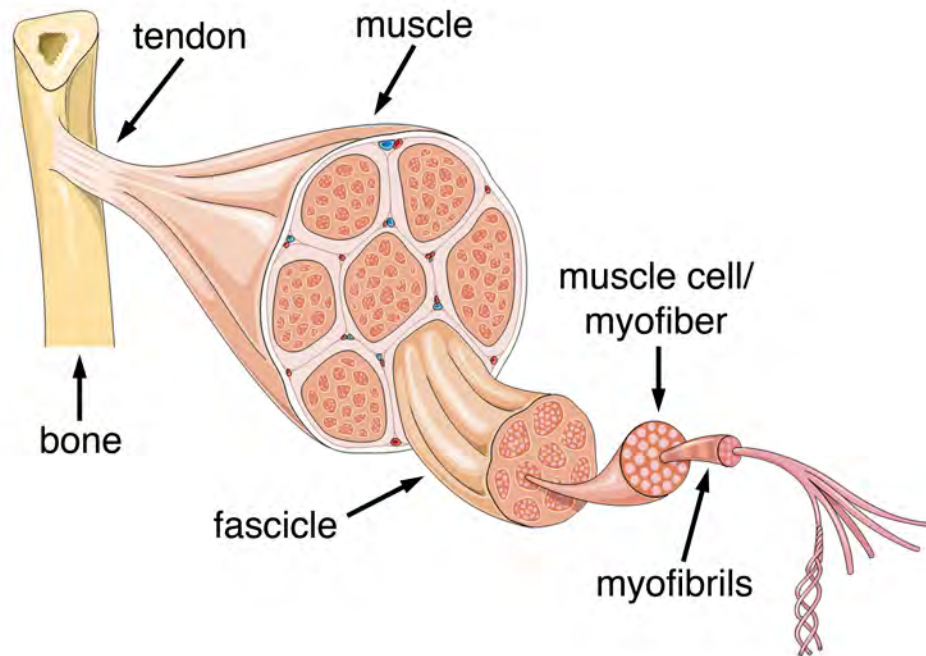
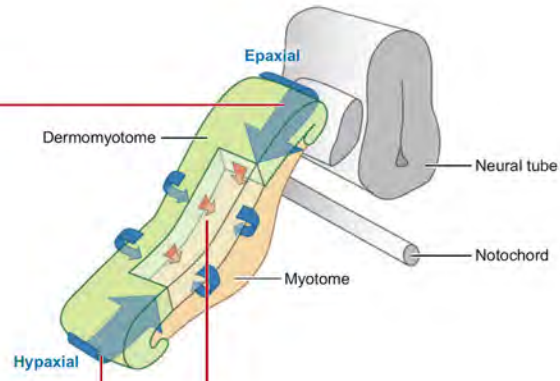


Figure 1.16. Vertebrate muscle is composed of bundles of myofibrils. Skeletal muscle in vertebrates is anchored to bones via tendons. Each muscle, sheathed by a layer of connective tissue (not indicated), contains multiple bundles of fascicles. Each fascicle contains many (100s or more) muscle cells, which are also called myofibers. Finally, each myofiber contains bundles of myofibrils, which are organized into sarcomeres. Further detail of the myofibril and sarcomere organization is shown in Figure 1.14. Image reproduced with permission from Servier Medical Art.

Myoblast specification

In mammalian embryos, skeletal muscle arises from mesodermal precursor cells (MPCs) from within the somites. Somites are transient, segmented blocks of paraxial mesoderm that develop in pairs flanking the neural tube during embryogenesis. The somite is patterned into dorsal (dermomyotome) and ventral (sclerotome) regions by instructional signals from the surrounding notochord, neural tube, and dorsal ectoderm, including Wnts, BMPs and Shh (Figure 1.17A). The dermomyotome is further regionalized into the dermatome and myotome, which gives rise to the dermis and muscle, respectively, while the ventral sclerotome will give rise to axial skeleton and ribs (Tajbakhsh et al., 1997). The transcription factor paired-box 3 (Pax3) is expressed in the paraxial mesoderm and marks the early embryonic myogenic precursors (Williams et al., 1994; Tajbakhsh et al., 2000). Pax3 is required for the formation of the trunk hypaxial muscles and for the delamination and migration of myogenic progenitors to sites of myogenesis such as the limb. *Pax3* null mice (*Spotch* mice) completely lack limb muscle; myogenic progenitor cells fail to delaminate from the dermomyotome and migrate to sites of limb myogenesis (Figure 1.17B) (Borycki et al., 1999). The Pax3 paralogue, Pax7, plays a partially overlapping role in myogenic specification and can substitute for Pax3 in the primary myotome (trunk), but cannot rescue the delamination and migration activities of Pax3 to form limb muscles (Bober et al., 1994; Relaix et al., 2004).

A



B

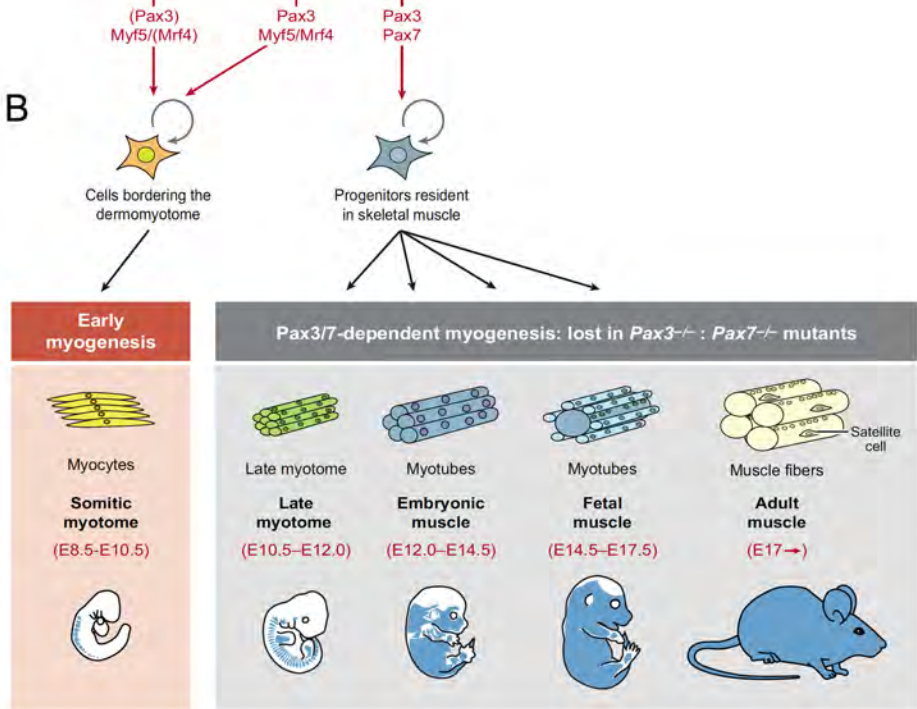


Figure 1.17. Overview of Pax3/7 function during mammalian skeletal muscle formation. (A) The epithelial dermomyotome (single somite, green) and the underlying myotome (beige) are formed by the delamination of cells from the dermomyotome (blue arrows). Pax3, Myf5 and Mrf4 (red) regulate these events. As the dermomyotome loses its epithelial structure, additional myogenic progenitors enter the myotome (red arrows). Pax3/7 (red) regulate these events. The location of the notochord and neural tube, which pattern the somite, are also shown. (B) Schematic of the myogenic cells, their muscle derivatives and timing of Pax3-independent and -dependent myogenesis. Blue shading indicates location of muscles affected. E, embryonic day. Used with permission from (Buckingham et al., 2007).

Pax3 and Pax7 operate in an intricate transcriptional regulatory network with the basic helix-loop-helix transcription factors myogenic factor 5 (Myf5) and myoblast determining protein (MyoD), two myogenic regulatory factors (MRFs) required for the determination of myogenic precursors (Pownell et al., 2002; Buckingham et al., 2007). In *Myf5/Myod* double mutants, skeletal muscle fails to form because muscle precursors are absent, and the cells, which would normally become myoblasts, adopt other mesodermal cell fates (Rudnicki et al., 1993; Tajbakhsh et al., 1996). Two additional MRFs act downstream of Myf5 and MyoD: Myf4 (myogenic factor 4) and myogenin. Unlike Myf5 and MyoD, which are required for the early determination of myogenic fate, Myf4 and myogenin are required for terminal differentiation of myoblasts into myocytes and myofibers. Muscle groups in myogenin-knockout mice lack myofibers and are instead composed of undifferentiated myoblasts (Hasty et al., 1993; Nabeshima et al., 1993).

Myoblast fusion and myotube formation

Once they have exited the cell cycle and begin to express the cadre of muscle-specific transcription factors, myoblasts can then fuse with one another to generate syncytial myofibers. Unlike in *Drosophila*, work to date has not yet supported the existence of distinct FC- and FCM-like cell populations in vertebrate models. Owing to the complexities of muscle development in mammals, relatively few studies exploring myoblast fusion have been carried out in *in vivo* mammalian systems.

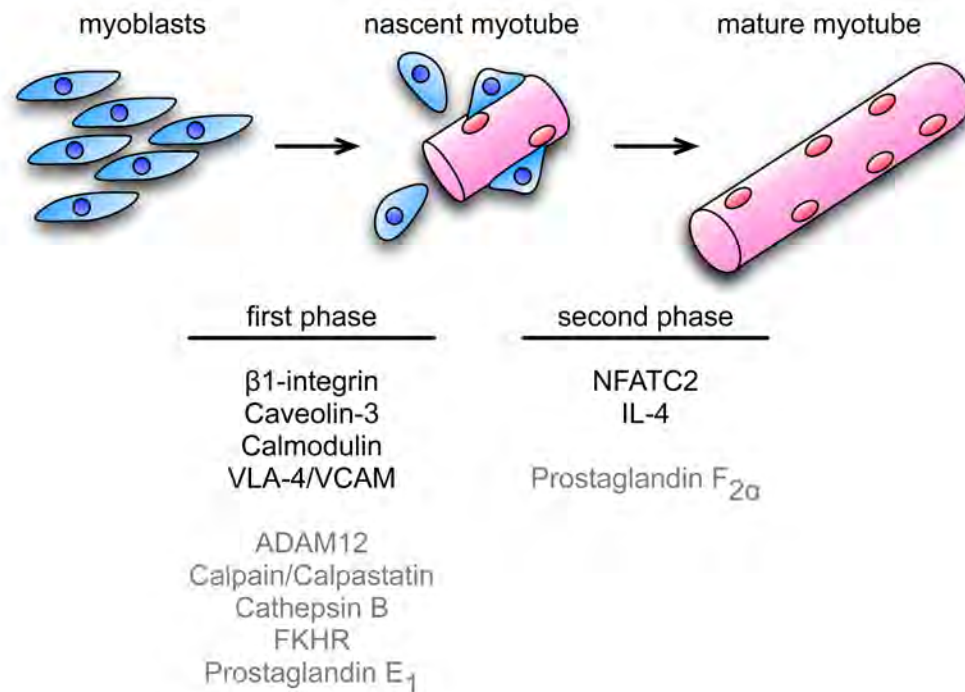


Figure 1.18. Two phases of mammalian myoblast fusion. During embryonic and adult myoblast fusion in the mouse, differentiated myoblasts (left) elongate and fuse with one another, giving rise to nascent, bi-nucleate myotubes (middle). Subsequent fusion of additional myoblasts with nascent myotube gives rise to the mature myotube (right). A number of molecules have been identified that are required for one phase and not the other phase of fusion. Molecules in black are discussed further in the text. Molecules in grey are excluded in the text but are included here for completeness and are further discussed in (Horsley et al., 2004).

Tissue culture systems have dramatically simplified this analysis. The basic events surrounding vertebrate myoblast fusion have been described using a variety of experimental approaches and have given us a general framework of the processes required for fusion. Existing data suggest that the basic cellular events underlying myoblast fusion in *Drosophila*, namely migration, recognition and adhesion and membrane fusion, are conserved in vertebrates (Figure 1.5) (Knudsen et al., 1977; Doberstein et al., 1997; Wakelam et al., 2005).

In mammalian myoblast fusion there are two phases of fusion (Figure 1.18) (Horsley et al., 2004). In the first stage, individual myoblasts undergo fusion with one another to generate nascent myotubes, which contain few nuclei. The second phase of fusion is characterized by further maturation of the nascent myofiber during which the myofiber increases in size and begins to express contractile proteins. This increase in size is a direct result of the incorporation of additional differentiated myoblasts into the nascent myotube. Although these phases appear similar, different molecules have been shown to regulate the two phases of fusion (Figure 1.18) (Horsley et al., 2004). For example, the membrane proteins β 1-integrin, VLA-4, VCAM and caveolin-3 have been shown to play roles in the fusion of myoblasts with one another, whereas the NFATC2 pathway, activated by calcium and calmodulin, and IL-4, a secreted cytokine, are critical for the fusion of myoblasts with nascent myotubes (Rosen et al., 1992; Galbiati et al., 1999; Horsley et al., 2001; 2004; Schwander et al., 2003).

Recognition and adhesion of myoblasts

In *Drosophila*, two distinct types of myoblasts, FCs and FCMs, must recognize one another and do so by expressing differential transmembrane proteins on their surfaces; Duf/Kirre and Rst are expressed on the surface of FCs, while Sns and Hbs are FCM-specific transmembrane proteins (Ruiz-Gomez et al., 2000; Bour et al., 2000; Strunkelnberg et al., 2001; Artero et al., 2001; Dworak et al., 2001; Galletta et al., 2004; Shelton et al., 2009). The mouse genome encodes orthologous proteins for Duf/Kirre/Rst and Sns/Hbs (Sellin et al., 2002; Sun et al., 2003; Ueno et al., 2003). Murine Kirrel (Duf/Kirre/Rst orthologs) and Nephrin (Sns/Hbs orthologs) proteins are well-characterized components of the slit-diaphragm, a specialized cell-cell adhesion complex that makes up the filtration barrier of the kidney (Patari-Sampo et al., 2006; Sun et al., 2003; Tryggvason et al., 2001). Nephrin (Nphs1) is expressed in developing mouse skeletal muscle and human fetal muscle cells undergoing fusion and is upregulated in two murine models of human muscular dystrophies (Table 1.1, Figure 1.19) (Sohn et al., 2009). Primary myoblasts isolated from Nphs1 null mice fail to fuse *in vitro*, suggesting that Nephrin plays a conserved role in vertebrate skeletal muscle fusion. Interestingly, cell-mixing experiments demonstrated an asymmetrical requirement for Nephrin during fusion. Nphs1 is required in myoblasts but not in myotubes. Thus, Nephrin may play a role that is analogous to that of *Drosophila* Sns, which is expressed on the surface of FCMs exclusively and suggests the

presence of FC- and FCM-like myoblast populations in vertebrate myoblast fusion (Bour et al., 2000; Sohn et al., 2009).

The protein/s with which mammalian Nphs1 interacts during fusion have not been identified. In the slit-diaphragm, Nephrin has been shown to interact with itself as well as with Kirrel1 and Kirrel2 (NEPH1/2; orthologs of *Drosophila* Duf/Kirre) (Barletta et al., 2003; Patari-Sampo et al., 2006; Gerke et al., 2003; Khoshnoodi et al., 2003). Whether the Duf orthologs play any role in myoblast fusion has not been examined; however, Kirrel1 deficient mice do not display a muscle phenotype, suggesting that if they play a role in muscle development, Kirrel1 and Kirrel2 may have redundant functions in myoblast recognition (Donoviel et al., 2001).

Additionally, various transmembrane proteins, such as the mannose receptor, CDO and BOC have been shown to regulate fusion in the mouse (Figure 1.19) (Jansen et al., 2006; Kang et al., 2004; Wegorzewska et al., 2003; Cole et al., 2004). Early *in vitro* work has indicated that the cadherins mediate the recognition and adhesion process in the mouse (Donalies et al., 1991; George-Weinstein et al., 1997); however, additional genes must be involved as M- and N-cadherin are not essential *in vivo* (Radice et al., 1997; Hollnagel et al., 2002). Other data has pointed to a contributing role for integrin family members and other transmembrane proteins in myoblast adhesion and alignment (Griffin et al., 2009; Horsley et al., 2004; Rosen et al., 1992; Schwander et al., 2003; Galbiati et al., 1999). Taken together, the existing data suggest that one protein family is not solely responsible for the recognition and adhesion of mouse myoblasts to one another, perhaps reflecting the additional complexities that underlie myoblast fusion in the mouse.

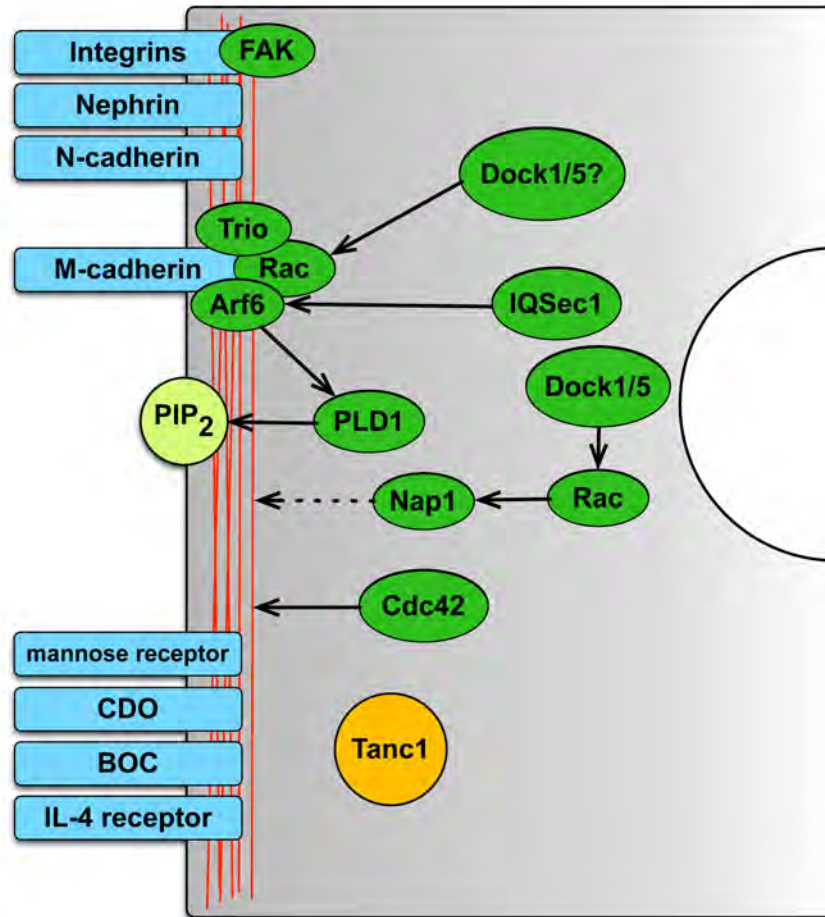


Figure 1.19. Overview of proteins required for mammalian myoblast fusion. The indicated proteins and pathways correspond to those that are included in the text. Transmembrane receptors that play a role in recognition and adhesion are blue. Proteins that regulate the actin cytoskeleton are green. Adaptor proteins that link the transmembrane receptors to the actin regulators are orange. Nuclei, white. Myoblast/tube, light grey. Actin wall, red filaments.

Adaptor proteins

The activity of the *Drosophila* downstream adaptor protein, Rols, is conserved in mammals (Table 1.1, Figure 1.19) (Avirneni-Vadlamudi et al., 2012). Mammals encode two Rols homologs: Tanc1 and Tanc2 (Chen et al., 2001; Han et al., 2010). *Tanc1* and *Tanc2* are expressed in numerous tissues, including the brain (Chen et al., 2001; Han et al., 2010; Suzuki et al., 2005). Only *Tanc1* is expressed in somites during myoblast fusion, suggesting that it is the functional ortholog of Rols (Chen et al., 2001). Knockdown of *Tanc1* in myoblasts results in a block in myoblast fusion *in vitro*. Furthermore, overexpression of Tanc1 also causes a fusion defect, suggesting that the levels or activity of Tanc1 are critical for proper fusion (Avirneni-Vadlamudi et al., 2012). Surprisingly, however, *Tanc1* knockout mice are viable and show no defects in growth or body size, hallmarks of defects in myogenesis, whereas *Tanc2* knockout mice die *in utero*, indicating that Tanc2 is necessary for embryonic development (Han et al., 2010). The role of Tanc2 in muscle development has not been tested and, despite the absence of its expression in somites, may play a redundant role with Tanc1.

Actin regulation during mammalian myoblast fusion

The connection between adhesion molecules on the surface of myoblasts and the downstream pathways that result in fusion are less clear in mammals than in

Drosophila. However, as in *Drosophila*, genetic and cell biological evidence in mammals points to the careful orchestration of the actin cytoskeleton and its many regulators in the cellular activities that underpin successful myoblast fusion (Massarwa et al., 2007; Kesper et al., 2007; Berger et al., 2008; Richardson et al., 2007; Schafer et al., 2007; Horsley et al., 2003; Jansen et al., 2006; Bondesen et al., 2007). For example, during differentiation, myoblasts undergo shape changes where they remodel from a nonpolarized, fibroblast-like morphology to an elongated conformation that is spindle-like in shape (Ohtake et al., 2006; Nowak et al., 2009). Differentiating myoblasts also form lamellipodia and filopodia, both of which are well described actin-based behaviors before and during their migration, another actin-based behavior (Nowak et al., 2009; Kawamura et al., 2004; Steffen et al., 2004; 2006; Ohtake et al., 2006). Treatment of differentiating mammalian myoblasts with Latrunculin A or Cytochalasin D, which interfere with F-actin remodeling by binding to actin monomers or actin branches, respectively, adversely affected myoblast migration and fusion consistent with a requirement of the actin cytoskeleton in the migration of myoblasts (Sanger et al., 1972; Constantin et al., 1995; Coue et al., 2001; Dhawan et al., 2004; Nowak et al., 2009). These migrations are thought to promote critical contacts between myoblasts and myotubes necessary for differentiation and fusion (Krauss et al., 2005).

During fusion, mammalian myoblasts elongate and align their membranes and a dense actin structure, termed the actin wall, develops (Figure 1.19) (Duan et al., 2009). Prevalence of this structure decreases over additional days of

culture in conditions that promote myoblast fusion *in vitro*, suggesting that the actin wall is transient. Like the *Drosophila* actin focus, the actin wall is asymmetric and appears only in one fusing partner. TEM further indicated that gaps appear in the actin wall and membrane-bound vesicles fill these gaps. Live imaging analysis of this process has not been achieved in mammalian myoblast fusion, leaving open the possibility that the mammalian actin wall and the *Drosophila* actin focus do not represent equivalent structures during fusion.

Though the actin focus or an actin focus-like structure has not been definitely identified in mammals, many of the proteins that regulate the actin focus play a conserved role in mammalian myoblast fusion. For example, the small GTPase Rac is required for fusion in *Drosophila* and mammals (Table 1.1, Figure 1.19) (Vasyutina et al., 2009; Richardson et al., 2007; Hakeda-Suzuki et al., 2002; Luo et al., 1994). A requirement for Rac in the fusion paradigm of mammals had not been experimentally demonstrated until recently. One reason for this is the complication of *in vivo* analysis in the mouse as a result of the importance of the small GTPase for early developmental events: *rac1* deficient mouse embryos die before E9.5, precluding analysis of myoblast fusion (Sugihara et al., 1998). As a result, an early study of Rac function in mammalian myoblast fusion, which concluded that Rac was required for fusion, was in an *in vitro* culture model and utilized a Rac-specific inhibitor rather than genetic perturbations (Charrasse et al., 2007). Recently, however, the analysis of conditional Rac1 knockout in migrating hypaxial muscle precursors revealed short, thin myofibers in the limbs, indicative of a fusion impairment *in vivo* and

established the conservation of Rac to the mammalian fusion process (Vasyutina et al., 2009). Interestingly, genetic ablation of Rac1 alone was sufficient to reveal a fusion defect in mice, whereas mutation of both *drac1* and *drac2* are required to obtain a fusion defect in *Drosophila* (Hakeda-Suzuki et al., 2002; Srinivas et al., 2007; Vasyutina et al., 2009). Primary myoblasts isolated from Rac1 conditional knockout mice were able to appropriately recruit early markers of adherence, α - and β -catenin, while the accumulation of polymerized actin, vinculin and Arp2/3 at the site of myoblast-myoblast adhesion was reduced (Vasyutina et al., 2009). This is unsurprising given the role of Rac in activating Arp2/3 to drive actin polymerization. However, this is in contrast to the accumulation and perdurance of F-actin foci in *Drosophila* Rac triple mutants (Richardson et al., 2007). Whether this difference indicates different roles for the Rac proteins in *Drosophila* versus mouse or is reflective of the fact that a site of fusion/actin focus has not yet been identified in mouse needs to be assessed further.

In *Drosophila*, Rac triple mutant FCMs remain rounded, which suggested that these myoblasts fail to migrate (Richardson et al., 2007; Hakeda-Suzuki et al., 2002; Gildor et al., 2009). Interestingly, the activity of Rac1 in the mouse does not appear to be required for the migration of one population of muscle precursors to the limb bud (Vasyutina et al., 2009). Similarly, Cdc42 does not appear to be required for the first phase of migration *in vivo*. Their requirement has not been tested in the second phase of fusion, leaving open the possibility that other proteins are required for the first migratory period. Additionally, the Rho

GTPases may be able to compensate for the loss of the other, explaining why precursors are able to migrate in single mutants.

The mouse homologs of Mbc, Dock1 and Dock5, also play a conserved role in myoblast fusion *in vitro* and *in vivo* (Table 1.1, Figure 1.19) (Pajcini et al., 2008; Laurin et al., 2008). Dock1 is essential for development. *Dock1* null embryos presented with hallmarks of defective primary myogenesis, showing a dramatic and general reduction in muscle content as a result of impaired myoblast fusion *in vivo* (Laurin et al., 2008). In contrast, Dock5 plays a nonessential role during embryogenesis though there appears to be a partially redundant role for Dock5 in myoblast fusion *in vivo*. This differs when compared to the requirement for Dock1 and Dock5 in myoblast fusion in zebrafish where both proteins are required equally for the fusion process (Moore et al., 2007). Furthermore, Dock1 colocalized with an indirect fluorescent reporter of the actin cytoskeleton at sites of myoblast-myoblast contact in C2C12 myoblasts (Nowak et al., 2009). Whether these sites of colocalization are analogous to the actin foci in *Drosophila* requires further study. Taken together, these data demonstrate that Dock1, a component of the fusion machinery discovered in *Drosophila*, has a conserved role in mammals (Pajcini et al., 2008; Laurin et al., 2008). In Chapter 4, we also demonstrate that Dock1 has a conserved role in mammalian myoblast fusion *in vitro*. In addition, we present data showing that Dock1 is not required for early steps in myoblast fusion, including differentiation and migration.

The role of the mammalian homolog of Loner, IQSec1 (Brag2/GEP₁₀₀) in muscle fusion is also conserved in mammals (Table 1.1, Figure 1.19) (Pajcini et

al., 2008). IQSec1 knockdown myoblasts exhibited a severe fusion defect *in vitro*. Data suggests that IQSec1 can act as a GEF for Arf6 *in vitro*. Consistent with the known roles of Arf6 in intracellular trafficking, paxillin, a component of focal adhesions, is improperly localized in IQSec1-knockdown myoblasts. Interestingly, the morphology of IQSec1-depleted myoblasts was distinct from that of the Dock1 knockdown myoblasts, supporting data from *Drosophila* that suggests Loner and Mbc have independent roles in myoblast fusion (Richardson et al., 2007; Pajcini et al., 2008). In Chapter 5, we present data that suggest that IQSec1 is not required for myoblast differentiation or migration and that IQSec1 plays a conserved role in myoblast fusion.

Unlike in *Drosophila*, where Arf6 was not required for myoblast fusion, knockdown of Arf6 impaired mammalian myoblast fusion *in vitro* (Table 1.1, Figure 1.19) (Bach et al., 2010). Further, Arf6 is activated during myoblast fusion *in vitro* and during muscle regeneration *in vivo*, suggesting that Arf6 activity is essential for muscle development and repair. During fusion *in vitro*, Arf6 physically interacted with M-cadherin, Trio, a Rac GEF required for fusion in the mouse *in vivo*, and Rac1 (O'Brien et al., 2000; Bach et al., 2010). This complex is localized to the site of myoblast-myoblast contact where it is suggested to act during fusion. The role of Arf6 in this complex is unclear as it does not appear to be required for Rac1 activation. In addition, Arf6 is known to regulate membrane traffic through its activation of phospholipase D (PLD) and phosphatidylinositol 4-phosphate 5-kinase (PIP5K) (Brown et al., 2001; D' Souza-Schorey et al., 2006; Gillingham et al., 2007). The activities of PLD and PIP5K respectively generate

phosphatic acid (PA) and phosphatidylinositol 4,5-bisphosphate [PI(4,5)P or PIP₂], two phospholipids important for changes to cortical actin, vesicular trafficking and membrane curvature, all essential events for myoblast fusion (Donaldson et al., 2008). During fusion, PLD1 accumulated at the site of myoblast-myoblast contact (Bach et al., 2010). This localization, as well as PLD1 activity, was lost in Arf6 knockdown myoblasts. In addition, PIP₂, visualized using the pleckstrin homology domain of PLCδ1 fused to GFP (PLCδ1^{PH}::GFP), which binds preferentially to PIP₂, was found to colocalize with M-cadherin at the site of fusion. PIP₂ was essential for mammalian myoblast fusion as treatment of C2C12 satellite cell-derived myoblasts with agents that reduce (calcimycin, LiCl) or mask (neomycin) PIP₂ blocked fusion. Further, live imaging of the PLCδ1^{PH}::GFP reporter indicated that membrane phospholipids accumulate at the site of myoblast fusion in mammals as in *Drosophila* (Nowak et al., 2009; Bach et al., 2010; Bothe, et al., in revision). Accumulations of PIP₂ were observed at sites of myoblast-myoblast or myoblast-myotube contact (Nowak et al., 2009; Bach et al., 2010; Tall et al., 2000). These accumulations were transient and dissipated prior to a fusion event (Nowak et al., 2009; Bach et al., 2010). Furthermore, PLCδ1^{PH}::GFP accumulations perdured in Nap1 (mammalian homolog of *Drosophila* Kette) knockdown myoblasts and failed to resolve, concomitant with a block in fusion (Nowak et al., 2009). A similar behavior was observed for *kette* mutants (Bothe, et al., in revision). In fixed analysis, PLCδ1^{PH}::GFP also colocalizes with actin, M-cadherin and Dock1 (mammalian homolog of *Drosophila* Mbc, known to be at site of fusion) (Nowak et al., 2009; Bach et al., 2010).

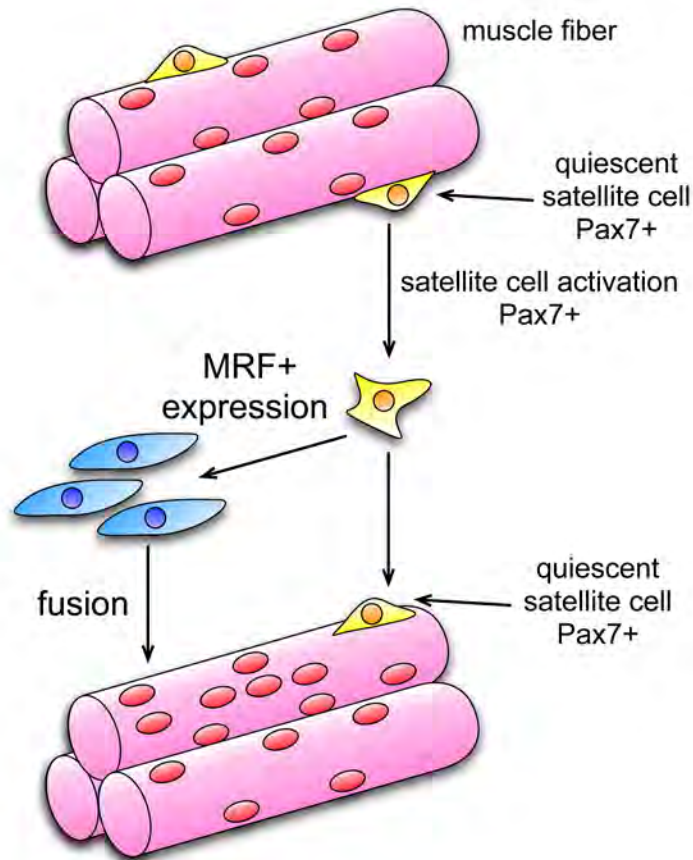


Figure 1.20. Adult muscle repair by satellite cells. In an uninjured muscle (pink), satellite cells (yellow), which express Pax7, are quiescent and can be found underneath the basal lamina of muscle cells. Upon muscle injury or during growth or regeneration, satellite cells become activated, proliferate and turn on the expression of MRFs, including MyoD. Pax7 is downregulated, and the differentiated myoblasts (blue) fuse with the injured myofiber or with one another to generate a new myofiber. The satellite cell population is also capable of self-renewal, and these satellite cells maintain high Pax7.

In Chapter 5, we present data further characterizing the role of PIP₂ during mammalian myoblast fusion. Our data suggest that PIP₂ accumulates asymmetrically during fusion and that PIP₂ is required for myoblast fusion *in vitro*.

Muscle repair

During the course of development, a subset of myoblasts, that are derived from the same progenitor pool in the dermomyotome as those that form embryonic muscle do not differentiate (Relaix et al., 2005; 2006; Gros et al., 2005; Seale et al., 2000). These cells, termed satellite cells, maintain expression of Pax3/7, do not express MRFs, proliferate and remain associated with the surface of the developing myofiber as quiescent cells (Figure 1.20). In mature muscle fibers, these cells line the basal lamina (sarcolemma) and are responsible for the postnatal growth and regeneration and repair of skeletal muscle.

In response to muscle damage as a result of natural causes (i.e. physical exertion, direct trauma) or inherent genetic predisposition to defects in the skeletal muscle (i.e. dystrophies), satellite cells become activated (Figure 1.20) (Campion et al., 1984; Hawke et al., 2001; Grounds et al., 2002). Subsequently, these cells proliferate, with some exiting the cell cycle and differentiating. These differentiated cells then fuse with the injured myofiber to repair the damage or fuse with one another to generate a new fiber. The activation and differentiation of satellite cells mimics the specification of myoblasts during development. For example, the expression of MRFs is essential in the differentiation of embryonic muscle

precursors; the expression of these same genes is required for the terminal differentiation of activated satellite cells (Cornelison et al., 2000; Zammit et al., 2002; Cooper et al., 1999; Yablonka-Reuveni et al., 1994; Maley et al., 1994; Cornelison et al., 1997; Fuchtbauer et al., 2004). Likewise, the genes underlying the fusion of activated satellite cells to the damaged myotube appear to overlap with those that are involved in the fusion of myoblasts during development. For example, the expression of M- and N-cadherin, which play roles in muscle development, are also upregulated in activated satellite cells, suggestive of a role for the cadherins in muscle repair (Radice et al., 1997; George-Weinstein et al., 1997; Hollnagel et al., 2002; Moore et al., 1993; Irintchev et al., 2004; Donalies et al., 2009). However, there are different mechanisms at play during repair that are absent or unnecessary for myoblast fusion during development. Evidence for this has come from analysis of both processes in desmin and Ii-4 mutant mice in which muscle formation proceeds normally; however, the repair process is impaired (Li et al., 1997; Smythe et al., 2001; Horsley et al., 2003). Taken together, these data suggest that understanding the mechanisms that underlie fusion during muscle development may inform aspects of satellite cell biology and repair, but differences between these processes exist.

C2C12 satellite cell-derived myoblasts

Owing to the complex structure of muscle in the mouse, *in vivo* analysis of muscle development has been difficult. Early attempts at *in vitro* study using muscle tissue

explants were hampered by the presence of additional, non-muscle cell populations in cultures. Furthermore, the composition of cell populations differed in normal and disease states (Powell et al., 1973; Parsons et al., 1974; Gallup et al., 1973). In contrast, large numbers of muscle satellite cells can be obtained by injuring a muscle a few days prior to satellite cell isolation/culture, making the generation of a homogenous population of muscle cells relatively simple. Widely used in *in vitro* studies, the mouse satellite cell line C2C12 was established from primary cultures isolated from the injured thigh muscle of a 2-month old C3H mouse after injury (Yaffe et al., 1977). Like other stem cell populations, satellite cells (including C2C12 satellite cell-derived myoblasts) are capable of self-renewal, making propagation of such cultures simple. Satellite cells derived in this manner are spindle-shaped, resembling myoblasts in newborn animals, and can fuse *in vitro*. Furthermore, satellite cells can fuse with muscle when injected into mouse making them useful for *in vivo* studies of fusion, repair and regeneration and the introduction of recombinant proteins (Yao et al., 1992; Cheng et al., 2005; Barr et al., 1991; Pajcini et al., 2008; Dhawan et al., 1991).

The actin cytoskeleton and its regulators

Actin structure and polymerization

Actin, the most abundant protein in most eukaryotic cells, is involved in many aspects of cellular function, and its primary sequence has been remarkably

conserved from protozoa to animals (Chhabra et al., 2007). The actin monomer, globular G-actin, is a 43-kDa molecule composed of two similar major domains (inner and outer) and polymerizes to form filamentous (F)-actin (Figure 1.21A) (Chhabra et al., 2007; Goley et al., 2006). F-actin has an inherent polarization due to the asymmetry of the monomer; one end of the filament is called the pointed (minus)-end and the other, the barbed (plus)-end. In most cellular contexts, actin polymerization occurs primarily at the barbed-end; however, in the F-actin-based thin filaments of striated muscle, polymerization is regulated at the pointed-end (Fischer et al., 2003; Pollard et al., 2000). Polymerization of actin, an adenosine triphosphatase (ATPase), requires ATP hydrolysis. ATP (or ADP) binds between the two domains of G-actin, although G-actin is only able to hydrolyze ATP very slowly. Once integrated into the filament, the ATPase activity of actin hydrolyzes ATP. ADP-bound actin monomers slowly dissociate from microfilaments at the pointed-end, at which point they release ADP, bind ATP and repeat the cycle.

The atomic structure of F-actin reveals that the outer domain of G-actin undergoes a 20° rotation relative to the inner domain in its transition from G- to F-actin (Oda et al., 2009). Interestingly, the effect of this rotation is to bring a residue likely involved in ATP hydrolysis closer to the phosphate groups of the ATP molecule. In addition to the 20° intramolecular rotation, each G-actin monomer rotates 167° in the F-actin structure, resulting in F-actin appearing as a double helix. Thirteen actin subunits are required for a single actin crossover (an exact helical repeat) and proteins that sever or depolymerize actin are

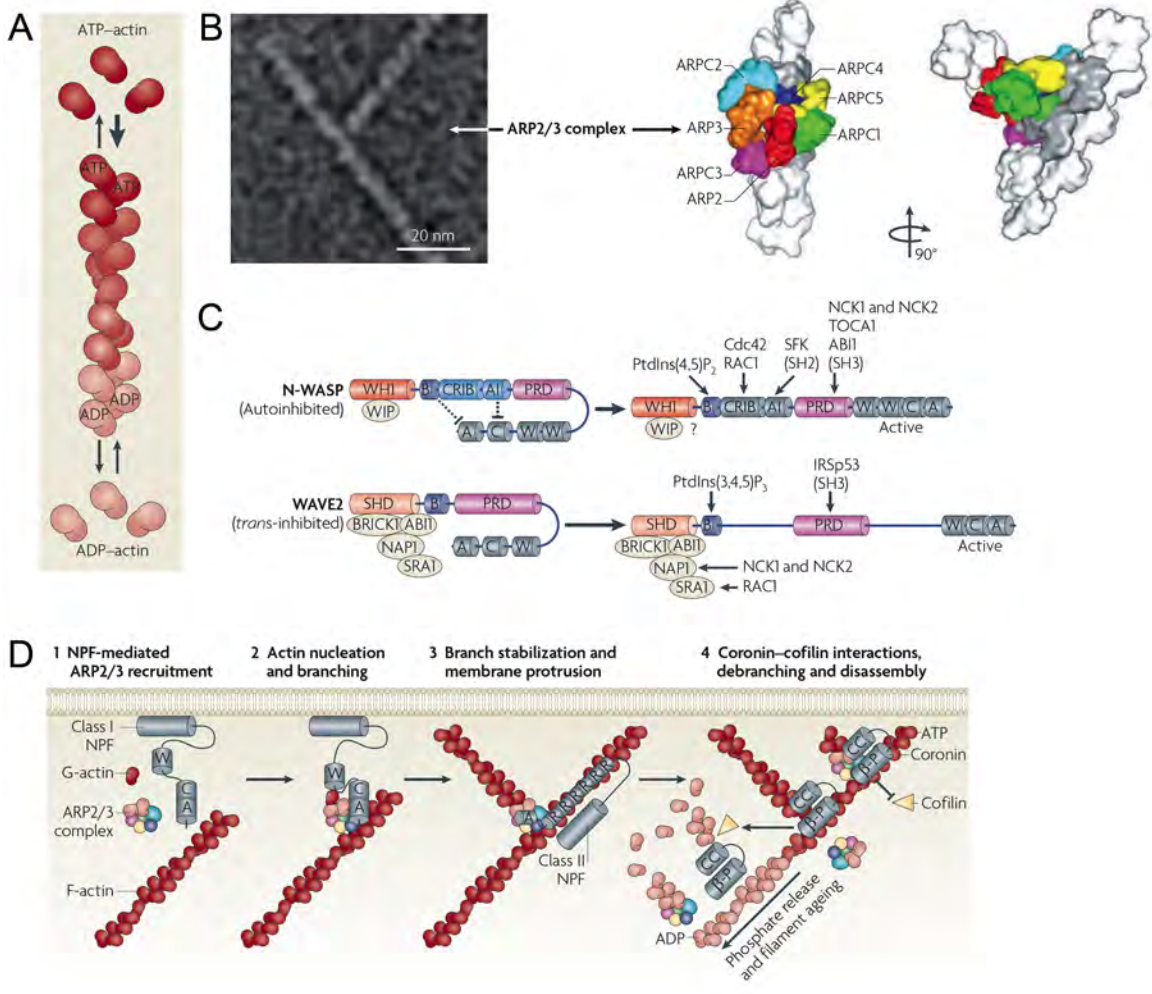


Figure 1.21. An overview of branched actin polymerization mediated by Arp2/3 and its NPFs. (A) Monomeric G-actin associates to form filamentous (F)-actin. This activity is coupled to ATP hydrolysis. ATP-bound G-actin is incorporated into F-actin and older ADP-bound monomers preferentially disassociate from the pointed end. (B) EM of a branched actin filament formed by the Arp2/3 complex (left). Structural models of Arp2/3 complex (colored) bound to F-actin (white) based on electron tomography (right). All seven subunits contact the existing filament, and Arp2 and Arp3 act as the first two subunits of the daughter filament. (C) WASp and N-WASp NPF activity is autoinhibited by interaction of its GBD (including the B, CRIB and AI domains) with the connector (C) and acidic (A) domains and with interactions with WIP family proteins. This inhibition is overcome by binding phosphoinositides, small GTPases and SH2 or SH3 domains. SCAR/WAVE activity is controlled by the WAVE complex, which includes HSPC300 (Brick1 in the figure), Abi1, Nap1 and Sra1. SCAR/WAVE is stimulated by Nck-Nap1 or Rac-Sra1 interactions, phosphoinositide-binding or SH3 domains. (D) A model for nucleation and branching. NPFs, via their WCA domains, recruit Arp2/3 (1). The activity of the WCA domain also brings Arp2/3 together with the first actin subunit in the daughter filament (2). Arp2/3 can be stabilized by cortactin, a class II NPF (3). Coronin family proteins interact with Arp2/3 to prevent cofilin-mediated disassembly of newly formed filaments (4). Coronin can also replace Arp2/3 to trigger debranching and depolymerization by cofilin. Finally, depolymerization happens spontaneously. A, acidic motif; C, connector; CC, coiled coil; GBD, GTPase-binding domain; NPF, nucleation promoting factor; PRD, Pro-rich domain; PtdIns(3,4,5)P₃, phosphatidylinositol-3,4,5-trisphosphate; W or WH, WAVE homology. Adapted with permission from (Campellone et al., 2010).

able to alter the length of the crossover as part of their mechanism (Oda et al., 2009; McGough et al., 1997).

Elongation of existing F-actin is favorable, particularly at the barbed-end, where the association of actin monomers is limited by the diffusion rate constant (Pollard et al., 1986; Goley et al., 2006). However, nucleation of actin filaments is inefficient due to the instability of small actin oligomers (dimers and trimers), and thus, it requires the activity of several classes of proteins to generate linear filaments and branched actin networks (Campellone et al., 2010; Pollard et al., 2007; Goode et al., 2007).

Branched actin polymerization

Arp2/3

The conserved Arp2/3 complex initiates actin filament branches on the sides of existing actin filaments, anchoring the pointed end of the daughter filament so that the barbed end grows away at a 70° angle (Figure 1.21B, D) (Pollard et al., 2007). This generates a network of branched actin filaments, a process known as dendritic nucleation, and, in the case of cell migration, the barbed ends of each “branch” push the cell membrane forward in an actin-rich structure called a lamellipodia.

The Arp2/3 complex consists of seven subunits including Arp2 and Arp3, two actin-related proteins, and five Actin-related protein complex proteins

(Arpc1-5) (Figure 1.21B) (Pollard et al., 2007). Arp2 and Arp3 are held in an inactive state, where they are separated by the five other members of the complex (Robinson et al., 2001; Nolen et al., 2004). Activation of the Arp2/3 complex brings Arp2 and Arp3 in close apposition in such a way that they mimic an actin filament end (Rouiller et al., 2008). The activation requires a substantial conformational change and in the resulting conformation, all seven subunits contact the existing mother filament.

Nucleation-promoting factors (NPFs)

Activators of Arp2/3 are collectively referred to as nucleation promoting factors (NPFs) (Pollard et al., 2007; Goley et al., 2006). The four NPF subfamilies are classified by their N-terminal domains and include the WASp (Wiskott-Aldrich syndrome protein), SCAR/WAVE (suppressor of cAMP receptor/WASp family verprolin homolog), WASH (Wiskott-Aldrich syndrome protein and SCAR homolog) and WHAMM/JMY (WASp homolog associated with actin, membrane and microtubules/junction-mediating regulatory protein) families (Derivery et al., 2010). The WASH and WHAMM/JMY families have only recently been identified (Linardopoulou et al., 2007; Campellone et al., 2008; Zuchero et al., 2009). All NPFs share a C-terminal WCA domain (also called a VCA) which is sufficient for Arp2/3 activation *in vitro* (Goley et al., 2006; Pollard et al., 2007). The WCA domain consists of a WH2 (WASp homology 2 or Verprolin homology) domain that recognizes actin, a connector and an acidic motif that binds Arp2/3 (Figure

1.21C). Thus, NPFs have affinity for actin (via the WC domains) and Arp2/3 (via the CA domains) and mediate the delivery of a new actin subunit to the Arp2/3 complex (Weaver et al., 2002; Marchand et al., 2001; Chereau et al., 2005). Additionally, the number of WH2 repeats differs amongst NPFs and are also found in other actin-binding proteins, including WIP (WASp-interacting protein) and Spire, indicating that it is a general actin-binding domain (Figure 1.23) (Quinlan et al., 2005; Pollard et al., 2007).

The mechanism by which NPFs activate Arp2/3 is unclear, but the mechanisms underlying NPF activation have been elucidated. WASp and N-WASp are autoinhibited via intramolecular interactions of their GTPase-binding domain (GBD), which also includes the CDC42/Rac-interactive binding (CRIB) domain, with the C motif (Figure 1.21C). This inhibition is overcome by PIP₂ and Rho-family GTPases, including Rac and Cdc42, which bind the GBD and displace the WCA domain. The SH3 domains of Nck and Grb2 can also activate N-WASp in the place of Cdc42 (Pollard et al., 2007). In addition, WASp and N-WASp interact with a family of proline-rich proteins [Verprolins or WASp-interacting proteins (WIPs)] via its WH1 domain. WIP and its homologs have an N-terminal WH2 domain, a proline-rich central domain and a C-terminal domain that binds WASp. The WIP/WASp interaction enhances the stability of WASp, contributes to its activation and is important for the translocation of WASp to sites of actin polymerization (Campellone et al., 2010). WIP can also inhibit WASp activity. Thus, it is unclear exactly how WIP influences WASp activity in this complex.

In contrast, SCAR/WAVE is constitutively active and is inhibited by binding in *trans* with the WAVE complex through its WHD [WAVE-homology domain, also SHD (SCAR homology domain)] (Figure 1.21C) (Ibarra et al., 2005; Pollard et al., 2007). In addition to SCAR/WAVE, the WAVE complex consists of four subunits: Abi (Abl-interacting protein), Nap1 (Nck-associated protein, Kette in *Drosophila*), PIR121/Sra1 (protein p53-inducible mRNA 121) and HSPC300 (Hematopoietic Stem Progenitor Cell 300). The role of the WAVE complex in regulating SCAR/WAVE activity is controversial and may be dependent on the amount of SCAR/WAVE and the WAVE complex available (Ibarra et al., 2005). Though the role of the WAVE complex is not fully understood, SCAR/WAVE is activated by Rac, which binds Sra1, or Nck, which binds Nap1 (Ibarra et al., 2005; Eden et al., 2002).

Unbranched actin polymerization

Formins

Formins strongly nucleate linear actin filaments, are universally present in eukaryotic cells and share three regions of homology, termed the formin homology domains 1-3 (FH1-3) (Figure 1.22) (Castrillon et al., 1994; Petersen et al., 1998; Higgs et al., 2005; Rivero et al., 2005). FH domains 1 and 3 are critical for regulating actin assembly and formin interaction with binding partners. The FH2 domain forms a donut-shaped dimer that is essential and sufficient for nucleating

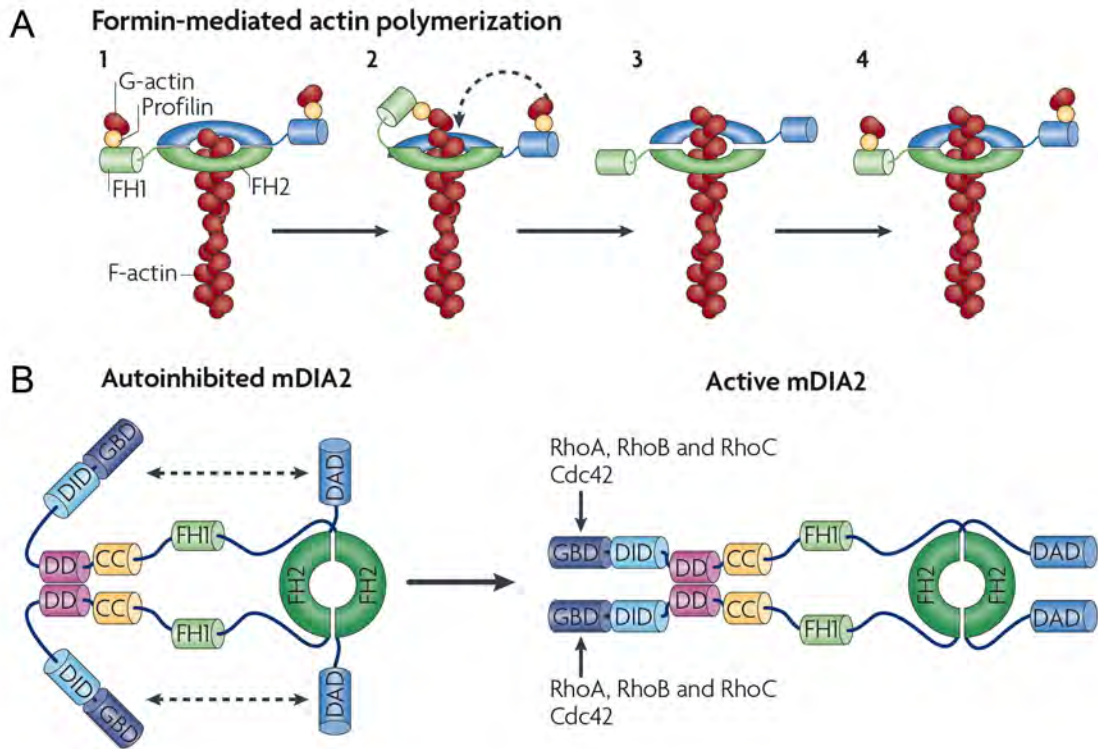


Figure 1.22. Overview of formin actin nucleators. (A) An FH2 dimer (blue and green rings) associates with the barbed end of an actin filament. The FH1 domains recruit profilin-actin complexes (1). The FH1 domain delivers profilin-actin to the FH2 domain. This is coupled to the FH2 domain moving towards the barbed end as additional monomers are incorporated (2). The second FH2 domain incorporates its actin monomer (3). Formin, in the closed conformation, prevents barbed end capping by capping proteins (4). (B) Diaphanous-related formins are dimeric and regulated by autoinhibition mediated by the interaction of the DAD with the DID (left). Autoinhibition is relieved by binding to Rho family GTPases, including RhoA/B/C, Cdc42 and Rac (right). CC, coiled coil; DAD, Diaphanous-autoinhibitory domain; DID, Diaphanous inhibitory domain; DD, dimerization domain; FH, formin homology; GBD, GTPase-binding domain. Adapted with permission from (Campellone et al., 2010).

actin polymerization. The presence of an FH2 domain, which also physically associates with the barbed-end of actin filaments, is the defining feature of formin proteins and phylogenetic analysis of this domain has divided the family into a number of groups (Higgs et al., 2005; Rivero et al., 2005; Evangelista et al., 2002; Goode et al., 2007).

The Diaphanous-related formins, including Dia1-3, the disheveled-associated activators of morphogenesis (DAAM1-2) and the formin-related proteins (FMNL1-3) are the best understood formins. The C-terminus of this group contains the FH1 and FH2 domains and the DAD (diaphanous autoregulatory domain) (Figure 1.22B). The FH1 domain, present in all formins, binds to profilin, a protein that associates with polymerization-ready ATP-bound actin monomers (Pollard et al., 2007). Thus, this domain is responsible for bringing profilin-actin complexes to the end of a growing filament. The DAD, a short, non-folded segment of ~17 residues, binds the N-terminal DID (diaphanous inhibitory domain) and maintains formins in an autoinhibited state {Alberts:2000fu, Goode:2007eq}. In addition to the DID, the N-terminus consists of a GTPase-binding domain (GBD), a dimerization domain (DD) and a coiled-coil (CC) region. The GBD binds activated (GTP-bound) Rho-family GTPases and the DD and CC domains mediate the N-terminal dimerization of Diaphanous-related formins.

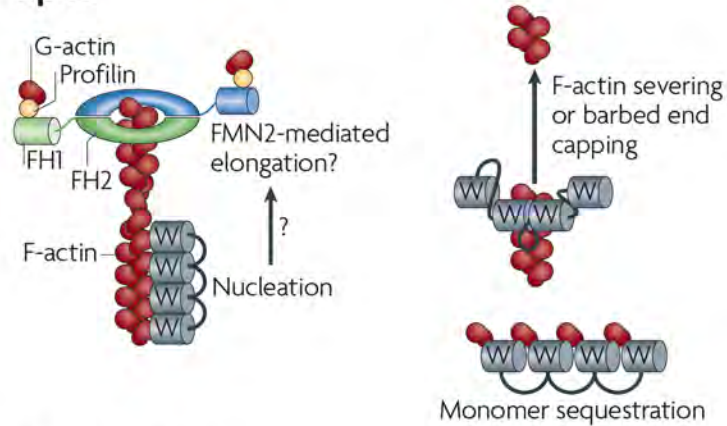
In contrast to Arp2 and Arp3, the FH2 domain of formins lack structural similarity to actin and bind actin monomers weakly (Goode et al., 2007; Rouiller et al., 2008). As expected, their mechanism of actin nucleation also differs.

Recent analyses suggest that formins nucleate actin by stabilizing spontaneously-formed actin dimers and/or trimers, which are highly unstable polymerization intermediates (Goode et al., 2007; Otomo et al., 2005; Pring et al., 2003; Shimada et al., 2004). In a mechanism termed “processive capping,” FH2 domains remain bound to the barbed-end of the actin filament for the addition of thousands of actin subunits (Figure 1.22B) (Pruyne et al., 2002; Sagot et al., 2002; Zigmond et al., 2003). The mechanism of how actin subunits insert themselves between the FH2 domain and the actin filament is still unclear. Further, how an FH2 dimer continues to track with the growing filament during this process is not known, though it is likely that bound formins (or the actin cytoskeleton) must undergo some rotation (Shemesh et al., 2005).

Spire

Spire, another linear actin polymerization nucleator, contains an N-terminal kinase non-catalytic C-lobe domain (KIND), a C-terminal FYVE domain and a central tandem WH2 domain and an additional G-actin-binding linker (Campellone et al., 2010). Together, the central WH2 domain and the linker region are able to bind four actin monomers, but its activity is dependent on the Spire/actin ratio within a cell (Figure 1.23A). At low Spire/actin ratios, Spire nucleates actin, while at high Spire/actin ratios, Spire sequesters actin (Quinlan et al., 2005; Campellone et al., 2010). Spire nucleates actin with similar activity to the *Drosophila* formin Cappuccino (Capu), but its mechanism of nucleation is unclear.

A Spire



B Leiomodrin

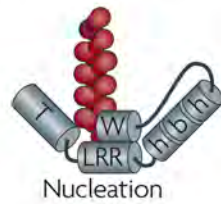


Figure 1.23. Models for actin nucleation and polymerization by Spire and Leiomodrin. (A) Spire can nucleate F-actin polymerization (left), which may be elongated by formins, sequester monomers (right) and cap and sever existing filaments. (B) Leiomodrin uses multiple G-actin-binding sequences to assemble trimeric actin nuclei. FH1/2, Formin homology 1/2; LRR, Leu-rich repeats; h-b-h, helix-basic-helix; T, tropomyosin- and actin-binding helices; W, WH2 homology. Adapted, with permission, from {Campellone:2010gd}.

Spire may also enhance pointed-end disassembly by severing filaments and inhibiting profilin-actin assembly at barbed-ends, indicating that Spire is a versatile regulator of actin dynamics (Figure 1.23A) (Bosch et al., 2007; Campellone et al., 2010).

In addition, Spire (mammalian SPIRE1/2) and Capu (mammalian FMN1/2) can physically interact and cooperate in actin assembly. This interaction is mediated by the Spire KIND domain and sequence near the C-terminus of FMN1/2 and results in the enhancement of Spire and inhibition of formin actin nucleation activities (Campellone et al., 2010).

Leiomodin

Leiomodins, muscle-specific actin nucleators, have only recently been identified (Chereau et al., 2008; Campellone et al., 2010). Similarly to tropomodulins, which cap F-actin pointed-ends, leiomodins contains N-terminal tropomyosin- and actin-binding helices and a central actin-binding Leu-rich repeat (LRR) (Figure 1.23B) (Conley et al., 2001). Leiomodin 2 (LMOD2), expressed in skeletal and cardiac muscle, also contains additional C-terminal domains, including a polyproline peptide, a WH2 domain and two predicted helices. Leiomodins are suggested to nucleate actin polymerization through the stabilization of an actin trimer via its three actin-binding domains. The LRR and C-terminal extension contain the minimal fragment with strong actin nucleation activity (Chereau et al., 2008). This activity was enhanced by the N-terminal region, which recruited tropomyosin and

localized leiomodin to sarcomere M-lines where tropomyosin and leiomodin coordinate to regulate sarcomere assembly.

Actin depolymerization

To maintain continuous polymerization, actin monomers must be recycled. In contrast to the slow rate of depolymerization of pure actin *in vitro* (0.044-1.14 $\mu\text{M}/\text{min}$), cellular rates of actin turnover occur rapidly (up to 9 $\mu\text{M}/\text{min}$), suggesting that this process is accelerated by proteins *in vivo* (Pollard et al., 1986; Theriot et al., 1991; Zigmond et al., 1993). Two classes of such proteins exist in most eukaryotic cells: the gelsolin/villin and the actin-depolymerizing factor (ADF)/cofilin families. Members of the both families can be found all eukaryotic organisms (Bamburg, 1999; Nag et al., 2013).

Gelsolin/villin

Gelsolin, part of a superfamily of calcium-dependent regulators of the actin cytoskeleton, severs, caps and nucleates actin filaments, and sequesters actin monomers (Nag et al., 2013). Gelsolin, the eponymous member of the superfamily, contains six copies of the gelsolin domain (G1-6), each of which folds into a five- or six-stranded β -sheet and are separated by two helices. Other members of the family, which in mammals includes CapG, Adseverin, Flightless I, Advillin, Villin, Villin-like and Supervillin, contain different numbers of the gelsolin domain.

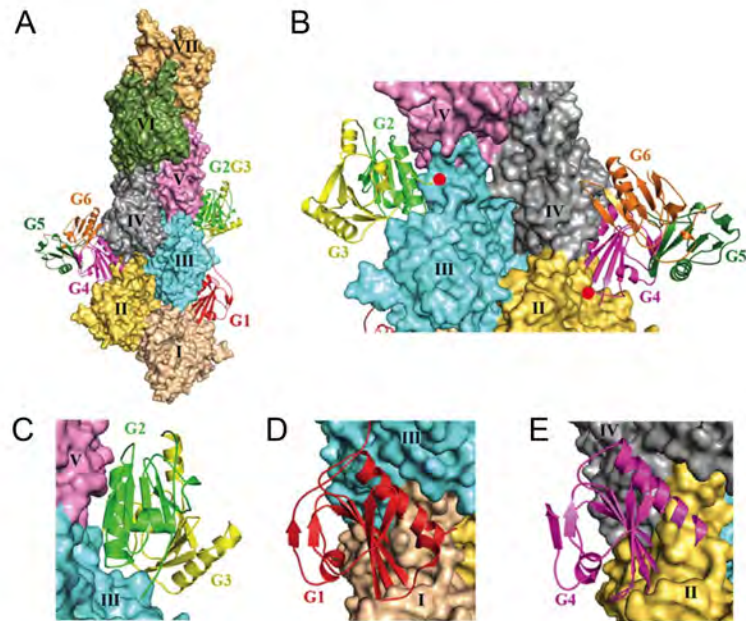


Figure 1.24. Model for actin severing by gelsolin. (A) Structure of the N-terminus (G1-G3) and C-terminus (G4-G6) of activated gelsolin attached to F-actin {Oda: 2009jq}. (B) Rotation of 180° of (A). (C) Interface of G2G3 linker that targets gelsolin to F-actin. G2 interacts with two adjacent protomers, III and V. (D) G1 binds to protomer III, which causes clashes with protomer I. (E) G4 binds to protomer IV, which causes clashes with protomer II. These steric clashes suggest that gelsolin severs F-actin by displacing the adjacent protomers. Used with permission from (Nag et al., 2013).

Gelsolin is maintained in an inactive state until it is required (dos Remedios et al., 2003). Three “latches” hold inactivated gelsolin in such a way that all actin-binding surfaces are hindered (Burtnick et al., 1997; 2004; Choe et al., 2002; Nag et al., 2013). The C-terminal tail latch is formed from the interaction of a C-terminal helix with the long helix of G2; the G1-G3 latch is formed by the apposition of the β -sheets of G1 and G3, and the G4-G6 latch is formed from the interactions of the core β -sheets of G4 and G6. Calcium ion binding to G6 activates gelsolin by opening these three latches. The tail latch is the first to be released and allows for subsequent opening of the other two latches and dramatic rearrangement of the gelsolin domains (Burtnick et al., 2004; Choe et al., 2002; Nag et al., 2013). Calcium binding also affects the affinity and the rate of binding of gelsolin to actin (Nag et al., 2013). Actin-binding, mediated through conserved actin-binding sites on G1, G2 and G4, further facilitates additional calcium ion sequestration and stabilizes the active conformation of gelsolin (Burtnick et al., 2004; Choe et al., 2002; Nag et al., 2013). Additional binding sites have been identified in G3 and G6 (Burtnick et al., 2004; Nag et al., 2013).

To sever actin filaments, the gelsolin domains cooperatively bind an F-actin filament with the G2G3 domain first binding to the side (Figure 1.24A-C). Subsequent competition between gelsolin fragments G1 and G4-G6 with adjacent actin monomers (also called protomers) results in a pincer-like movement that severs the filament (Figure 1.24D-E) (Nag et al., 2013). The initial binding of gelsolin to an actin filament may promote changes in the twist of F-

actin, which would destabilize lateral monomer contacts and allow for G1 and G4-G6 to insert between protomers and sever the filament. Once the filament is severed, the G1 and G4-G6 fragments also act as filament cappers, and each fragment is capable of sequestering a single actin monomer.

The ADF/cofilin family of proteins

ADF was named for its ability to depolymerize F-actin to form a 1:1 complex of ADF:G-actin, whereas cofilin (cofilamentous structures with actin) was named for its ability to cosediment with F-actin (Nishida et al., 1984; Bamburg et al., 1980). Despite these differences in behavior, however, both proteins increase the pool of actin monomers in a pH-dependent manner. Genetic evidence suggests that ADF can functionally rescue cofilin null mutants in yeast (Moon et al., 1993; Iida et al., 1993). Thus, ADF and cofilin are often considered to be redundant proteins with similar activities.

Structure

At the sequence level, ADF and cofilin within the same organism share close to 70% identity (Figure 1.25). When compared over the entire family, homology ranges from 25-71% amino acid identity (Bamburg, 1999). ADF/cofilin family members are defined by the presence of a single ADF-homology (ADF-H) structural motif, which spans almost the entire length of the protein. The ADF-H consists of a hydrophobic core composed of 4-5 mixed β -sheets surrounded by

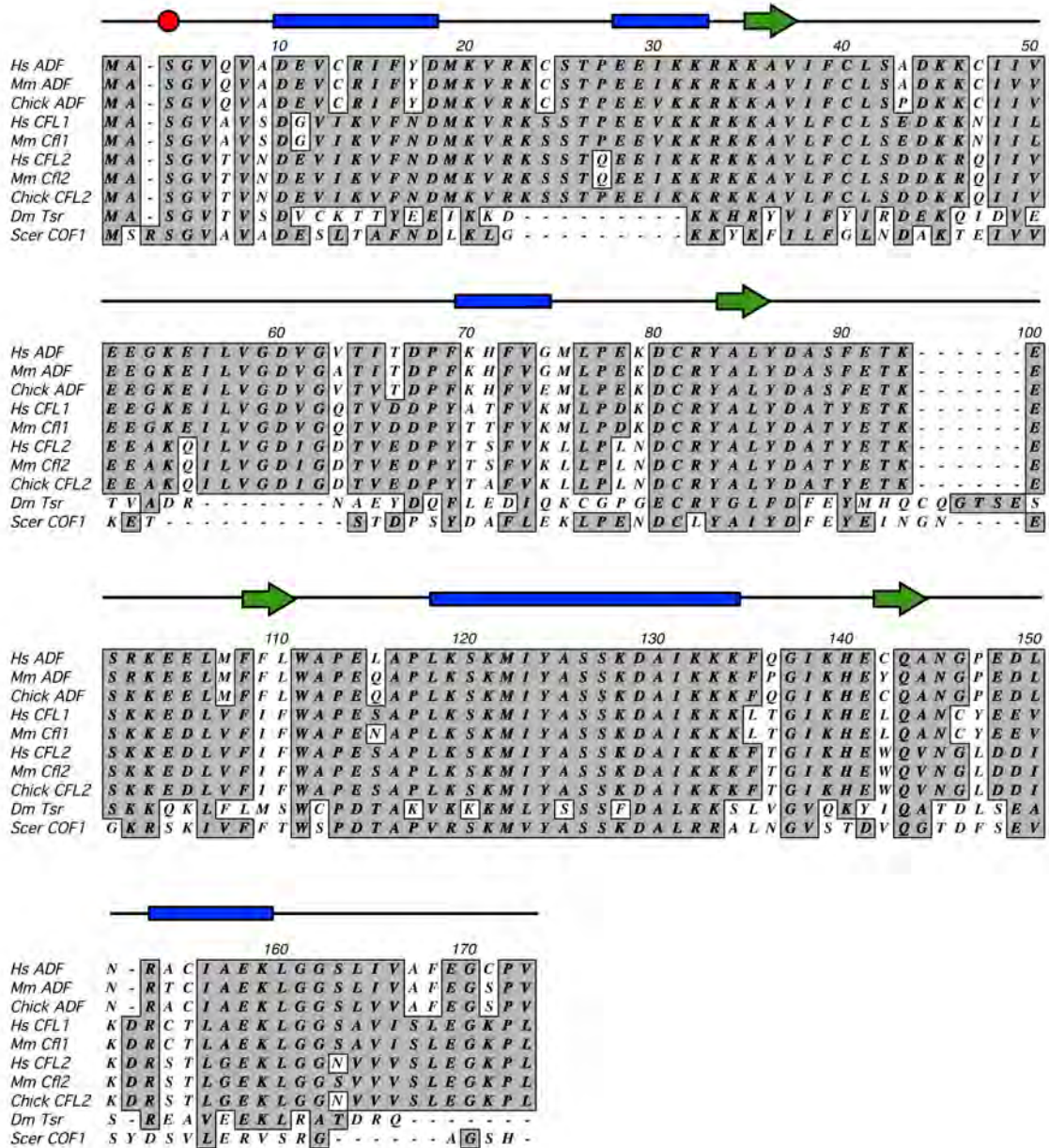


Figure 1.25. Alignment of cofilin homologs. Amino acid alignment of select ADF and cofilin family members in human, mouse, chicken, *Drosophila* and yeast. Conserved amino acids are bolded and shaded in grey. Red circle indicates conserved regulatory Ser3. Green arrows indicate β -sheets. Blue bars indicate α -helicies. Hs, *Homo sapiens*; Mm, *Mus musculus*; Chick, chicken; Dm, *Drosophila melanogaster*; Scer, *Saccharomyces cerevisiae*.

pairs of α -helices (Lappalainen et al., 1998; Puius et al., 1998). The regions of highest homology within the ADF-H domain are the two actin-binding domains, which include a completely conserved serine (Ser3 in animals and insects, Ser6 in plant ADF). The residues of the actin-binding domains fall into two categories: those that are required for actin-binding and those that confer F-actin-binding specificity. The N-terminus, conserved serine residue and a portion of the long helix α 3 and the turn connecting the β 5 strand and α 4 helix compose the residues/secondary structure required for actin-binding. Residues from the β 4 strand and α 4 helix are essential for F-actin-binding specificity. That the N-terminus of ADF/cofilin is required for actin-binding is supported by a number of studies, including zero length cross-linking between ADF/cofilin and actin and mutagenesis of yeast and chicken cofilin, (Muneyuki et al., 1985; Sutoh et al., 1989; Lappalainen et al., 1997). In addition, a twelve-peptide region within the actin-binding domain of cofilin can also bind the phosphoinositides, PI, PIP and PIP₂ in a manner that precludes cofilin from also binding actin (Yonezawa et al., 1990; 1991). A similar sequence is found in all members of the ADF/cofilin family, suggesting that this interaction is conserved. Further, the ADF-H motif shares structural features with some segments of the gelsolin family of actin regulatory proteins though only low sequence homology exists between the two protein families, suggesting that ADF/cofilin family members may interact with actin similarly to the gelsolin family (Hatanaka et al., 1996; Leonard et al., 1997; Wriggers et al., 1998).

Mutagenesis of yeast cofilin also identified a second region of high homology outside of the actin-binding domain. Phylogenetic conservation indicates that both regions are likely important for binding to the actin interacting protein 1 (AIP1), an accessory protein that greatly enhances the severing activity of cofilin (Lappalainen et al., 1997; Rodal et al., 1999; Amberg et al., 1995). Regions of non-homology, which include three insertions in the larger members of the family (vertebrate, *C. elegans*, *Drosophila*), occur in loops between the conserved secondary structures and do not appear to impact their three-dimensional structure.

ADF/cofilin-actin interface

To date, it has not been possible to generate a co-crystal structure of the ADF/cofilin-monomeric actin interface. This is likely due to the fact that ADF/cofilin also binds F-actin, which cannot be crystallized (Bamburg et al., 1999; Oda et al., 2009). Use of electron cryomicroscopy coupled with image reconstruction has provided a picture of the cofilin-actin interface and demonstrated that cofilin binds to two adjacent actin subunits (McGough et al., 1997; Galkin et al., 2011). Interestingly, the interaction of cofilin and actin is similar to binding of gelsolin with actin (Puius et al., 1998; McGough et al., 1998; Bamburg et al., 1999). Despite these similarities, however, striking differences exist. The binding of cofilin to F-actin induces a change in the twist of the bound filament (from -167° to -162°); this property appears to be unique to the ADF/cofilin family (Figure 1.26)

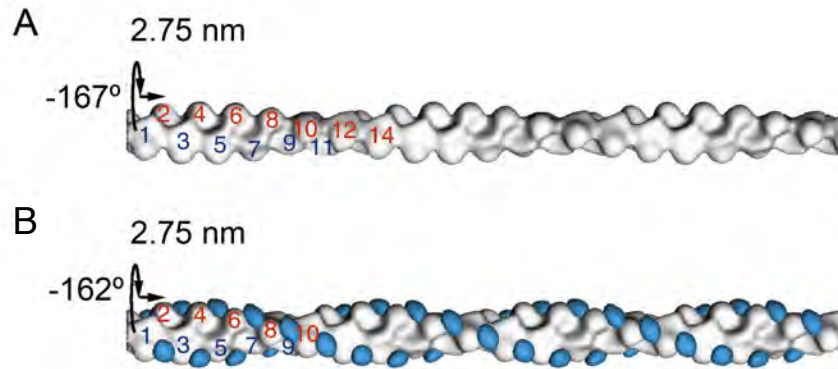


Figure 1.26. Effect of cofilin-binding on F-actin structure. (A-B) Reconstitution of F-actin obtained by electron cryomicroscopy without bound cofilin (A) or with bound cofilin (B) from {McGough: 1997vc}. (A) F-actin, formed from the polymerization of actin monomers (numbered), winds in a left-handed sense and gives the appearance of two parallel helices (numbered in blue and red). In most F-actin structures, 13 monomers constitute a single crossover. Two adjacent actin monomers are related by an axial rise of 2.75 nm and a rotation of -167° . (B) In the presence of human cofilin (blue), F-actin is twisted by approximately 5° per subunit, and the rise is unaffected. The number of subunits per crossover is reduced to 10. Used with permission from (Bamburg et al., 1999).

(McGough et al., 1997). As a consequence, the length of the actin crossover, which is typically 13 actin subunits, is reduced to around 10 subunits per crossover. The unique ability of ADF/cofilin proteins to twist F-actin may also explain other properties of this protein family. For example, the ability of muscle and non-muscle tropomyosins to bind F-actin is competitively inhibited by the binding of ADF/cofilin to actin filaments (Bamburg, 1999; Bamburg et al., 1999). This is likely a result of the change in filament twist induced by ADF/cofilin proteins (McGough et al., 1997).

ADF/cofilin enhance the dynamics of actin assembly

Coupled with the key finding that severing occurs at the junction between cofilin-bound and cofilin-free regions of F-actin, the increase in torsion of the F-actin filament induced by cofilin-binding explains the structural basis of cofilin-mediated severing (McGough et al., 1997; Bravo-Cordero et al., 2011; Galkin et al., 2011). The twist disrupts longitudinal interfaces, which is propagated to cofilin-free regions of the actin filament (Galkin et al., 2011). Regions of the actin filament decorated with cofilin are stabilized by the formation of a cofilin 'bridge' that maintains a connection between longitudinal interfaces, while regions that are cofilin-free are unstable due to the absence of the cofilin 'bridge' and, as a result, severing occurs.

The role of ADF/cofilin in actin depolymerization has been less clear. Initial studies that suggested cofilin increases the dissociation rate constants for

monomeric actin subunits from the pointed end of F-actin failed to take into account the generation of free barbed ends, which can be used to nucleate actin polymerization, by filament severing (Carlier et al., 1997; Bravo-Cordero et al., 2013). Branches on these new filaments are nucleated by Arp2/3; however, cofilin can also dissociate these branches (Bravo-Cordero et al., 2013). Moreover, cofilin can locally depolymerize filaments. Thus, the activity of cofilin can result in depolymerization and polymerization with a single severing event, and the relative concentration of G-actin appears to be the determining factor. At physiological concentrations of ATP-bound G-actin and due to the association and dissociation rates of monomers at the pointed and barbed ends, respectively, net polymerization occurs at sites of actin severing. Further, through its promotion of depolymerization, cofilin helps to maintain G-actin at physiological levels. The balance between polymerization and depolymerization is also affected by other actin-modulating proteins such as AIP1 (actin interacting protein 1; Flare in *Drosophila*), gelsolin and coronin (discussed in more detail below) (Bravo-Cordero et al., 2013; Uetrecht et al., 2006; Nag et al., 2013). AIP1 potentiates cofilin severing and tips the balance towards net depolymerization (Bravo-Cordero et al., 2013). Gelsolin activity also results in net depolymerization (Nag et al., 2013). Coronin plays both roles: preventing cofilin from binding to new actin filaments and enhancing cofilin binding to older actin filaments.

Regulation of ADF/cofilin activity

Expression

Single cell eukaryotes and *Drosophila* appear to encode only a single ADF/cofilin family member while other multicellular organisms contain additional members, likely to handle tissue- and temporal-specific needs for actin dynamics/regulation (Bamburg, 1999). In *C. elegans*, the two ADF/cofilin members, UNC-60A and UNC-60B are splice variants encoded by the *unc-60* gene (McKim et al., 1994). UNC-60A is ubiquitously expressed and is essential for viability (Ono et al., 1999). In contrast, UNC-60B is muscle-specific isoform expressed during muscle differentiation and is important for muscle actin assembly and organization.

Mice and humans contain 3 members of the ADF/cofilin family: ADF (or destrin), a ubiquitously expressed cofilin (CFL1) and a muscle-specific cofilin (CFL2) (Ono et al., 1994). In embryonic muscle, CFL1 and ADF are expressed at high levels; however, as myogenesis progresses, ADF levels decline and CFL1 is replaced by CFL2 *in vivo* and *in vitro*. In regenerating and dystrophic muscle, CFL2 expression is upregulated while ADF levels remain low (Ono et al., 1994; Bamburg et al., 1987; Abe et al., 1989; Nagaoka et al., 1996; Akkila et al., 1997; Thirion et al., 2001; Morgan et al., 1993; Hayakawa et al., 1993; Ono et al., 1998).

Compartmentalization

ADF/cofilin are predominantly cytoplasmic; however, ADF/cofilin in mammals, *C. elegans* and *Drosophila* contain an insertion which encodes a nuclear localization sequence (NLS) just prior to the second strand of the β -sheet. The NLS is opposite the actin-binding surface, suggesting that it can still be recognized by the importin pathway, even in the context of bound actin, which has no NLS (Bamburg, 1999). Consistent with this, mammalian ADF/cofilin can be induced to accumulate in the nucleus with actin to form actin rods. This translocation of ADF/cofilin into the nucleus, which can deplete by as much as 100% of the cytoplasmic ADF/cofilin, is often induced by stress, though its role is unclear. In Chapter 2, we will demonstrate that *Drosophila* Twinstar can also translocate to the nucleus.

Phosphorylation

With the exception of yeast and *Dictyostelium* cofilin, the activity of ADF/cofilin family members are regulated by phosphorylation at a single, conserved serine residue within the conserved N-terminal actin-binding domain (Figure 1.27) (Bamburg, 1999). Phosphorylation of Ser3 (or Ser6 in plant ADF) by LIM domain-containing kinases 1 and 2 (LIMK1/2) and the dual specificity testis-specific protein kinases 1 and 2 (TESK1/2) inactivates ADF/cofilin and prevents it from binding to actin, and thus from depolymerizing or severing filaments

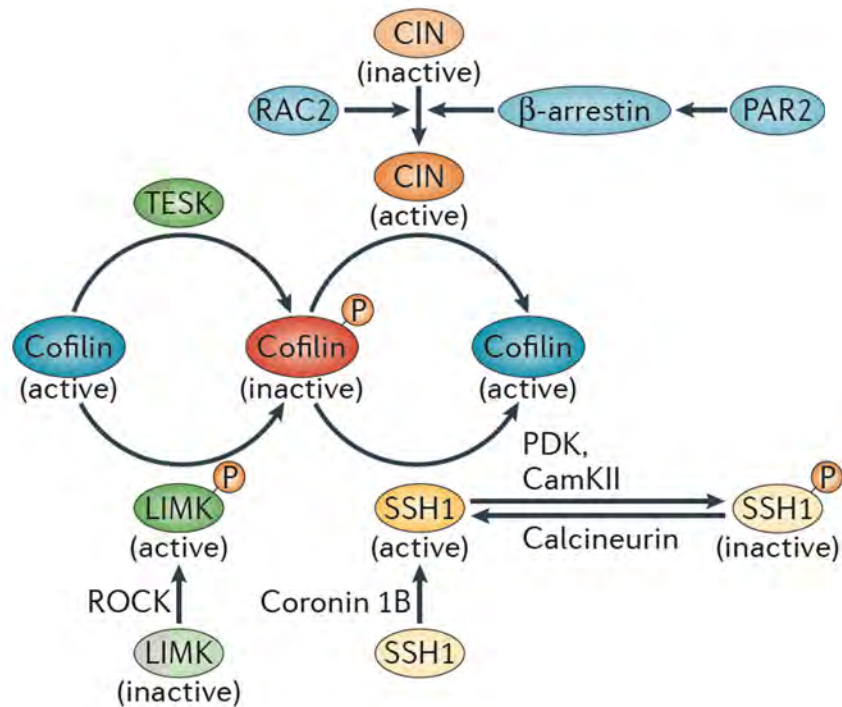


Figure 1.27. Regulation of cofilin by kinases and phosphatases. Cofilin is regulated by inhibitory phosphorylation at Ser3 by LIMK1/2 (*Drosophila* LIMK1) and TESK1/2 (*Drosophila* Cdi). LIMK is activated by Rho-associated protein kinase (ROCK). Cofilin is activated by dephosphorylation at Ser3 by the phosphatases chronophin (CIN, *Drosophila* CG5567) and Ssh1 (*Drosophila* Ssh). Localization and activation of Ssh is mediated by the type I coronin, Coro1B (discussed in more detail in following sections). Ssh can also be regulated by other kinases and phosphatases. CIN is activated by a number of mechanisms, including by Rac2. Used with permission from (Bravo-Cordero et al., 2011).

(Bamburg, 1999; Morgan et al., 1993; Wang et al., 2007; Bravo-Cordero et al., 2013). Consistent with this, mutation of Ser3 to glutamic acid (S3E), which mimics the phosphorylated state, results in only 10% of the actin depolymerization activity as wild-type ADF *in vitro* (Agnew et al., 1995). Dephosphorylation at Ser3 by Slingshot (Ssh) or Chronophin (CIN) reactivates ADF/cofilin (Bravo-Cordero et al., 2013; Wang et al., 2007; Agnew et al., 1995). Dephosphorylation occurs rapidly (30s) in response to cell stimulation and results in changes in cytoskeleton organization and assembly, including the breakdown of stress fibers and redistribution of actin to membrane ruffles. Further, activated cofilin becomes concentrated to regions of the cell cortex where actin is dynamic.

Taken together, these data suggest that phosphorylation state of ADF/cofilin regulates actin dynamics. Thus, one would expect in stimulated conditions, the pool of dephosphorylated/activated ADF/cofilin increases at the expense of phosphorylated pool. In some systems, however, actin dynamics occur without the expected decrease in the ratio of phosphorylated to dephosphorylated ADF/cofilin (Bamburg, 1999). Instead, the ratio is unchanged but the turnover of the regulatory phosphate increases, indicating that at least some ADF/cofilin regulatory pathways act by affecting both the kinase and the phosphatase responsible for the activity cycle and that the turnover rate may be more critical in regulating actin dynamics than a net change in phosphorylation state. In Chapter 2, we show that the Tsr phospho-regulators LIMK1, Cdi and Ssh are also required for muscle development in the *Drosophila* embryo.

In vivo functions of ADF/cofilin: evidence from genetic model organisms

Yeast

Saccharomyces cerevisiae and *Schizosaccharomyces pombe* each express a single ADF/cofilin family member (Moon et al., 1993). This protein is named Cofilin as it shares slightly more homology with mouse cofilin than human ADF (41% versus 37%). The essential role of ADF/cofilin was first demonstrated in *S. cerevisiae*. Disruption of yeast Cofilin is lethal as yeast are not able to divide. This phenotype could be rescued by expressing either mammalian ADF or Cofilin, demonstrating a functional similarity between these proteins (Moon, et al., 1993).

Caenorhabditis elegans

The two ADF/cofilin family members in *C. elegans* are derived from alternative splicing of the *unc-60* gene (McKim et al., 1994; Ono et al., 1998). UNC-60A is ubiquitously expressed and is essential for viability (Ono et al., 1999). In support of this, no mutations have been isolated in the *unc-60A* gene, suggesting that UNC-60A is similar to ADF or non-muscle cofilin (Ono et al., 1994). In contrast, UNC-60B is muscle-specific isoform and is upregulated in the developing body wall muscle, suggesting that UNC-60B is more similar to mammalian CFL2 (Abe et al., 1989; Nagaoka et al., 1996; Ono et al., 1994; 1998; 1999).

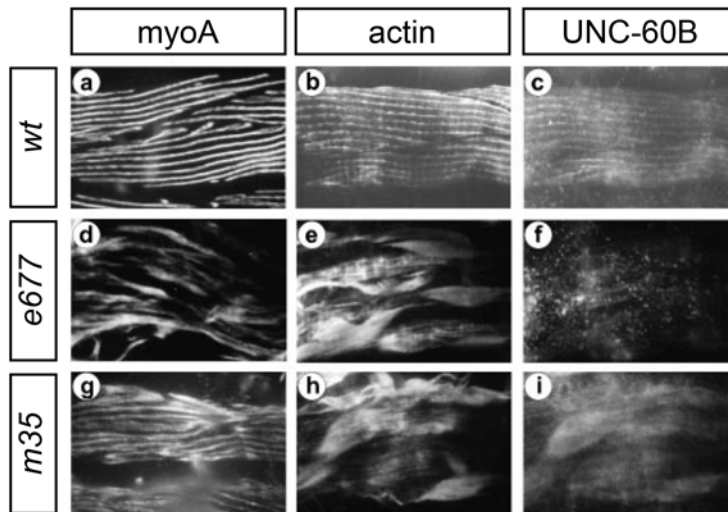


Figure 1.28. Defects in adult myofibril organization in *unc-60* mutants. Localization of myosin (*myoA*), actin and UNC-60B in the adult body wall muscle of wild-type and the *unc-60b* mutants, *e677* and *m35*. Actin and UNC-60B were observed by double staining. In *unc-60b* mutants, sarcomeric actin is disorganized. Bar, 10 μ m. Used with permission from (Ono et al., 1999).

UNC-60B is localized to both the cytoplasm and striations in myofibrils. Mutations in *unc-60B* result in severe disorganization of myofibrils, including actin filament organization (Figure 1.28). In *unc-60B* mutants, actin filaments formed thick bundles and accumulations in embryonic and adult body wall muscle, suggesting that UNC-60B is required for proper actin filament organization in muscle fibers (Ono et al., 1999).

Chicken

Chick ADF was the first identified member of the ADF/cofilin family, and chicken cofilin was identified 10 years later (Bamburg et al., 1980; Abe et al., 1990). Both ADF and cofilin are expressed in young myogenic cells, but ADF decreases during muscle development and cannot substitute for the absence of cofilin (Bamburg et al., 1987; Abe et al., 1989). Microinjection of an antisense morpholino oligonucleotide (MO) to cofilin into 3-day old (developing) chicken skeletal myotubes disrupted the formation of striated actin filament bundles and partially disrupted α -actinin organization at Z-bands *in vitro* (Miyachi-Nomura et al., 2012). When the antisense MO was injected into 5-day old, “developed” myotubes, however, actin was not disrupted despite the clear depletion of cofilin, suggesting that cofilin is required for the assembly of actin during myofibrillogenesis but not for its maintenance in the short-term. This is consistent with previous observations that indicate that actin in developing myotubes is more sensitive to the actin drug, Latrunculin A, than actin in mature myotubes (Wang et al., 2005). Furthermore,

overexpression of cofilin caused transient disorganization of actin, suggesting that proper concentration/activity/regulation of cofilin required for proper actin organization during sarcomere assembly (Miyachi-Nomura et al., 2012).

Drosophila melanogaster

Drosophila encodes a single ADF/cofilin family member, Twinstar (Tsr) (Edwards et al., 1994; Gunsalus et al., 1995). Tsr is most closely related to nonvertebrate homologs, with sequence identities ranging from 36-39% (Gunsalus et al., 1995; Bamberg et al., 1999; Lappalainen et al., 1998). Twinstar retains distinct homology to the described NLS identified in mammals and birds, suggesting that it can translocate to the nucleus; however, until this study (Figure 2.1G) there was not yet evidence that it did (Gunsalus et al., 1995). Furthermore, homologs of the kinases and phosphatases responsible for regulating cofilin, Limk1/2 (only LIMK1 in *Drosophila*) and Tesk1/2 (Cdi in *Drosophila*) and Slingshot and chronophin (CG5567), respectively, are present in *Drosophila*, and they play a conserved role when it has been analyzed (Niwa et al., 2002; Ohashi et al., 2000; Sese et al., 2006).

Unsurprisingly, Tsr function has been implicated in a number of actin-dependent processes during *Drosophila* development, including cytokinesis in mitotic (larval neuroblast) and meiotic (larval testis) cells (Gunsalus et al., 1995). For example, spermatocytes homozygous for a hypomorphic allele of *tsr* (*tsr¹*) exhibit defects in aster migration and separation during early stages of meiosis and

the presence of large actin accumulations at the site of contractile ring formation, which fail to disassemble, at the end of meiosis. Twinstar is also required during ovary development and oogenesis for the convergence and extension needed to form terminal filament cells and the protrusion of lamellipodia during border cell (BC) migration (Chen et al., 2001; Zhang et al., 2011). In both contexts, F-actin accumulates aberrantly in *tsr* mutants, indicating that Tsr plays a conserved role in actin turnover during these morphogenetic events. In fact, the accumulation of F-actin is a hallmark of cofilin/Tsr mutant phenotypes. Moreover, Tsr activity must be properly regulated during BC migration: overexpression of constitutively active Tsr (S3A) or dominant negative Tsr (S3E) both resulted in significantly shorter protrusions at the leading edge of BCs, indicating that the rate of actin turnover must be finely tuned to generate protrusions of the optimal length (Zhang et al., 2011). Tsr is also required for the planar cell polarity (PCP) pathway. *tsr* mutants have PCP pathway-like defects in wing, thorax, leg, abdomen and eye (Blair, et al., 2006). To date, a role for Tsr in muscle development in *Drosophila* has not been described. In Chapter 2, I will present data showing that Tsr is required for the proper development of and the proper function of the embryonic and larval body wall muscles, respectively.

Mouse

Mice encode three ADF/cofilin family members, ADF (or destrin), Cofilin 1 (Cfl1), and Cofilin 2 (Cfl2), which play tissue-specific roles in actin depolymerization and

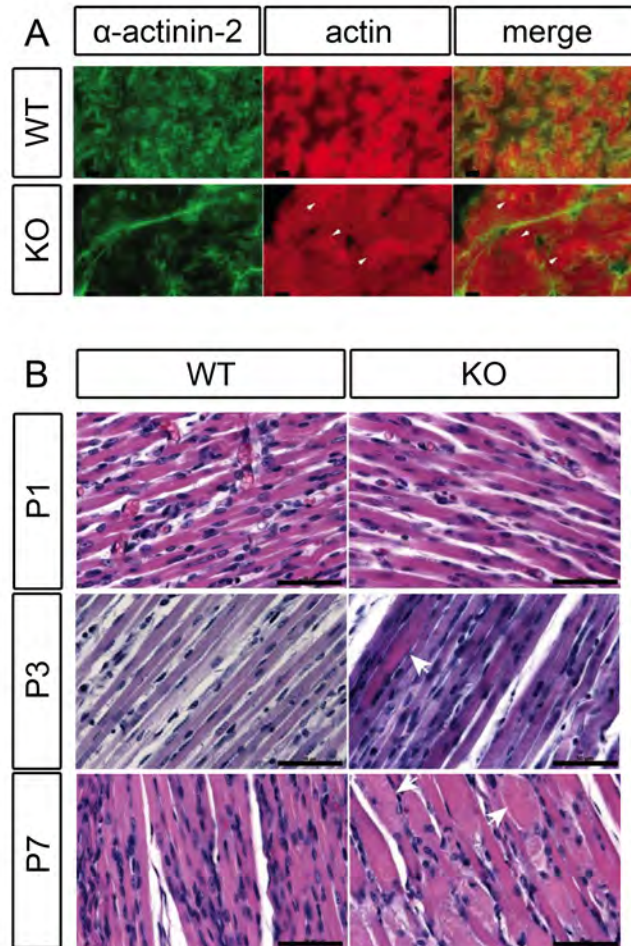


Figure 1.29. Progressive muscle defects in *Cfl2^{-/-}* mice. (A) Muscle sections from WT and *Cfl2^{-/-}* (KO) mice were immunostained with anti-actinin-2 (green) and phalloidin (red). Actin accumulations in *Cfl2^{-/-}* sections are indicated by arrowheads. Bar, 10 mm. (B) H&E staining of muscle sections from WT and *Cfl2^{-/-}* (KO) mice at post-natal (P) days 1, 3 and 7. At P1, the muscles from WT and KO mice appear similar. By P3, occasional degenerating muscles are observed in KO mice (arrow). On P7, numerous degenerated fibers are present in KO mice (arrows). Bar, 50 mm. Modified with permission from (Agrawal et al., 2012).

have different requirements for development. Destrin is expressed at low levels in the developing embryo and is nonessential for development (Gurniak et al., 2005). Cfl1 is highly and broadly expressed throughout development and is essential for embryonic development. At E9.5, homozygous *cfl1* null embryos appear wild-type and are present at the expected ratio; however, at E10.5, mutant embryos are significantly smaller and display a number of phenotypes, including defects in neural tube closure and somite pair alignment (Gurniak et al., 2005; Mahaffey et al., 2013).

In contrast, *Cfl2* is predominantly expressed in skeletal muscle and is dispensable for embryonic development (Gurniak et al., 2005; Ono et al., 1994; Thirion et al., 2001; Agrawal et al., 2012). *Cfl2* null mice are indistinguishable from their wild-type littermates and are born at the expected ratio (Agrawal et al., 2012). By post-natal (P) day 7, however, they are significantly smaller, and none survive longer than P8. Histological analysis of several muscle groups revealed a proportional decrease in muscle size, a progressive disruption in sarcomere organization and accumulations in F-actin (Figure 1.29). Thus, *Cfl2* does not appear to be required for muscle development but is essential for muscle maintenance in the mouse.

The coronin family of proteins

Unlike other Arp2/3-binding proteins, coronin family proteins inhibit Arp2/3 actin nucleation activity. Coronins also regulate the ADF/cofilin pathway to enhance actin disassembly or to prevent cofilin-mediated severing. Thus, the emerging

consensus indicates that coronin family proteins balance the activities of Arp2/3 and ADF/cofilin proteins to modulate actin dynamics by enhancing the assembly/disassembly cycle (Chan et al., 2011). The first coronin family member was identified in *Dictyostelium discoideum* and was so named because it localized to crown-like dorsal projections (de Hostos et al., 1991). Coronins have since been identified in the majority of eukaryotic organisms and are separated into three classes based on their sequence (Xavier et al., 2008; de Hostos et al., 2008; Utrecht et al., 2006; Clemen et al., 2008).

Structure

Coronin family proteins are defined by the presence of five canonical WD40 repeats, which form β -propeller structures and mediate protein-protein interactions, flanked by short, highly conserved extensions, which may also regulate coronin interactions with other proteins (Figure 1.29A) (de Hostos et al., 1991; Appleton et al., 2006). Together, these form a seven-bladed β -propeller (Appleton et al., 2006). The N- and C-terminal extensions also contain residues that do not participate in the formation of the β -propeller structure, but appear to play important roles in regulating coronin function or in maintaining the stability of the β -propeller. For example, the highly basic N-terminal extension contains an important phosphorylation site that regulates interaction of coronin with other proteins and a portion of the C-terminal extension packs tightly against the β -propeller for additional stabilization of the structure (Cai et al., 2005). Most

coronins also contain a C-terminal coiled-coil domain that mediates homo-oligomerization, which is linked to the conserved β -propeller unit by a highly variable unique region (Cai et al., 2005; Goode et al., 1999; Oku et al., 2005; Gatfield et al., 2005). Oligomerization is required for the full activity of coronins and has been shown to be important for bundling actin filaments (Goode et al., 1999). This structure is generally conserved amongst the three classes of coronins; however, Type II coronins contain additional conserved residues that are predicted to form loops in the β -propeller structure and differ greatly in their unique region from Type I coronins. Furthermore, Type III coronins completely lack the coiled-coil domain, but do encode two complete β -propeller units, which may bypass the need to oligomerize (Figure 1.29A) (Rybakin et al., 2005).

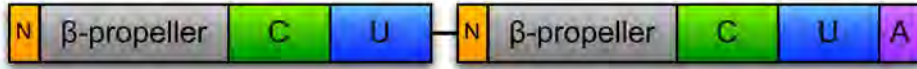
Type I, II, III coronins

With the exception of yeast, which only encodes a single Type I coronin (CRN1), most organisms contain a short form Type I/II (450-650 amino acids) and a long form Type III (925-1075 amino acids) coronin (Utrecht et al., 2006; de Hostos et al., 2008; Clemen et al., 2008). *Dictyostelium*, *Drosophila* and *C. elegans* each encode a single short and long form coronin; the short form coronin in these organisms is generally considered to be Type I-like. In vertebrates, however, all three classes of coronins are present (Utrecht et al., 2006). For example, seven coronin genes are present in mammals: four Type I coronins, two Type II coronins (unique to vertebrates) and a single Type III coronin.

A Type I/II Coronins



Type III Coronins



B

		10	20	30	40	50	60	70
<i>Hs CORO1A</i>	MS	RQVVRSSKFRHVFGQ	PAKA	DQCYEDV	RVRSQTTWDS	GFCAVNPKFVALIC	EASGGGAFLVLP	LGKTGR
<i>Mm Coro1a</i>	MS	RQVVRSSKFRHVFGQ	PAKA	DQCYEDV	RVRSQTTWDS	GFCAVNPKFMALIC	EASGGGAFLVLP	LGKTGR
<i>Dm Coro</i>	MS	FRVVRSSKFRHVYGA	LKR	EQCYDNR	IRVRSKSSWDS	TFCAVNPKFLAIV	ESAGGGAFLVLP	HNKVGR
<i>Scer CRN1</i>	MSG	KFVRAISKYRHVFGQ	AAKK	ELQYEK	LKVTNNAWDS	NLLKTNKGFIAV	NWNASGGGAFAV	ITPEVIGK

		80	90	100	110	120	130	140
<i>Hs CORO1A</i>	V	DKNAPTVC	GHGHTAPVLDIAWCP	HNDNVIASGSEDC	TVMVWEIPDG	GLMLPLR	-----	EPVVTLEIGH
<i>Mm Coro1a</i>	Y	DKNAPLV	CGHTAPVLDIAWCP	HNDNVIASGSEDC	VMVWEIPDG	GLVLP	-----	EPVITLEIGH
<i>Dm Coro</i>	I	AADHPLV	GHGHTAPVLDIAWCP	HNDNVIASGSEDC	VKVMQIPDG	GLSRTLT	-----	EPVVDLVFHH
<i>Scer CRN1</i>	A	PQVPLFR	GHGHTAPVLDIAWCP	HNDNVIASGSDDS	KIIGIWDIPENY	KFHDHVD	EDGEPIDIK	PKVFLTIGH

		150	160	170	180	190	200	210
<i>Hs CORO1A</i>	T	KRVGIVAWHTA	CNVLLSAGC	DNVTIMVWDV	GTGAAMLT	LGREVHPDT	IYSVDWSR	DGGLICT
<i>Mm Coro1a</i>	T	KRVGIVAWHPTA	CNVLLSAGC	DNVTIMVWDV	GTGAAMLT	LGREVHPDT	IYSVDWSR	DGGLICT
<i>Dm Coro</i>	Q	RRVGLVLWHPSA	LNVLLTAGS	DNQVVIWNVGTGE	ILVRIID	SHPDIVYSA	CFNW	DGSKLVIT
<i>Scer CRN1</i>	A	RKVGIVLYHPVA	ENVLAS	SSGDYTYIKLWN	VETGKDMITL	LK--	HPDMVTSMS	FSDGNYLATAVARDKKL

		220	230	240	250	260	270	280
<i>Hs CORO1A</i>	R	IIEPRKIGTVVA	EKDRP	HEGTRPV	RAVFEVSE	GKILTTGFSR	MSE	ROVALWDTKHLEEP--
<i>Mm Coro1a</i>	R	VIEPRKIGTVVA	EKDRP	HEGTRPV	HAVFVSE	GKILTTGFSR	MSE	ROVALWDTKHLEEP--
<i>Dm Coro</i>	R	IYDPRTAELLES	EA-MCHEGSKA	TRAIFLRH	GLIFTTGFNR	SERQYS	LRA	PDALENEP--
<i>Scer CRN1</i>	R	VWNTRIEEKIVS	EG-PAHITGAK	KNQRYVWLGNS	DRLAT	TGFSKLS	SDRQTG	IWDAFNIEKGLDGGFYTVDDQS

		290	300	310	320	330	340	350
<i>Hs CORO1A</i>	S	GVLLPFFDP	DTNIVYLCGKGDSS	IRYFEITS	EA	PFLHYLSMFS	SKES	ORGMGYMPKRGLEVNKCEIARF
<i>Mm Coro1a</i>	S	GVLLPFFDP	DTNIVYLCGKGDSS	IRYFEITS	EA	PFLHYLSMFS	SKES	ORGMGYMPKRGLEVNKCEIARF
<i>Dm Coro</i>	N	GMVMPFLYDADT	NMIYLCGKGDSS	IRYFEVTEP	PEPFVHYINT	FQTT	EP	QRGIGLMPKRGCDVITCEVAKEF
<i>Scer CRN1</i>	S	GLMPFFYDEGNR	ITLYLVGKGDGN	IRYYE	FONDE--	LF	LS	EFQSTEAQRGFALVAPKRMVNVKENEVLKIG

		360	370	380	390	400	410	420
<i>Hs CORO1A</i>	Y	KLHER-RCEPI	AMTVPRKSDLFQEDLYP	P	TAGP	DPALTAEEWLGGRDAG	P	LLISLKDGYVPRKLSRE--
<i>Mm Coro1a</i>	Y	KLHER-KCEPI	AMTVPRKSDLFQEDLYP	P	TAGP	DPALTAEEWLGGRDAG	P	LLISLKDGYVPRKLSRE--
<i>Dm Coro</i>	Y	RMNNGLCQV	ISMTVPRKSDLFQEDLYP	O	TLA	EDAATAEEWIDGKDA	D	PITFSLKGGYVSSVNSKSL
<i>Scer CRN1</i>	F	KITVVQDR	IEPVSFFVPRRSE	EFQEDLYP	DA	PSNK	PALTAEEWFS	GKSV

		430	440	450	460	470	480	490
<i>Hs CORO1A</i>	---	LRVNRG	---	LDTGR	---	RRAAPEAS	GT	PS
<i>Mm Coro1a</i>	---	LRVNRG	---	LDSAR	---	RRATPEPS	GT	PS
<i>Dm Coro</i>	P	AKRAGN	I	LNKPRGDS	A	SSGATSS	S	AGGGNFA
<i>Scer CRN1</i>	H	EAKR	PQOPT	GETAL	E	EKK	EQPK	V

		500	510	520	530	540	550	560
<i>Hs CORO1A</i>	---	---	---	SDA	V	SRLE	EE	MRK
<i>Mm Coro1a</i>	---	---	---	S	D	V	SRLE	EE
<i>Dm Coro</i>	---	---	---	E	K	L	R	T
<i>Scer CRN1</i>	L	K	K	S	S	D	I	D

		570	580	590	600	610	620	630
<i>Hs CORO1A</i>	---	---	---	---	---	---	---	---
<i>Mm Coro1a</i>	---	---	---	---	---	---	---	---
<i>Dm Coro</i>	S	D	A	P	A	S	A	G
<i>Scer CRN1</i>	Q	E	Q	S	L	P	Q	E

		640	650	660
<i>Hs CORO1A</i>	---	---	---	---
<i>Mm Coro1a</i>	---	---	---	---
<i>Dm Coro</i>	---	---	---	---
<i>Scer CRN1</i>	L	E	D	V

Figure 1.30. Coronin family of proteins. (A) Domain structure of type I/II and type III coronins. Type I and II coronins share a similar structural organization, including N-terminal (N) and C-terminal (C) extensions, which flank a β -propeller, a unique region (U) and a coiled-coil domain (CC). Type III coronins lack a CC, but are comprised of two full β -propeller units and a C-terminal acidic region (A). (B) Amino acid alignment of selected type I coronins. Conserved amino acids are bolded and shaded grey. *Hs*, *Homo sapiens*; *Mm*, *Mus musculus*; *Dm*, *Drosophila melanogaster*; *Scer*, *Saccharomyces cerevisiae*.

Type III coronins are distinct in both structure (discussed above) and function. Members of this coronin subfamily include *CORO7* (mammals), *pod-1* (*C. elegans*), *pod1* (*Drosophila*) and *CRN7* (*Dictyostelium*) (Rybakin et al., 2004; Rappleye et al., 1999; de Hostos et al., 1993; Rothenberg et al., 2003). Interestingly, the sequence of Type III coronins is highly conserved across species, but their function appears to have diverged in mammals. Type III coronins in *C. elegans*, *Drosophila* and *Dictyostelium* are involved in actin-dependent processes, including cell polarity and vesicular trafficking in *C. elegans*, growth cone guidance in *Drosophila* and directed migration and phagocytosis in *Dictyostelium* (Shina et al., 2010; 2011; Maniak et al., 1995; Rothenberg et al., 2003; Tagawa et al., 2001; Rappleye et al., 1999). Human Coro7, however, does not appear to interact with the actin cytoskeleton and plays a role in Golgi morphology and membrane trafficking (Rybakin et al., 2004).

F-actin-binding

Coronin was originally identified based on its ability to bind F-actin, and with the exception of mammalian Coronin 7, all coronins to date also show F-actin-binding activity (Rybakin et al., 2004; 2005; Chan et al., 2011). Coronins bind actin filaments sides with high affinity where it can bundle filaments and synergize with ADF/cofilin to sever filaments (de Hostos et al., 1991; Goode et al., 1999; Briehner et al., 2006; Cai et al., 2007; Gandhi et al., 2009). The human Type I coronin, Coro1B, exhibits a 50-fold higher affinity for newer ATP/ADP + Pi filamentous actin over

older ADP-bound F-actin (Cai et al., 2007). A similar observation has been made for budding yeast Crn1p suggesting that this is a shared property of Type I coronins (Gandhi et al., 2009).

Early attempts using recombinant fragments to map the domain(s) responsible for actin-binding have been problematic and nearly every portion of coronin has been suggested to have actin-binding ability (Goode et al., 1999; Gatfield et al., 2005; Spoerl et al., 2002; Liu et al., 2006; Oku et al., 2003; Uetrecht et al., 2006). A number of these studies agree that at least one actin-binding site resides in the β -propeller (Appleton et al., 2006; Cai et al., 2007; Galkin et al., 2008h; Goode et al., 1999; Oku et al., 2003; Uetrecht et al., 2006). Systematic mutation of residues within the β -propeller have provided a higher resolution picture of the residues responsible for actin-binding (Cai et al., 2007; Kimura et al., 2010; Tsujita et al., 2010; Gandhi et al., 2010). In *S. cerevisiae*, five conserved surface residues (Crn1-2, Crn1-6, Crn1-13, Crn1-17, Crn1-19), which form a ridge across the β -propeller structure and are encoded in four of the seven blades of the β -propeller, are important for actin-binding (Gandhi et al., 2010). Similarly, mutation of a single conserved residue (Arg30) in a charged patch on the β -propeller surface of three Type I coronins, Coro1A, Coro1B and Coro1C diminished F-actin binding (Cai et al., 2007; Gandhi et al., 2010; Kimura et al., 2010; Tsujita et al., 2010). This residue is not conserved in Type II coronins, suggesting that they may utilize an alternative actin-binding surface (Cai et al., 2007).

S. cerevisiae Crn1 also harbors a potential second actin-binding site in its coiled-coil domain (Gandhi et al., 2009). Importantly, Crn1 in which the coiled-coil domain is deleted (Crn1 Δ CC) is still able to bind F-actin, albeit with a lower affinity than full-length Crn1, suggesting that multiple actin-binding domains contribute to the ability of coronin to bind F-actin. A more recent study, however, failed to detect actin-binding with a fragment containing the coiled-coil domain (Liu et al., 2011).

Interactions with ADF/cofilin

One mechanism by which coronin regulates actin dynamics is by modulating ADF/cofilin activity (Figure 1.31). This was first observed in yeast where mutations in *CRN1* genetically synergized with mutations in *cof1* and has since been shown for a number of contexts in which dynamic actin regulation is required (Goode et al., 1999; Gandhi et al., 2010). In *Listeria*, for example, Coro1A and Aip1 enhance the cofilin-based disassembly of actin comets, and depolymerization from the barbed ends occurs in bursts (Kueh et al., 2008). In addition, coronin regulates cofilin by both preventing cofilin from binding to new actin filaments and enhancing cofilin binding to older actin filaments (Bravo-Cordero et al., 2013; Chan et al., 2011). Full-length Crn1p and human Coro1B block the binding of cofilin to ATP-bound F-actin (Cai et al., 2007; Gandhi et al., 2009). Deletion of coiled-coil domain enhances cofilin-binding to F-actin, suggesting that the coronin coiled-coil domain is responsible for regulating this activity.

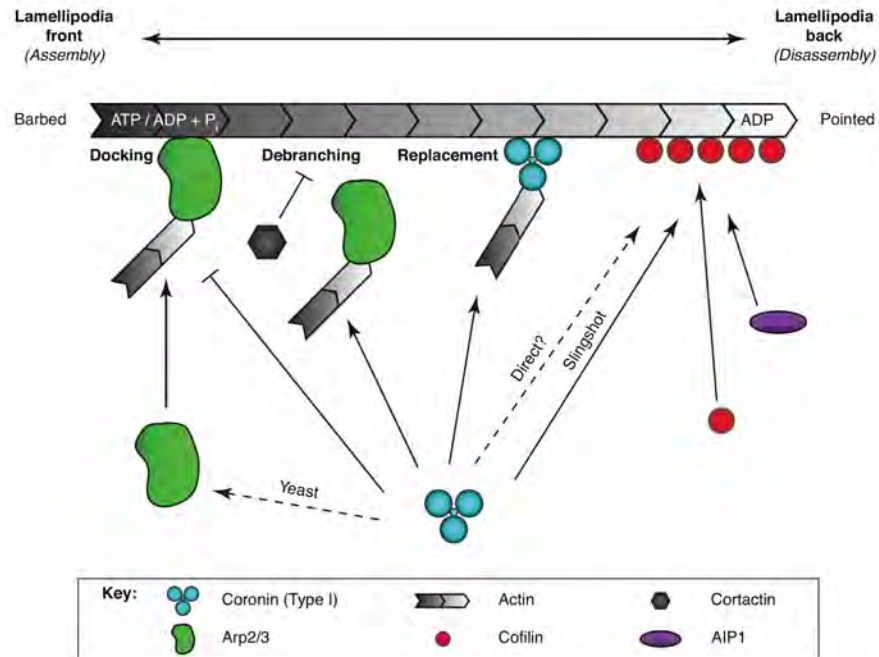


Figure 1.31. Model of type I coronin function. Coronin (blue) coordinates Arp2/3-based actin polymerization (left) and cofilin-mediated disassembly (right). At sites of active polymerization, Arp2/3 promotes actin assembly by nucleating new branches. Coronin inhibits Arp2/3 function by inhibiting Arp2/3 docking or facilitating debranching in a mechanism that antagonizes cortactin. Coronin can also replace Arp2/3 at actin branches and create more flexible branches. At sites of depolymerization, cofilin facilitates actin disassembly. Coronin enhances the activity of cofilin either directly or by targeting the Ssh. Dashed lines indicate interactions that have only been observed in one model organism or require further validation by functional studies *in vivo*. Used with permission from (Chan et al., 2011).

In addition, Coro1B interacts with the cofilin-activating phosphatase Ssh and directs Ssh to sites of active actin remodeling (Cai et al., 2007). Depletion of Coro1B suppresses overexpression phenotypes of Ssh, suggesting that the interaction of Coro1B and Ssh has a functional consequence.

Interactions with Arp2/3

Type I coronins also directly interact with Arp2/3 and inhibit its ability to nucleate actin filaments by stabilizing Arp2/3 in an inactive conformation, preventing the docking of Arp2/3 onto existing actin filaments (Figure 1.31) (Rodal et al., 2005; Cai et al., 2007; Humphries et al., 2002). Coronin family members are the only known protein inhibitors of Arp2/3. However, yeast coronins demonstrate a concentration-dependent regulation of Arp2/3, inhibiting at low concentrations and activating at high concentrations (Chan et al., 2011). This activity is mediated by a CA-like sequence that is not conserved in higher organisms, suggesting that it may not be a conserved property. In addition to preventing Arp2/3 from binding to existing filaments, coronin proteins also induce the dissociation of Arp2/3 from F-actin (Figure 1.31). This function seems to be mediated by inhibition of the class II NPF, cortactin, which, in addition to activating Arp2/3, also stabilizes Arp2/3 branches (Weaver et al., 2002; Chan et al., 2011). Thus, the mechanism of Arp2/3 inhibition by coronin may be two-fold. Finally, Coro1B has been observed to replace Arp2/3 at branch sites, and its presence alters the branch angle from about 70° to 80°

degrees. This function might serve to generate a more flexible actin network and aid in the formation of actin arcs (Chan et al., 2011).

In vivo functions of coronin: evidence from genetic model organisms

Dictyostelium discoideum

The first coronin family member was identified in *Dictyostelium* in a screen to isolate new actin-binding proteins essential for driving shape changes and chemotaxis (de Hostos et al., 1991). CRN12 (Type I, also corA) localizes to crown-like projections on the dorsal surface of cells during the growth phase and strongly accumulates in regions where actin is also enriched. In aggregating cells, projections are restricted to actin-rich lamellipodia and filopodia at the cellular front; accordingly, CRN12 is also enriched here, suggesting that CRN12 is an actin-binding protein *in vivo*. Mutation of both short and long coronins (Type III, CRN7, also corB) results in growth and migration defects (de Hostos et al., 1993). Importantly, cells migrate with the proper orientation, suggesting that chemotaxis is unaffected. Additionally, coronin null cells become multinucleated and further analysis indicates this is due to a defect in cytokinesis. In contrast, however, mutation of CRN7 alone does not affect growth, migration or cytokinesis, suggesting that the defects observed are due to the loss of CRN12 alone (Shina et al., 2010; 2011).

CRN12 and CRN7 are also localized to phagocytic cups in *Dictyostelium* (Maniak et al., 1995; Shina et al., 2010). The rate of phagocytosis decreases in the absence of both coronins or of CRN12 alone, while the loss of CRN7 has pathogen-dependent effects on phagocytosis, suggesting that while Type I and Type III coronins participate in the same developmental processes, they can have opposing roles (Maniak et al., 1995; Shina et al., 2010; 2011). Somewhat surprisingly, however, both CRN12 and CRN7 are dispensable for actin polymerization, actin filament localization and crown formation (de Hostos et al., 1993).

Saccharomyces cerevisiae

A single coronin family member, Crn1p, has been identified in *S. cerevisiae*. Crn1p is most similar to *Schizosaccharomyces pombe* coronin (70%), but retains high similarity to *C. elegans* (48%), *Dictyostelium* (57%) and human (56%) coronins (Figure 1.29B) (Heil-Chapdelaine et al., 1998). Crn1p also contains an insertion that shares homology with the microtubule-binding region of MAP1B (Noble et al., 1989; Goode et al., 1999). Consistent with this, Crn1p can bind both actin and microtubules, promote actin assembly and cross-link actin filaments into bundles and microtubules with actin filaments (Goode et al., 1999). In budding yeast, Crn1p colocalizes to cortical patches with actin in a manner similar to *Dictyostelium* coronins at the dorsal crown (de Hostos et al., 1993; Heil-Chapdelaine et al., 1998; Goode et al., 1999).

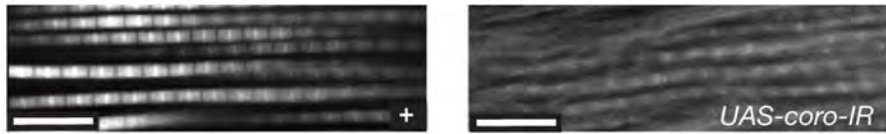


Figure 1.32. Muscle-specific depletion of *coronin* results in frayed myofibrils in adult indirect flight muscles. *Dmef2-Gal4* was used to express *UAS-coro-IR* in the *Drosophila* musculature. Thoraces were bisected and immunolabeled with phalloidin (grey scale) to label actin. Depletion of *coro* resulted in thin, frayed myofibrils (right) compared to wild-type (left). Used with permission from (Schnorrer et al., 2010).

Further, Crn1p localization to cortical patches depends on F-actin (Heil-Chapdelaine et al., 1998; Goode et al., 1999). Surprisingly, however, deletion of *CRN1* does not affect any actin-based behaviors, including polarized growth and secretion, endocytosis or bud-site selection, perhaps reflecting differences in coronin function from *Dictyostelium* to budding yeast or the presence of redundantly acting proteins. Indeed, mutating *CFL1* (cofilin) or *ACT1* (actin) in *crn1* null cells results in growth defects, an accumulation of actin filaments near the bud neck and partial depolarization of cortical actin patches (Goode et al., 1999).

Drosophila melanogaster

Drosophila encodes a single Type I-like coronin, Coro (Figure 1.29B) (Bharathi et al., 2004). *coro* is expressed at a high level throughout embryonic development in all tissues, including the embryonic central nervous system (CNS) (Graveley et al., 2010; Gelbart et al., 2010; Bharathi et al., 2004; Chintapalli et al., 2007). Mutations in *coro* affect a number of adult structures, including the eye, leg and wing (Bharathi et al., 2004). Eyes display a rough eye phenotype and, in the most severe cases, could be completely absent; legs appear short and thick and, in the most severe cases, could be lost completely and wings show vein thickening, Delta-like phenotypes and loss of anterior and/or posterior wing margins. These phenotypes are similar to those observed when the actin cytoskeleton is disrupted. Further analysis of imaginal discs indicates that the

actin cytoskeleton is disrupted, consistent with a role for coronin family members in actin regulation.

To date, the role of coronins in muscle development has not been explored in depth in any system. Data from a systematic screen of muscle morphogenesis in *Drosophila*, however, points to a role for Coro in the development of the adult indirect flight muscles (IFMs): muscle-specific knockdown of *coro* results in thinner myofibrils that appear frayed at muscle ends (Figure 1.32) (Schnorrer et al., 2010). The role that Coro plays during muscle development has not been further explored in *Drosophila* muscle. In Chapter 3, I will describe experiments that indicate Coro has a role in muscle development in the embryo and in muscle function in the larvae and adult.

Summary

Though some differences exist, the formation of multinucleated skeletal muscle is remarkably similar in *Drosophila* and mammals. Both organisms specify mononucleated myoblasts from mesodermal precursors, which then undergo a conserved set of cellular behaviors required for their fusion (Rochlin et al., 2009). Though not discussed in detail here, myofibers in each organism subsequently attach to tendons, assemble their sarcomeres and become innervated by the nervous system, allowing for organism-specific movement. At the molecular level, myoblast specification in *Drosophila* and mammals relies on the activity of bHLH

transcription factors, and myoblast fusion in both systems requires the proper regulation of the actin cytoskeleton.

The actin cytoskeleton is a dynamic microfilament network that is essential for many cellular functions during muscle development. To fulfill its many roles, the actin cytoskeleton is regulated by a host of conserved actin-binding proteins which affect its polymerization (or depolymerization) into F-actin. The contribution of actin depolymerization to muscle development, however, is under appreciated in any system. To address this, we explored the requirement of the sole ADF/cofilin family member, Tsr, and its regulators to muscle development in *Drosophila* (Chapters 2 and 3). In contrast, the necessity of actin polymerization during fusion, particularly Arp2/3-based branched actin, is well-studied in *Drosophila*, and the same processes and proteins are being shown to have a conserved role in mammalian muscle development. We explored whether actin accumulates at the fusion site and Dock1 and IQSec1, mammalian homologs of two GEFs required for myoblast fusion in *Drosophila*, are also required for myoblast fusion using an *in vitro* mouse myoblast line (Chapters 4 and 5). The characterization of the roles of these proteins during muscle development and function will be described in the following chapters.

CHAPTER TWO:

**Twinstar is required for muscle development,
maintenance and function in *Drosophila***

Chapter Overview

The requirement for regulators of actin polymerization during myoblast fusion, including Arp2/3, SCAR/Wave, WASp and Rac has been well documented (Rochlin et al., 2009). Actin filaments, formed by polymerization of actin monomers, must be turned over to replenish the pool of monomers available for continued polymerization. Two families of proteins - the gelsolin/villin and ADF/cofilin families - are responsible for generating free monomers in *Drosophila* and mammals. Despite the identification of these protein families, the role of actin depolymerization has not been described in depth in any muscle system. Work in *C. elegans* indicates that *unc-60B*, the *C. elegans* muscle-specific cofilin, plays a role in sarcomere organization in striated muscle; however, *C. elegans* muscle does not fuse, precluding analysis of the role of cofilin homologs in this process (Ono and Benian, 1998; Ono et al., 1999). Mice null for the muscle-specific cofilin, *Cfl2*, develop normally, likely due to the earlier functions of *Cfl1*, but eventually present with defects in muscle organization and function (Agrawal et al., 2012). Recent studies have identified mutations in Cofilin 2 in two families affected with Nemaline myopathy, suggesting that cofilin may have a role in muscle function after development (Agrawal et al., 2007; Ockeloen et al., 2012). Thus, work to date supports a role for ADF/cofilin homologs in later muscle function, but have yet to describe a role for them in earlier muscle development.

Here, we show that Twinstar (*Tsr*), the only *Drosophila* homolog of the ADF/cofilin family, is expressed in *Drosophila* muscle, and *tsr* mutant embryos

display a number of muscle defects. In addition, Tsr is essential in the muscle: muscle-specific depletion of *tsr* is larval lethal and results in the progressive loss of sarcomeric organization, overall growth defects and locomotor deficiencies. Together, these data demonstrate an essential role for actin depolymerization in muscle development and function in *Drosophila*.

Results

Tsr is expressed in Drosophila body wall muscle

Prior work has examined *tsr* expression in *Drosophila*. *tsr* is maternally loaded [0-2 hours after egg laying (AEL)] and expressed at a high level throughout development (Figure 2.1A) (Gelbart and Emmert, 2010; Graveley et al., 2010). In the embryo, *tsr* is expressed at different stages: at the onset of *twist* (mesoderm-specific transcription factor) and *Dmef2* (muscle-specific transcription factor) expression (2-4 hrs AEL), during myoblast fusion (6-14 hrs AEL), myotendinous junction formation (8-16 hrs AEL) and sarcomere assembly (16-18 hrs AEL). *tsr* expression also remained high throughout larval, pupal and adult stages, where it is expressed in all larval and adult tissues analyzed, including the larval trachea, the larval/adult central nervous system (CNS), digestive system, fat body and salivary gland and the adult head, eye, heart and reproductive systems (Chintapalli et al., 2007). Thus, Tsr appears to be ubiquitously expressed at a high level during *Drosophila* development.

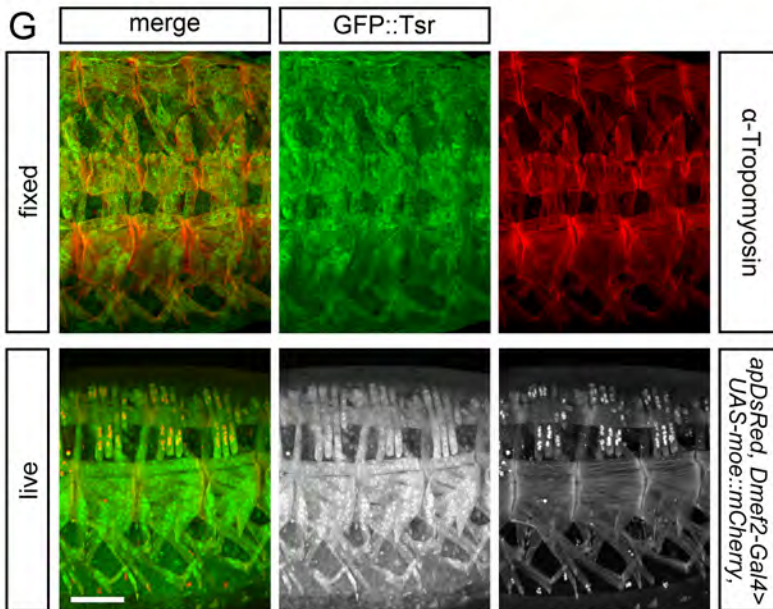
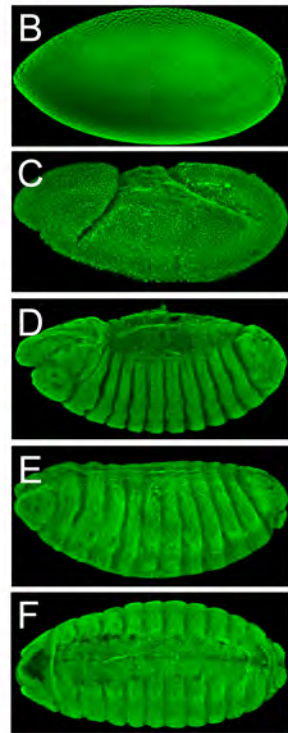
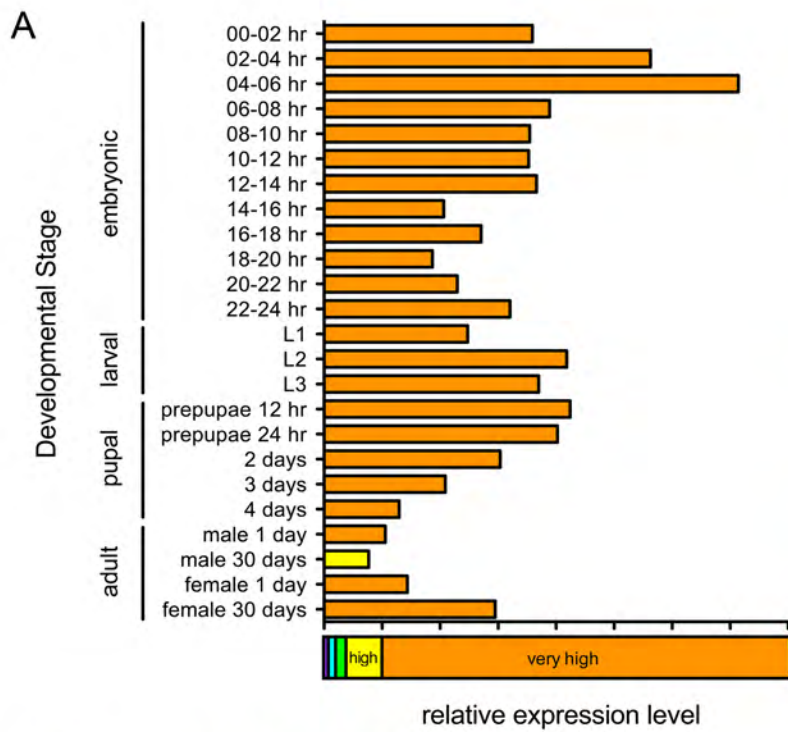


Figure 2.1. Tsr is expressed throughout development and in the somatic body wall muscles of the *Drosophila* embryo. (A) Summary of *tsr* expression over *Drosophila* development. *tsr* is highly expressed throughout embryonic, larval, pupal and adult stages. Modified from (Gelbart et al., 2010; Graveley et al., 2010). (B-F) Maximum intensity projection of *ZCL2393* embryos at stage 5 (B), stage 8 (C), stage 13 (D) and stage 16 (E, lateral view and F, ventral view) labeled with an antibody against GFP (green) to label GFP::Tsr. (G, fixed) Maximum intensity projection of a stage 16 embryo labeled with an antibody against GFP (green) to label GFP::Tsr and Tropomyosin (red) to visualize the embryonic body wall muscle. Three representative hemisegments are shown. (G, live) Endogenous GFP::Tsr was without antibody staining. A live reporter for muscle (*apRed, Dmef2-Gal4>UAS-moe::mCherry*), which labels muscle actin and the nuclei of the lateral transverse (LT) muscles, was used to identify the body wall muscle. Bar, 50 μ m.

Using three Tsr GFP protein trap lines (collectively referred to as GFP::Tsr) where expression of GFP::Tsr is under the control of the endogenous promoter and enhancer elements, we observed Tsr expression and localization *in vivo* (Figure 2.2 A) (Buszczak et al., 2007; Kelso et al., 2004; Morin et al., 2001; Quiñones-Coello et al., 2007). Importantly, in 2 of the 3 lines that we used (*ZCL0613*, *ZCL2393*), the insertion is not lethal, suggesting that the insertion location of GFP does not disrupt normal Tsr function (statement from FlyTrap) (Buszczak et al., 2007; Kelso et al., 2004; Morin et al., 2001; Quiñones-Coello et al., 2007). We found that Tsr is expressed throughout embryonic development, consistent with data reported by modENCODE (Figure 2.1B-F) (Gelbart and Emmert, 2010; Graveley et al., 2010). Further, Tsr is expressed in the embryonic body wall muscles at stage 16 (Figure 2.1G). In fixed imaging, Tsr appeared to be cytoplasmic with no obvious subcellular accumulation within the muscle fiber. Using live analysis of Tsr localization, we again observed cytoplasmic GFP::Tsr localization in embryonic muscle (Figure 2.1G, live). We also detected nuclear accumulation of GFP::Tsr, which had been predicted based on the presence of a nuclear localization sequence, but not previously demonstrated for *Drosophila* Tsr. Expression of *tsr* in muscle is further supported by a genome-wide ChIP-on-chip study in which regions of *Dmef2*-binding enrichment were identified in the 5' untranslated region (UTR) of *tsr* (Figure 2.2A) (Zinzen et al., 2009). Taken together, these data indicate that Tsr is expressed in *Drosophila* body wall muscle and suggest that Tsr could play a role in muscle development. In addition, these expression data indicate that *tsr* is widely expressed and likely plays a role in regulating the actin cytoskeleton in many cell types and tissues.

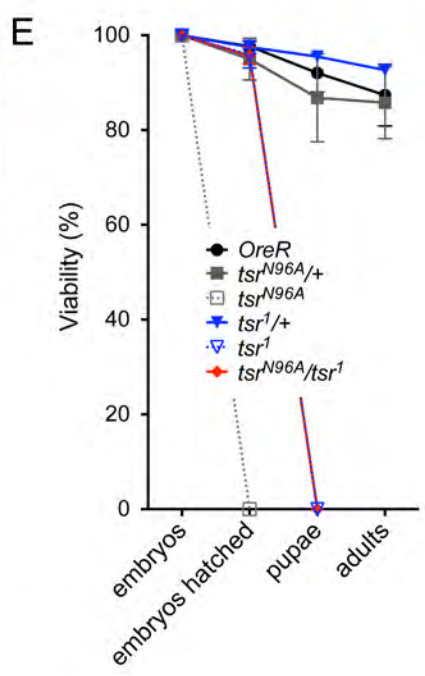
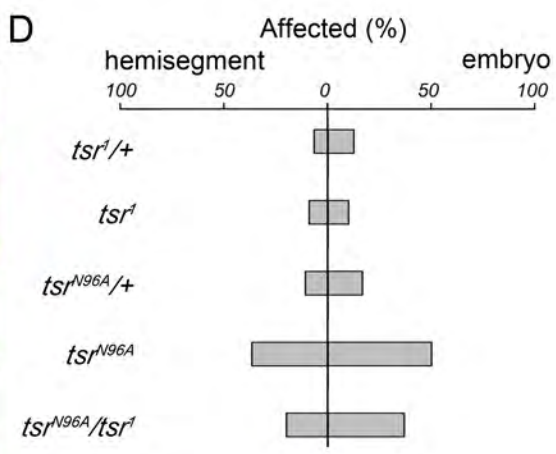
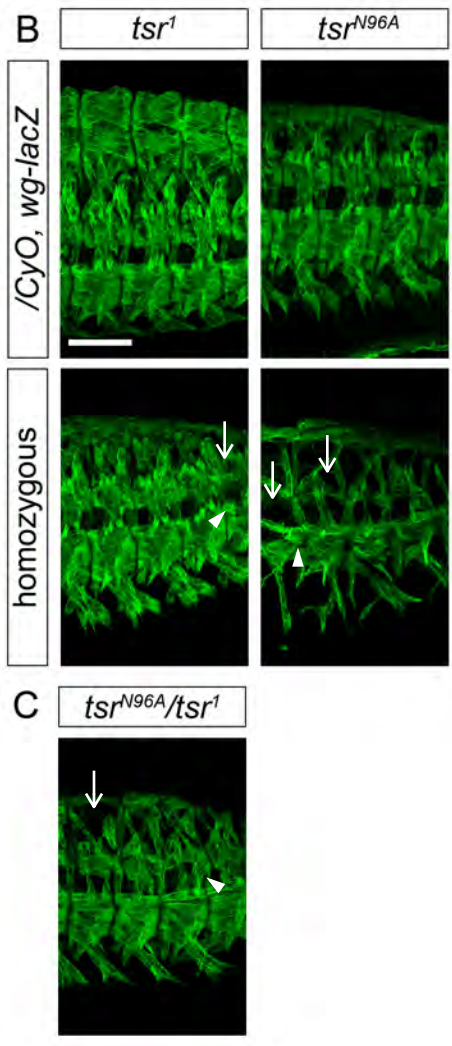
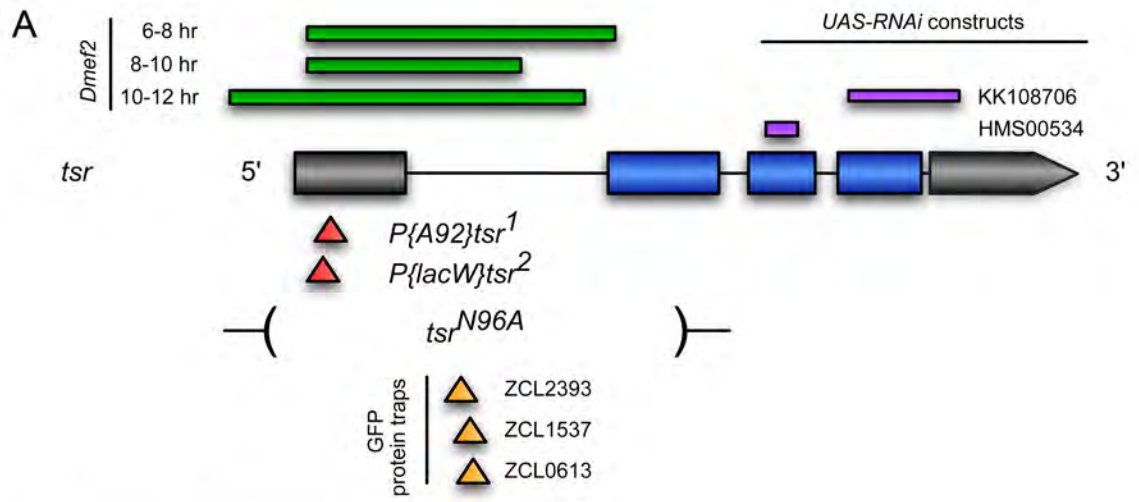


Figure 2.2. Mutation of *tsr* results in defects in embryonic muscle patterning (A) Schematic diagram of the *tsr* locus in *Drosophila*. Green bars above the locus represent regions enriched for Dmef2-binding (Zinzen et al., 2009). Purple bars indicate region targeted by *UAS-RNAi* constructs. Alleles used in this study are indicated below the locus. Grey bars, untranslated regions. Blue bars, exons. Red and orange triangles, P-element insertions. Deletions that remove portions of the *tsr* locus are schematized by a gap in the chromosome bracketed by parentheses. (B-C) Maximum intensity projection of a stage 16 embryo labeled with an antibody against Myosin heavy chain (green) to visualize the embryonic body wall muscle. Three representative hemisegments are shown for each genotype. Arrows indicate missing muscles. Arrowheads indicated misattached muscles. (D) Quantification of the percentage of affected hemisegments (left) and embryos (right) of each genotype indicated. n = 20 embryos, 100 hemisegments. (E) Viability of the indicated genotypes. n = 100. Bar, 50 μ m.

Tsr is required for muscle development in the Drosophila embryo

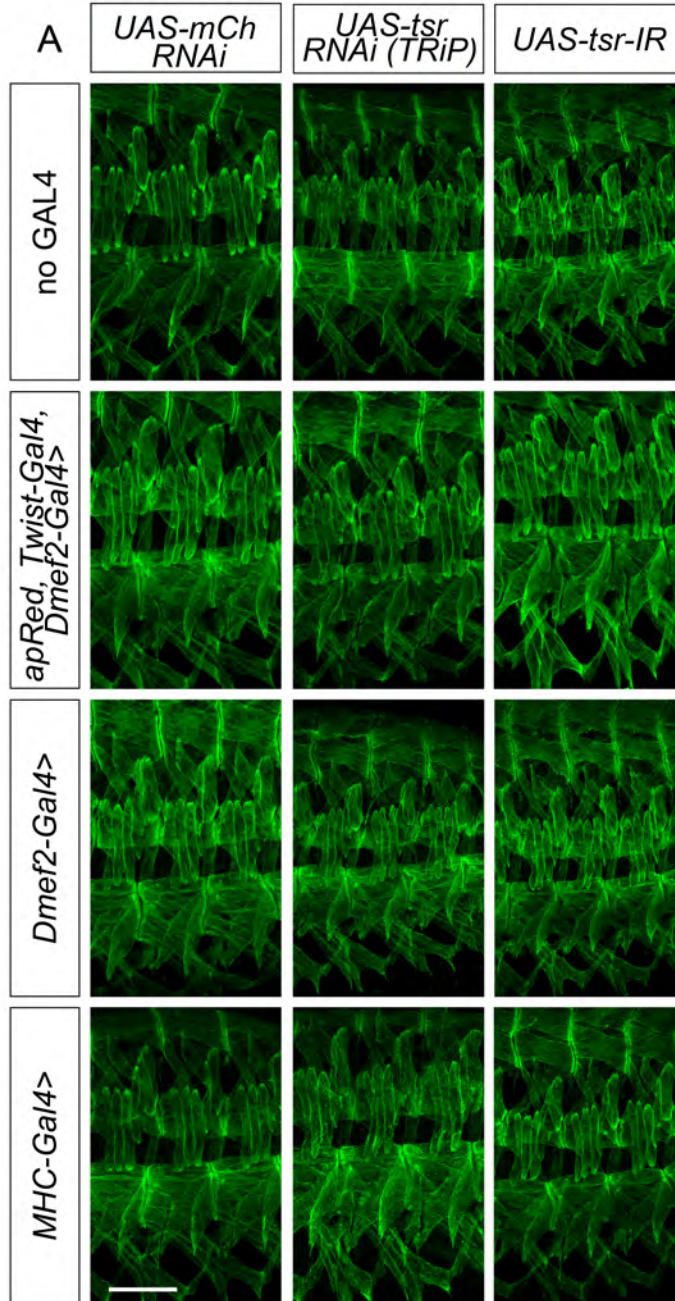
To determine if Tsr is required for muscle development in *Drosophila*, we obtained two well-characterized *tsr* mutant alleles. *tsr¹* is a hypomorphic allele generated by the insertion of a lacZ enhancer trap/P-element in the 5' UTR of *tsr* (Figure 2.2A) (Gunsalus et al., 1995). Approximately 20% of wild-type transcript was detected by Northern analysis in *tsr¹* homozygotes. *tsr^{N96A}* is a null allele, generated from the imprecise excision of a second lacZ enhancer trap, *P{lacW}* *tsr²*. *tsr²* is inserted 19 base pairs upstream of *P{A92}tsr¹* in the 5' UTR, and its imprecise excision deleted ~600 base pairs from the *tsr* locus, including the entire 5' UTR, the initiator ATG codon and nearly half of the first intron (Figure 2.2A) (K. Gunsalus, Ph.D thesis, personal communication).

We found a number of muscle defects in *tsr^{N96A}* mutant embryos, including muscle loss and misattachment (Figure 2.2B, D). These embryos completely failed to hatch, indicating that *tsr* is essential for viability (Figure 2.2E). Fewer muscle defects were observed in *tsr¹* mutant embryos, consistent with it being a hypomorphic allele (Figure 2.2B, D). These embryos were able to hatch into larvae, though the larvae failed to develop past the first instar (L1) stage (Figure 2.2E). *tsr^{N96A/1}* transheterozygous embryos displayed similar defects in embryonic muscle patterning to each of the single mutants and a similar viability profile to *tsr¹* mutant embryos (Figure 2.2C-E). Together, these data indicate that Tsr is essential for proper muscle development.

Tsr plays an essential, muscle-autonomous role in Drosophila

Tsr function has been implicated in numerous developmental contexts (Blair et al., 2006; Chen et al., 2001; Gunsalus et al., 1995); therefore, we next determined if Tsr was required specifically in the musculature. We specifically depleted *tsr* in the muscle using two independent RNAi lines, *UAS-tsr RNAi TRiP* (DRSC, HMS00534) and *UAS-tsr-IR* (VDRRC, KK108706) (Figure 2.2A) and three mesoderm- and/or muscle-specific Gal4 drivers, a combination of *twist-Gal4*; *Dmef2-Gal4* or *Dmef2-Gal4* alone and *MHC-Gal4*. All combinations of driver and RNAi construct failed to produce embryonic muscle phenotypes, most likely due lack of sufficient knockdown in these heavily maternally-loaded individuals (Figures 2.1A, 2.3A). We did, however, observe complete lethality at early larval stages when either RNAi construct was expressed with *twist-Gal4*; *Dmef2-Gal4* or *Dmef2-Gal4* alone (Figure 2.3B-C) and later lethality when *UAS-tsr RNAi TRiP* was expressed using *MHC-Gal4* (Figure 2.3D), suggesting that Tsr has an essential role in the muscle after embryonic muscle development in *Drosophila*.

To demonstrate that this phenotype was due to depletion of *tsr* and not an off-target effect, we attempted to rescue viability by expressing constructs encoding wild-type (*UAS-tsr^{w^t}*), constitutively active (*UAS-tsr^{S3A}*) or dominant negative (*UAS-tsr^{S3E}*) Tsr. Importantly, expression of these constructs alone using *Dmef2-Gal4* caused few defects, and animals were viable (Figure 2.3E). We could partially rescue defects in viability associated with *Dmef2-Gal4>UAS-tsr-IR* expression by



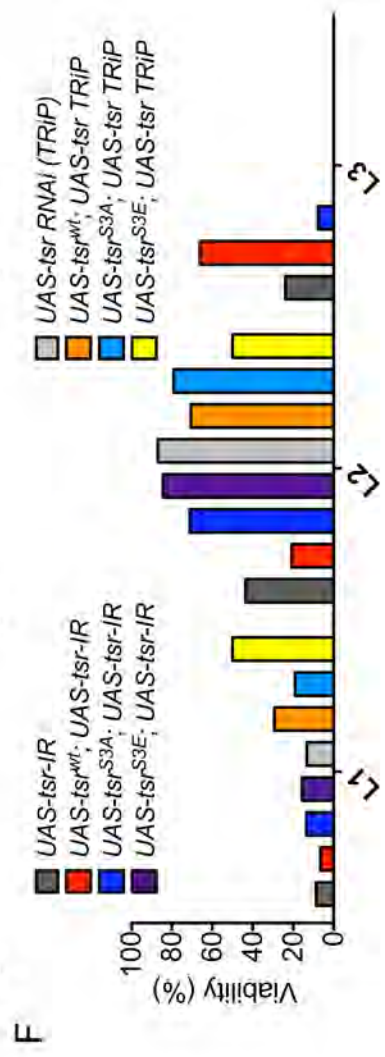
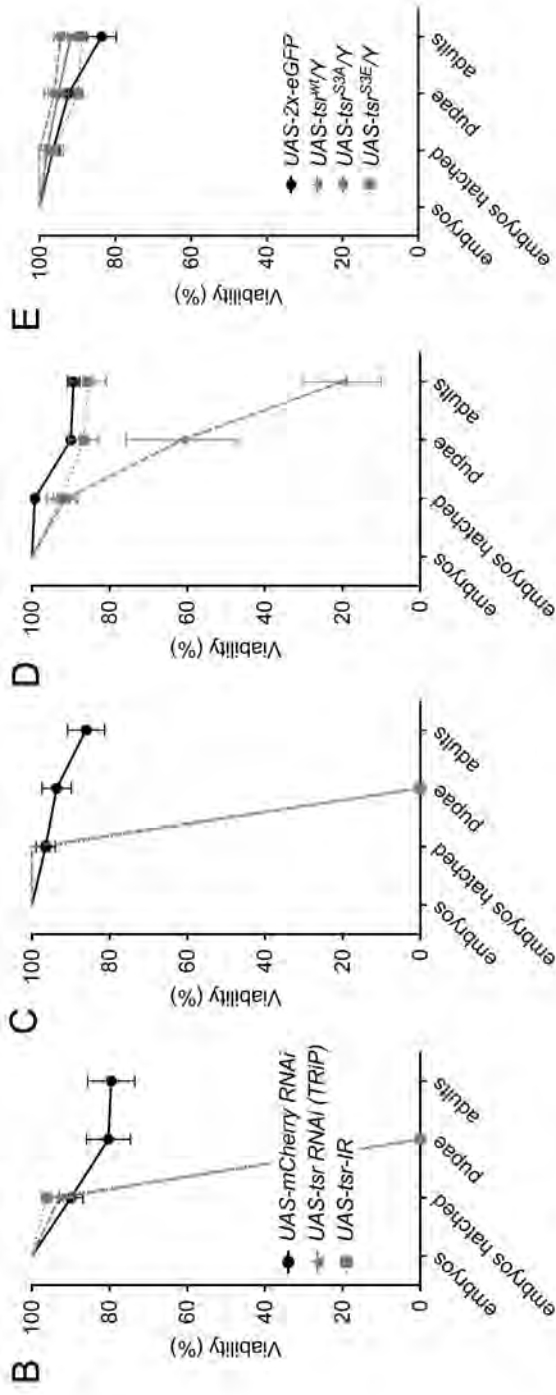


Figure 2.3. Tsr is required specifically in the muscle. (A) Maximum intensity projection of a stage 16 embryo labeled with an antibody against Tropomyosin (green) to visualize the embryonic body wall muscle. Three representative hemisegments are shown for each genotype. (B-D) Viability of the expression of the indicated *UAS-RNAi* construct using (B) *apRed, twist-Gal4; Dmef2-Gal4* (C) *Dmef2-Gal4* or (D) *MHC-Gal4*. n = 100. (E) Viability of *Dmef-Gal4* driving the expression of the indicated *UAS* constructs. n = 100. (F) Detailed viability over larval stages when the indicated *UAS* constructs are expressed using *Dmef2-Gal4*. n>50. Bar, 50 μ m.

overexpressing a wild-type (*UAS-tsr^{wt}*) Tsr construct (Figure 2.3F). In contrast to *UAS-tsr-IR* alone, which died as first or second instar larvae, a high percentage of *UAS-tsr^{wt}* rescue larvae developed into third instar larvae. Further, rescue third instar larvae appeared to be developmentally stalled: they failed to pupate but survived as third instar larvae for over 10 days, twice as long as normal larval development (data not shown). We also attempted to rescue *tsr* knockdown using *UAS-tsr^{S3A}* (constitutively active) or *UAS-tsr^{S3E}* (dominant negative) expression. In both cases, we were unable to rescue viability compared to *UAS-tsr-IR* alone (Figure 2.3F), suggesting that Tsr activity must be properly regulated. We were unable to rescue viability defects associated with the second *UAS-tsr RNAi* construct (Figure 2.3E); however the similarity in phenotypes we observed with both RNAi constructs suggests that both specifically target *tsr*. Together, these data indicate that Tsr is required specifically in muscle where it is essential for development. Further, our ability to partially rescue the viability of *Dmef2-Gal4>UAS-tsr-IR* by expressing wild-type *tsr* suggests that the phenotype we observe is due to *tsr* depletion and not off-target effects.

Founder cells (FC) and adult progenitors (APs) appear to be specified correctly in tsr mutant embryos

The prevalent loss of muscles in *tsr^{N96A}* mutant embryos prompted us to examine whether founder cell (FC) specification is affected. We analyzed the expression

of three transcription factors, Even-skipped (Eve), Krüppel (Kr) and Slouch (Slou), which are present in distinct FC populations (Figure 1.4) (Beckett and Baylies, 2007). We found that all three identity genes were properly expressed in *tsr^{N96A}* mutant embryos, suggesting that FC specification was not affected by loss of Tsr (Figure 2.4A). We also examined the expression of Twi, which marks the APs that are specified from the same cell divisions as FCs. As expected, the number of Twi-positive APs was unaffected in *tsr^{N96A}* mutant embryos (Figure 2.4B). Together, these data indicate that the muscle loss we observe in *tsr* mutants is not due to misspecification or loss of FCs.

Tsr plays a role in generating proper muscle-tendon attachments

The high percentage of misattached muscles in *tsr^{N96A}* mutant embryos suggested that Tsr may also play a role in myotendinous junction (MTJ) formation. Proper MTJ formation relies on reciprocal signaling between differentiating tendon cells and elongating myotubes. Thus, Tsr could be required in muscle cells to promote elongation towards tendon cells, in tendon cells to attract muscles or in both cell types to form the junction. Since early signals that pattern the entire embryo are responsible for the initial specification of tendon precursors, we examined denticle belt organization as a read-out for proper embryo patterning. We found that the cuticle in *tsr^{N96A}* mutant embryos appeared grossly wild-type and that overall denticle arrangement was unperturbed, suggesting that initial tendon field specification was not affected (Figure 2.5A).

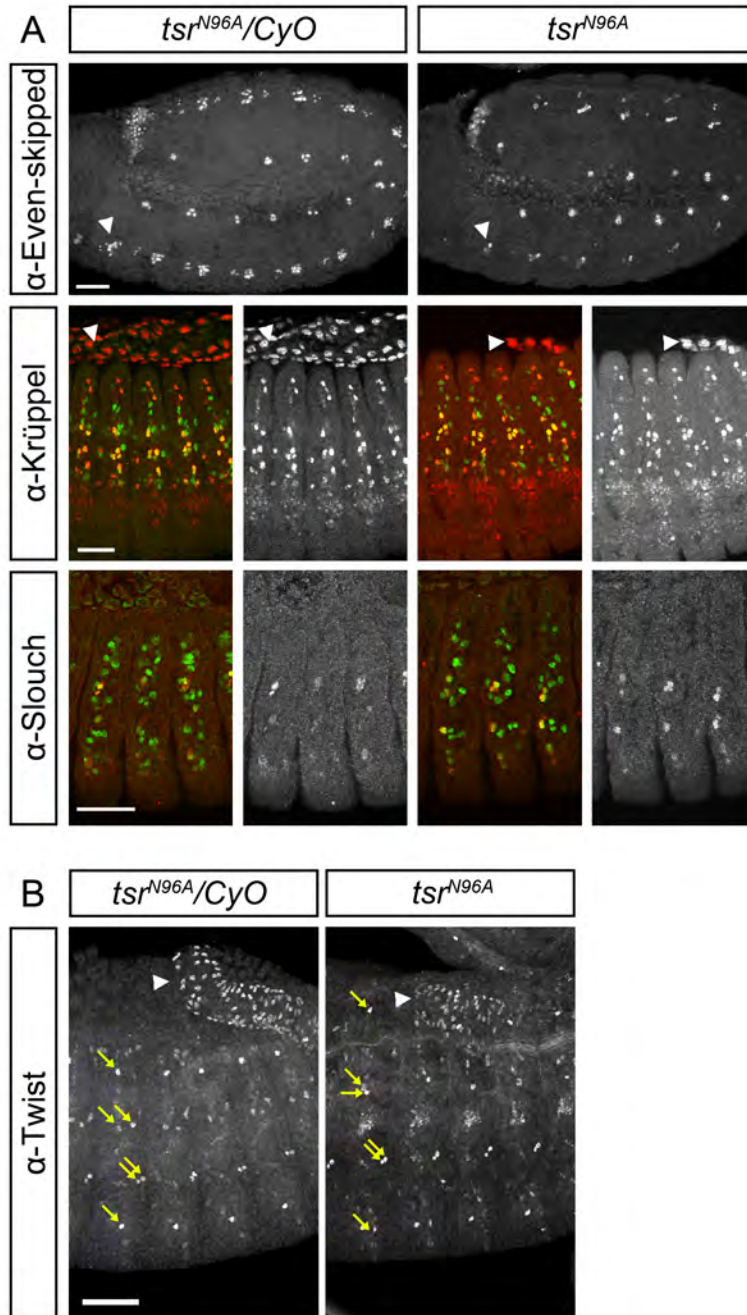


Figure 2.4. Founder cell (FC) and adult progenitor (AP) specification is unaffected in *tsr^{N96A}* mutant embryos. (A-B) Maximum intensity projection of embryos of the indicated genotype immunolabeled with an antibody against the transcription factors (A) Eve, Kr and Slou (red, greyscale) or (B) Twi (greyscale) to mark (A) FCs and (B) APs. Arrowheads in Eve panels indicate ventral nerve cord staining. Arrowheads in other panels indicate background staining. Yellow arrows (B) indicate the six APs in a single hemisegment. Bar, 50 μ m.

Early tendon precursors and mature tendon cells express the transcription factors StripeB (SrB) and StripeA (SrA), respectively. To determine if the terminal differentiation of tendon cells was stalled at either developmental time point upon the loss of Tsr, we examined the expression of these two factors. In *tsr^{N96A}* embryos, the pattern of tendon precursors expressing SrB appeared unaffected (Figure 2.5B). Similarly, SrA was expressed appropriately in the mature tendons in *tsr^{N96A}* embryos, indicating that tendon cell differentiation was normal.

Though muscles were often misattached, we did not find evidence indicating that the attachment itself was defective. For example, β PS integrin normally accumulates at the MTJ in *tsr^{N96A}* embryos (Figure 2.5C). In addition, when MTJ strength is compromised, as is the case for mutants in β PS integrin, muscles often detach at stage 17 after they begin to fully contract (Brown, 1994; Newman and Wright, 1981). Using live imaging analysis, we find that muscles in *tsr^{N96A}* mutant embryos remain properly attached to tendons at stage 17, indicating that although muscles make incorrect attachments to tendons, the MTJ itself is not functionally compromised and suggests that Tsr is not required for this process (data not shown).

We also used *Stripe-Gal4*, a tendon-specific Gal4 driver, to express either *UAS-tsr RNAi* or *UAS-tsr-IR* in Stripe-expressing tendon cell types. Depletion of *tsr* in tendons did not affect embryo hatching, but we observed a decrease in the rate of pupariation of larvae with expression of *UAS-tsr RNAi* and a later decrease in rate of eclosion of pupae with expression of *UAS-tsr-IR*, suggesting that Tsr also has a tendon-specific role during development (Figure 2.5D).

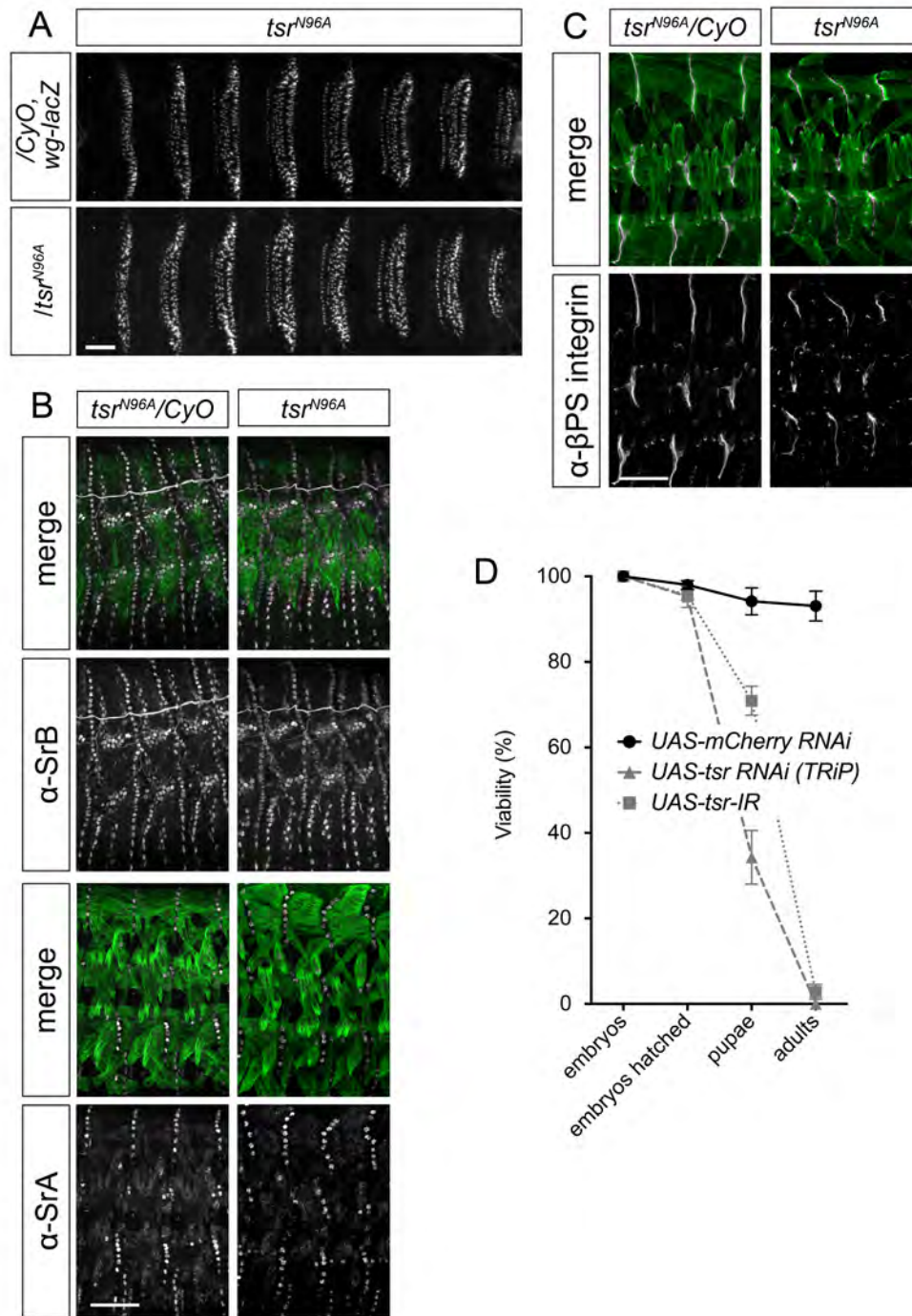


Figure 2.5. Tendon specification and differentiation are unaffected in *tsr^{N96A}* mutant embryos. (A) Cuticle preparations of stage 17 embryos of the indicated genotype. Denticle belts are in white. (B) Maximum intensity projection of embryos of the indicated genotype immunolabeled with antibodies against Myosin heavy chain (green) and Stripe B or Stripe A (greyscale) to label tendon precursors and mature tendons, respectively. (C) Maximum intensity projection of embryos of the indicated genotype immunolabeled with antibodies against Tropomyosin (green) and β PS integrin (greyscale) to label the MTJ. Bar, 50 μ m. (D) Viability of the expression of the indicated UAS-RNAi constructs using *Stripe-Gal4*. n = 100.

In support of this, the majority of pupae exhibited similar defects in metamorphosis to pupae with compromised muscle function, and the few adults that did emerge were flightless (data not shown). Due to the normal rate of embryo hatching with tendon-specific RNAi and the lack of muscle detachment upon contraction in *tsr^{N96A}* mutants, we did not pursue this phenotype further.

Regulators of Tsr are also required for embryonic muscle development

The regulation of ADF/cofilin activity by the phosphorylation state of Ser3 has been well-documented (Bamburg, 1999). Phosphorylation by two kinase families, LIM domain-containing kinases (LIMK1/2, *Drosophila* LIMK1) and testis-specific protein kinases [TESK1/2, *Drosophila* Center divider (Cdi)], inhibits ADF/cofilin activity, while dephosphorylation by two phosphatases, Slingshot (Ssh) and Chronophin (CG5567 in *Drosophila*), activates ADF/cofilin family proteins (Agnew et al., 1995; Bamburg, 1999; Bravo-Cordero et al., 2013; Morgan et al., 1993; Wang et al., 2007). In addition, AIP1 [*Drosophila* Flare (Flr)] synergizes with ADF/cofilin to drive actin dynamic processes (Bamburg, 1999). We wanted to establish whether this same pathway was at work in muscle.

As a first step, we determined if any of these proteins were expressed in *Drosophila* muscle. Because no antibodies were available to detect the endogenous *Drosophila* proteins, we surveyed available *in situ* databases and searched for endogenous protein trap reporter stocks for each of the Tsr-interacting proteins.

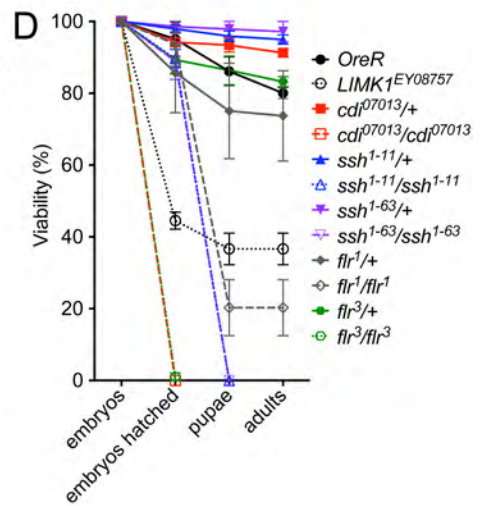
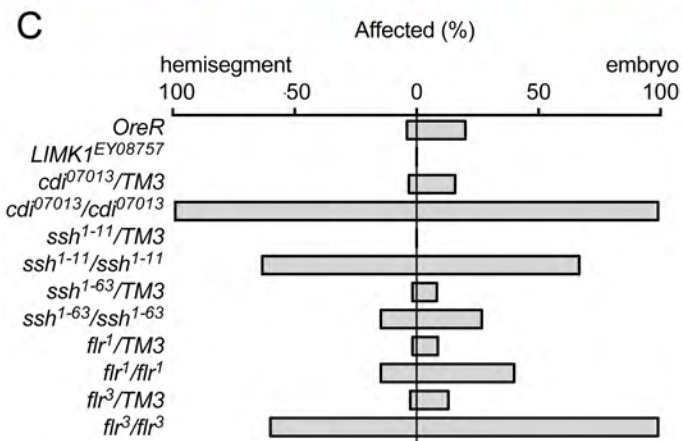
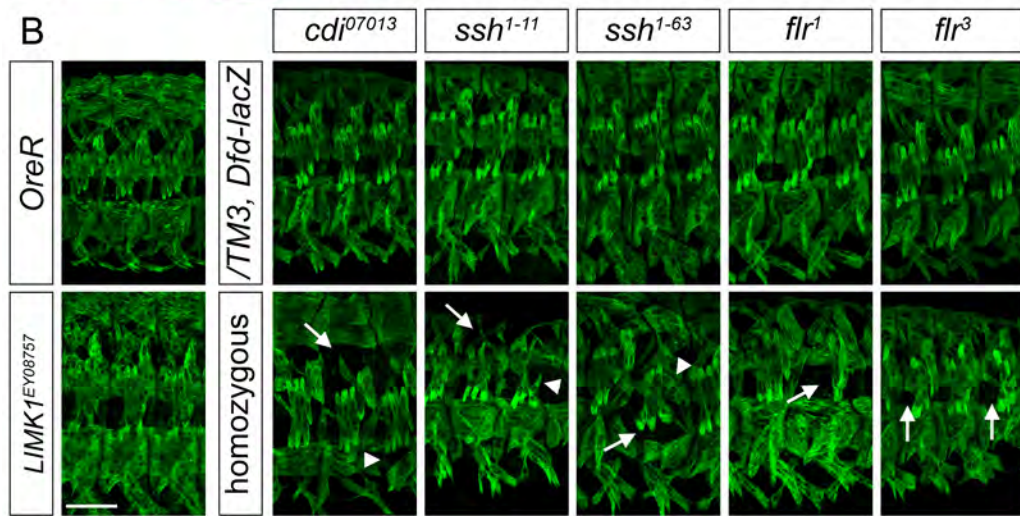
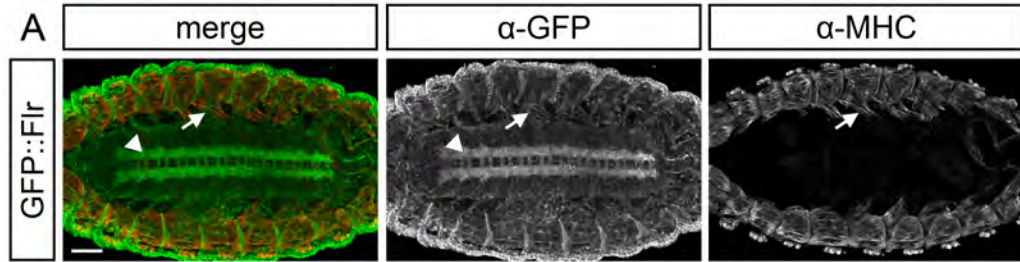


Figure 2.6. Tsr-interacting proteins are required for proper muscle development. (A) Maximum intensity projection of a stage 16 embryo labeled with an antibody against GFP (green) to label GFP::*Flr* and Myosin heavy chain (red) to visualize the embryonic body wall muscle. Muscle expression is indicated by an arrow. Ventral nerve cord expression is indicated by an arrowhead. (B) Maximum intensity projection of stage 16 embryos labeled with an antibody against Myosin heavy chain (green) to visualize the embryonic body wall muscle. Three representative hemisegments are shown for each genotype. Arrows indicated missing muscles. Arrowheads indicate misattached muscles. (C) Quantification of the percentage of affected hemisegments (left) and embryos (right) of each genotype indicated. n = 20 embryos, 100 hemisegments. (D) Viability of the indicated genotypes. n = 100. Bar, 50 μ m.

We found that *flr* is expressed in the embryonic somatic body wall muscles (Tomancak et al., 2002; 2007). GFP::Flr, a Flr GFP protein trap line, was also expressed in the embryonic body wall muscle, where it appeared to be enriched at MTJs as well as in the ventral nerve cord (Figure 2.6A) (Buszczak et al., 2007; Kelso et al., 2004; Morin et al., 2001; Quiñones-Coello et al., 2007). *LIMK1* was ubiquitously expressed throughout embryonic development, and *CG5567* was not detected in the body wall muscle, though it did appear to be present in pharyngeal and visceral muscle types (Tomancak et al., 2002; 2007). We have demonstrated that the Tsr-regulator Coro is expressed in *Drosophila* embryonic and larval muscle (Figures 3.2 and 3.15). These data suggest that at least some of the traditional Tsr-regulating proteins are also expressed in *Drosophila* muscle.

To examine their role in *Drosophila* muscle development, we obtained mutant alleles for *LIMK1*, *cdi*, *ssh* and *flr*. Embryos homozygous for *LIMK1^{EY08757}* appeared wild-type (Figure 2.6B-C). These flies were homozygous viable and fertile though there was an overall decrease in fitness (Figure 2.6D). As it was generated by a P-element insertion in the 5' UTR, the *LIMK1^{EY08757}* allele is likely a hypomorphic allele. *cdi⁰⁷⁰¹³* contains an intronic P-element insertion (Spradling et al., 1999). Embryos homozygous for the *cdi⁰⁷⁰¹³* allele had a number of muscle defects (Figure 2.6B-C). Most strikingly, however, was the nearly complete and specific loss of the dorsal oblique (DO) muscles (Figure 1.6). These embryos failed to hatch into larvae (Figure 2.6D). We also obtained two null alleles of *ssh*, *ssh¹⁻¹¹* and *ssh¹⁻⁶³*. Homozygous mutant embryos displayed a similar phenotype to one another with missing and

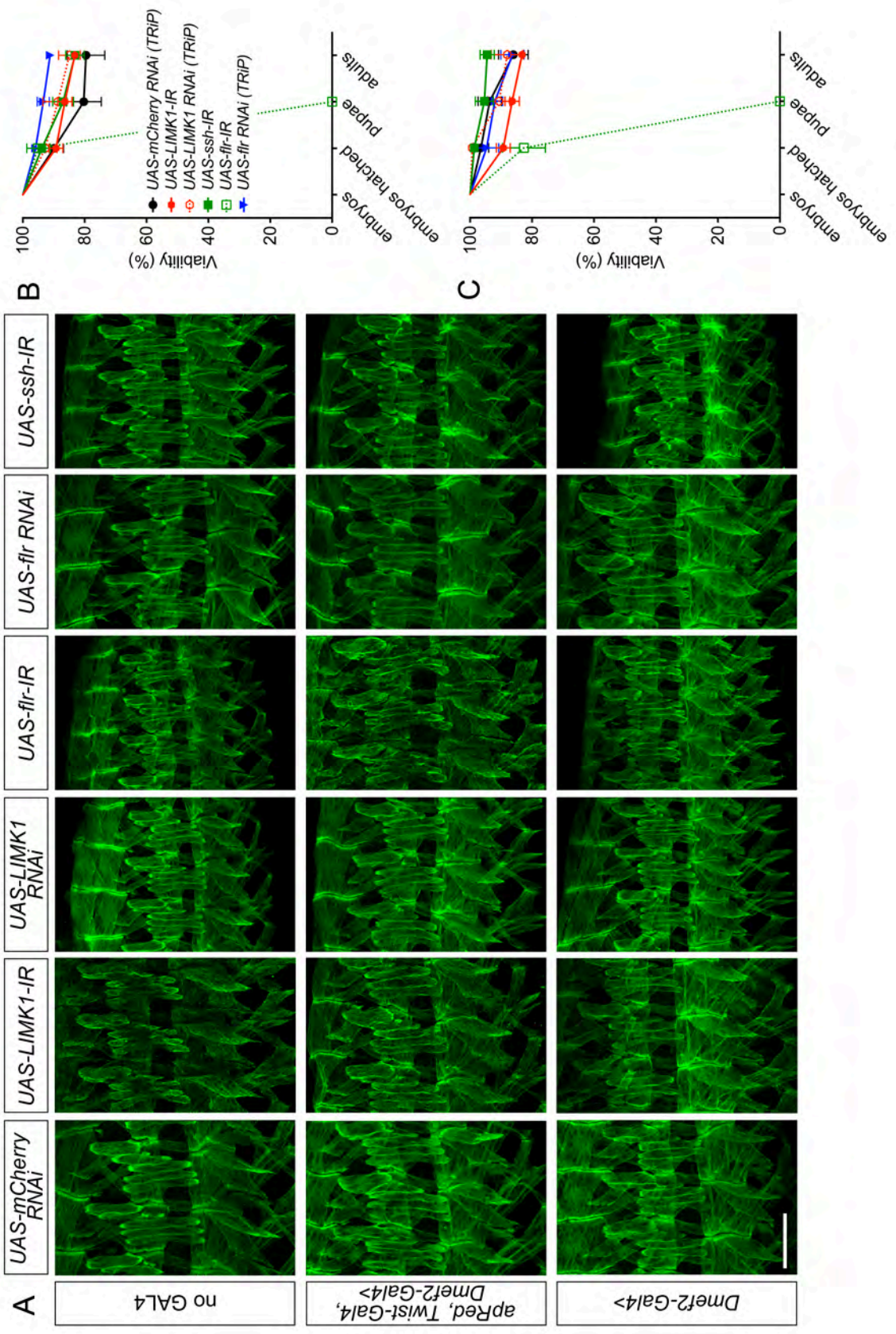


Figure 2.7. Muscle-specific depletion of Tsr-interacting proteins does not result in any embryonic muscle phenotypes. (A) Maximum intensity projection of stage 16 embryos labeled with an antibody against Tropomyosin (green) to label the embryonic body wall muscle. Three representative hemisegments are shown for each genotype. n = 20 embryos, 100 hemisegments. (B-C) Viability of the expression of the indicated *UAS-RNAi* constructs using (B) *apRed, twist-Gal4; Dmef2-Gal4* and (C) *Dmef2-Gal4*. n = 100. Bar, 50 μ m.

misattached muscles though embryos homozygous for the *ssh*¹⁻¹¹ allele were more often affected. These embryos hatched but died at early larval stages (Figure 2.6B-D). Two alleles of *flr*, *flr*¹ and *flr*³, generated by EMS mutagenesis, also resulted in general muscle patterning defects in homozygous mutant embryos. *flr*³ mutant embryos, which had a more penetrant phenotype, failed to hatch, while the majority of *flr*¹ mutants died during larval development (Figure 2.6B-D). Together, these data indicate that the Tsr-interacting proteins, Cdi, Ssh and Flr are essential for *Drosophila* development and are required for proper muscle morphogenesis in the embryo.

Muscle-specific depletion of Tsr regulators does not affect embryonic muscle development

We also obtained *UAS-RNAi* constructs which targeted mRNAs encoding Tsr-interacting proteins to examine their muscle-autonomous roles. As with *tsr* RNAi (Figure 2.3), we failed to observe defects in the embryonic musculature when RNAi constructs were expressed using *twist-Gal4*; *Dmef2-Gal4* or *Dmef2-Gal4* alone (Figure 2.7A). In addition and in contrast to data obtained by depleting *tsr*, presumptive depletion of *LIMK1* and *ssh* did not affect later viability, suggesting that either LIMK1 and Ssh were not sufficiently depleted or that they are not required muscle-autonomously for the proper development and function of *Drosophila* muscle (Figure 2.7B-C). We suspect that a combination of insufficient knockdown and high maternal loading is masking a role for these proteins.

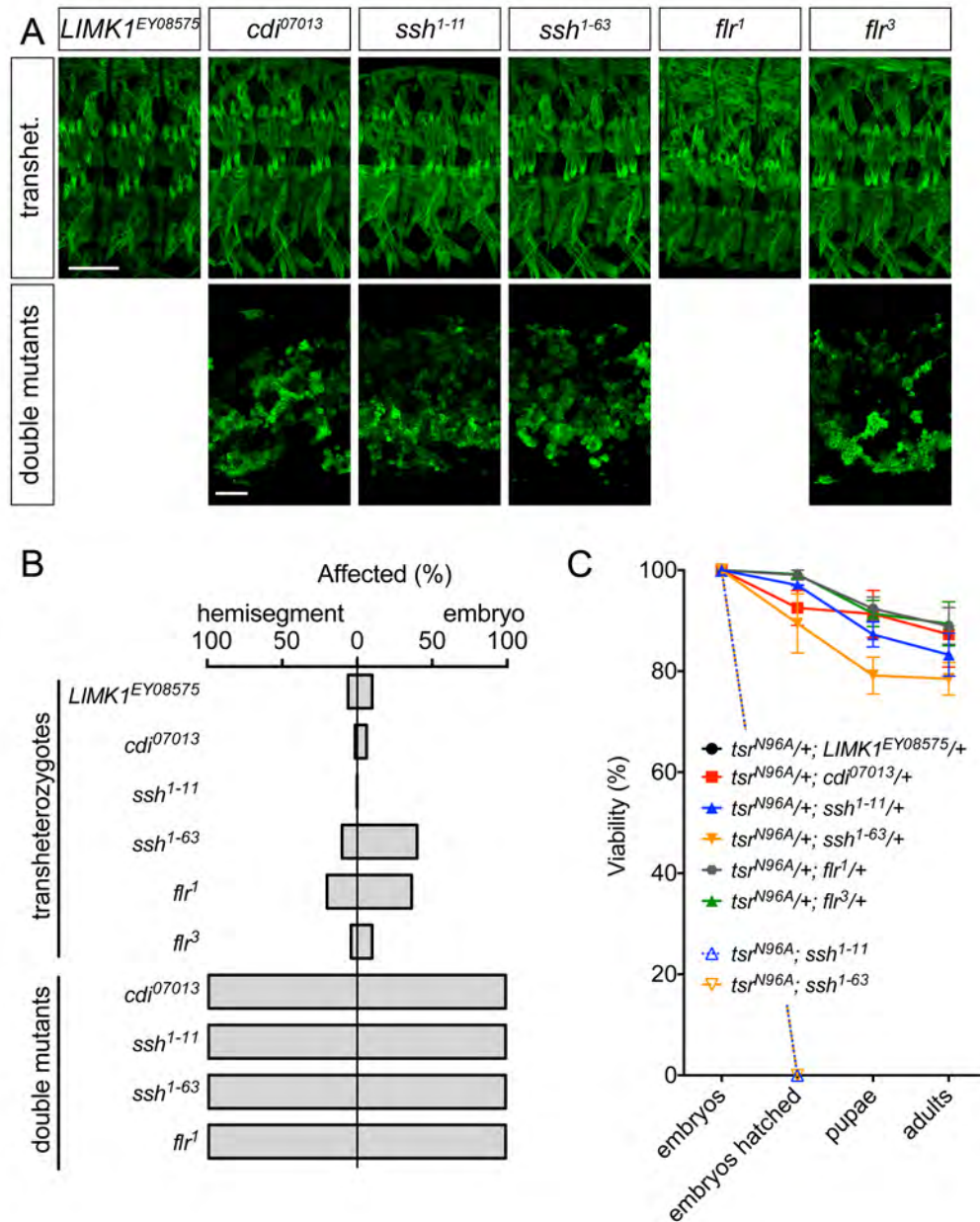


Figure 2.8. Tsr genetically interacts with Cdi, Ssh and Flr in the *Drosophila* body wall muscle. (A) Maximum intensity projection of stage 16 embryos labeled with an antibody against Myosin heavy chain (green) to label the body wall muscle. The *tsr^{N96A}* allele was used for transheterozygote and double mutant analysis. (B) Quantification of the percentage of affected hemisegments (left) and embryos (right) of each genotype indicated. n = 20 embryos, 100 hemisegments. (C) Viability of the indicated genotypes. n = 100. Bar, 50 μ m.

Depletion of *flr*, however, resulted in larval lethality (Figure 2.7B-C), suggesting that Flr has an essential muscle-specific role.

Tsr genetically interacts with Cdi, Ssh and Flr in embryonic muscle

To determine whether these proteins interacted genetically with Tsr in the muscle, we examined transheterozygous and double mutant embryos. In all transheterozygous embryos, the embryonic muscle pattern appeared wild-type, and there were no defects in viability (Figure 2.8A-C). In contrast, *tsr^{N96A}; ssh¹⁻¹¹* and *tsr^{N96A}; ssh¹⁻⁶³* double mutant embryos had severe and early defects in dorsal closure, germband retraction and mesoderm patterning. Most strikingly, however, the myoblasts in these embryos completely failed to fuse. Unsurprisingly, these embryos did not hatch. We observed similar defects in *tsr^{N96A}; cdi⁰⁷⁰¹³* and *tsr^{N96A}; flr³* double mutant embryos (Figure 2.8). These data suggest that Ssh, Cdi and Flr genetically interact with Tsr during muscle development in *Drosophila*.

Tsr is required for myoblast fusion

Given the role of Tsr in regulating actin dynamics and the critical nature of the F-actin focus to myoblast fusion, we hypothesized that the myoblast fusion defect in double mutant embryos was the result of misregulation of actin at the site of fusion.

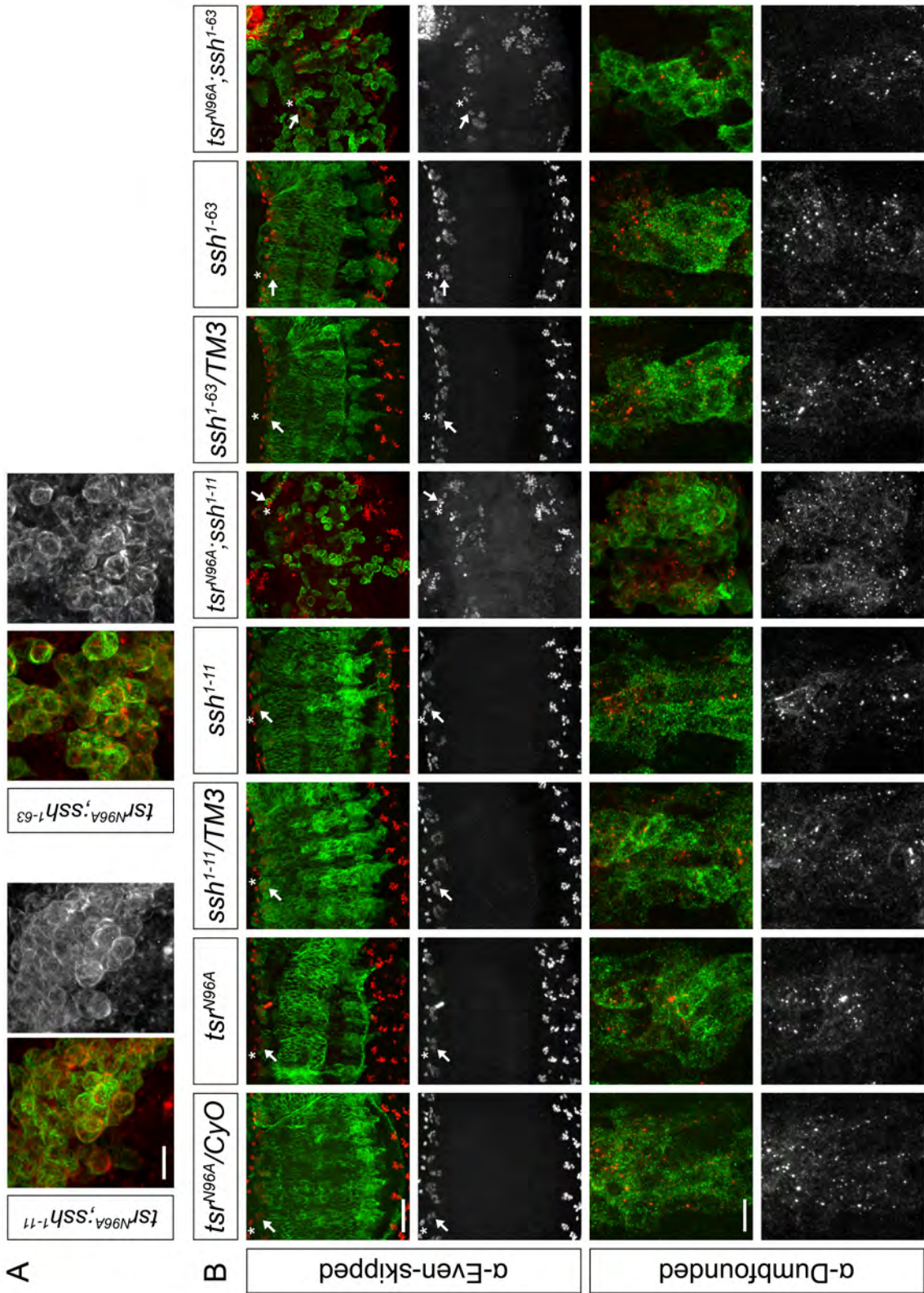


Figure 2.9. *tsr; ssh* double mutant myoblast are capable of making contact with one another but do not form an actin focus. (A) Maximum intensity projection of embryos labeled with an antibody against Myosin heavy chain (green) to label the body wall muscle and phalloidin (red, greyscale) to label the actin cytoskeleton. Bar, 8 μm . (B) (Top) Maximum intensity projection of stage 14 embryos labeled with an antibodies against Myosin heavy chain (green) to label the developing body wall muscle and Eve (red, greyscale) to label the DA1 FC, pericardial cells and the ventral nerve cord. Pericardial cells are indicated by an asterisk. DA1 FCs are indicated by an arrow. Bar, 50 μm . (Bottom) Maximum intensity projection of embryos labeled with an antibodies against Myosin heavy chain (green) to label the developing body wall muscle and Dumbfounded (red, greyscale) to label sites of FC-FCM contact. Bar, 8 μm .

Thus, we examined actin localization in *tsr; ssh* double mutant embryos. Surprisingly, we failed to detect actin foci at sites of presumptive FC-FCM contact (Figure 2.9A), suggesting that the observed fusion block was caused by defects more upstream of F-actin foci formation.

Defects in FC specification could also result in a myoblast fusion phenotype. FCs are specified by two sequential cell divisions, and *Tsr* has been previously implicated in cytokinesis (Gunsalus et al., 1995). To determine whether FCs were properly specified in *tsr; ssh* double mutants, we examined the expression of the transcription factor and identity gene *Eve*. *Eve* is expressed in the FC that gives rise to DA1 as well as in the ventral nerve cord and pericardial cells (Figure 1.4) (Frasch et al., 1987). We detected *Eve* in a number of MHC-positive myoblasts in double mutant embryos, indicating that these *Eve*-positive cells were FCs and not pericardial cells (Figure 2.9B). Further, this suggests that at least some FCs are properly specified and defects in FC specification are not likely to be the underlying cause of the fusion defect we observed.

We next analyzed whether FCs and FCMs were able to make contact with one another, a prerequisite for foci formation, by examining the localization of *Dumbfounded* (*Duf*), one the FC-specific transmembrane proteins that mediates FC-FCM adhesion (Ruiz-Gomez et al., 2000; Strünkelberg et al., 2001). We found that *Duf* properly accumulated at sites of contact between presumptive FCs and FCMs in double mutant embryos (Figure 2.9B), demonstrating that contact was initiated between the two myoblast types.

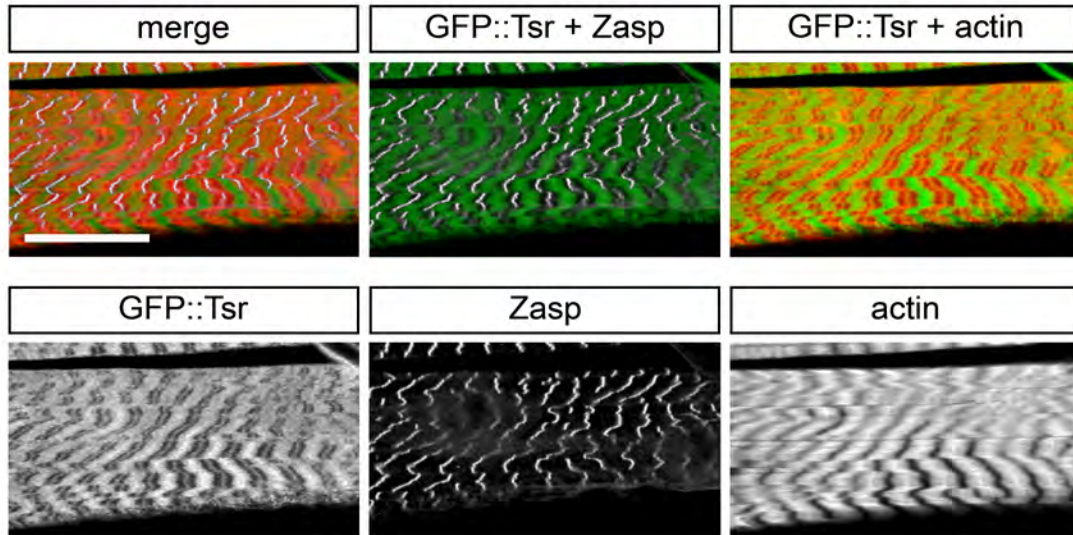


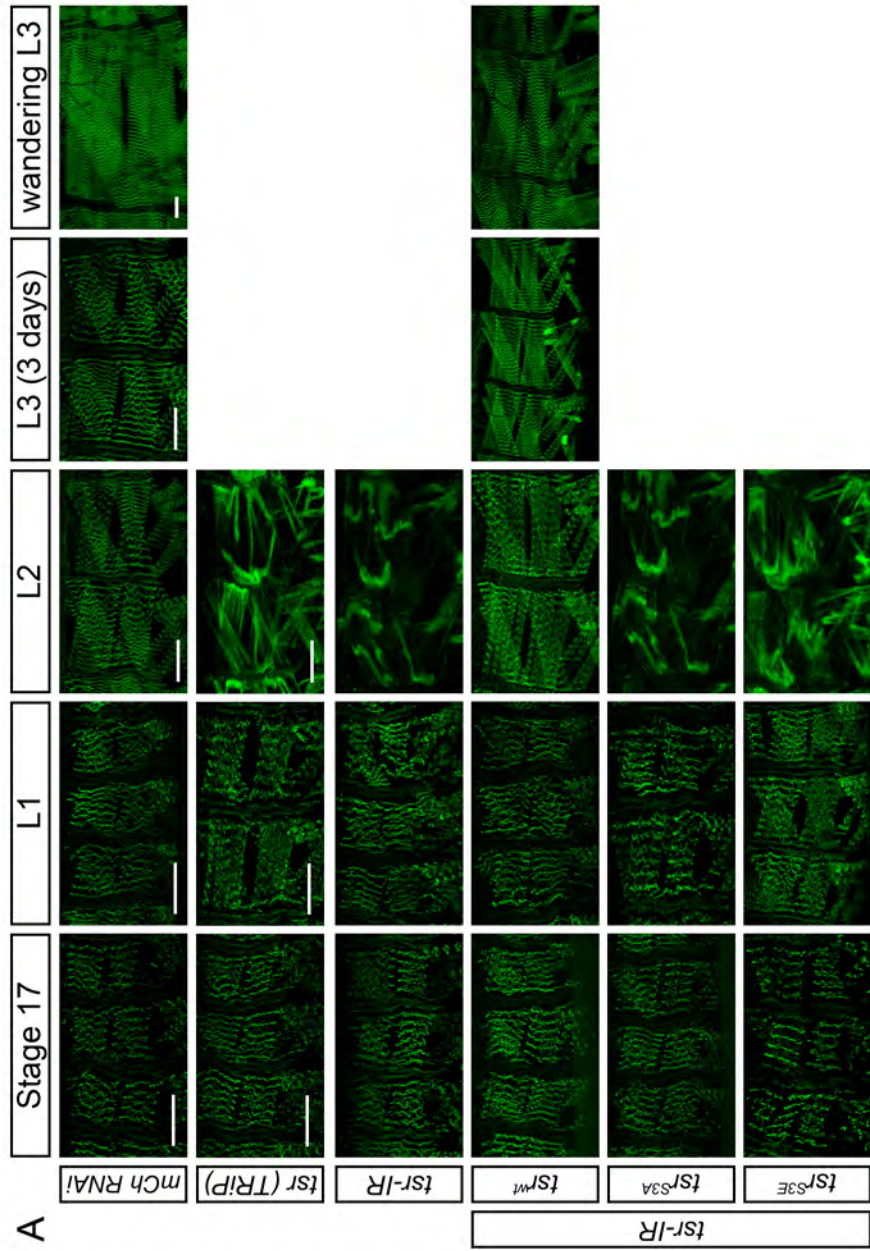
Figure 2.10. Tsr is localized to the Z-disc and H-zone in *Drosophila* larval muscle. Maximum intensity projection of an L3 larvae labeled with an antibody against GFP (green) to label GFP::Tsr, Zasp (white) to mark Z-discs and phalloidin (red) to visualize thin filaments. GFP::Tsr colocalizes with Zasp at Z-discs (GFP::Tsr + Zasp). Bar, 50 μ m.

Together, these data demonstrate that Tsr is required for myoblast fusion after FC-FCM contact in *Drosophila*. The high level of cortical actin and absence of actin foci in *tsr; ssh* double mutant embryos suggests that Tsr may play a role in the initial formation of the actin focus by helping to reorganize the cortical actin network to generate free actin monomers that are subsequently polymerized to form the actin focus.

Tsr is localized to the larval sarcomere

Data from other model systems has indicated that cofilin homologs play a role in sarcomere maintenance (Agrawal et al., 2007; 2012; Miyauchi-Nomura et al., 2012; Ono et al., 1999). This has neither been explored in *Drosophila* nor the mechanism by which it acts at the sarcomere made clear. In support of a role for Tsr in sarcomere development, our analysis of *tsr* alleles and muscle-specific *tsr* depletion identified few embryonic defects in muscle, likely owing to maternal loading of *tsr*, yet a consistent decrease in viability during larval development, suggesting a role for Tsr after muscle formation.

We analyzed the localization of Tsr in dissected third instar larvae using the GFP::Tsr protein trap line. We found that GFP::Tsr was expressed in the larval body wall muscle where it colocalized with Zasp at Z-discs (Figure 2.10). GFP::Tsr was also localized to the H-zone, a region where the thick filament does not overlap with the thin filament (Clark et al., 2002). A similar localization was observed for CFL2 in human skeletal muscle (Papalouka et al., 2009).



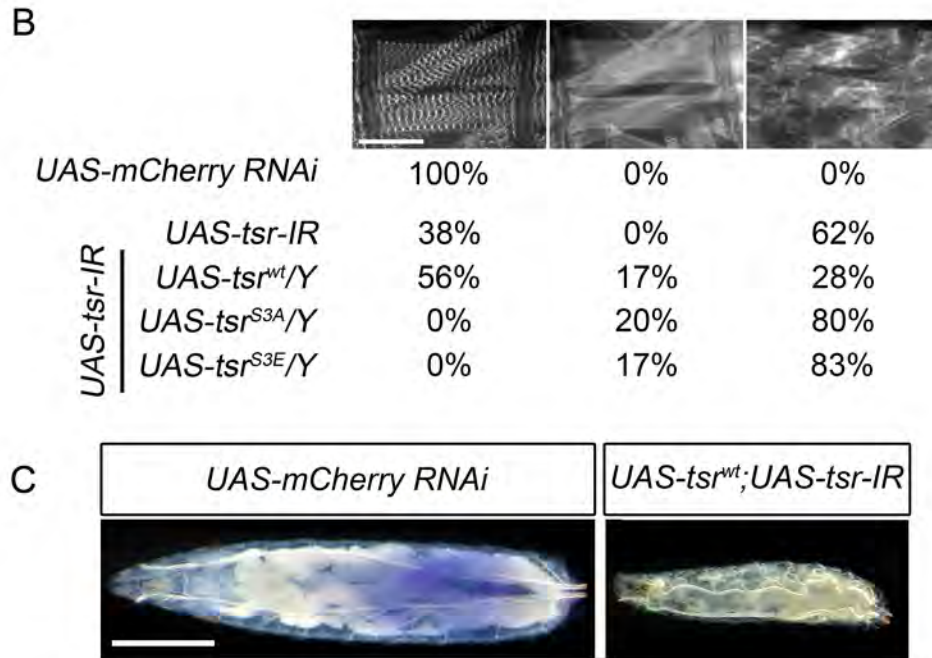


Figure 2.11. Muscle-specific depletion of Tsr results in severe and progressive loss of sarcomere organization. (A-B) *Dmef2-Gal4* was used to express the indicated *UAS* construct(s). *GFP::Zasp66* was used to visualize Z-discs. (A) Maximum intensity projection of embryos and larvae at the indicated developmental stage. *GFP::Zasp66* is in green. Bar, 50 μ m. (B) Single z-section of L2 larvae. *GFP::Zasp66* is in white. Percentages indicate the prevalence of each sarcomere organization class. $n > 20$. (C) *Dmef2-Gal4* was used to express the indicated *UAS* constructs. Larvae were fed on normal food and then switched to blue food after the L2 molt.

Tsr is required for sarcomere organization and maintenance

In *Drosophila*, sarcomeres form in the late embryo (stage 17), when the cuticle has formed and antibody staining is difficult. Further, early larval stages (first and, to a degree, second) are too small to dissect and stain. Thus, sarcomeres have not been traditionally analyzed until third instar (after *Dmef2-Gal4>UAS-tsr RNAi* and *UAS-tsr-IR* animals have died). To bypass the need for antibody staining, yet examine the development of the sarcomere, we obtained a GFP protein trap fly line in which GFP is fused in frame to Zasp66 (*GFP::Zasp66*), an isoform of Zasp and a Z-disc protein (Buszczak et al., 2007; Katzemich et al., 2013; Kelso et al., 2004; Morin et al., 2001; Quiñones-Coello et al., 2007).

Using *GFP::Zasp66, Dmef2-Gal4*, we observed sarcomere development in the embryo as well as throughout larval development. In control animals (*UAS-mCherry RNAi*), sarcomeres properly assemble at stage 17 and increase in number as the larval muscle increases in size during larval development (Figure 2.11A). Expression of either *UAS-tsr RNAi (TRiP)* or *UAS-tsr-IR* did not affect sarcomere formation at stage 17, and sarcomere organization appeared wild-type in first instar (L1) larvae. In contrast to control larvae at L2, however, *tsr*-depleted L2 larvae exhibited severe sarcomere disorganization and did not develop beyond this point.

To demonstrate that this phenotype was due to knockdown of *tsr* and not to off-target effects, we attempted to rescue the sarcomere organization defects by expressing *UAS-tsr^{wt}*, *UAS-tsr^{S3A}* or *UAS-tsr^{S3E}* in *tsr*-depleted larvae.

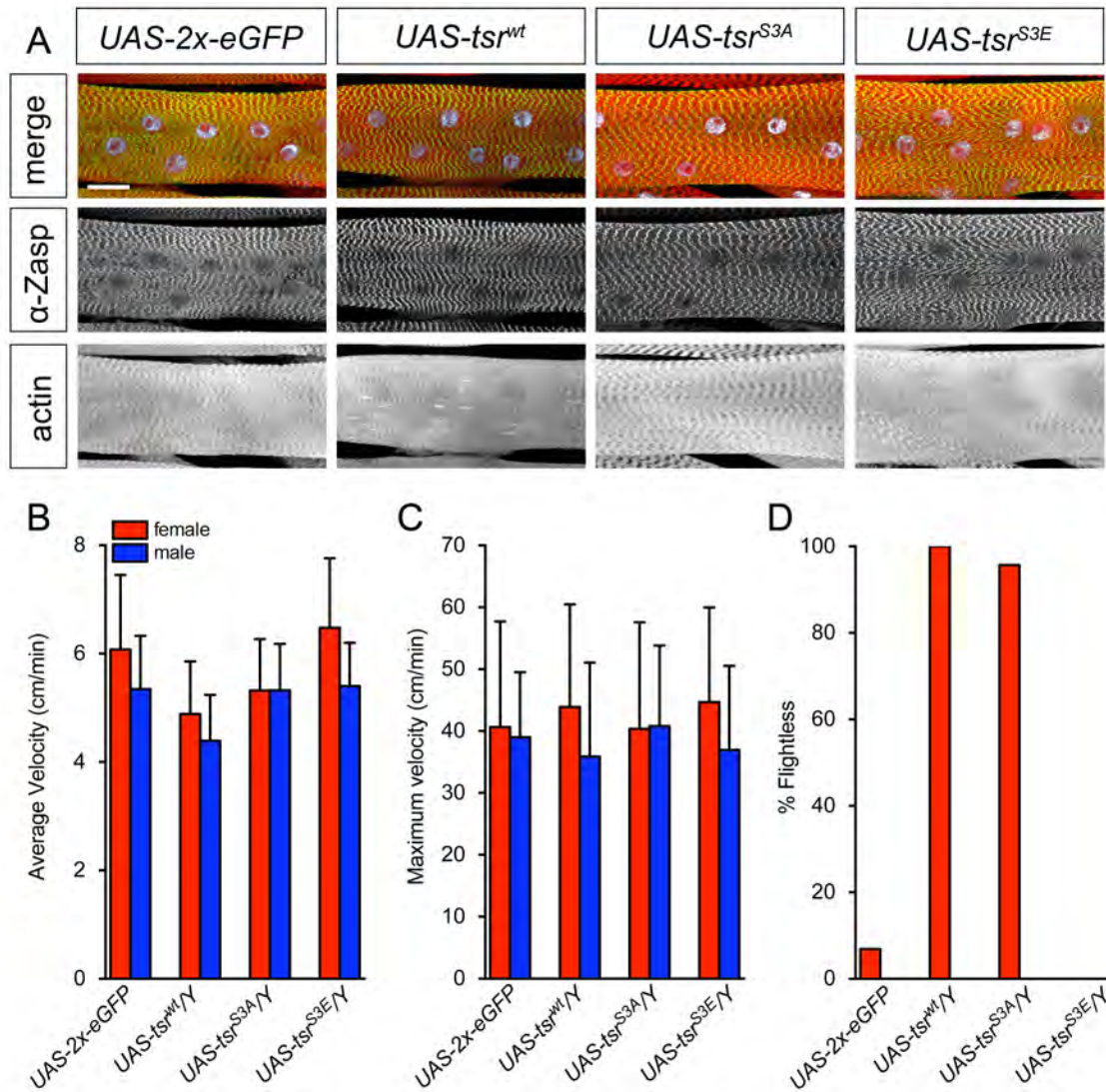
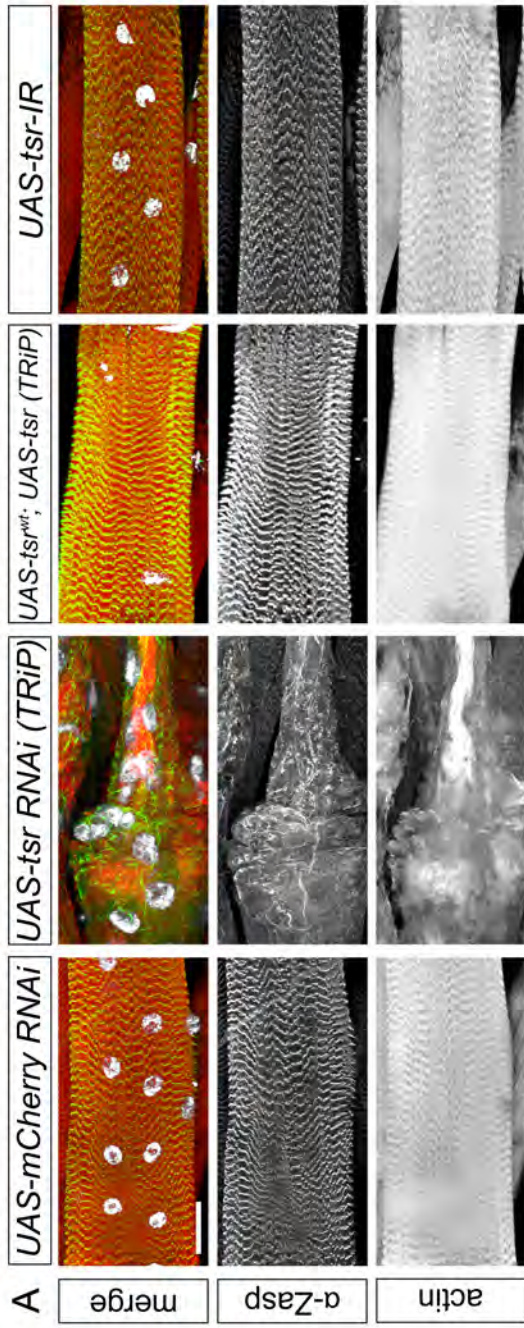


Figure 2.12. Muscle-specific overexpression of Tsr does not affect larval muscle function but does cause flightlessness in adults. (A) Maximum intensity projection of dissected third instar larvae in which *Dmef2-Gal4* was used to express the indicated *UAS* construct. Larval fillets were labeled with an antibody against Zasp (green), phalloidin (red) and Hoechst (white). (B-C) Larvae of the indicated genotype were tracked as described previously (Louis et al., 2008a; 2008b). Average velocity (B) and maximum velocity (C) are plotted. (D) Emerged adults were examined for their ability to fly. (B-D) *UAS-tsr* constructs are carried on the X chromosome, and thus, are not present in males, which were used as controls. $n > 30$. Bar, 50 μ m.

Importantly, expression of these constructs alone using *Dmef2-Gal4* did not affect sarcomere organization in L3 larvae or larval crawling (Figure 2.12A-C). However, overexpression of *UAS-tsr^{wt}* and *UAS-tsr^{S3A}* causes flightlessness in adults, suggesting that overexpression of these constructs does have some functional consequence (Figure 2.12D).

When we expressed *UAS-tsr^{wt}* in animals in which *tsr* is depleted using *UAS-tsr-IR*, sarcomeres formed normally at stage 17 (Figure 2.11A). Over larval development, the sarcomeres remained properly organized and increased in number through the wandering third instar stage, indicating that *UAS-tsr^{wt}* is able to rescue *tsr* knockdown by *UAS-tsr-IR*. The rescue, however, was not complete as rescue larvae remained smaller than controls after L2 (Figure 2.11C). They also ceased eating and excreting, which was measured by the presence of absence of blue food in the gut, suggesting defects in pharyngeal and/or visceral muscle function. Further, though larvae survived until control larvae became wandering third instar, rescued larvae failed to pupate and survived as L3 larvae for at least five days longer than normal.

We also attempted to rescue *tsr* knockdown using *UAS-tsr^{S3A}* (constitutively active) or *UAS-tsr^{S3E}* (dominant negative) expression. In both cases, we were unable to rescue the sarcomere organization phenotype, suggesting that Tsr activity must be properly regulated (Figure 2.11A). Further, as with viability (Figure 2.3E), we were unable to rescue the associated sarcomere organization phenotype obtained by depleting *tsr* using *UAS-tsr RNAi (TRiP)* (Figure 2.11A and data not shown).



B

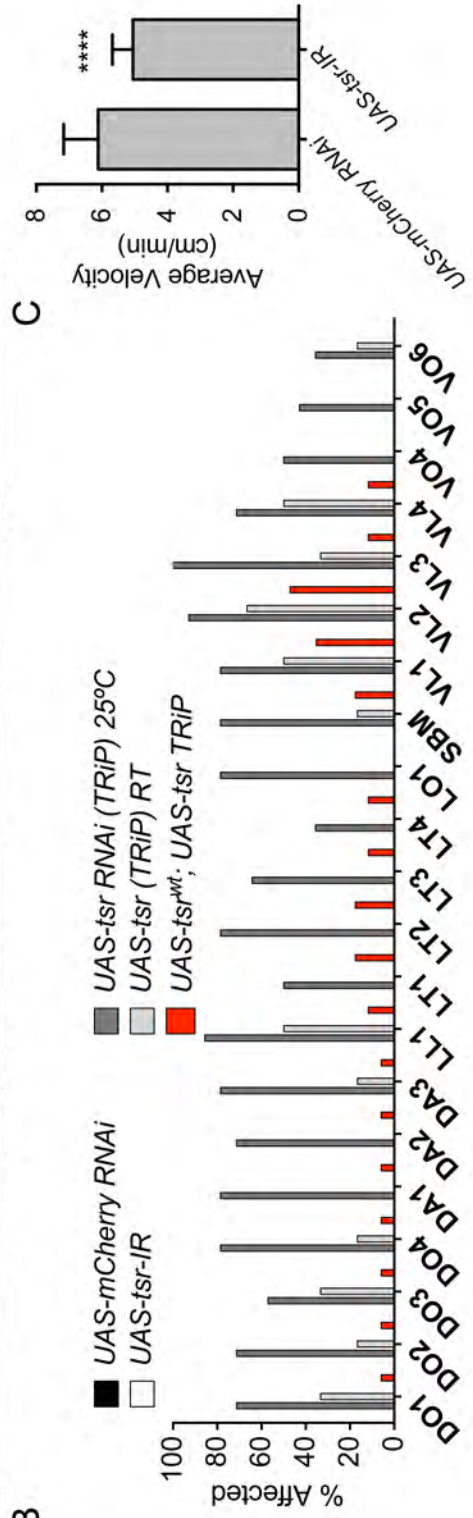


Figure 2.13. Depletion of *tsr* results in hyperpolymerization of actin and severe defects in sarcomere organization. (A) Maximum intensity projection of dissected third instar larvae in which *Dmef2-Gal4* was used to express the indicated *UAS* construct(s). Larval fillets were labeled with an antibody against Zasp (green), phalloidin (red) and Hoechst (white). (B) Quantification of percentage of affected muscles in the indicated genotypes. $n > 10$ hemisegments. (C) Larvae of the indicated genotype were tracked as described previously (Louis et al., 2008a; 2008b). Average crawling velocity is plotted. **** $p < 0.0001$. $n = 30$ larvae. Bar, 50 μm .

To determine whether this phenotype progressed through any intermediate stage, we examined Z-disc organization *in vivo* from L1-L2 (Figure 2.11B). We found that sarcomeres progressively deteriorate, first resembling immature, assembling sarcomeres before attaining the severe phenotype we described above. Taken together, these data indicate that Tsr plays a conserved role in sarcomere maintenance in *Drosophila*.

Muscle-specific depletion of tsr results in excessively polymerized actin

Because Tsr is a well-characterized actin depolymerization protein, we were interested in looking at the effect depleting *tsr* would have on actin in muscle. Expression of either RNAi construct using *MHC-Gal4* allows *tsr*-depleted larvae to develop into L3 larvae that can be easily dissected (Figure 2.3D). Sarcomeres in control L3 larvae were properly organized with Z-discs, visualized using an antibody against Zasp, and actin uniformly spaced across the muscle (Figure 2.13A-B), whereas sarcomeres in *UAS-tsr TRiP* larvae were severely disrupted, and Z-discs appeared similar to the Z-disc disorganization that we observed using *Zasp66::GFP, Dmef2-Gal4* (Figure 2.13A-B). Further, instead of being organized into thin filaments of uniform size, actin appeared to be excessively polymerized into rods, consistent with a role for Tsr in actin depolymerization. We found that this affected the majority of muscles (Figure 2.14B). These defects were less severe though still present in animals raised at room temperature, and we could partially rescue these defects by expressing *UAS-tsr^{mt}* in combination with *UAS-tsr-IR*

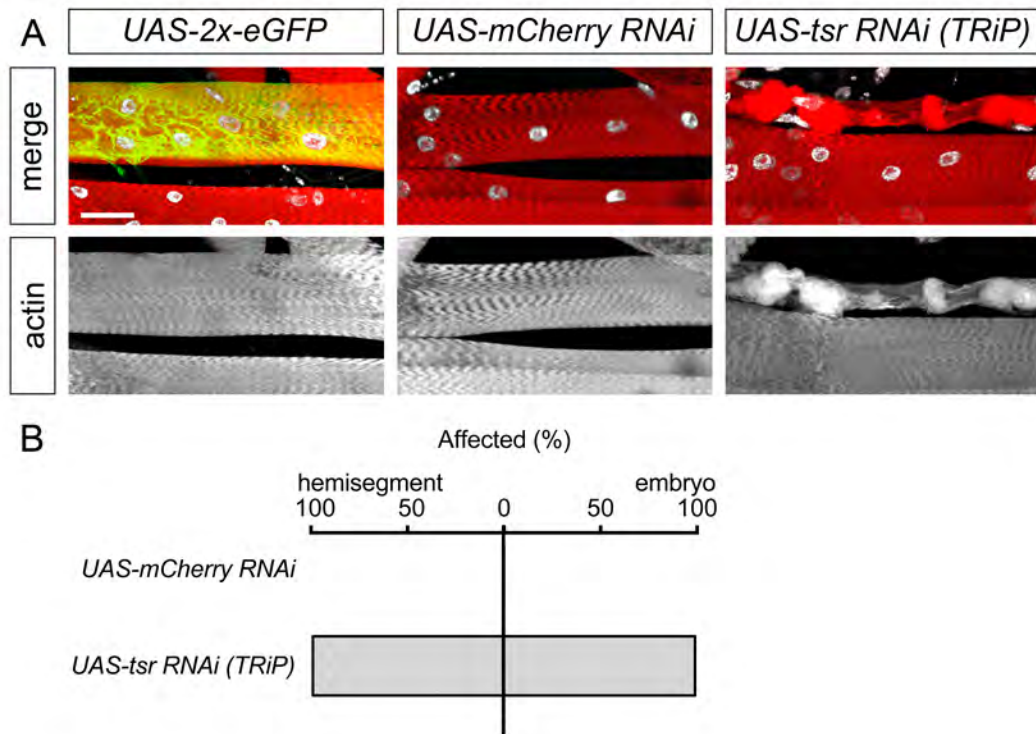


Figure 2.14. Expression of *UAS-tsr RNAi* in a single muscle causes a severe defect in sarcomere organization. (A) Maximum intensity projection of dissected third instar larvae in which *Dmef2-Gal4* was used to express the indicated *UAS* construct. Larval fillets were labeled with an antibody against GFP (green) to indicate muscle VL1 and phalloidin (red) and Hoechst (white) to label the actin cytoskeleton and nuclei, respectively. (B) Quantification of the percentage of affected hemisegments (left) and embryos (right) of the indicated genotype. n=10 hemisegments. Bar, 50 μ m.

(Figure 2.13A-B). Of the six rescue larvae we analyzed, the sarcomere organization in one larvae appeared completely wild-type, while the others showed improvements in only some muscles. In contrast, sarcomere organization in *UAS-tsr-IR* larvae appeared similar to sarcomeres in control larvae, and no muscles displayed the severe sarcomere organization phenotype we observe with *UAS-tsr RNAi (TRiP)* (Figure 2.13A-B). Despite their wild-type appearance, however, these larvae crawled slower than control larvae in a larval locomotion assay, suggesting that some aspect of muscle function is affected (Figure 2.13C).

As an additional approach, we also used *5053-Gal4* to drive *UAS-tsr RNAi (TRiP)* in a single muscle, VL1 (Figure 2.14A, *UAS-eGFP*), reasoning that targeting the RNAi to a single muscle would likely not affect the overall health and size of the animal, making dissection easier and providing an internal control for scoring muscle defects. Quite strikingly, we found a severe defect in sarcomere organization similar to the defect observed when either RNAi construct was expressed using *Dmef2-Gal4* specifically in muscle VL1 (Figure 2.11A). These data indicate that Tsr is required to regulate actin polymerization and maintain sarcomere organization in larval muscle.

Tsr is required for muscle-dependent events in metamorphosis

At the onset of pupariation, third instar larvae shorten their larval body and evert their anterior spiracles and head (Fraenkel and Rudall, 1940).

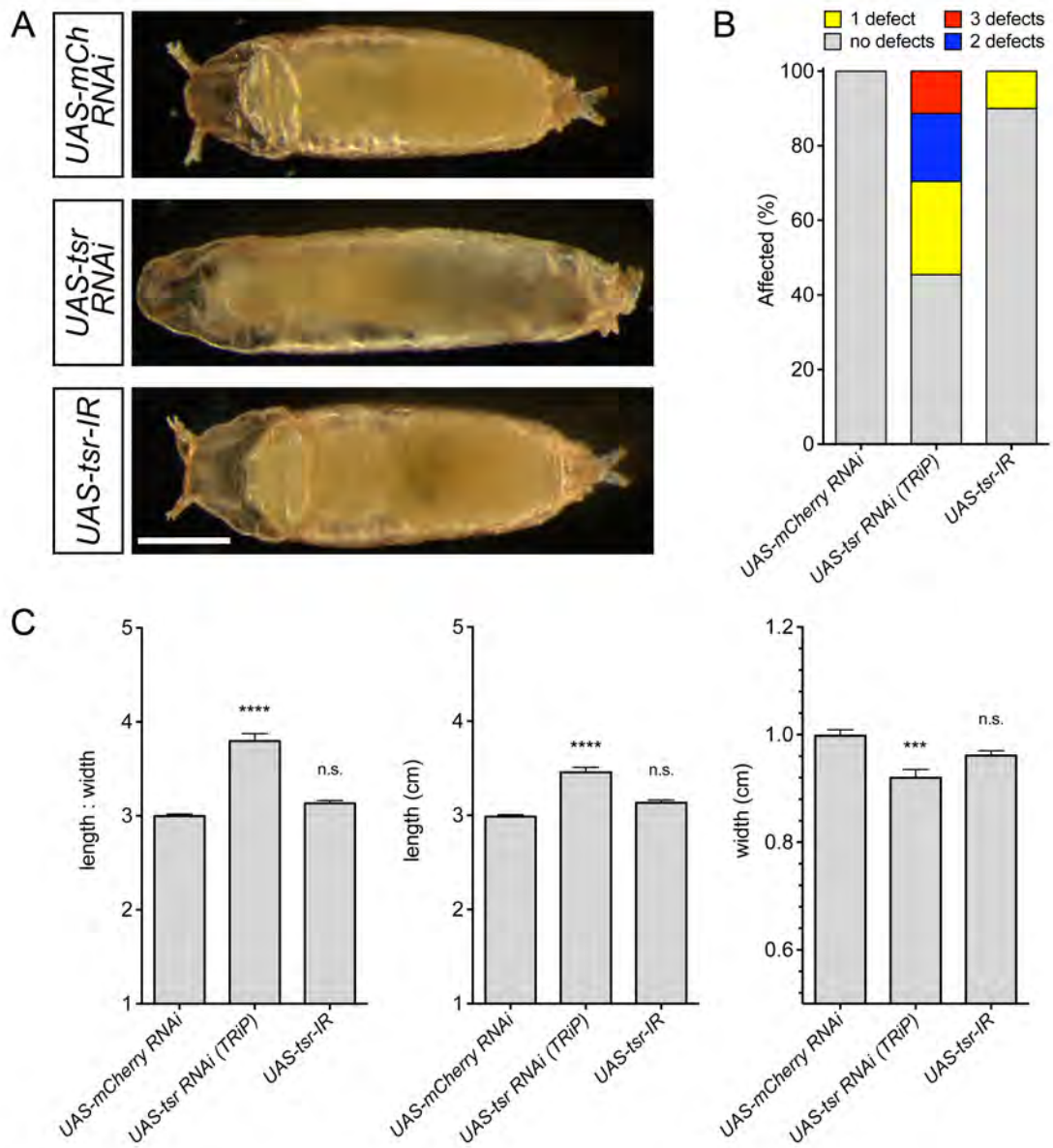


Figure 2.15. Tsr is required for muscle-dependent events during *Drosophila* metamorphosis. (A) Whole-mount pupal cases in which the indicated *UAS* construct is expressed using *MHC-Gal4*. The *UAS-tsr RNAi* larvae depicted has defects in spiracle eversion, head eversion and gas bubble translocation. (B) Quantification of the defects observed during metamorphosis in pupae of the indicated genotype. (C) The ratio of pupal case length:width (left), pupal case length (middle) and pupal case width (right). Bar, 500 nm. *** $p < 0.001$. **** $p < 0.0001$. n.s., not significant. $n = 30$ pupae.

These events require contraction of the body wall and pharyngeal dilator muscles and the generation of hydrostatic pressure driven by the translocation of an abdominal gas bubble (Fraenkel and Rudall, 1940; Fristrom, 1965; Robertson, 1936). To determine whether these muscle-dependent events in metamorphosis also required Tsr function, we examined the development of pupae in which *tsr* was depleted using *MHC-Gal4*. In *UAS-mCherry RNAi* pupae, we did not observe any defects in gas bubble translocation or head and spiracle eversion (Figure 2.15A-B). Similarly, pupae in which *tsr* was depleted using *UAS-*tsr-IR** appeared wild-type, and only the occasional defect in metamorphosis was detectable (Figure 2.15A-B). Depletion of *tsr* using *UAS-*tsr* RNAi (TRiP)*, however, generated a noticeable change in pupal appearance. Pupae appeared longer and thinner, and a high percentage of pupae had defects in at least one of the muscle-dependent metamorphic events (Figure 2.15A-B).

To quantify the defects in larval body shortening, we measured the length and width of pupal cases in each genotype. We found that expression of *UAS-*tsr-IR** did not affect larval body shortening as the length, width and the length:width ratio was not statistically significantly different from measurements obtained from *UAS-mCherry RNAi* pupae (Figure 2.15C). In contrast, we found that *UAS-*tsr* RNAi (TRiP)* pupae failed to appropriately contract their body wall at pupariation. Larvae were longer and thinner than controls, and accordingly, the ratio of the pupal length:width was increased compared to *UAS-mCherry RNAi* pupae. Together, these defects indicate that Tsr is required in multiple larval muscle types during metamorphosis.

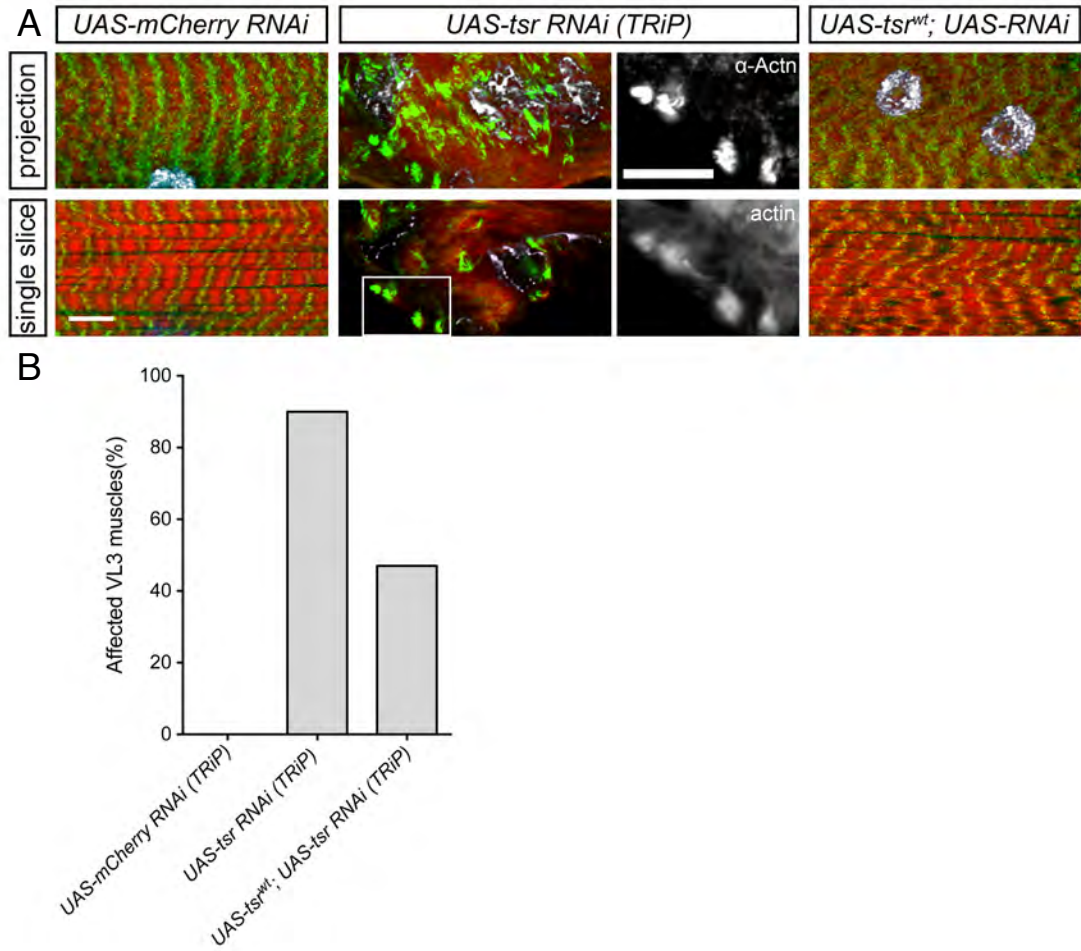


Figure 2.16. Accumulations resembling nemaline bodies are present in muscle in which *tsr* is reduced. (A) (Top) Maximum intensity projection of dissected third instar larvae in which *MHC-Gal4* was used to express the indicated *UAS* constructs. Larval fillets were labeled with an antibody against α -Actinin (green) to label Z-discs, and phalloidin (red) and Hoechst (white) to label the actin cytoskeleton and nuclei, respectively. (Bottom) Single z-section taken from top panels. (B) Percentage of VL3 muscles affected when the indicated *UAS* constructs are expressed using *MHC-Gal4*. Bar, 8 μ m.

Drosophila as a disease model for Nemaline myopathy

Recently, two different recessive mutations in human muscle-specific ADF/cofilin, CFL2, were identified in two patients affected with Nemaline myopathy (NM) (Agrawal et al., 2007; Ockeloen et al., 2012). NM, the most common type of congenital myopathy, is a disease of the sarcomere thin filaments and is characterized by the presence of “nemaline bodies,” muscle weakness and, often, feeding difficulties (Sanoudou and Beggs, 2001a). Nemaline bodies are electron-dense accumulations that are largely composed of actin, α -Actinin (Actn) and other Z-disc proteins. To determine if the actin accumulations we observed were similar to nemaline bodies, we examined the localization of Actn in *UAS-tsr RNAi (TRiP)* L3 larvae. We found that Actn organization was severely disrupted upon knockdown of *tsr*, similar to the phenotype observed with Zasp organization when *tsr* was reduced (Figures 2.13 and 2.17). Further, Actn could be found in accumulations with actin, a defining characteristic of nemaline bodies, suggesting that these are nemaline body-like structures (Figure 2.16, inset) (Sanoudou and Beggs, 2001a). Additionally, these defects can be partially rescued by expression of *UAS-tsr^{wt}* (Figure 2.16A-B).

Both reported missense mutations in *CFL2* (G19A and A35T) identified in patients affected with NM are hypothesized to be loss of function mutations (Agrawal et al., 2007; Ockeloen et al., 2012). *Cfl2*-null mice and *tsr* depleted larvae share phenotypic characteristics with affected patients, including the presence of nemaline bodies and actin accumulations (Figure 2.16A) (Agrawal et al., 2007; 2012; Ockeloen et al., 2012). The defects in the mouse and larvae are

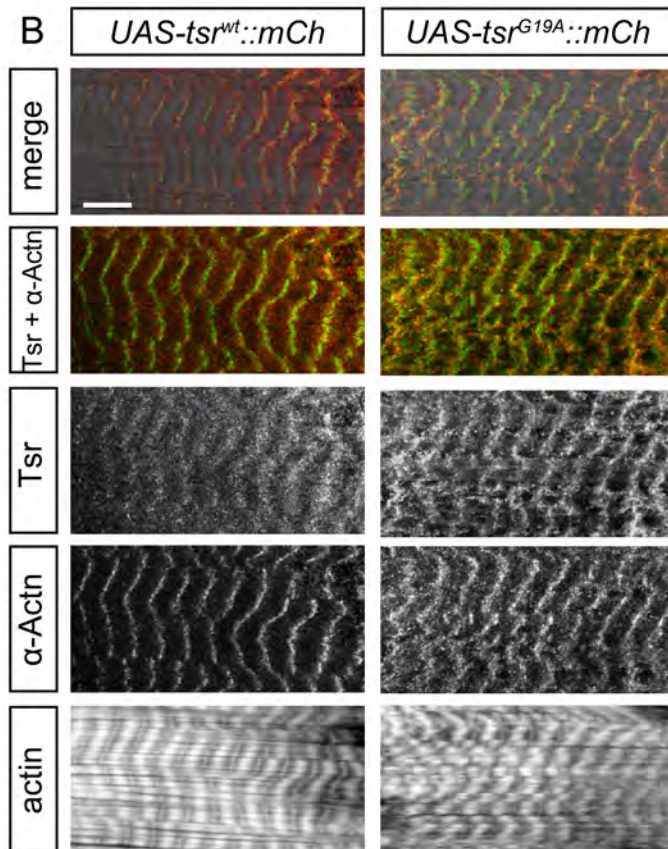
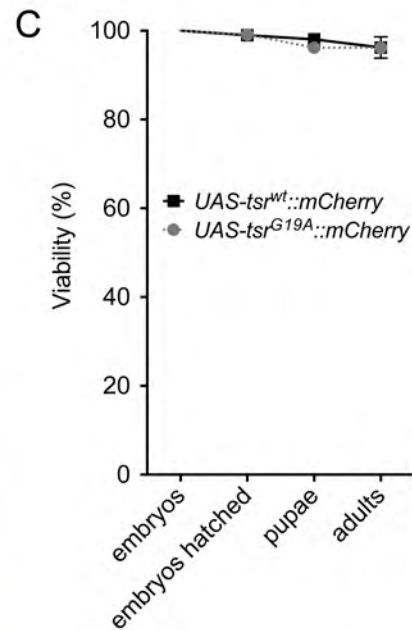
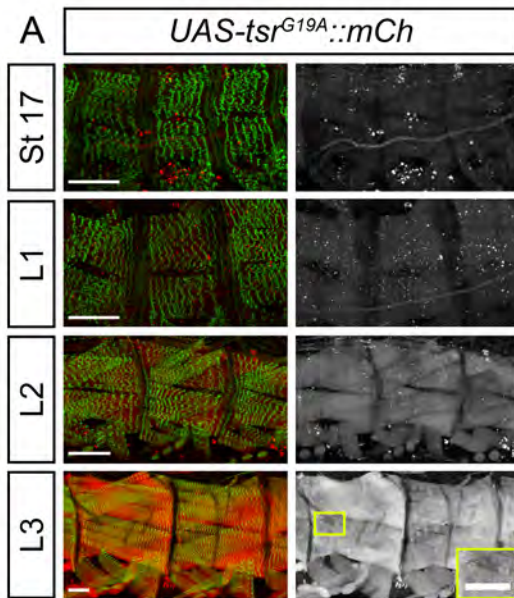


Figure 2.17. *UAS-tsr^{G19A}::mCherry* is properly localized to Z-discs in larval muscle. (A) Maximum intensity projection of embryos and larvae at the indicated developmental stage. *GFP::Zasp66* (green) was used to visualize Z-discs. *UAS-tsr^{G19A}::mCherry* is in red and was expressed using *Dmef2-Gal4*. Inset highlights nuclear localization of *UAS-tsr^{G19A}::mCherry*. (B) Maximum intensity projection of dissected third instar larvae in which *Dmef2-Gal4* was used to express the indicated *UAS* construct. Larval fillets were labeled with antibodies against dsRed (red) to label the Tsr::mCherry fusion protein and α -Actinin (Actn, green) to label Z-discs. Phalloidin (white) was used to label the actin cytoskeleton. (C) Viability of indicated *UAS* constructs when expressed using *Dmef2-Gal4*. Bar, 50 μ m.

more severe than those observed in patients with *CFL2* mutations though, suggesting that there is some residual activity retained by these alleles. Neither disease allele has been modeled *in vivo*.

One *CFL2* disease-associated mutation, G19A, which results in a Valine to Methionine amino acid change (Val7Met), affects a conserved nucleotide in *Drosophila* (Figure 1.25) (Ockeloen et al., 2012). Thus, we introduced the G19A mutation into full-length *tsr* and fused this to mCherry (*UAS-tsr^{G19A}::mCherry*). We also generated the full-length wild-type *tsr* (*UAS-tsr^{wt}::mCherry*) as a control. Live observation of *UAS-tsr^{G19A}::mCherry* expression driven by *Dmef2-Gal4* indicated that expression of *UAS-tsr^{G19A}::mCherry* increased from stage 17 to L3 (Figure 2.17A). Using this method, we were unable to discern any distinct subcellular localization of *UAS-tsr^{G19A}::mCherry*; however, we were able to observe translocation of the mutated protein to the nucleus, indicating that this function of Tsr is not affected (Figure 2.17A, inset). To get a better understanding of *UAS-tsr^{G19A}::mCherry* subcellular localization in muscle, we expressed both mutated and wild-type *tsr* using *Dmef2-Gal4*. *UAS-tsr^{wt}::mCherry* localized to Z-discs in L3 larvae (Figure 2.17B). The localization of *UAS-tsr^{wt}::mCherry* in L3 muscle was similar to that observed with the *GFP::Tsr* protein trap, suggesting that the addition of an mCherry tag did not affect Tsr localization (Figure 2.10). *UAS-tsr^{G19A}::mCherry* could also be observed at Z-discs, suggesting that the G19A mutation does not affect Tsr localization. Expression of either the disease allele or wild-type Tsr using *Dmef2-Gal4* did not affect the viability of embryos (Figure 2.17C). We next determined to what degree *UAS-tsr^{G19A}::mCherry* was

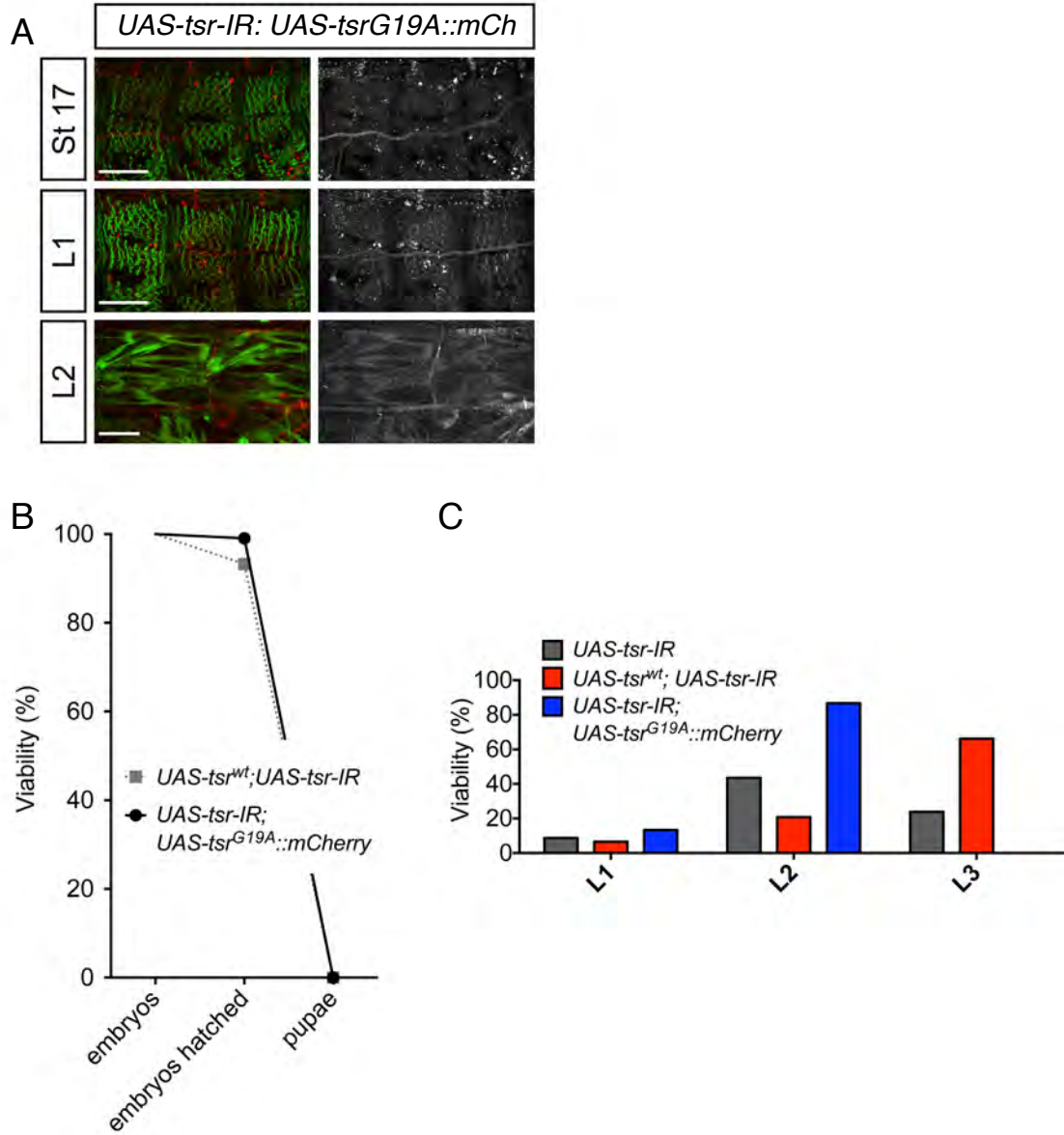


Figure 2.18. *UAS-tsr^{G19A}::mCherry* is unable to rescue *tsr* depletion. (A) Maximum intensity projection of embryos and developing larvae in which *Dmef2-Gal4* was used to express the indicated *UAS* constructs. *GFP::Zasp66* was used to mark Z-discs (green), and *UAS-tsr^{G19A}::mCherry* is in red (or greyscale in the adjacent single channel panel). (B) Viability of indicated *UAS* constructs when expressed using *Dmef2-Gal4*. (C) Breakdown of viability over larval development. Bar, 50 μ m.

able to rescue depletion of *tsr* by *UAS-*tsr*-IR*. Expression of *UAS-*tsr*^{wt}* is capable of partially rescuing *tsr* depletion (Figures 2.3F, 2.11). We found that *UAS-*tsr*^{G19A}::mCherry* expression did not improve sarcomere organization defects or decreases in viability associated with *tsr* depletion (Figure 2.18A-C). Together, our data indicate that *UAS-*tsr*^{G19A}::mCherry* cannot functionally substitute for wild-type Tsr, which is consistent with data in humans patients affected with NM that carry the same mutation.

Discussion

The ADF/cofilin family of actin regulators is responsible for turning over actin filaments to generate free monomers, which is critical to fuel subsequent actin polymerization (Bamburg, 1999). Regulators of actin polymerization, including Arp2/3, SCAR/Wave, WASp and Rac, play an essential role during muscle development in *Drosophila* (Rochlin et al., 2009). Despite this, the role of actin depolymerization has not been fully appreciated or characterized in any muscle system. Work in *C. elegans* and mouse have indicated that muscle-specific cofilins play a late role in sarcomere organization in striated muscle (Agrawal et al., 2012; Ono and Benian, 1998; Ono et al., 1999). However, *C. elegans* muscle does not fuse, and initial muscle development in *Cfl2* null mice is normal, likely due to the earlier functions of Cfl1 (Agrawal et al., 2012; Gurniak et al., 2005;

Ono et al., 1999). Thus, a role for ADF/cofilin proteins in muscle development has not been described.

Here, we demonstrate that Tsr is expressed in the body wall muscle of the *Drosophila* embryo. We further show, for the first time in any muscle system, a role for actin depolymerization at multiple steps during muscle development, including mesoderm migration, early patterning, actin focus formation during myoblast fusion and proper muscle-tendon attachments. With the exception of AIP1, which is also required for sarcomere organization in *C. elegans* (Ono, 2001), to our knowledge, the role of Tsr-interacting proteins has not been examined in muscle development and function. Our analysis indicates that this pathway is conserved during muscle development in *Drosophila*. In addition, we demonstrate that Tsr is also essential for sarcomere organization. Depletion of *tsr* specifically in the muscle results in progressive loss of sarcomere organization and defects in muscle function, indicating that muscle cofilins play a late, conserved role in this process.

Given the importance of regulators of actin polymerization to myoblast fusion in *Drosophila*, we were surprised that we did not observe fusion phenotype in *tsr^{N96A}* mutant embryos or in embryos in which *tsr* was depleted using either RNAi construct. It is likely that maternal transcript loading is allowing them to bypass these steps. To further reduce *tsr*, we combined *tsr^{N96A}* with null alleles of *ssh*, hypothesizing that loss of the Tsr-activating phosphatase would essentially render remaining Tsr protein inactive. *tsr*; *ssh* double mutant embryos displayed a number of defects in early developmental processes, including germband

retraction and dorsal closure, actin-dependent processes. In addition, we found that mesoderm migration was impaired and that myoblasts failed to fuse in *tsr*; *ssh* double mutants, suggesting that Tsr plays a broad role in embryonic mesoderm development, consistent with it being the only ADF/cofilin family member in *Drosophila*.

We decided to focus on later steps in muscle development, particularly understanding the underlying defect in myoblast fusion. In *Drosophila*, myoblast fusion occurs between two myoblast cell types, founder cells (FCs) and fusion competent myoblasts (FCMs) (Rochlin et al., 2009). Adhesion of FCs and FCMs results in the formation of an F-actin structure, termed the actin focus, at the site of contact, which resolves prior to fusion (Richardson et al., 2007). The actin focus has proven to be a valuable tool for highlighting functional differences between essential fusion proteins (Table 1.1, Figure 1.9). We failed to see any actin accumulations at presumptive sites of FC-FCM contact in *tsr*; *ssh* double mutant embryos, suggesting that Tsr was required upstream of F-actin focus formation and placing Tsr in the first class of fusion mutants, which consist of the four known transmembrane proteins required for FC/myotube-FCM adhesion (Richardson et al., 2007).

To gain additional insight to the role of Tsr during myoblast fusion, we examined the cellular behaviors that precede actin focus formation. We determined that FC specification was unaffected. We also demonstrated that FC-FCM contact was unaffected, despite the complete absence of foci formation. Thus, these data point to a role for Tsr in the formation of the actin focus

immediately downstream of FC-FCM contact. How Tsr may regulate focus formation is not clear. We did observe an increased level of cortical actin in unfused *tsr*, *ssh* double mutant myoblasts compared to cortical actin in unfused myoblasts which are capable of building a focus, suggesting that Tsr may turn over cortical actin so that it may be reorganized, recycled and used to construct the F-actin focus. The pathway/signal that would direct this function of Tsr is not clear. LIMK1 is activated by Rac, which is required for myoblast fusion and is found at the site of fusion in *Drosophila*, but this pathway inhibits cofilin activity (Bamburg, 1999; Hakeda-Suzuki et al., 2002; Haralalka et al., 2011; Luo et al., 1994; Richardson et al., 2007). Similarly, PIP₂, which is also required at the site of fusion, inhibits cofilin activity (Yonezawa et al., 1991; Bothe et al., in revision). These data suggest that Tsr activity would be suppressed at the site of fusion, and do not explain Tsr regulation upstream of focus formation. Thus, elucidating the mechanism that would activate Tsr at this step should be an important future goal. After successful FC/myotube-FCM contact, the fusion machinery, including Blow, Mbc and D-Wip, is recruited to the site of fusion (Haralalka et al., 2011; Kim et al., 2007; Massarwa et al., 2007; Richardson et al., 2007). It will be interesting to see if this still occurs in *tsr*, *ssh* double mutant embryos.

We also found that Tsr is required for proper muscle-tendon attachment, though it is unclear at which step Tsr functions. Tendon cells are properly specified in *tsr* null embryos. Further, using live imaging analysis, we determined that muscles do not detach in stage 17 *tsr^{N96A}* mutant embryos despite sustained

embryo contraction. It is possible that *tsr^{N96A}* mutant embryos are not capable of generating strong enough contractions to detach muscles, but we could not measure this directly. We did, however, observe a lack of coordinated, peristaltic-like contractions during this period in *tsr^{N96A}* mutant embryos, which is indicative of nervous system defects and consistent with a known role for Tsr in nervous system development (Gunsalus et al., 1995). Thus, Tsr does not appear to be required for tendon specification or for building a stable MTJ.

Prior to MTJ formation, myotubes extend growth cone-like filopodia towards tendon cells. Tsr is required for cell motility in other cell types (Chen et al., 2001). Thus, one possibility is that Tsr is required in extending (“migrating”) myotubes as they search out their proper tendon attachment site. In cases where myotubes are not able to extend to the appropriate tendon, they select an alternative site and continue normally with MTJ formation. Alternatively, the expression of or reception of cues by either myotubes or tendon cells may require Tsr activity.

Tsr does appear to have an essential role in tendon cells. Though we did not observe any defects in tendon cell specification or differentiation in *tsr^{N96A}* mutant embryos, depletion of *tsr* in tendons was pupal lethal, and pupae exhibited similar defects in metamorphosis to pupae in which *tsr* was depleted in the muscle. The MTJ, which connects muscle to the epidermis to allow for force generation, is a hemi-adherens junction that links the internal actin cytoskeleton of one cell to a neighboring cell or extracellular matrix (Tepass and Hartenstein, 1994). Depletion of *tsr* may disrupt this connection, causing defects in muscle

contraction. Importantly, we did not examine the muscle pattern in embryos in which *tsr* was depleted specifically in tendons. These embryos hatched at normal rates, suggesting that tendon function was not compromised enough to affect viability, but examination of the muscle pattern here would perhaps offer additional insight into the cause of the muscle attachment defects that we observed in *tsr^{N96A}* mutant embryos.

In human striated muscle, CFL2 is found at Z-discs where it colocalizes with α -Actinin (Papalouka et al., 2009). We found that Tsr is also localized to Z-discs in the larval muscle in *Drosophila* and colocalizes with Zasp, another Z-disc protein. Z-discs define the lateral sarcomere boundaries and anchor the plus (barbed) end of thin filaments (Clark et al., 2002). In contrast to F-actin in other cellular contexts, thin filaments elongate from the minus (pointed) end (Fischer and Fowler, 2003; Pollard et al., 2000). It is unclear what function Cofilin/Tsr would have at Z-discs. Tsr may be part of a mechanism to ensure that actin polymerization does not occur at the plus end. The plus end of the thin filament is also capped by CapZ (Clark et al., 2002); thus, there may be multiple proteins involved in limiting actin lengthening at this end. We also observed Tsr accumulation in the H-zone, which was not detected in analysis of human CFL2 localization. The H-zone is devoid of thin filaments, and this is necessary to allow for sarcomere shortening during muscle contraction (Clark et al., 2002). Tsr may also function here to establish a thin filament-free zone.

Depletion of *tsr* specifically in the muscle bypassed the defects we observed in muscle development in *tsr^{N96A}* mutant embryos but was still lethal,

indicating that Tsr is essential in the muscle. When *tsr* was depleted, sarcomere formation at stage 17 was normal, and defects in sarcomere organization became apparent at L1. L2 larvae were severely affected, and the majority of larvae developmentally arrested at this stage. Additionally, we found that when *tsr* was reduced, actin became hyperpolymerized; these defects were similar to those observed in UNC-60B and *CFL2* null worms and mice, respectively (Agrawal et al., 2012; Ono et al., 1999), indicating that cofilin homologs play a conserved role in the maintenance of sarcomere organization.

We found that *tsr* depletion affected the majority of muscles, though there was a slight preference towards more severe and more frequent sarcomere defects in muscles that attached to the segment border at each end (i.e., DO1-4, DA1-3, LL1, LO1, SBM, VL1-4) compared to muscles that did not attach at the segment border (i.e., LT1-4) (Figure 2.14B). This may reflect the additional/extra tension they are under compared to muscles that are attached on one side or neither side to the segment border.

We were not able to completely rescue the phenotypes associated with depletion of *tsr* using *UAS-ts^r-IR*. *UAS-ts^r-IR* targets a region of the *tsr* transcript including the third exon and 3' UTR (Figure 2.2A). The 3' UTR is absent in all *UAS-ts^r* constructs; thus, it is likely that *UAS-ts^r-IR* may still target *UAS-ts^r* constructs but perhaps less efficiently than endogenous *tsr*. Further, our rescue constructs do not contain 'wobble' codons, which also impact the effectiveness of rescue. Though we have not probed this biochemically, we have noticed that expression levels of *UAS-ts^r::mCherry* appear reduced in animals that also

express *UAS-tsr-IR*, providing support of our assumption that rescue constructs are also being depleted by RNAi constructs. We were also unable to rescue viability defects associated with the second *UAS-tsr RNAi* construct (Figure 2.3E), which targets the second exon, and therefore would be expected to target the *UAS-tsr* overexpression constructs as effectively as endogenous *tsr* transcript. Due to the similarity in phenotypes we observed with both RNAi constructs, we feel confident that both phenotypes are due to *tsr* depletion.

Surprisingly, our inability to rescue viability in *UAS-tsr-IR* larvae does not appear to be the result of an inability to rescue the somatic muscle sarcomere organization defects. In rescue larvae, sarcomere organization appeared normal, and Z-discs increased in number over larval development as in control larvae. Despite this, however, rescue larvae remained smaller than controls and did not pupate, suggesting that additional functions of Tsr were not rescued. Consistent with this, we found that depletion of *tsr* resulted in the cessation of eating and excreting and that these functions were not rescued with the expression of *UAS-tsr^{wt}*. These defects may be attributable to issues in the visceral mesoderm. Dmef2 is expressed in all muscle cell types, including the visceral mesoderm which surrounds the midgut (Nguyen et al., 1994). Visceral mesodermal cells are binucleated, striated and contain sarcomeric repeats which share features with somatic muscle sarcomeres (Stronach et al., 1999; Tepass and Hartenstein, 1994). Thus, it is likely that Tsr is also required in the visceral mesoderm for proper sarcomere organization. Why expression of wild-type Tsr would rescue *tsr*

depletion in the body wall muscle but not the visceral mesodermal cells is unclear.

Recent studies have identified mutations in Cofilin 2 in two families affected with Nemaline myopathy (Agrawal et al., 2007; Ockeloen et al., 2012). Nemaline myopathy is a disease of the sarcomere thin filaments and is characterized by the presence of electron dense nemaline bodies composed of actin, α -Actinin and other Z-disc proteins and muscle weakness (Sanoudou and Beggs, 2001b). The defects we observed with muscle-specific depletion of *tsr* resembled the disease state in patients with mutated *CFL2*. Muscle in *tsr* RNAi larvae contained overpolymerized actin that formed cores and nemaline body-like accumulations that contained both actin and α -Actinin. In addition, larvae were weak and displayed difficulties feeding.

Since one *CFL2* disease-associated mutation (*CFL2^{G19A}*) occurred at a conserved nucleotide (Ockeloen et al., 2012), we generated the corresponding *Drosophila* disease allele under *UAS* control. We found that *UAS-ts^{G19A}::mCherry* localized to Z-discs and retained the ability to translocate to the nucleus. However, *UAS-ts^{G19A}::mCherry* was not able to rescue *UAS-ts-IR* depletion of *tsr*, suggesting that it is not a fully functional protein.

It has been suggested that since *CFL2^{G19A}* results in a Val7Met amino acid change, *CFL2^{G19A}* could be alternatively translated to truncate the first six amino acids, including the regulatory Ser3 and a number of residues essential for both G- and F-actin binding (Bamburg et al., 1999; Ockeloen et al., 2012). One would expect this truncated protein to behave similarly to dominant negative Tsr. As with

UAS-tsr^{G19A}::mCherry, *UAS-tsr^{S3E}* is not able to rescue *tsr* depletion. This could be more directly addressed by determining whether Tsr(Val7Met) is capable of binding actin using *in vitro* approaches and could provide additional mechanistic insight into how Tsr/CFL2 activity is deficient.

In summary, using a combination of traditional alleles and other genetic tools, we are able to show that Tsr is required for both the development and function of *Drosophila* body wall muscle, likely fulfilling the roles of Cfl1 and Cfl2 in mammalian development. This approach highlights the strengths of *Drosophila* as a model system to study normal development. Our analysis suggests that *Drosophila* can also be a powerful system in which to model human muscle disorders. To our knowledge, this is the first description of a *Drosophila* model for Nemaline myopathy, a significant advance which will provide both a system for studying this disease and a platform for drug screening.

CHAPTER THREE:

**Coro is required for muscle development and
function in *Drosophila***

Chapter Overview

In a screen to identify genes which were differentially expressed in founder cells (FCs) compared to fusion competent myoblasts (FCMs), we identified the actin regulator *coronin* (*coro*) as upregulated in two different FC populations (Dobi et al., submitted). Coronin family proteins, present in the majority of eukaryotic organisms, are suggested to enhance the dynamics of actin filament turnover by coordinating Arp2/3-based actin polymerization with ADF/cofilin-based filament disassembly and severing (Figure 1.31) (Chan et al., 2011).

Drosophila coro was originally identified in a GAL4 enhancer-trap screen for segmentally-repeating expression patterns (Bharathi et al., 2004). Mutation of *coro* produces a number of defects in the eye, leg and wing, which are consistent with disruption in the actin cytoskeleton. To date, however, no in depth characterization of *coro* has been done in muscle in any system. We have recently demonstrated that the *Drosophila* ADF/cofilin family member Twinstar (Tsr) is required for proper muscle development and function in *Drosophila* (this study, Chapter 2). The cooperation of ADF/cofilin and coronin in numerous developmental contexts prompted us to investigate whether Coro is also required for muscle development in *Drosophila* (Brieher et al., 2006; Cai et al., 2007; Kueh et al., 2008; Lin et al., 2010).

We found that Coro is expressed in the body wall muscle of the embryo and larvae and that *coro* mutants had a number of embryonic muscle defects. Further, we demonstrate that Coro is required autonomously for muscle function

in the larvae and adult. Muscle-specific depletion of *coro* resulted in reduced viability and in the inability of adults to fly. Together, our data indicate that Coro is required for the proper development and function of the *Drosophila* muscles.

Results

Coro is expressed in the body wall muscle of the Drosophila embryo

In *Drosophila*, *coro* is maternally loaded (0-2 hrs AEL) and highly expressed throughout development (Figure 3.1B) (Gelbart and Emmert, 2010; Graveley et al., 2010). Genome-wide chromatin immunoprecipitation (ChIP)-on-chip data of the mesoderm- and muscle-specific transcription factors, Twist and Dmef2, respectively, identified regions of Twist- and DMef2-binding enrichment in the 5' and 3' UTRs of *coro*, suggesting that *coro* is expressed in mesoderm and muscle of the embryo (Figure 3.1A) (Zinzen et al., 2009). *in situ hybridization* data available through the Berkeley *Drosophila* Genome Project (BDGP) also detected mesoderm and early muscle expression of *coro* (up to stage 12); later stages are not available (Tomancak et al., 2002; 2007).

We performed *in situ hybridization* to *coro* to confirm the *in situ* analysis provided by the BDGP and to determine where *coro* was expressed in the late embryo (Figure 3.2A). Consistent with the available data from high-throughput studies, we found that *coro* was maternally loaded and expressed early in the

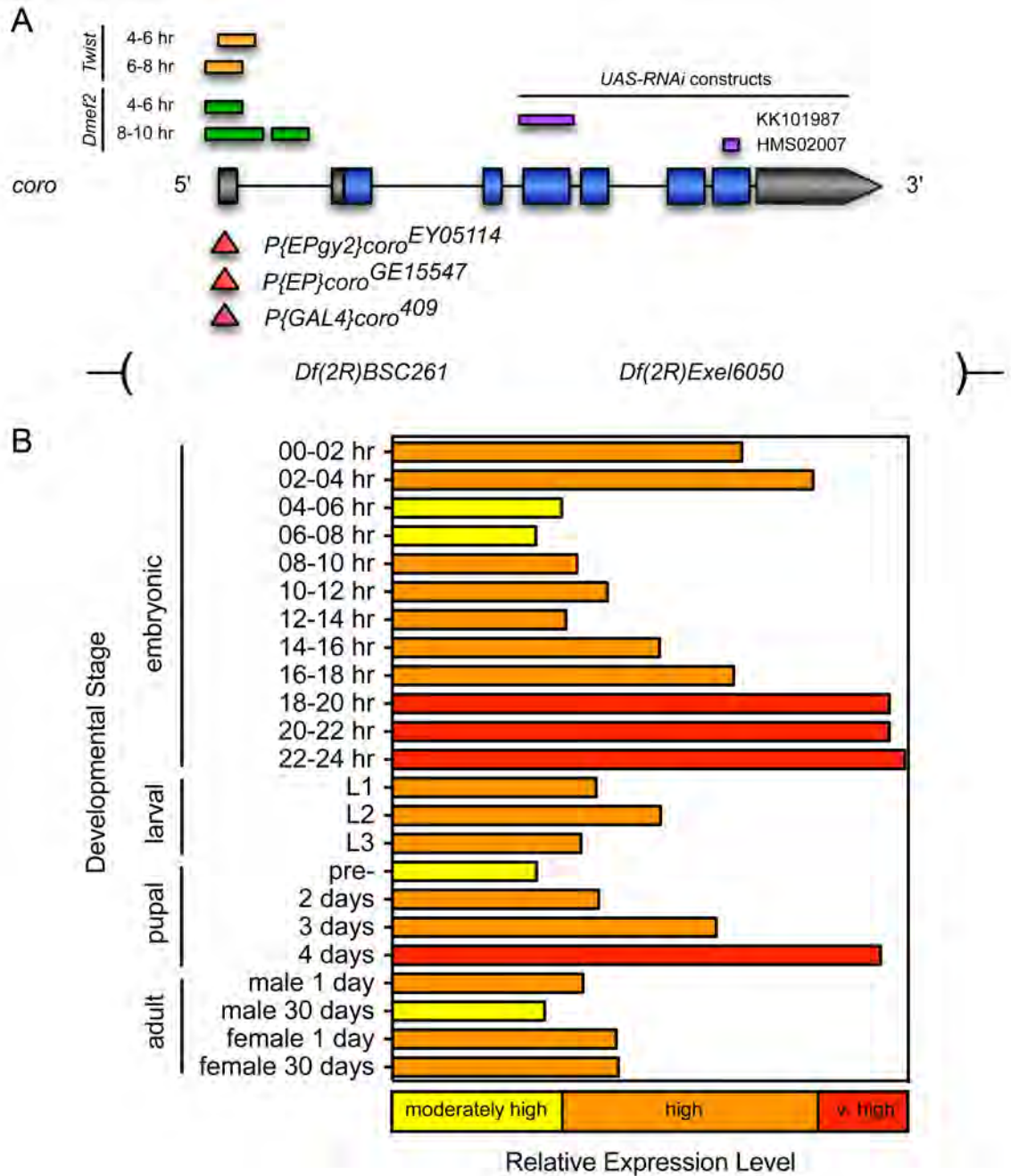


Figure 3.1. *coro* is highly expressed throughout *Drosophila* development. (A) Schematic diagram of the *coro* locus in *Drosophila*. Orange and green bars above the locus represent regions enriched for Twist and Dmef2-binding, respectively (Zinzen et al., 2009). Purple bars indicate region targeted by *UAS-RNAi* constructs. Alleles used in this study are indicated below the locus. Grey bars, untranslated regions. Blue bars, exons. Red triangles, P-element insertions. Deletions that remove portions of the chromosome, including *coro*, are schematized by a gap in the chromosome bracketed by parentheses. (B) Summary of *coro* expression over *Drosophila* development. *coro* is highly expressed throughout embryonic, larval, pupal and adult stages. Modified from (Gelbart et al., 2010; Graveley et al., 2010).

mesoderm (Figure 3.2A left and middle panels) (Gelbart and Emmert, 2010; Graveley et al., 2010; Tomancak et al., 2002; 2007; Zinzen et al., 2009). At stage 16, *coro* is also expressed in a pattern that is strikingly similar to the final muscle pattern of the embryo (Figure 3.2A, right panel). Using the 409-GAL4 enhancer insertion, mapped to the 5' untranslated region (UTR) of *coro*, to drive expression of *UAS-lacZ*, we found that *lacZ* is expressed in all myosin heavy chain (MHC)-positive muscles of the embryonic body wall, suggesting that Coro is expressed in embryonic muscle and plays a general role in *Drosophila* muscle development and/or function (Figures 3.1A, 3.2B) (Bharathi et al., 2004).

We also observed high expression in the salivary glands and additional non-muscle cells, indicating that Coro is broadly expressed (Figure 3.2B). Notably, we did not detect *coro* or β -gal (as a read-out of Coro) in the central nervous system (CNS), though previous *in situ hybridization* analysis has reported its expression there (Bharathi et al., 2004). The BDGP *in situ* collection also failed to detect *coro* expression in the CNS (Tomancak et al., 2002; 2007). Tsr is expressed in the CNS where it plays a well-characterized role in nervous system development and function (Gunsalus et al., 1995; Ng and Luo, 2004). It is possible that Coro does not cooperate with Tsr in every context; however, we cannot rule out the possibility that our analyses only partially recapitulate the *coro* expression pattern *in vivo* (Figure 3.2B).

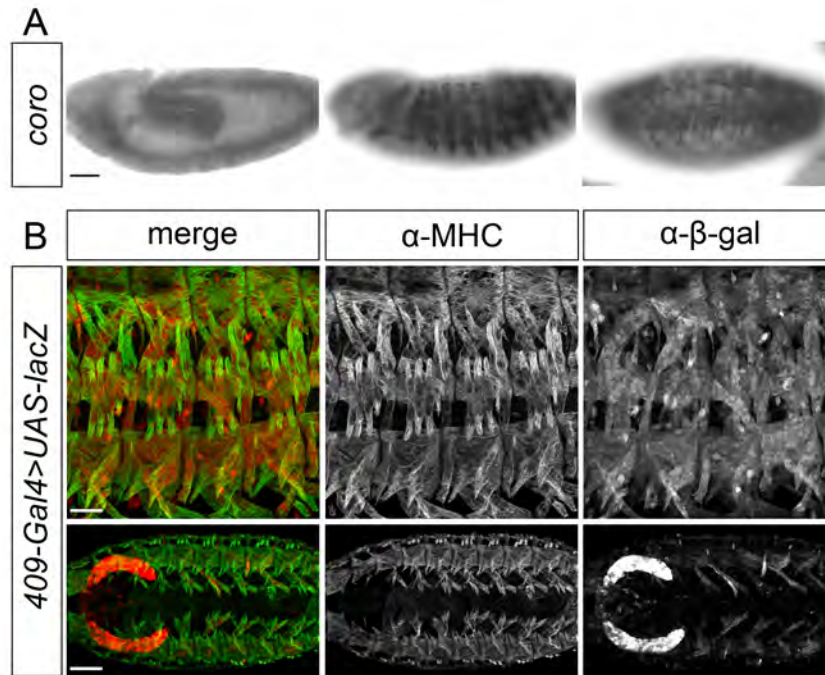


Figure 3.2. Coro is expressed in the embryonic body wall muscle of *Drosophila*. (A) *coro* is expressed at stage 9 in the mesoderm (left), at stage 14 in early muscle (center) and at stage 16 in the developed muscle (right) of the *Drosophila* embryo (courtesy of M. Halfon). (B) *409-Gal4*, *UAS-lacZ*, a reporter for Coro (α - β -gal, red), colocalizes with Myosin heavy chain (α -MHC, green) in somatic muscle at stage 16. *lacZ* is also expressed in non-muscle cells, including the salivary glands. Bar, 50 μ M.

Coro is required for the proper development of the embryonic body wall muscle

To test whether Coro is required for muscle development, we obtained three *coro* mutant alleles, *coro*^{EY05114}, *coro*^{GE15547} and *coro*⁴⁰⁹, all P-element insertions mapped to the 5' UTR of *coro*, and two deficiencies, *Df(2R)Exel6050* and *Df(2R)BSC261*, which completely remove the *coro* locus (Figure 3.1A). A list of the genes removed in each deficiency is presented in Table 3.1. The muscle pattern in embryos homozygous for any of the P-element insertions appeared wild-type (compare to *OreR*, Figure 3.3A-B). This was unsurprising given that these stocks are homozygous viable and fertile and suggested that none of the P-element insertions appreciably affects Coro function, that Coro is not essential for muscle development and viability, or that maternal loading is sufficient for embryonic muscle development.

Similarly, the majority of hemisegments in embryos homozygous for either of the two deficiencies that remove *coro*, *Df(2R)BSC261* and *Df(2R)Exel6050*, appeared wild-type (Figure 3.4A, C). However, these embryos failed to hatch, suggesting that *coro* or other gene(s) removed are essential for viability (Figure 3.4B). To reduce the number of genes that are homozygously deleted, we analyzed embryos transheterozygous for the two deficiencies (Table 3.1, overlapping). The muscle pattern of *Df(2R)Exel6050/Df(2R)BSC261* embryos also appeared wild-type (data not shown) but failed to hatch, narrowing the list of genes required for viability but not clearly implicating *coro* (Figure 3.4C). A summary of these data are available in Table 3.2.

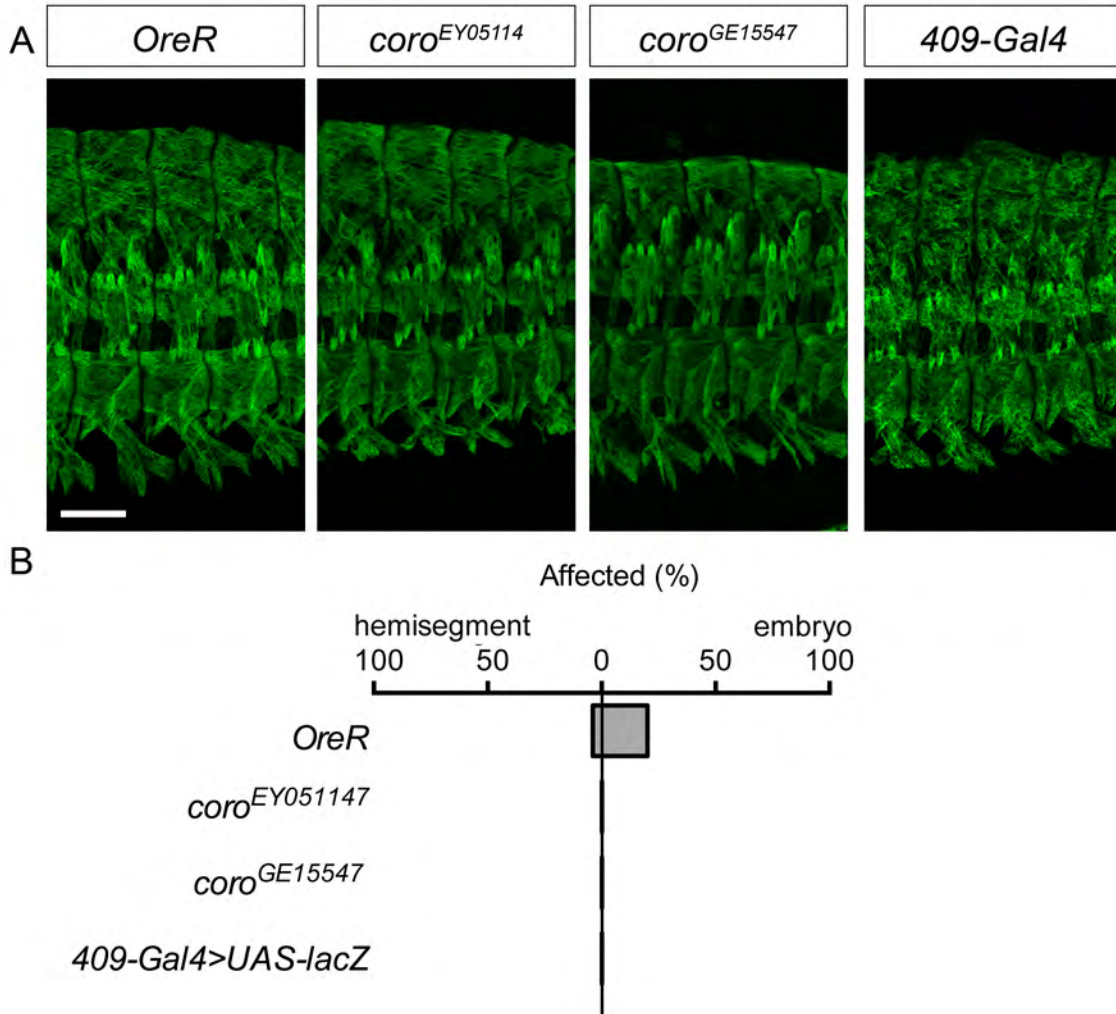


Figure 3.3. P-element insertions in *coro* do not disrupt the embryonic muscle. (A) Maximum intensity projection of a stage 16 embryo labeled with an antibody against Myosin heavy chain (green) to visualize the embryonic body wall muscle. Three representative hemisegments are shown for each genotype. (B) Quantification of the percentage of affected hemisegments (left) and embryos (right) of each genotype indicated. n = 20 embryos, 100 hemisegments. Bar, 50 μ m.

In addition to the P-element and deficiencies described above, we obtained several *coro* excision alleles. The *coro* excision (*coro^{ex}*) alleles (*ex³*, *ex⁴*, *ex⁶*, *ex⁷*, *ex⁸* and *ex¹¹*) were generated by the imprecise excision of the *409-GAL4* enhancer trap (*coro⁴⁰⁹*) in the 5' UTR of *coro* (Figure 3.1A) (Bharathi et al., 2004). All ten alleles generated (we obtained the six listed above) reportedly belonged to a single complementation group and showed varying degrees of lethality (summarized in Table 3.3). In addition, the molecular lesions in the *coro* locus were identified in all four alleles analyzed (*ex⁶*, *ex⁸*, *ex¹⁰* and *ex¹¹*), suggesting that the phenotypes observed are due to mutations in *coro*. Importantly, the muscle pattern in embryos homozygous for *coro⁴⁰⁹* appeared wild-type, indicating that the insertion itself did not affect Coro activity (Figure 3.3).

Embryos homozygous for either *coro^{ex3}* or *coro^{ex4}* alleles had a wild-type muscle pattern (Figure 3.5A-B) but they had defects in viability later in development (Figure 3.5C), suggesting that the maternal contribution of *coro* is sufficient for muscle development in the embryo and/or that these are weak hypomorphic alleles. In contrast, embryos homozygous for *coro^{ex6}*, *coro^{ex7}*, *coro^{ex8}* and *coro^{ex11}* had a number of striking muscle patterning defects, which affected a high percentage of hemisegments per embryo (Figure 3.5A-B). Further, the viability of these embryos was decreased and ranged from 0-50% of adults eclosing, indicating that Coro is important for viability (Figure 3.5C). The eclosion rate of heterozygous controls ranged from 60-75% and could reflect a decrease in fitness due to the heterozygous *coro* mutation; however, it is more likely due to a decrease in fitness associated with the balancer chromosome.

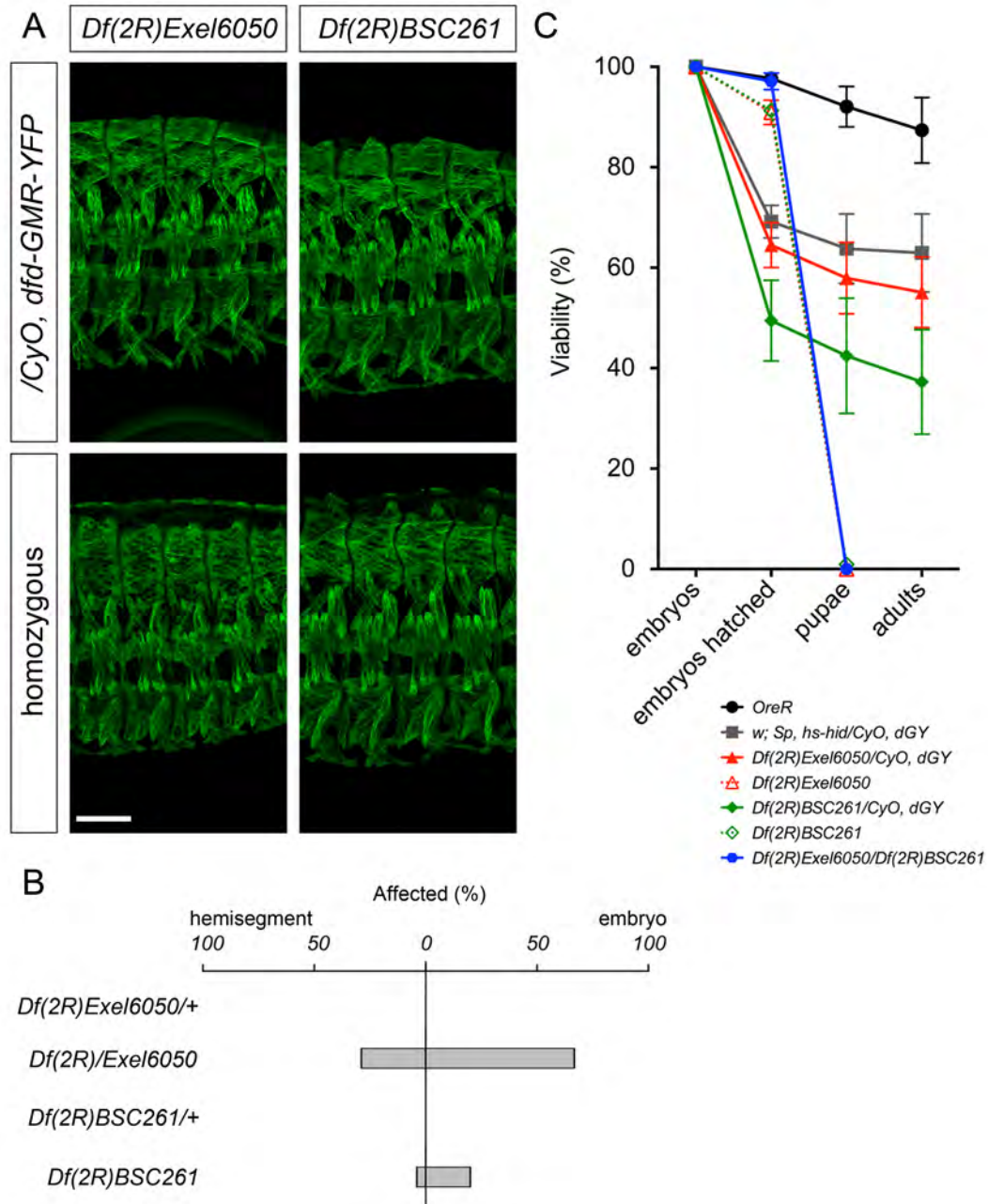


Figure 3.4. Deficiencies which remove *coro* do not cause an embryonic muscle phenotype. (A) Maximum intensity projection of a stage 16 embryo labeled with an antibody against Myosin heavy chain (green) to visualize the embryonic body wall muscle. Three representative hemisegments are shown for each genotype. (B) Quantification of the percentage of affected hemisegments (left) and embryos (right) of each genotype indicated. A single hemisegment with 1-2 affected muscles was affected in more than half of the embryos homozygous for *Df(2R)Exel6050*. $n = 20$ embryos, 100 hemisegments. (C) Quantification of the viability of each genotype at the indicated developmental stage. $n = 100$ embryos. Error bars, s.e.m. Bar, 50 μm .

Table 3.1. A list of unique and overlapping genes deleted in two deficiencies that remove *coro*

<i>Df(2R)Exel6050</i>	overlapping	<i>Df(2R)BSC261</i>
<i>phtf</i>	<i>Epac</i>	<i>CG9447</i>
<i>CG3267</i>	<i>Cyp6a2</i>	<i>Spn42Da-e</i>
<i>Eb1</i>	<i>SdhB</i>	<i>CG30158</i>
<i>CG3420</i>	<i>CG15237</i>	<i>CG3358</i>
<i>CG9436</i>	<i>ubl</i>	<i>mim</i>
	<i>koi</i>	<i>CheB42a-c</i>
	<i>CG15236</i>	<i>ppk25</i>
	<i>CG34215</i>	<i>Cyp6u1</i>
	<i>CG9445</i>	<i>CG30157</i>
	<i>coro</i>	<i>vimar</i>
		<i>CG44171</i>
		<i>CG30156</i>
		<i>CG17002</i>
		<i>Tsp42Ea-f</i>
		<i>CG30159</i>
		<i>CG30160</i>
		<i>CG43646</i>
		<i>CG43647</i>

In support of this, viability of *w; Sp, hs-hid/CyO, dGY*, which should not harbor any lesions in *coro*, also eclosed at a lower rate (~65-70%) than wild-type controls (data not shown).

Upon closer analysis of the muscle phenotype, we observed that the lateral transverse (LT) muscles were particularly affected. We found that 15-47% of LTs were affected, while defects for other muscle groups ranged from 0-7% in the same embryos, which is similar to the percentage observed in heterozygous controls (Figure 3.6). We further classified these defects and found that muscle loss and muscle misattachment were the most prevalent defects, while events like muscle duplication/addition were more rare (Table 3.3). A summary of these data are available in Table 3.4.

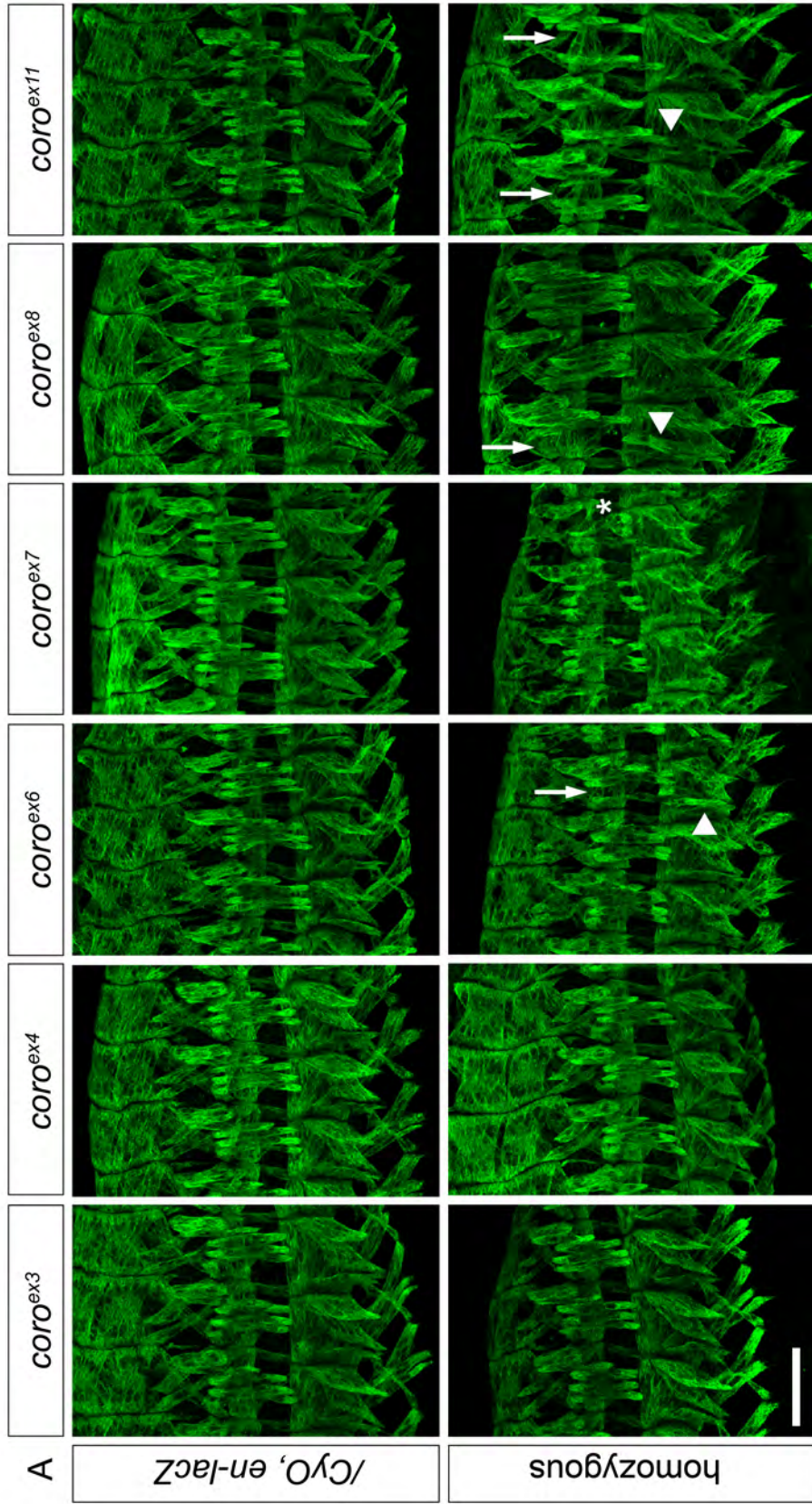
Coro is required for muscle function

To determine whether its mutation impacted muscle function, we assayed larval locomotion in *coro* mutants using an automated tracking system wherein third instar larvae are motivated to crawl towards an odorant and the average and maximum crawling velocities are calculated (Louis et al., 2008a; 2008b). Larvae homozygous for either P-element insertion displayed a nearly 33% reduction in average crawling velocity compared to *OreR* controls, indicating that although *coro*^{EY051147} and *coro*^{GE15547} animals are viable, fertile and have no obvious embryonic muscle phenotypes, some aspect of muscle function is impaired (Figure 3.7). Moreover, compared to heterozygous control larvae,

Table 3.2. Summary of phenotypes observed in homozygous embryos.

genotype	viability ^a	fertility	embryonic defects ^b	larval locomotion defects ^c	adult phenotypes ^d
<i>coro</i> ^{GE15547}	Viable	Fertile	No	Yes	Yes
<i>coro</i> ^{EY05114}	Viable	Fertile	No	Yes	No
<i>Df(2R)Exel6050</i>	0% hatch	NA	No	NA	NA
<i>Df(2R)BSC261</i>	0% hatch	NA	No	NA	NA
<i>409-GAL4</i>	Viable	Fertile	No	NT	No

^aSee also Figure 3.3C ^bSee also Figure 3.3A-B ^cSee also Figure 3.6 ^dSee also Figure 3.7. NA=not applicable, NT=not tested.



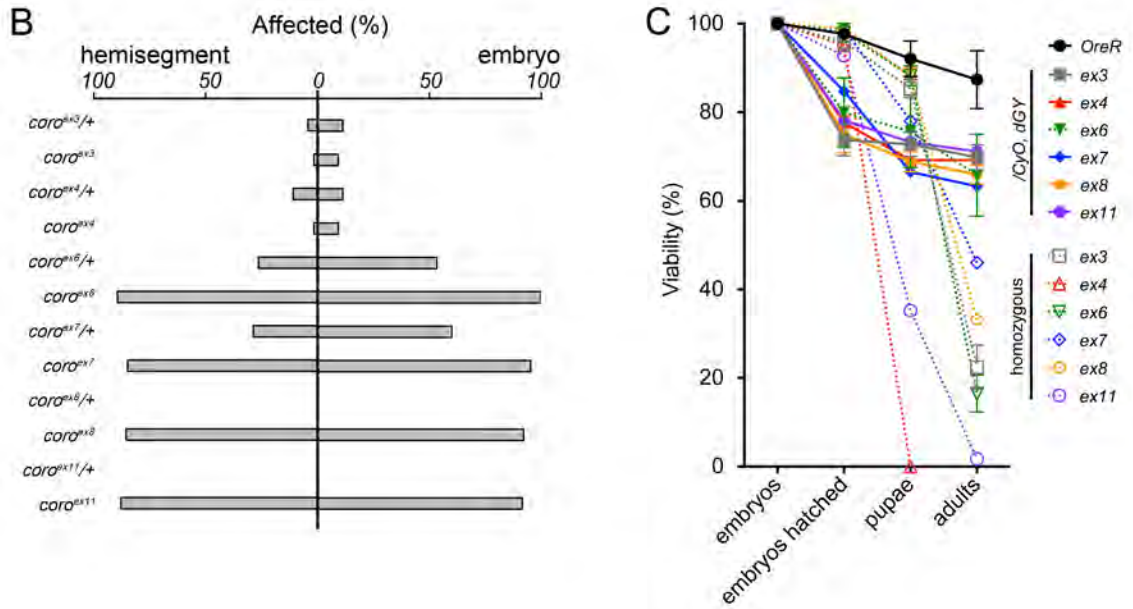


Figure 3.5. *coro^{ex}* alleles have embryonic muscle defects. (A) Maximum intensity projection of a stage 16 embryo labeled with an antibody against Myosin heavy chain (green) to visualize the embryonic body wall muscle. Three representative hemisegments are shown for each genotype. Some defects are indicated by arrows (muscle loss), arrowheads (muscle attachment defects) and asterisks (muscle shape defects). (B) Quantification of the percentage of affected hemisegments (left) and embryos (right) of each genotype indicated. n = 20 embryos, 100 hemisegments. (C) Quantification of the viability of each genotype at the indicated developmental stage. n = 100 embryos. Error, s.e.m. Bar, 50 μ m.

larvae homozygous for *coro^{ex3}* had no statistically significant defect in larval locomotion. This was not unexpected as *coro^{ex3}* mutant embryos had few muscle defects and pupate at a rate similar to *OreR* controls (Figure 3.5). In contrast, however, larvae homozygous for *coro^{ex6}*, *coro^{ex7}* and *coro^{ex8}* alleles, which all exhibited defects in embryonic muscle development (Figure 3.5), displayed statistically significant decreases in larval crawling velocity compared to heterozygous control larvae, indicating that Coro is required for muscle function in the larvae (Figure 3.7). Importantly, we cannot rule out a possibility that Coro is acting in the nervous system. In addition to not properly signaling to the muscles, nervous system defects can also include issues in odorant sensing; however, we did not see evidence for this as larvae did crawl towards the odorant.

To test whether adult muscle was affected in genotypes that were able to eclose (Figure 3.5C), we used an assay to observe adult behaviors, including walking, jumping and flying. We found that *OreR* control flies use a variety of approaches to scale the graduated cylinder, including walking, jumping and flying. Compared to *OreR* control adults, *coro^{EY051147}* adults did not display a statistically significant impairment in completing the assay and displayed all three behaviors (Figure 3.8B). *coro^{GE15547}* adults were only slightly impaired. In contrast, *coro^{ex3}*, *coro^{ex6}*, *coro^{ex7}* and *coro^{ex8}* adults were severely impaired in their ability to mount the graduated cylinder, maintain their attachment to the cylinder walls while walking and reach the marked line before the end of the assay.

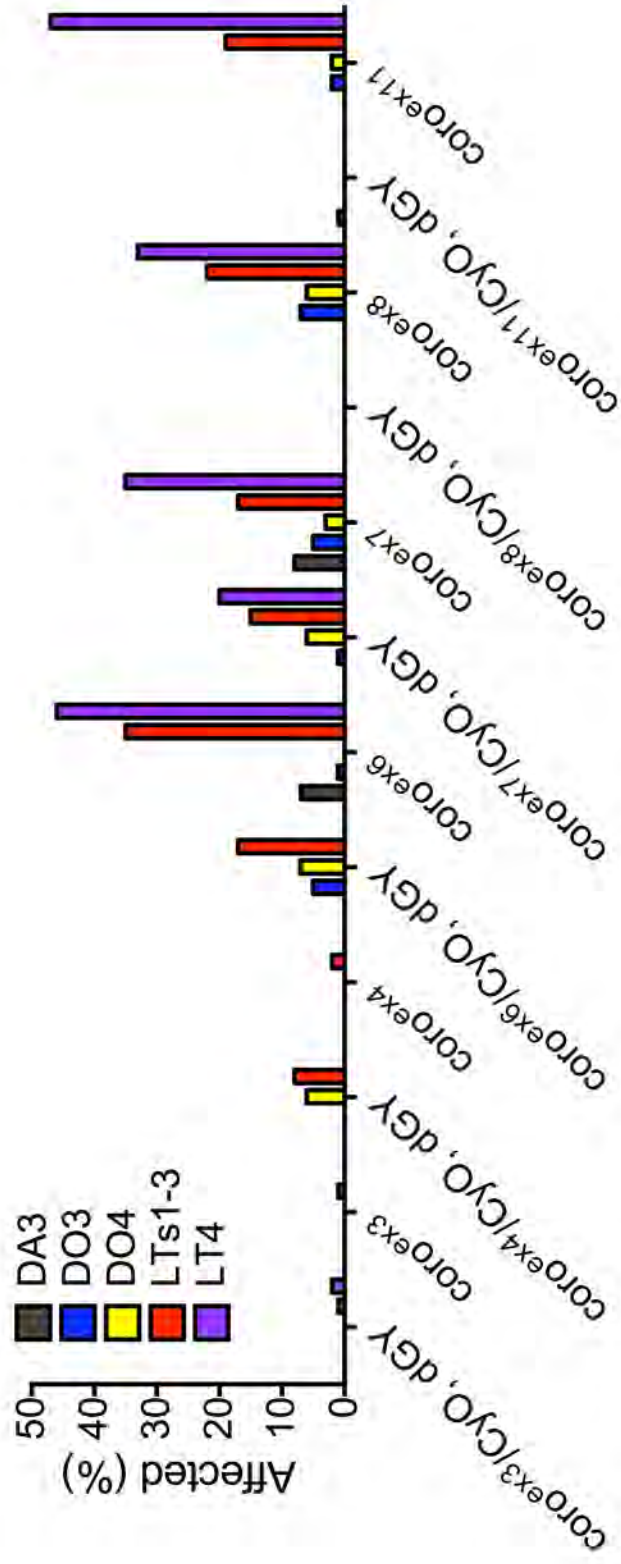


Figure 3.6. The lateral transverse (LT) muscles are specifically affected in *cororex* mutants. Histogram depicting the percentage of affected muscles of the indicated muscle identity in each genotype. Other muscle groups, including the segment border muscle, ventral acute muscles 1-3 and ventral oblique muscles 4-6 were not included here as the percentage of affected muscles was less than five in all genotypes analyzed. n = 20 embryos, 100 hemisegments.

These locomotor defects suggested that adult muscle was affected. Together with the dorso-ventral muscles (DVMs), dorsal longitudinal muscles (DLMs) make up the adult indirect flight muscles (IFMs). DLMs are six bilaterally symmetric muscles and are responsible for generating wing depression during wing beating (Figure 3.9) (See also Introduction, page 58) (Crossley, 1978). All *coro^{ex}* heterozygotes analyzed (only *coro^{ex8}/If* is shown) contained the proper number and organization of DLMs. In the *coro^{ex}* mutant adults analyzed, we identified a number of defects, including muscle loss (*coro^{ex3}*), disruption of the bilateral symmetry (*coro^{ex6}*, *coro^{ex7}* and *coro^{ex8}*) and muscle gain (*coro^{ex8}*). Overall, however, only a small percentage (10%) of mutant adults displayed any gross change in DLM organization, while nearly every mutant fly analyzed had defects in movement, suggesting that the underlying muscle defect may be on a more subcellular level than we analyzed (Figure 3.8). Additionally, we did not analyze the tergal depressor of the trochanter (TDT, or jump muscle) or the leg muscles; however, the phenotypes we observed in walking and jumping suggest that they are also affected. Again, we cannot rule out the possibility that these defects are the result of the loss of Coro in the nervous system.

Verifying coro is disrupted in coro^{ex} alleles

Imprecise P-element excision can generate lesions at or nearby the initial insertion site as well as disrupt genes at a new landing site. Importantly, we observed no embryonic phenotypes with the original Gal4 insertion, *coro⁴⁰⁹*,

Table 3.3 Summary of defects observed with *coro^{ex}* alleles

genotype	number of hemisegments	loss	addition	not shifted ^a	mis-attachment ^b	shape	gap	total defects
<i>coro^{ex3}/CyO, en-lacZ</i>	70	0 (0)	0 (0)	0 (0)	1 (50)	0 (0)	1 (50)	2
<i>coro^{ex3}</i>	55	0 (0)	1 (100)	0 (0)	0 (0)	0 (0)	0 (0)	1
<i>coro^{ex4}/CyO, en-lacZ</i>	50	0 (0)	4 (25)	0 (0)	4 (25)	8 (50)	0 (0)	16
<i>coro^{ex4}</i>	55	1 (100)	0 (0)	0 (0)	0 (0)	0 (0)	0 (0)	1
<i>coro^{ex6}/CyO, en-lacZ</i>	75	14 (51.9)	5 (18.5)	2 (7.4)	3 (11.1)	0 (0)	3 (11.1)	27
<i>coro^{ex6}</i>	95	58 (42)	0 (0)	5 (3.6)	46 (33.3)	11 (8)	18 (13)	138
<i>coro^{ex7}/CyO, en-lacZ</i>	100	13 (20)	8 (12.3)	0 (0)	3 (4.6)	40 (61.5)	1 (1.5)	65
<i>coro^{ex7}</i>	115	30 (29.7)	1 (1)	6 (5.9)	33 (32.7)	17 (16.8)	14 (13.9)	101
<i>coro^{ex8}/CyO, en-lacZ</i>	50	0 (0)	0 (0)	0 (0)	0 (0)	0 (0)	0 (0)	0
<i>coro^{ex8}</i>	70	11 (16.7)	3 (4.5)	3 (4.5)	24 (36.4)	13 (19.7)	12 (18.2)	66
<i>coro^{ex11}/CyO, en-lacZ</i>	55	0 (0)	0 (0)	0 (0)	0 (0)	0 (0)	0 (0)	0
<i>coro^{ex11}</i>	65	9 (14.3)	2 (3.2)	6 (9.5)	26 (41.3)	11 (17.5)	9 (14.3)	63

Number in parentheses indicates percentage of total defects in a particular category. ^a L4-specific defect ^b Includes cross-over attachment defects.

indicating that the original insertion did not cause the observed phenotype and did not already contain a second hit that causes the observed phenotype (Figure 3.3). To rule out the possibility that a second lesion was generated upon imprecise excision of the *coro*⁴⁰⁹ P-element which is responsible for the *coro*^{ex} phenotype, we assessed the ability of each *coro*^{ex} allele to complement one another. We first analyzed the viability and fertility of all transheterozygous combinations of *coro*^{ex} alleles (Table 3.5). We found that only 1-9% of *coro*^{ex3/ex4} adults eclosed (33% expected if alleles fail to complement). Similarly, any pairwise combination of *coro*^{ex6}, *coro*^{ex7}, *coro*^{ex8}, or *coro*^{ex11} resulted in only 0-8% of adults emerging, independent of which allele came from which parent. Transallelic combinations of *coro*^{ex3} or *coro*^{ex4} with *coro*^{ex6}, *coro*^{ex7}, *coro*^{ex8}, or *coro*^{ex11} resulted in 14-52% of the transheterozygous progeny emerging, suggesting that multiple complementation groups may be present. With any combination of alleles, however, we found a defect in fertility of the transheterozygous progeny. We did not test to see if this was sex-specific. We also analyzed the viability of each *coro*^{ex} allele in trans to *coro*^{GE15547}. We found that crossing *coro*^{GE15547} adults to adults of each *coro*^{ex} allele produced viable and fertile transheterozygous adults at the expected frequency independent of the direction of the cross.

In addition, we analyzed the muscle pattern in embryos transheterozygous for *coro*^{ex6/ex7} and *coro*^{ex6/ex11}. These embryos displayed a similar muscle phenotype to embryos homozygous for the individual alleles (Figure 3.10A). Again, the LT muscles were almost exclusively affected, and missing and

Table 3.4. Summary and comparison of phenotypes observed in animals homozygous for *coro* alleles used in this study and in Bharathi et al., 2004.

genotype	viability				adult phenotypes		
	this study ^a	Bharathi et al., 2004.	fertility	embryonic defects ^b	larval locomotion defects ^c	this study ^d	Bharathi et al., 2004.
<i>coro</i> ^{ex3}	<25% eclose	Early pupal	NF	No	No	Yes	NA
<i>coro</i> ^{ex4}	0% pupate	Early pupal	NF	No	NA	NA	NA
<i>coro</i> ^{ex6}	<20% eclose	Early pupal	NF	Yes	Yes	Yes	NA
<i>coro</i> ^{ex7}	<50% eclose	Early pupal	NF	Yes	Yes	Yes	NA
<i>coro</i> ^{ex8}	<35% eclose	Pharate adult	NF	Yes	Yes	Yes	NA
<i>coro</i> ^{ex11}	<10% eclose	10% eclose	NF	Yes	NT	Yes	Yes
<i>coro</i> ^{ex6/ex7}	<50% eclose	NT	NF	Yes	NT	Yes	NT
<i>coro</i> ^{ex6/ex11}	<65% eclose	Pharate adult	NF	Yes	NT	Yes	Yes ^e

^aFigure 3.5C ^bFigure 3.5A-C ^cFigure 3.6 ^dFigure 3.6 ^eAnalyzed pharate adults
 NF=not fertile, NA=not applicable, NT=not tested

misattached LT muscles were the most prevalent defect observed (data not shown). Further, this phenotype was highly penetrant, affecting nearly 100% of hemisegments in almost all embryos analyzed (Figure 3.10B). Surprisingly, the viability of transheterozygous animals improved upon the viability of animals homozygous for a single allele, suggesting that additional modifiers or lesions may be present in allele backgrounds (Figure 3.10C). The viability reported here was greatly increased compared to the viability reported in Table 3.5. This was likely due to the different approaches we used to assess viability. Though viability was improved, transheterozygous adults displayed the same defects in walking, jumping and flying that we observed in adults homozygous for a single allele (data not shown). Taken together, these data implicate the disruption of a single gene, *coro*, to give the observed muscle phenotype.

For additional confirmation, we examined each *coro^{ex}* allele in trans with each deficiency (Figure 3.1). To our surprise, we failed to see any embryonic muscle phenotype with any combination of allele and deficiency, though the occasional hemisegment had 1-2 affected muscles (Figure 3.11A, B). Furthermore, all embryos hatched and developed into adults at a similar rate to *OreR* control embryos, indicating that maternal loading is not a sufficient explanation for the lack of embryonic phenotype we observed (Figure 3.11C). One interpretation of these data is that mutation of *coro* is not responsible for the phenotypes described above and that a second mutation, carried on all of the *coro^{ex}* alleles is responsible for the phenotype.

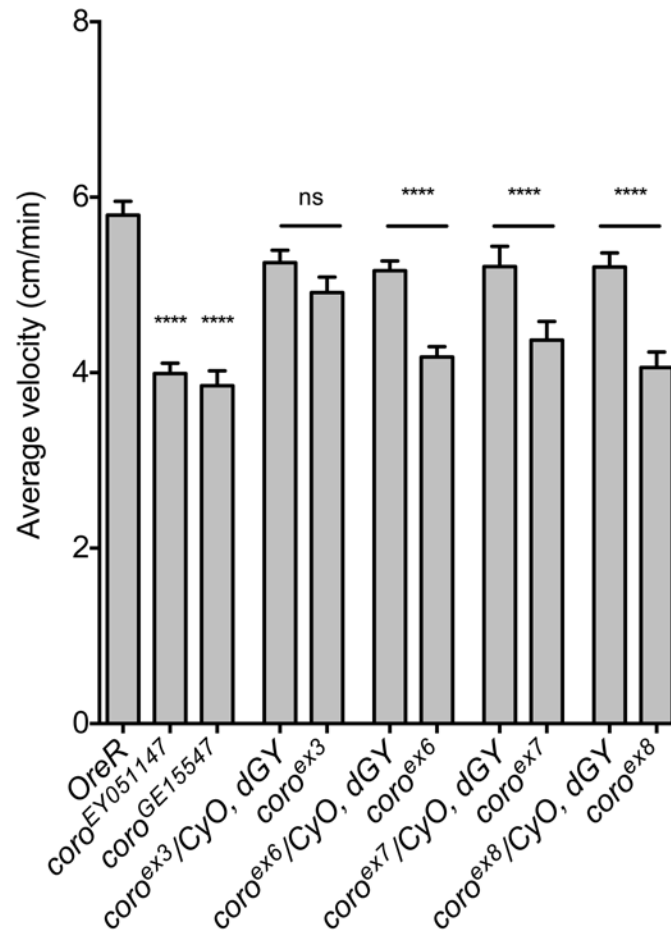


Figure 3.7. *coro* is required for larval locomotion. Third instar larvae of the indicated genotype were tracked using an automated system (Louis et al., 2008a; 2008b). *coro^{EY051147}* and *coro^{GE15547}* mutant larvae crawl at a reduced averaged velocity compared to *OreR* control larvae. *coro^{ex3}* mutant larvae do not display any defects in larval crawling compared to heterozygous controls. In contrast, *coro^{ex6}*, *coro^{ex7}* and *coro^{ex8}* mutant larvae are significantly impaired in their average velocity compared to heterozygous control larvae. n = 30 larvae. Error bars, s.e.m. ****p < 0.0001. ns, not significant.

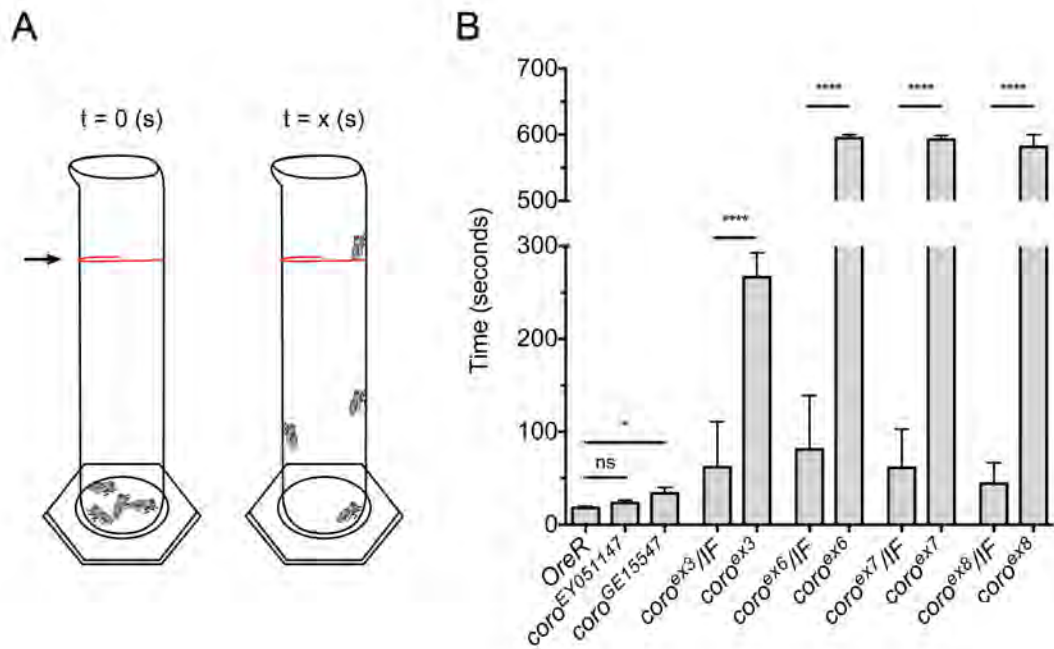


Figure 3.8. *coro* mutant adults have defects in walking, jumping and flying. (A) Groups of 10 adult flies were placed in a graduated cylinder and tapped until all flies were at the base. The time it took for each fly to reach a line drawn at 7 cm (arrow) was determined and plotted in (B). Flies that failed to reach the end point were given a time score of 600 seconds. $n > 30$. Error bars, s.e.m. * $p < 0.5$, **** $p < 0.0001$. ns, not significant.

Alternatively, as the lesions in *coro* are thought to be regulatory in nature (Bharathi et al., 2004) and the deficiencies appear to rescue *coro^{ex}* phenotypes, we hypothesized that *coro* is overexpressed in these alleles. To test this hypothesis, since there is no antibody available to detect *Drosophila* Coro, we wanted to reduce *coro* in the muscle using RNAi in *coro^{ex6}* embryos (Figure 3.12).

Muscle-specific knockdown of coro does not affect embryonic muscle development

We first determined the embryonic phenotype associated with muscle-specific *coro* depletion alone. Previous work has indicated that adult myofibrils are “frayed” in *coro* knockdown adults though the mechanism was not explored and a requirement for Coro earlier in muscle development was not addressed (Figure 1.32) (Schnorrer et al., 2010). We used two *UAS-RNAi* constructs to target *coro*, *UAS-coro RNAi* (TRiP HMS2007, DRSC) and *UAS-coro-IR* [VDRC KK101987, used in (Schnorrer et al., 2010)] (Figure 3.1A). Expression of either *UAS-RNAi* construct using both *twist-Gal4* and *Dmef2-Gal4* or *Dmef2-Gal4* alone did not result in any embryonic defects compared to embryos in which either *UAS-RNAi* construct was crossed to *yw* (no GAL4) or in which *UAS-mCherry RNAi* was expressed as a control (Figure 3.12A-B). These data suggested that either *coro* is not being sufficiently reduced, perhaps due to the maternal loading of *coro*, or that Coro is not required for embryonic muscle development.

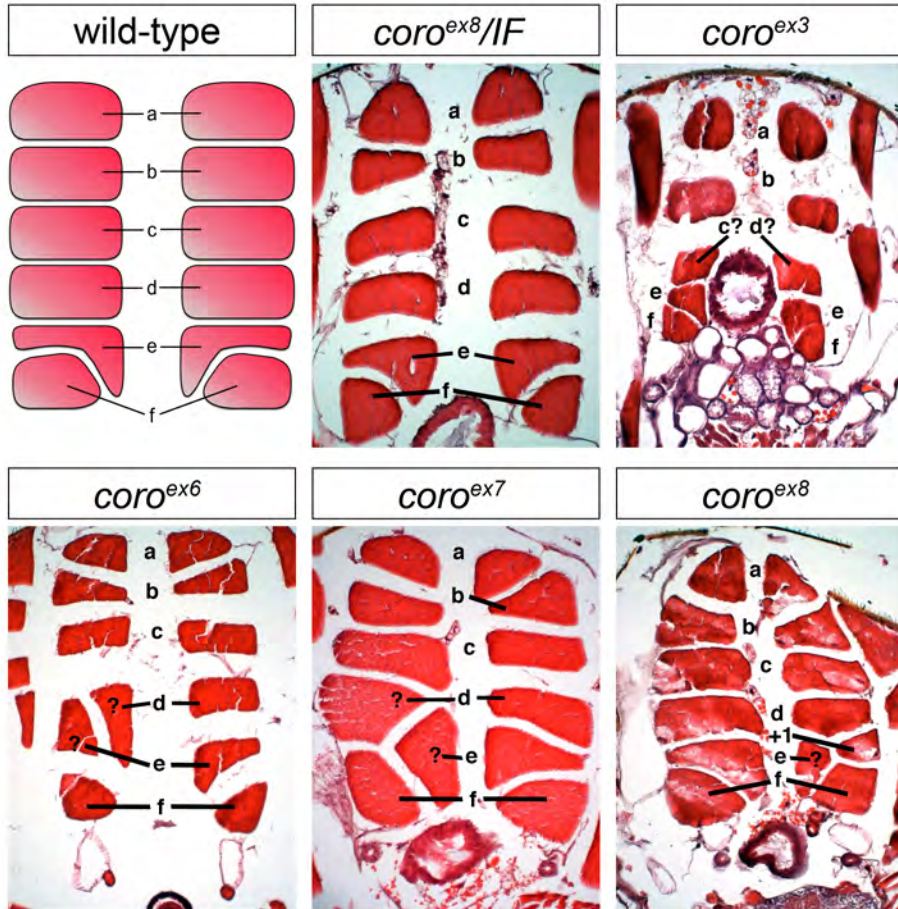


Figure 3.9. *coro* mutant adults have aberrant DLMs. Dorsal longitudinal muscles (DLMs) are six bilaterally symmetric muscles (labeled a-f, dorsal is oriented up) with a characteristic shape and organization, particularly with respect to “e” and “f” muscles. Heterozygous adults (*coro^{ex8}/IF* shown as a representative) contain the proper number and organization of DLMs. Mutant adults have occasional missing DLMs (*coro^{ex3}*), loss of bilateral symmetry coupled with changes in muscle shape and organization (*coro^{ex6}*, *coro^{ex7}* and *coro^{ex8}*) and muscle gain (*coro^{ex8}*). n = at least 3 for each genotype.

Expression of *UAS-coro RNAi (TRiP)* was larval lethal and expression of *UAS-coro-IR* was partially lethal at later stages (Figure 3.12C-D). Interestingly, expression of *UAS-coro RNAi* using *Dmef2-Gal4* resulted in larvae that failed to pupate. These larvae appeared developmentally paused as they survived as larvae for more than ten days, similarly to larvae in which *tsr* was depleted using the same driver (Figure 2.3).

When *coro* was depleted in *coro^{ex6}* mutants, embryos presented with defects similar to those observed in *coro^{ex6}* mutants, but there was some reduction in the percentage of hemisegments affected in comparison to *coro^{ex6}* mutants in which *coro* RNAi was not expressed (Figure 3.13A, B). In addition, the viability of these animals was increased compared to that of *coro^{ex6}* homozygous mutants and was similar to the viability of *coro^{ex6}* heterozygotes (Figure 3.13C). Thus, while there was not a complete rescue of *coro^{ex6}* phenotypes, reducing *coro* in the muscle attenuated some of the defects associated with the *coro^{ex6}* allele. However, the nature of the alleles is still unclear.

Sequencing coro alleles

To better understand the *coro* phenotype, we sequenced additional *coro^{ex}* alleles to identify the molecular lesions generated by the P-element excision. Previously published sequencing data of RT-PCR transcripts of the *coro^{ex6}* allele identified a 231 base pair (bp) translocation from *CG16791* on the third chromosome into the third exon of *coro*, though normal-sized PCR product is also detectable

Table 3.5. Viability and fertility of *coro* transheterozygotes.

	male	<i>coro</i> ^{GE15547}	<i>coro</i> ^{ex3}	<i>coro</i> ^{ex4}	<i>coro</i> ^{ex6}	<i>coro</i> ^{ex7}	<i>coro</i> ^{ex8}	<i>coro</i> ^{ex11}
virgin								
<i>coro</i> ^{GE15547}			V, F					
<i>coro</i> ^{ex3}	V, F		(1) NF	(9), NF	(22), NF	(26), NF	(28), NF	(24), NF
<i>coro</i> ^{ex4}	V, F		(42) NF	(30), NF	(29), NF	(22), NF	(24), NF	(29), NF
<i>coro</i> ^{ex6}	V, F		(52) NF	(20), NF	(1), NF	NV	NV	(7), NF
<i>coro</i> ^{ex7}	V, F		(14), NF	(26), NF	NV	(2), NF	(8), NF	(8), NF
<i>coro</i> ^{ex8}	V, F		(14), NF	(20), NF	NV	NV	NV	NV
<i>coro</i> ^{ex11}								

Number in parenthesis indicates the percentage of mutant adults that emerged. Viability (V, NV) refers to the viability of transallelic combinations. Fertility (F, NF) refers to the fertility of transallelic stocks (second generation). V=viability, NV, not viable, F=fertile, NF=not fertile. n > 100 adults.

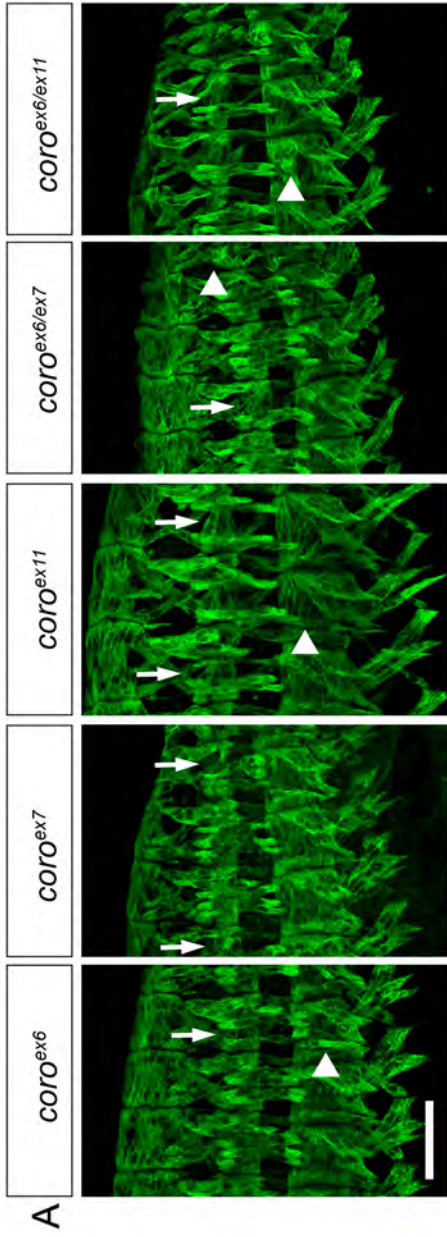
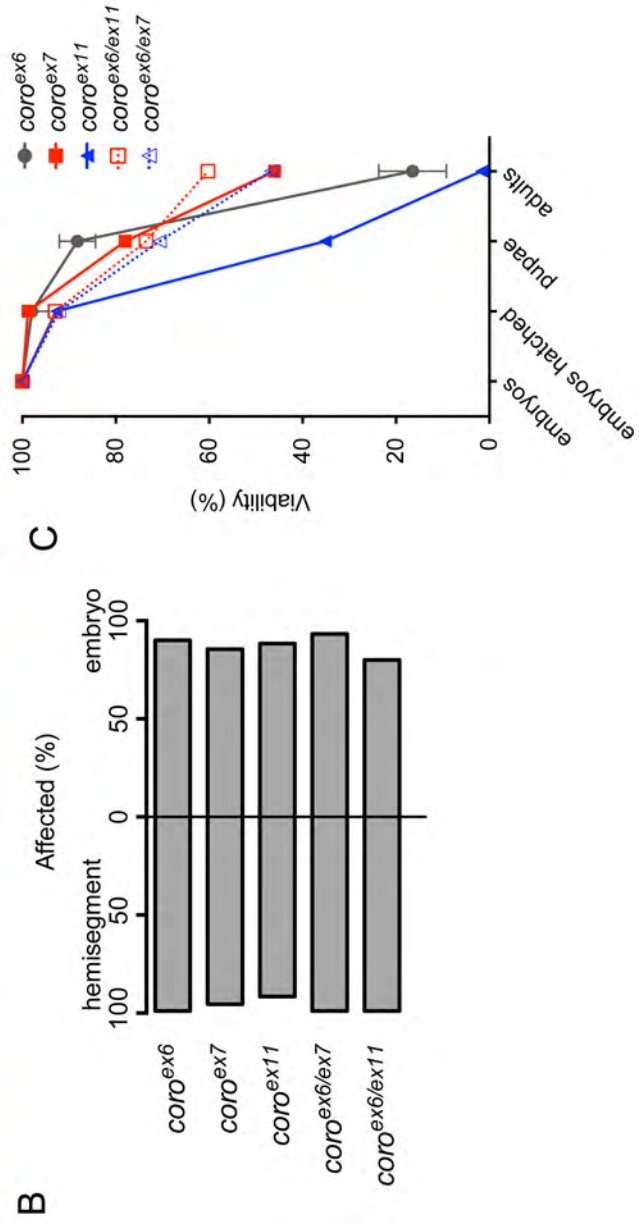
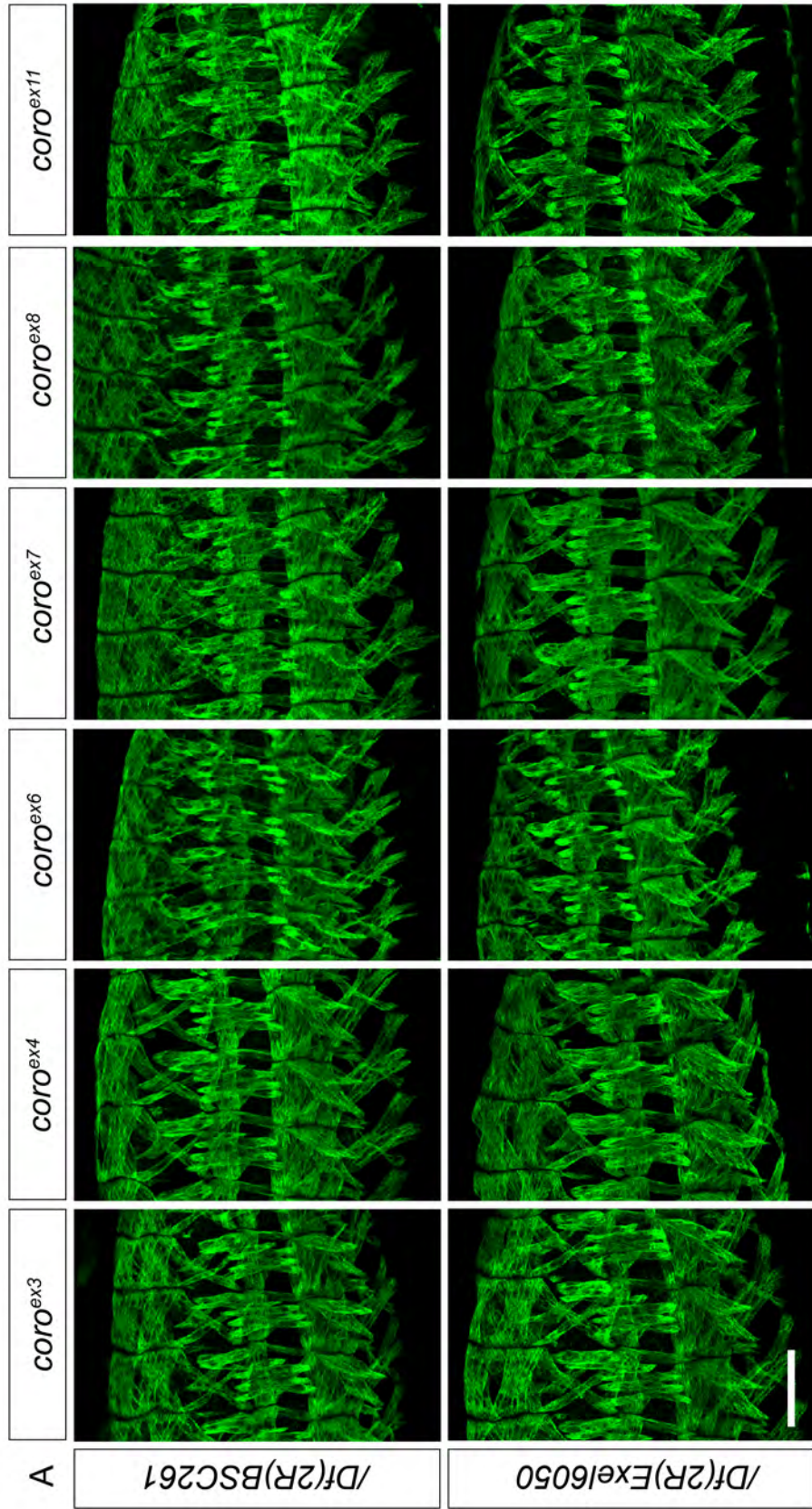


Figure 3.10. Transheterozygous embryos phenocopy single allele mutants. (A) Maximum intensity projection of a stage 16 embryo labeled with an antibody against Myosin heavy chain (green) to visualize the embryonic body wall muscle. Three representative hemisegments are shown for each genotype. Some defects are indicated by arrows (muscle loss), arrowheads (muscle attachment defects) and asterisks (muscle shape defects). (B) Quantification of the percentage of affected hemisegments (left) and embryos (right) of each genotype indicated. $n = 20$ embryos, 100 hemisegments. (C) Quantification of the viability of each genotype at the indicated developmental stage. $n = 100$ embryos. Error, s.e.m. Bar, 50 μm .



(Figure 3.14A, green triangle) (Bharathi et al., 2004). Sequencing genomic DNA from *coro^{ex6}* larvae also identified a 100 bp deletion 1250 bp upstream of the transcription start site (Figure 3.14A). This deletion removes the 3' UTR of *CG9447*, however, no transcript of *CG9447* could be detected in wild-type embryos or larvae. Further, residual GAL4 activity could be detected in *coro^{ex11}*, indicating an incomplete excision of the P-element. An internal deletion within the P-element was confirmed with PCR and sequencing, and no other lesion was detected in *coro^{ex11}* (Figure 3.14A, dashed red triangle).

We identified a 702 bp deletion approximately 1.5 kb upstream of the transcription start site in *coro^{ex6}*, *coro^{ex7}* and *coro^{ex8}* adults, but not in *409-Gal4*, *UAS-lacZ* or *coro^{ex3}* adults (Figure 3.14B, data not shown). This deletion was also present in *yw* controls but not in *OreR* controls, suggesting that it is not likely contributing to the phenotype. Surprisingly, we failed to identify the 100 bp deletion or the 231 base pair insertion (dashed grey triangle) previously reported in the *coro^{ex6}* allele (Figure 3.14B) (Bharathi et al., 2004). We did not sequence any additional regions from *409-Gal4*, *UAS-lacZ*, *coro^{ex7}* or *coro^{ex8}* genomic DNA (dashed lines). Given our inability to confirm any of the published sequencing data, we are continuing to work on identifying the molecular lesion associated with the *coro* alleles, while exploring alternative methods to elucidate a role for Coro in muscle development.



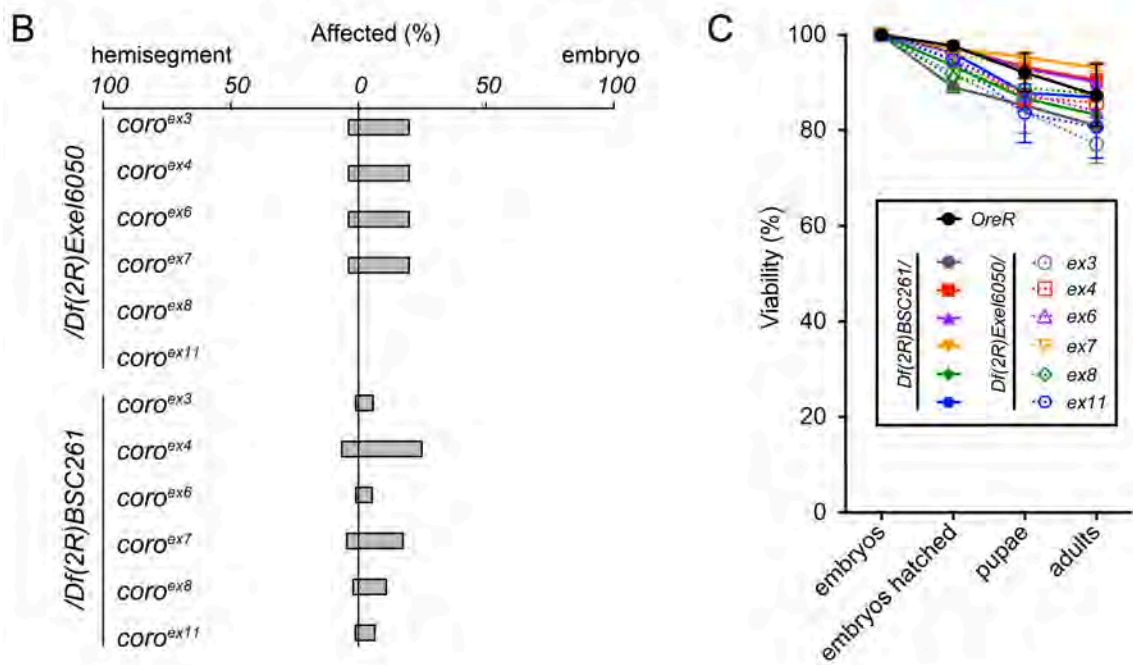


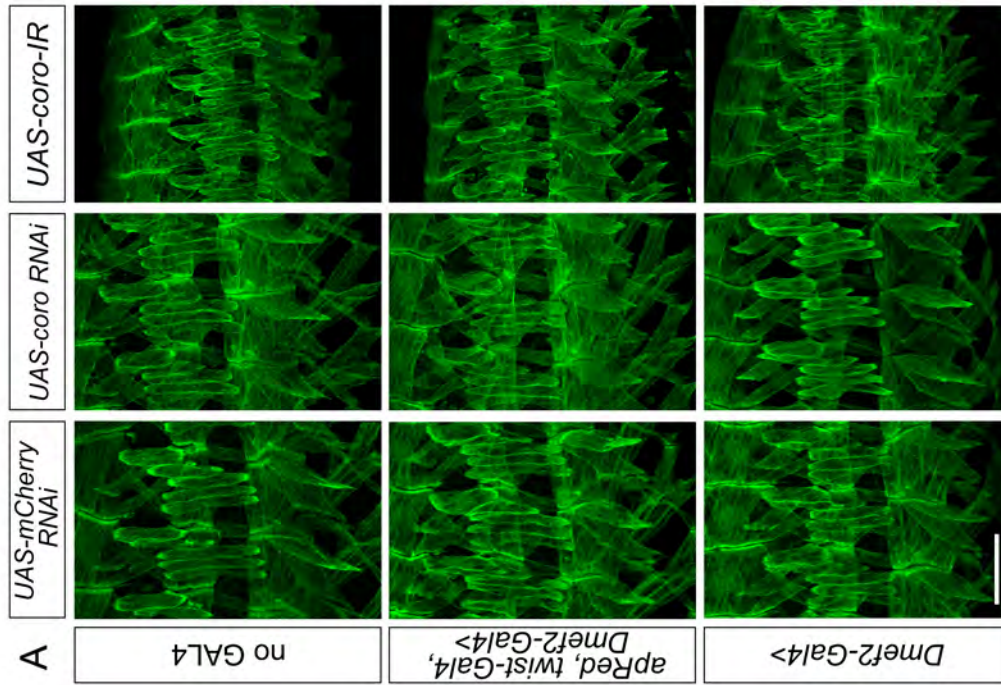
Figure 3.11. *coro*^{ex} alleles complement deficiencies which completely remove *coro*. (A) Maximum intensity projection of a stage 16 embryo labeled with an antibody against Myosin heavy chain (green) to visualize the embryonic body wall muscle. Three representative hemisegments are shown for each genotype. (B) Quantification of the percentage of affected hemisegments (left) and embryos (right) of each genotype indicated. n = 20 embryos, 100 hemisegments. (C) Quantification of the viability of each genotype at the indicated developmental stage. n = 100 embryos. Error, s.e.m. Bar, 50 μ m.

Coro is expressed in the *Drosophila* larval muscle where it is required for muscle activity

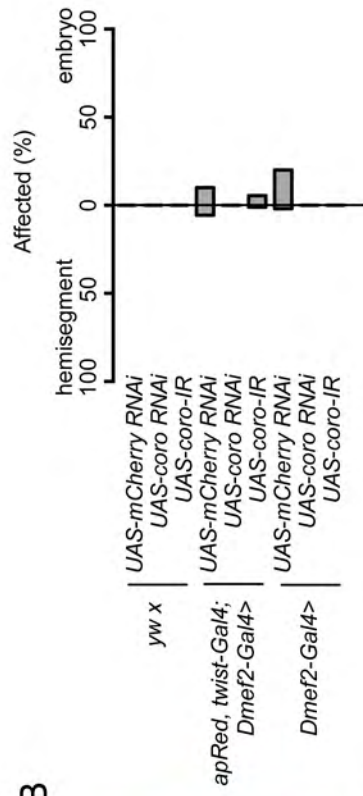
The observed decrease in viability during larval stages when *coro* was reduced in muscle suggested that *Coro* may play a later role in muscle function (Figure 3.12C-D). Using the 409-Gal4 *coro* enhancer trap line, we examined whether *Coro* was expressed in the L3 larval musculature. We found that β -gal, a readout of *Coro* expression, was detectable in all of the body wall muscles examined (Figure 3.15).

Using *Dmef2-Gal4* to express the *UAS-RNAi* constructs described above, we analyzed sarcomere organization in larvae in which *coro* was depleted. The organization of sarcomeres in L3 larvae in which *coro* was depleted using *UAS-coro-IR* appeared mostly wild-type (Figure 3.16A). However, 20% of these larvae had other types of muscle defects, including muscle splitting (Figure 3.16A, right-most panels). Further, *coro*-depleted L3 larvae displayed a modest, but statistically significant decrease in crawling velocity, suggesting that there may be a more subtle defect in these animals which affects muscle function. In support of this, *Dmef2-Gal4>UAS-coro-IR* adults were flightless as previously reported (Figure 3.16D) (Schnorrer et al., 2010).

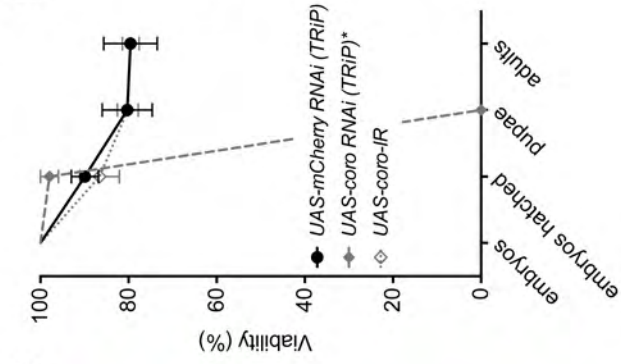
We also analyzed the muscle pattern in larvae in which *coro* was depleted using *UAS-coro RNAi* (TRiP) using our method for assessing sarcomere organization *in vivo*. We found that *UAS-coro RNAi* did not affect



B



C



D

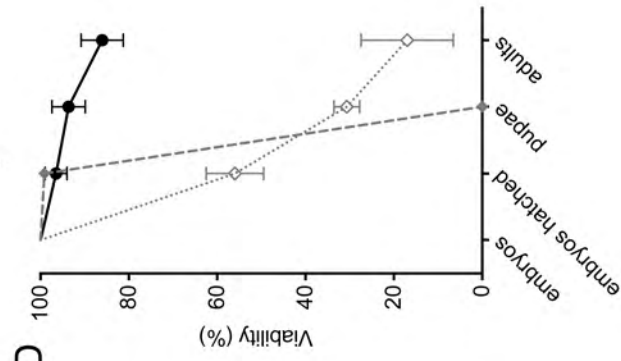


Figure 3.12. Muscle-specific depletion of *coro* does not result in embryonic phenotypes. (A) Maximum intensity projection of stage 16 embryos labeled with an antibody against Tropomyosin (green) to visualize the embryonic body wall muscle. Three representative hemisegments are shown for each genotype. (B) Quantification of the percentage of affected hemisegments (left) and embryos (right) of each genotype indicated. (A-B) n = 20 embryos, 5 hemisegments/embryo. (C) Quantification of the viability of each RNAi construct expressed using *apRed*, *twist-Gal4*, *Dmef2-Gal4* at the indicated developmental stage. (D) Quantification of the viability of each RNAi construct expressed using *Dmef2-Gal4* at the indicated developmental stage. (C-D) n = 100 embryos, 100 hemisegments. Error, s.e.m. Bar, 50 μ m.

sarcomere formation at stage 17 or the maintenance of sarcomere organization at the larval stages analyzed, despite the complete failure of these larvae to pupate (Figure 3.16C). Together, these data indicate that Coro is required for muscle function in the larvae and adult.

Discussion

Coronin family members uniquely interact with and coordinate the activities of both the Arp2/3 and ADF/cofilin pathways, playing an important role in balancing actin dynamics (Chan et al., 2011). Arp2/3 and ADF/cofilin as well as their regulators have been shown to play essential roles in many aspects of muscle development in *Drosophila* (Rochlin et al., 2009; this study). Thus, we hypothesized that Coro may also be required for muscle development.

We describe for the first time in *Drosophila* the expression of Coro in the embryonic and larval musculature. Though an earlier analysis of RNAi phenotypes indicated that *coro* depletion resulted in adult myofibril phenotypes and flightlessness (Schnorrer et al., 2010), this study is the first to identify a role for Coro in muscle development in the embryo and muscle function in the larvae. Our analysis also suggests that Coro is required for a number of key steps in muscle development in the embryo, including a role in establishing the full complement of muscles and proper muscle attachment. Defects in the LT muscles were most commonly observed, suggesting that Coro may have an LT-specific function despite its expression in all muscles of the *Drosophila* embryo.

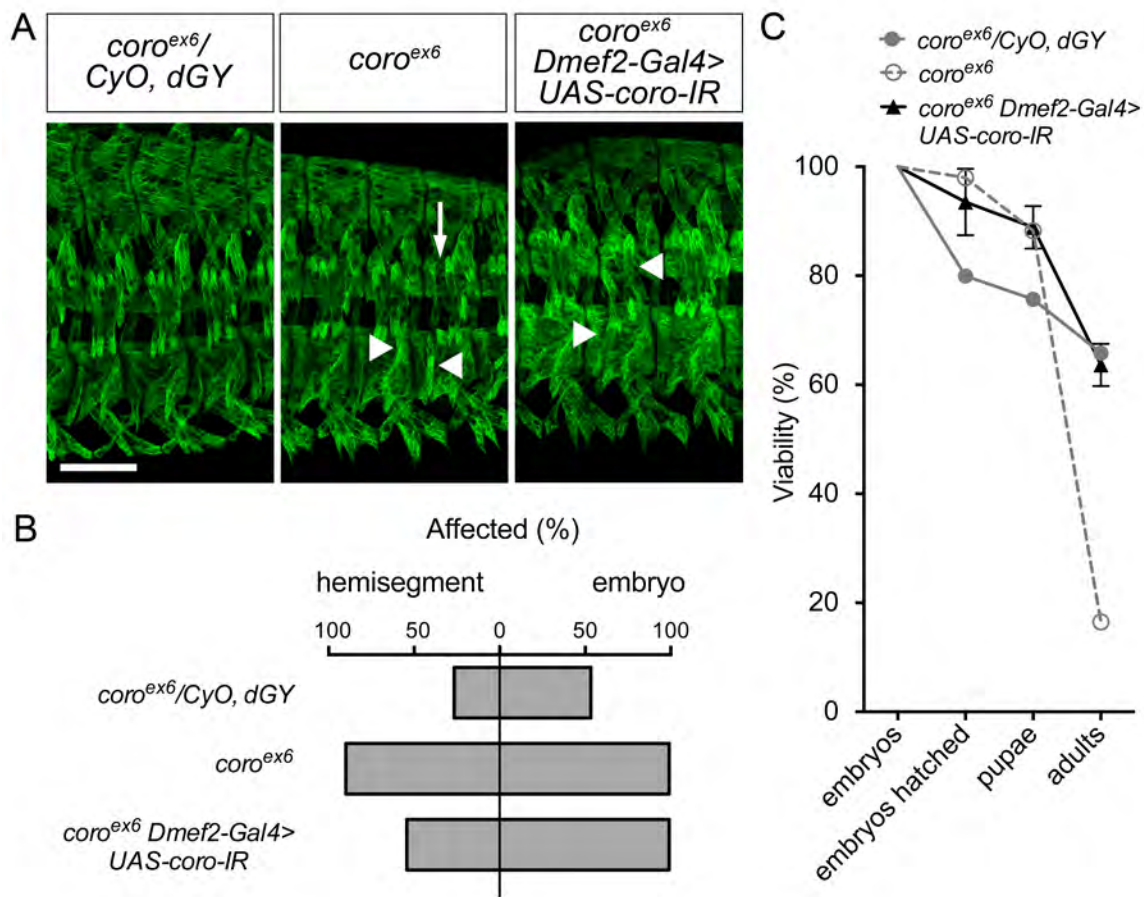


Figure 3.13. Muscle-specific depletion of *coro* using RNAi in *coro^{ex6}* mutant embryos. (A) Maximum intensity projection of a stage 16 embryo labeled with an antibody against Myosin heavy chain (green) to visualize the embryonic body wall muscle. Three representative hemisegments are shown for each genotype. (B) Quantification of the percentage of affected hemisegments (left) and embryos (right) of each genotype indicated. $n \geq 10$ embryos, 50-100 hemisegments. (C) Quantification of the viability of each genotype at the indicated developmental stage. $n = 100$ embryos, 100 hemisegments. Error, s.e.m. Bar, 50 μm .

However, LTs are often disrupted upon genetic perturbation of genes involved in muscle development and thus, may be somehow more sensitive than other muscles.

Additional evidence suggests that *Coro* is required more generally than in LTs. In *coro^{ex}* adults, we observed gross defects in adult IFM morphogenesis, including aberrant DLM number, which is indicative of the earlier loss of DLM template muscles (see Introduction, page 56) (Farrell et al., 1996; Fernandes and Keshishian, 1996). The second thoracic hemisegment muscles DO1-3, which are the DLM template muscles, are formed in the embryo and are unique in that they are not destroyed during metamorphosis (Crossley, 1978; Fernandes et al., 1991). As our analysis of *coro* mutant phenotypes focused on the formation of the abdominal musculature, we do not have direct data indicating that the thoracic template muscles were not properly specified and formed. However, given the high degree of muscle loss observed in abdominal hemisegments, we would expect them to also be missing occasionally. Thus, the irregular DLM number in *coro^{ex}* mutant adults is an indirect read-out of the presence/absence of the thoracic DO1-3 muscles and suggests that *Coro* is likely required in multiple, if not all, muscles.

We were not able to unequivocally demonstrate that the *coro^{ex}* alleles represent *bona fide* mutations in *coro*. However, a number of reasons hint that they are. For example, the alleles fail to complement one another, and the embryonic defects we observe are absent in the parental *coro⁴⁰⁹* stock, suggesting that a second hit was not present at the outset.

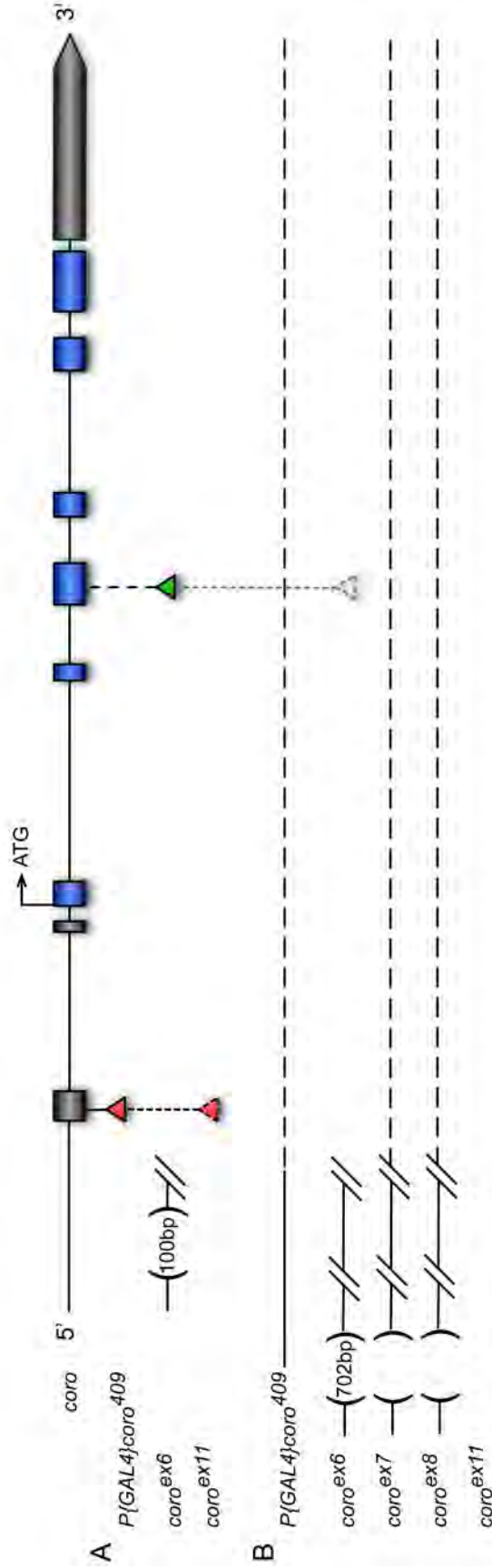


Figure 3.14. Graphical representation of *coro* allele sequencing data. (A) Summary of sequencing data reported in (Bharathi et al., 2004). $P\{GAL4\}coro^{409}$ is inserted in the 5' untranslated region (UTR) of *coro* (red triangle). Imprecise excision of $P\{GAL4\}coro^{409}$ generated a number of independent $coro^{ex6}$ alleles. $coro^{ex6}$ contains a 100 base pair (bp) deletion upstream of the transcription start site and a 231 bp translocation from $CG16791$ on the third chromosome into the third exon of *coro* (green triangle). The only lesion identified in $coro^{ex11}$ is an internal deletion in the P-element (dashed red triangle). (B) Summary of sequencing data reported in this study. All $coro^{ex}$ alleles sequenced contain a 702 bp deletion that is also found in y,w but not $OreR$ controls (not shown) or in $P\{GAL4\}coro^{409}$. This was not reported in the original analysis. The lesions previously reported in the $coro^{ex6}$ allele were not identified in this study. We did not sequence further regions of the $coro^{ex7}$ or $coro^{ex}$ alleles (dashed line)

Coro is expressed in the embryonic and larval body wall musculature, and muscle-specific depletion of *coro*, though it does not cause early embryonic phenotypes like those in *coro^{ex}* mutants, does result in defects in muscle activity. Thus, the observed phenotype is consistent with both the expression of Coro in muscle and a muscle-specific role Coro has in regulating proper muscle function later in development.

However, we cannot yet explain why we fail to see any defects in muscle development or function when *coro^{ex}* alleles are in trans to deficiencies which remove *coro*. One deficiency, *Df(2R)Exel6050*, completely removes *coro* coding sequence, but leaves 5' regulatory regions intact. One possibility is that transvection is occurring between the remaining upstream regulatory sequence on the *Df(2R)Exel6050* chromosome and the *coro^{ex}* allele on the homologous chromosome. Transvection has been observed at numerous loci in *Drosophila*, including *decapentaplegic*, *eyes absent*, *yellow* and *wupA* (the *Drosophila* homolog of troponin I) (Duncan, 2002; Marín et al., 2004). Though formally possible, this is not the most plausible explanation, and it does not explain why we obtain rescue with the second deficiency. An additional reason may be that *coro* activity is upregulated in the *coro^{ex}* alleles such that it is rescued by removal of the second *coro* locus. We had some success testing this hypothesis by reducing *coro* in *coro^{ex6}* mutants, but we cannot conclusively state that this is what is occurring.

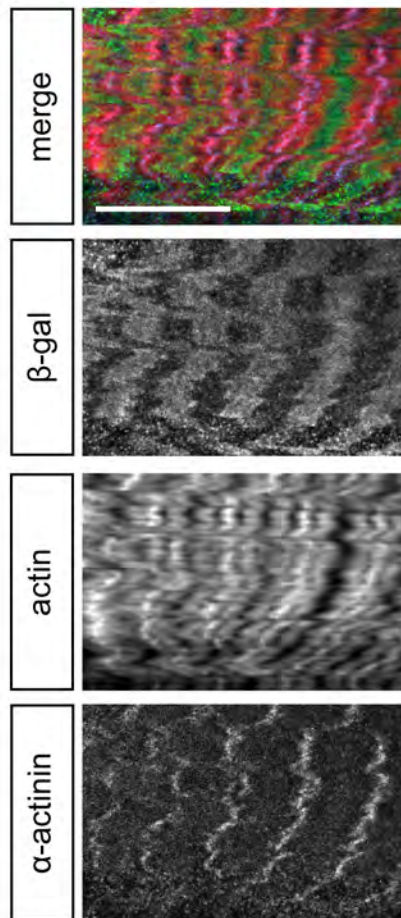


Figure 3.15. Coro is expressed in the *Drosophila* larval muscles. *409-Gal4, UAS-lacZ* L3 larvae were dissected and stained with antibodies against β -gal (green) and α -actinin (white). Phalloidin (red) was used to label the actin cytoskeleton. A single optical section of muscle VL3 is shown. Bar, 20 μ m.

There are additional methods for resolving these confusing data, including quantitative PCR to examine the levels of *coro* transcript expressed in *coro^{ex}* alleles and test more directly whether *coro* is overexpressed in *coro^{ex}* animals. We can also attempt to rescue the *coro^{ex}* phenotype by expressing full-length, wild-type *coro* ubiquitously or specifically in the muscle. Both of these strategies are being explored.

We have previously demonstrated that Tsr is required for many aspects of muscle development and function throughout *Drosophila* development (this study). It is not clear whether Coro coordinates Tsr activity in all contexts. Coro is the least well-studied of all Tsr regulators, particularly in an *in vivo* setting. This study suggests that at least in *Drosophila* muscle, Coro and Tsr are both required for aspects of development and function. It has not been addressed in this study or elsewhere whether they work together in the muscle or if they play independent roles.

Data from budding yeast indicates that mutation of *CRN1* (coronin) alone is not sufficient to affect actin-based behaviors such as polarized growth, endocytosis or bud-site selection (Goode et al., 1999; Heil-Chapdelaine et al., 1998). However, mutating *CFL1* (cofilin) in *crn1* null cells produces defects in growth, actin filament organization near the bud neck and the polarization of cortical actin patches (Goode et al., 1999). Together, these data indicate that Crn1p is less critical to actin dynamics than Cfl1p in yeast. Our data also support a more minor, but important role for Coro in muscle development. Muscle-specific depletion of *tsr* caused severe and early sarcomere organization defects, which

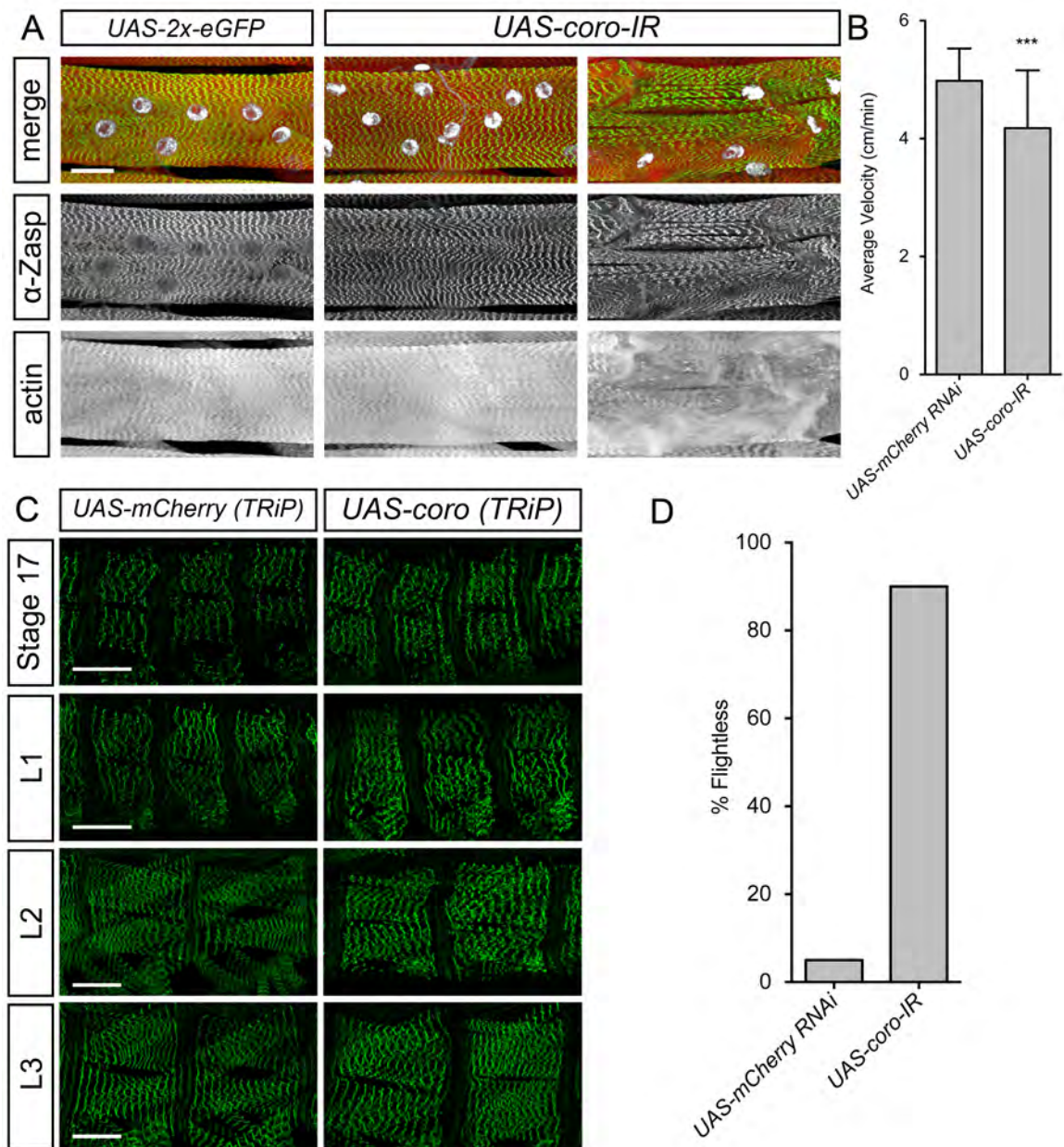


Figure 3.16. Coro is required for muscle function in the larvae and adult. (A) Maximum intensity projection of dissected L3 larvae labeled with an antibody against Zasp (green). Phalloidin (red) and Hoechst (white) were used to label actin and nuclei, respectively. *Dmef2-Gal4* was used (B) Quantification of average crawling velocity of L3 larvae of the indicated genotype. *** $p < 0.001$ (C) *Dmef2-Gal4*, *Zasp66::GFP* was used to express the indicated RNAi and to label the Z-discs of the sarcomere at the indicated developmental stages *in vivo*. (D) Percentage of flightless adults generated from the expression of each RNAi construct using *Dmef2-Gal4*. Bar, 50 μm .

were lethal (this study). In contrast, expression of RNAi which targets *coro* using the same Gal4 drivers was only partially lethal and caused a modest defect in muscle function in larvae with no gross defects in sarcomere organization. Thus, Coro may be required to fine-tune actin dynamics, causing subtle defects that have functional consequences. However, whether *coro* is actually depleted by these RNAi constructs has not been addressed and leaves open the possibility that the phenotypes we observed are due to off-target effects. It is also feasible that *coro* is not sufficiently depleted and that phenotypes we have reported here do not reflect the complete muscle-specific *coro* “null.”

We observed occasional myofibril “splitting” in larvae in which *coro* was depleted. A similar class of defects was identified in larvae in the same genome-wide screen that described adult IFM “fraying” after *coro* depletion (Schnorrer et al., 2010). We suspect this analysis likely overlooked the splitting phenotype in *coro*-depleted larvae since we only observed a small percentage of larvae affected. Myofibril splitting, most notably, was observed upon knockdown of α -*Actinin* (*Actn*), which is localized to Z-discs and costameres (Clark et al., 2002; Schnorrer et al., 2010). Myofibril splitting suggests that costameres, which connect myofibrils to one another (Clark et al., 2002; Sparrow and Schöck, 2009), are compromised, and this is consistent with the known function of Actn. Though the subcellular localization of Coro in muscle is not known, the larval myofibril splitting phenotype suggests that Coro may function at the costameres and/or Z-discs to regulate actin dynamics. In addition, the adult “frayed”

phenotype previously reported in *coro*-depleted adults may also be the result of the loss of costamere integrity (Schnorrer et al., 2010).

In summary, we have explored the role of the type I coronin, Coro, in muscle development in *Drosophila*. This study is the first to describe a role for Coro in muscle morphogenesis. Despite its importance in regulating actin dynamics (Chan et al., 2011), very few studies on the activity of type I coronins have been conducted in multicellular organisms *in vivo*. Though knockout mice for the type I coronins Coro1a and Coro1b have been analyzed, they have not identified a role for type 1 coronins in muscle development *in vivo*, perhaps due to redundancy amongst coronins (Chan et al., 2011; Foger et al., 2011; Föger et al., 2006). Thus, the conservation of Coro function to muscle development remains to be addressed.

CHAPTER FOUR:

Dock1 and IQSec1, homologs of the fusion proteins Myoblast city and Loner, respectively, play a conserved role in mammalian myoblast fusion

Chapter Overview

Using a forward genetics approach in *Drosophila*, a number of labs have identified genes which, when mutated, lead to a block in myoblast fusion (Rochlin et al., 2009). From these genetic screens, much has been learned about the kinds of proteins required for fusion to occur successfully. While these gene products fall into distinct classes, a number of proteins converge upon the actin cytoskeleton. For example, mutation of *myoblast city* (*mbc*) or *loner* (also known as *schizo*), genes that encode guanine nucleotide exchange factors (GEFs) that regulate the small GTPase Rac, leads to a strong fusion defect in *Drosophila* (Chen et al., 2003; Erickson et al., 1997; Nolan et al., 1997; Rushton et al., 1995). Rac, in turn, exerts its effects on the cytoskeleton through its regulation of the WAVE complex, which binds to SCAR/WAVE, a potent activator of Arp2/3-mediated actin polymerization (Goley and Welch, 2006).

While these studies have been informative, there remains a significant gap in our knowledge of the cellular and molecular mechanisms that orchestrate myoblast fusion in mammals. Some insight to this process can be gained by exploiting the homology between fusion proteins identified in *Drosophila* and mammalian proteins. We chose to focus our analysis on the mammalian homologs of two *Drosophila* GEFs required for fusion: the Mbc homolog, Dock1 and the Loner homolog, IQSec1.

Drosophila Mbc and mammalian Dock1 directly regulate Rac and are founding members of the CDM (CED-5, Dock1, Myoblast city) superfamily of

GEF proteins (Brugnera et al., 2002; Cote, 2002; Erickson et al., 1997; Kiyokawa et al., 1998a; Nolan et al., 1997). Their GEF activity is imparted by the Dock Homology Region-2 (DHR-2) domain, a novel catalytic domain that distinguishes CDM family GEFs from the canonical Dbl homology-pleckstrin homology domain (DH-PH)-containing family of GEF proteins (Cote, 2002; Côté and Vuori, 2007; Kiyokawa et al., 1998a; Meller, 2005). CDM family members play key roles in a variety of fundamental biological processes, including cell migration (Côté et al., 2005; Erickson et al., 1997; Gumienny et al., 2001; Meller et al., 2005; Wu et al., 2002), phagocytosis of apoptotic cells (Gumienny et al., 2001; Wang, 2003), neuronal polarization (Gumienny et al., 2001) and myoblast fusion (Erickson et al., 1997; Laurin et al., 2008; Nolan et al., 1997; Pajcini et al., 2008; Rushton et al., 1995).

Loner/IQSec1 contain a central catalytic domain with significant homology to the yeast Sec7 domain and have activity towards Arf6 *in vitro* and *in vivo* (Chen et al., 2003; Dunphy et al., 2007; Hiroi et al., 2006; Morishige et al., 2007; Someya, 2006; Someya et al., 2001). Arf6 is known to function at the cell periphery in endocytosis, cell migration, adherens junction turnover and actin cytoskeletal remodeling (D'Souza-Schorey and Chavrier, 2006; Donaldson, 2003; Radhakrishna et al., 1999) (Radhakrishna and Donaldson, 1997). Consistent with this, IQSec1 knockdown myoblasts have aberrant Paxillin localization and adhesion defects (Pajcini et al., 2008). Recent data also suggest Arf6 is also required for the spatial restriction of Rac activation, suggesting that Loner/IQSec1 may function to localize Rac activity (Palamidessi et al., 2008).

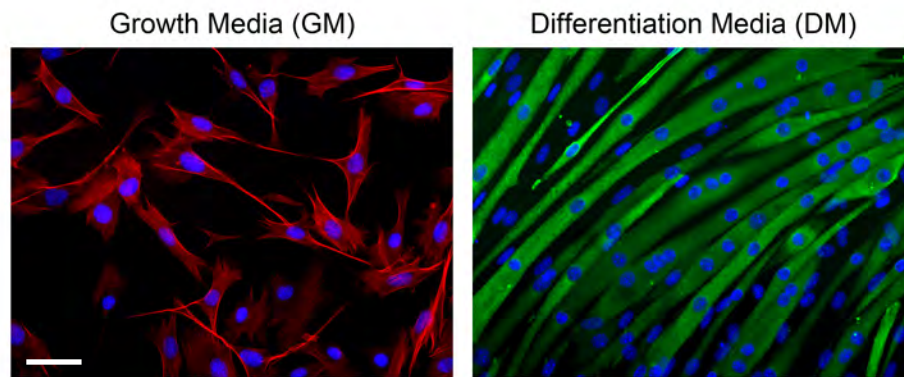


Figure 4.1. C2C12 satellite cell-derived myoblasts fuse *in vitro*. **(Left)** Mononucleate myoblasts are maintained and proliferate in growth medium (GM, left panel) Actin (phalloidin, red) and nuclei (DAPI, blue) are shown. **(Right)** Upon serum starvation achieved by changing the media to differentiation medium (DM, right panel), C2C12 myoblasts fuse to form multinucleate myotubes that express myosin heavy chain (green). Bar, 50 μm .

Here, we demonstrate that Dock1 plays a conserved role in myoblast fusion in C2C12 myoblasts. This has been corroborated by publications from other laboratories during my dissertation research (Laurin et al., 2008; Pajcini et al., 2008). We further these analyses by identifying the cellular step at which Dock1 acts during fusion. We show that Dock1 is not required for the differentiation or migration of myoblasts *in vitro*. Further, we determine that Dock1 is not required for myoblast-myoblast adhesion and conclude that Dock1 is required at the fusion site as is the case for Myoblast city. Finally, our data also suggest that IQSec1 is not required for earlier steps of myoblast fusion, including myoblast differentiation, migration and adhesion.

Results

Generation of stable clones expressing shRNAs against Dock1 and IQSec1

To study mammalian muscle development, we use the C2C12 mouse myoblast cell line derived from the satellite cells of a normal C3H mouse (Yaffe and Saxel, 1977). The differentiation and fusion of C2C12 myoblasts is controlled through the presence or withdrawal of mitogens provided in the culture media. C2C12 myoblasts are grown and maintained in media supplemented with serum (growth media, GM) and C2C12s are directed to fuse by withdrawing serum [differentiation medium, (DM)]. After five days in DM, C2C12 myoblasts fuse to form arrays of multinucleated myotubes *in vitro* (Figure 4.1).

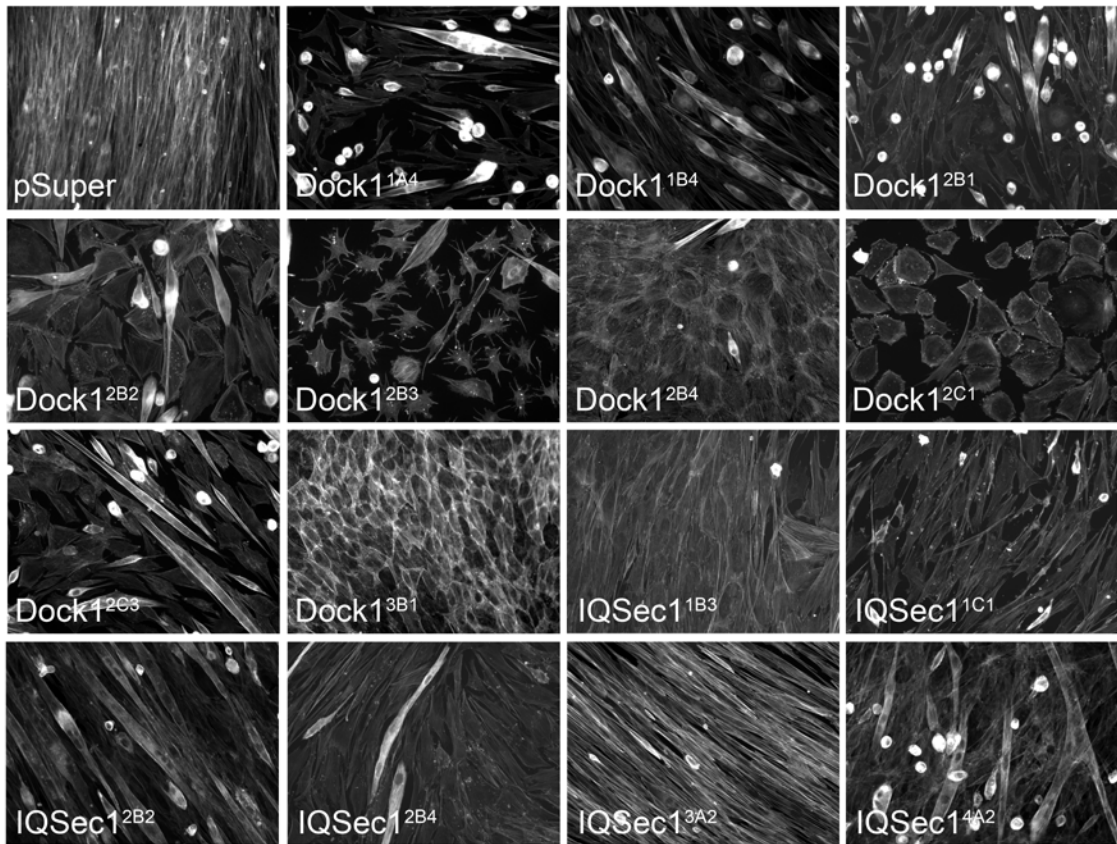


Figure 4.2. Screening cell lines with putative reduction of Dock1 and IQSec1. C2C12 myoblasts expressing the indicated shRNA were switched to differentiation medium and cultured for 5 days before being fixed and labeled with phalloidin (greyscale) to label the actin cytoskeleton. These lines were prepared by S. Nowak. Bar, 75 μ m.

To determine whether Dock1 and/or IQSec1 are required for mammalian myoblast fusion, our lab generated a number of independent C2C12 myoblast lines that stably express shRNAs targeted against either Dock1, IQSec1 or a control shRNA plasmid (pSuper). These clonal cell lines were shifted to differentiation medium for five days, and phalloidin was used to label the F-actin cytoskeleton to allow us to quickly assess fusion. A subset of these cell lines are shown in Figure 4.2. Nearly all the cell lines we generated displayed reduced fusion, providing the initial evidence that Dock1 and IQSec1 play a conserved role in mammalian myoblast fusion.

Knockdown of Dock1 and IQSec1 blocks fusion but not differentiation

We selected a few cell lines with presumed Dock1 or IQSec1 depletion for further analysis. In contrast to the arrays of Myosin heavy chain (MHC)-positive, multinucleate myotubes that we observed in untreated control and pSuper cell lines after five days of culture in DM, few myotubes formed in cell lines expressing shRNAs against Dock1 or IQSec1 (Figure 4.3A). Quantification of the fusion index confirmed the reduction in fusion, which ranged from 5-25% in these cell lines (Figure 4.3C). We hypothesize that the range in fusion phenotype may reflect different levels of protein knockdown. Importantly, myoblasts in each cell line expressed MHC upon differentiation, indicating that a failure in differentiation is not the cause of the fusion block (Figure 4.3A-B). Together, these data suggest that Dock1 and IQSec1 are required for mammalian myoblast fusion but not myoblast differentiation.

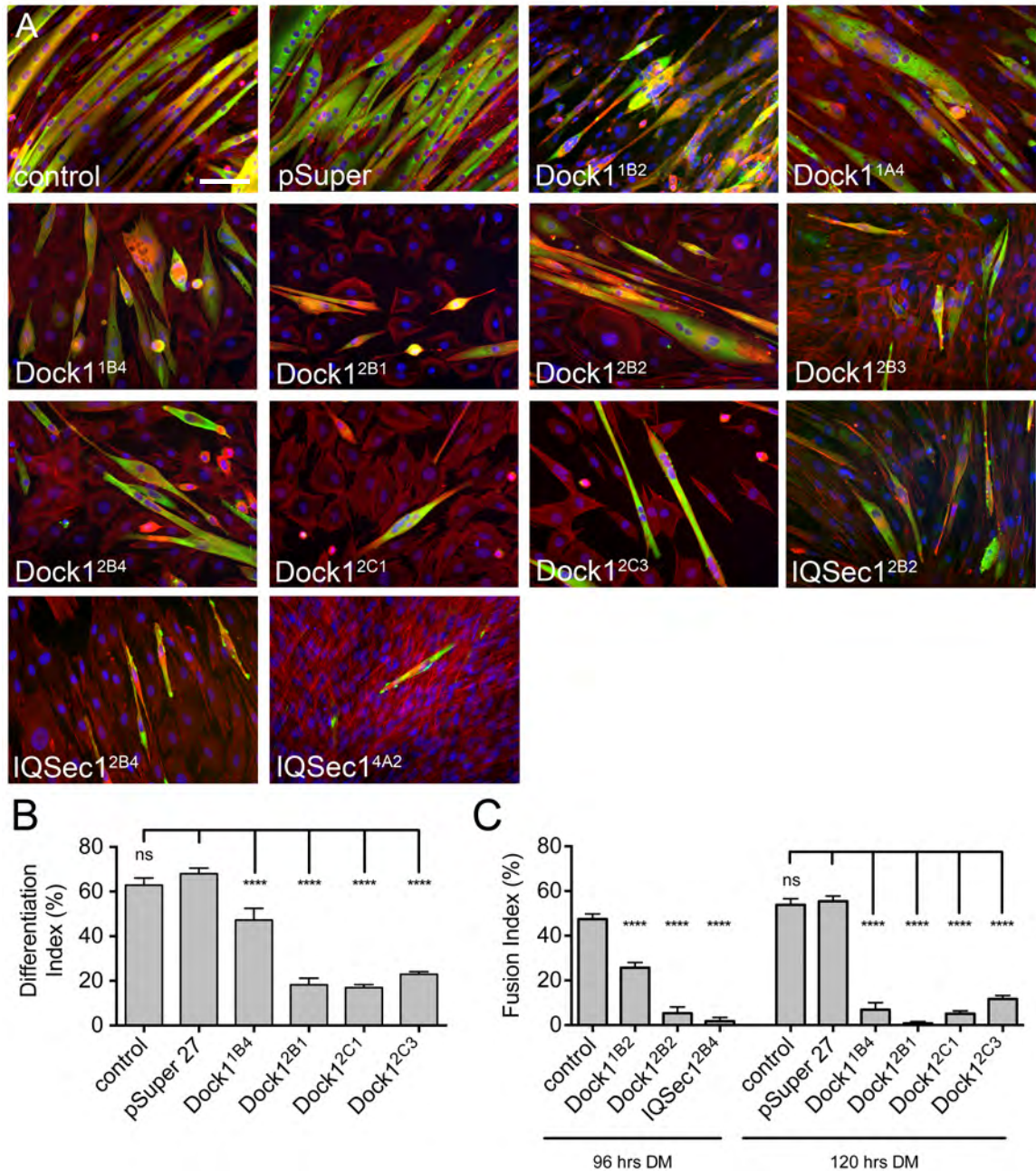


Figure 4.3. Reduction of Dock1 and IQSec1 result in myoblast fusion defects *in vitro*. (A) Stable cell lines were cultured in differentiation medium for five days before being fixed and immunostained with an antibody against Myosin Heavy Chain (MHC, green) and phalloidin (actin, red) and DAPI (nuclei, blue). (B) Quantification of the differentiation index (number of MHC-positive nuclei/total number of cells x 100) at 120 hours in DM. (C) Quantification of the fusion index (number of MHC-positive nuclei in myotubes that contain more than two nuclei/total number of nuclei x 100) at 96 hours and 120 hours in DM. Bar, 75 μ m.

Dock1 is reduced in a subset of cell lines

We focused first on understanding the role Dock1 is playing in mammalian myoblast fusion. Many behaviors are necessary for successful myoblast fusion, including myoblast differentiation, cell shape remodeling, migration and adhesion and alignment (Chen, 2010; Chen et al., 2007; Nowak et al., 2009). For our analysis, we wanted to define the cellular step at which Dock1 activity is required. Dock1 is expressed in both proliferating C2C12 myoblasts and myotubes throughout the fusion process *in vitro*, suggesting that it may be important in both cell types (Figure 4.4).

As a first step, we determined in which of our lines Dock1 was actually depleted. Western blot analysis of whole-myoblast lysates indicated that Dock1 was depleted in the Dock1^{1B4}, Dock1^{2B1}, Dock1^{2B2}, Dock1^{2B4}, Dock1^{2C1}, Dock1^{2C1.2}, and Dock1^{2C3} lines (Figure 4.5A). Though there was some variability between Western blots, Dock1 was not depleted in the Dock1^{1C1}, Dock1^{2A3}, Dock1^{2B4.2}, Dock1^{2B3} and Dock1^{2C2} lines, suggesting that off-target effects and/or the clonal selection process is likely the cause of the observed fusion defect (Figures 4.2, 4.3, 4.5A and data not shown). We also used the Dock1 antibody to examine the levels of Dock1 protein by immunofluorescence in Dock1^{2C1} and Dock1^{2C3} myoblast lines (Figure 4.5B). Compared to wild-type and pSuper controls, Dock1 appeared reduced in both knockdown myoblast lines, consistent with our Western blot analysis.

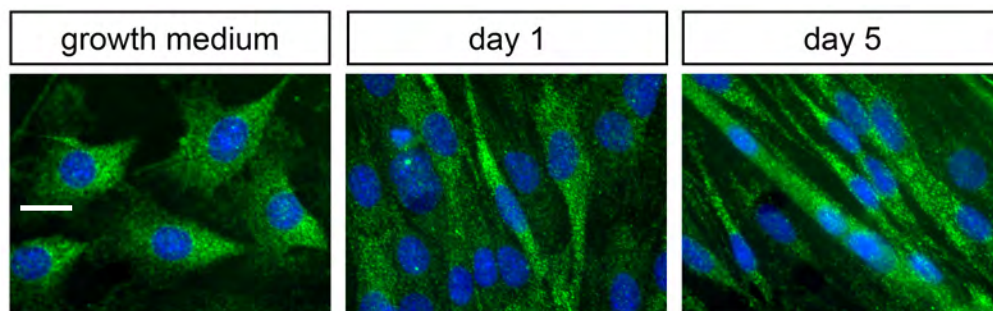


Figure 4.4. Dock1 is expressed throughout myoblast fusion *in vitro*. C2C12 myoblasts were cultured in growth medium (left) or in differentiation medium for one day (middle) or five days (right) before being fixed and immunostained with an antibody against Dock1 (green). Nuclei are labeled with DAPI (blue). Dock1 is expressed in myoblasts and myotubes and is cytoplasmically localized. Bar, 25 μm .

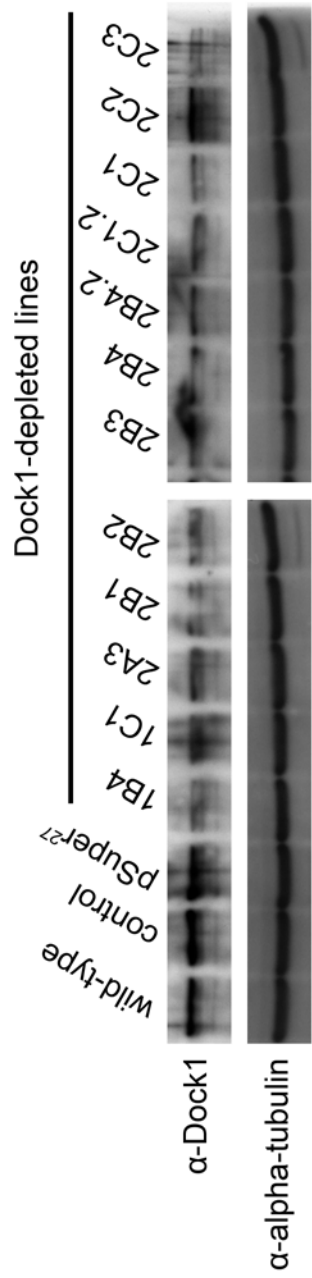


Figure 4.5. Dock1 is depleted in a subset of the presumptive Dock1 knockdown myoblast lines. Western blot analysis of total protein levels of Dock1 in the indicated myoblasts cultured in growth medium (GM). α-tubulin is used as a loading control.

Because they gave the most consistent protein knockdown via Western blot, we chose to focus on the Dock1^{1B4}, Dock1^{2B1}, Dock1^{2B4}, Dock1^{2C1}, and Dock1^{2C3} lines (Figure 4.5 and data not shown).

Dock1 is not required for myoblast shape changes

Our earlier analysis indicated that Dock1 is not required for myoblast differentiation (Figure 4.3). Therefore, we examined the ability of knockdown myoblasts to change shape from a fibroblast-like morphology to a bipolar, spindle-like morphology, which is a prerequisite for myoblast fusion (Nowak et al., 2009). To do this, we transfected control and Dock1^{2C3} myoblasts with plasmids encoding fluorescent reporters and performed live imaging analysis (Figure 4.6). At the onset of imaging, control myoblasts resembled fibroblasts and were highly motile (Figure 4.6A). Control myoblasts eventually attained a bipolar cell shape. Similarly, Dock1^{2C3} myoblasts had an irregular cell shape that ultimately remodeled into a spindle-like morphology, indicating that Dock1 is not required for myoblast cell shape rearrangements (Figure 4.6B).

Dock1 is not required for myoblast migration in vitro

Differentiating myoblasts form lamellipodia and filopodia and migrate before fusing (Kawamura, 2004; Nowak et al., 2009; Ohtake, 2006; Steffen et al., 2006; 2004). These migrations are thought to promote critical contacts between

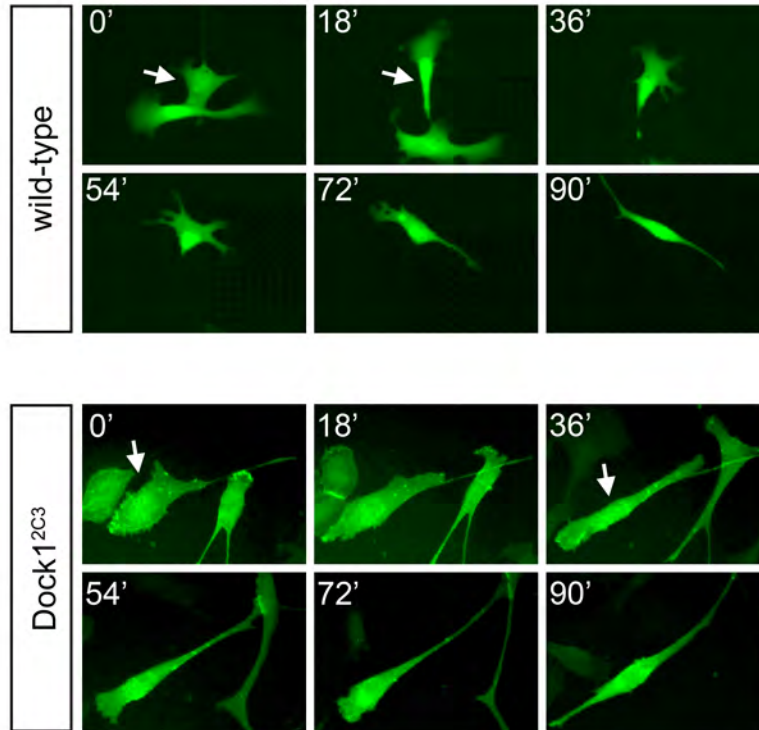


Figure 4.6. Dock1 knockdown myoblasts are able to remodel into spindle-shaped cells. Stills from live imaging demonstrating that wild-type and Dock1^{2C3} myoblasts, which express eGFP or a membrane-localized eGFP, respectively, remodel from a fibroblast-like shape to a bipolar, spindle-like shape. Myoblasts were cultured in differentiation medium for 24 hours prior to the onset of live imaging. Images were acquired every 18 minutes for an additional 24 hours. The arrow indicates the myoblast of interest.

myoblasts and myotubes necessary for differentiation and fusion (Krauss et al., 2005). During cell spreading and migration, data in mammalian cell lines indicate that Rac is activated by a signaling cascade triggered by integrin binding to fibronectin, which, through interactions with the adaptor proteins, p130^{CAS} and Crk, recruits Dock1 to focal adhesions (Kiyokawa et al., 1998a; 1998b; Meller, 2005). Overexpression of the Dock1-Crk-p130^{CAS} complex enhances Rac activation, cell spreading and migration (Kiyokawa et al., 1998a; 1998b), whereas depletion of Dock1 inhibits these behaviors (Côté et al., 2005; Meller, 2005). *Drosophila* Mbc is also implicated in cellular migration. *mbc* mutant embryos display defects in border cell migration during oogenesis and in dorsal closure, which is driven by the migration of epidermal cells during embryogenesis (Duchek et al., 2001; Erickson et al., 1997; Nolan et al., 1997). Thus, we hypothesized that Dock1 likely plays a universal role in cell migration and that the defect in myoblast fusion observed in Dock1-depleted myoblasts was due to impaired myoblast migration.

Though we observed Dock1 knockdown myoblasts migrating in our analysis of myoblast cell shape changes (Figure 4.6), suggesting that Dock1 was not required for myoblast migration, we wanted to quantify myoblast migration to determine if subtle defects in migration velocity or migration distance existed. To analyze myoblast migration, we again labeled control and Dock1 knockdown myoblasts and performed live imaging analysis under different culturing conditions and for different time intervals (Figure 4.7). When control and Dock1-depleted myoblasts were cultured in growth medium and imaged for 12 hours,

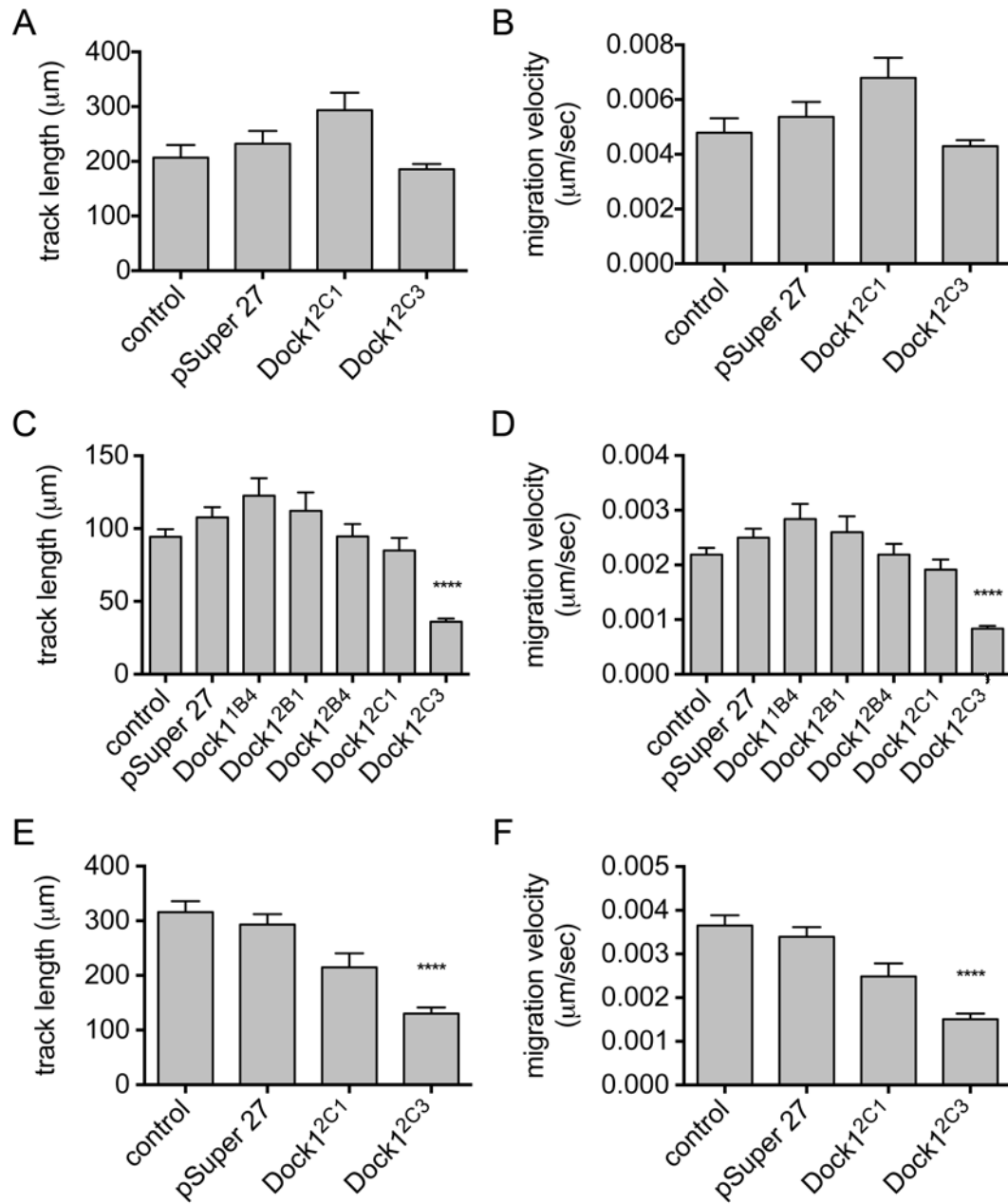


Figure 4.7. Dock1 knockdown myoblasts are capable of migrating. (A-F) Quantification of migration characteristics from live imaging. The indicated myoblasts lines were cultured in growth medium for 12 hours (A-B), in differentiation medium for 12 hours (C-D) or in differentiation medium for 24 hours (E-F). Total track length (A, C, E) and migration velocity (B, D, F) are shown. ****p<0.0001.

all myoblasts were highly motile, and we did not observe any statistically significant changes in track length or migration velocity (Figure 4.7A-B). When myoblasts were cultured in differentiation medium and imaged for the same time frame, all cell lines migrated shorter distances with slower velocities compared to the same cells cultured in growth medium, consistent with previously published observations, but there was no statistically significant difference between control cell lines and cell lines in which Dock1 was knocked down (compare Figure 4.7C-D to Figure 4.7A-B) (Griffin et al., 2010). Interestingly, one Dock1-depleted cell line, Dock1^{2C3}, showed a statistically significant decrease in migration distance and velocity (Figure 4.7C-D). This is likely an off-target effect as other cell lines in which Dock1 is depleted to a similar degree do not display migration defects. In addition, analysis of myoblast migration over a longer time period did not change the significance of any data points; however, the increase in track distance between the 12 hour and 24 hour tracking experiments demonstrate that myoblasts continue to migrate for at least 24 hours in DM (Figure 4.7E-F). Thus, these data indicate that Dock1 is not required for myoblast migration and that a migration defect is not responsible for the observed fusion defect. Though some Dock1 protein perdures and could be sufficient for myoblast migration, the absence of a migration phenotype in Dock1-depleted myoblasts is consistent with data showing that Nap1, part of the WAVE complex and downstream of Dock1 activation of Rac, is also not required for myoblast migration *in vitro* (Nowak et al., 2009).

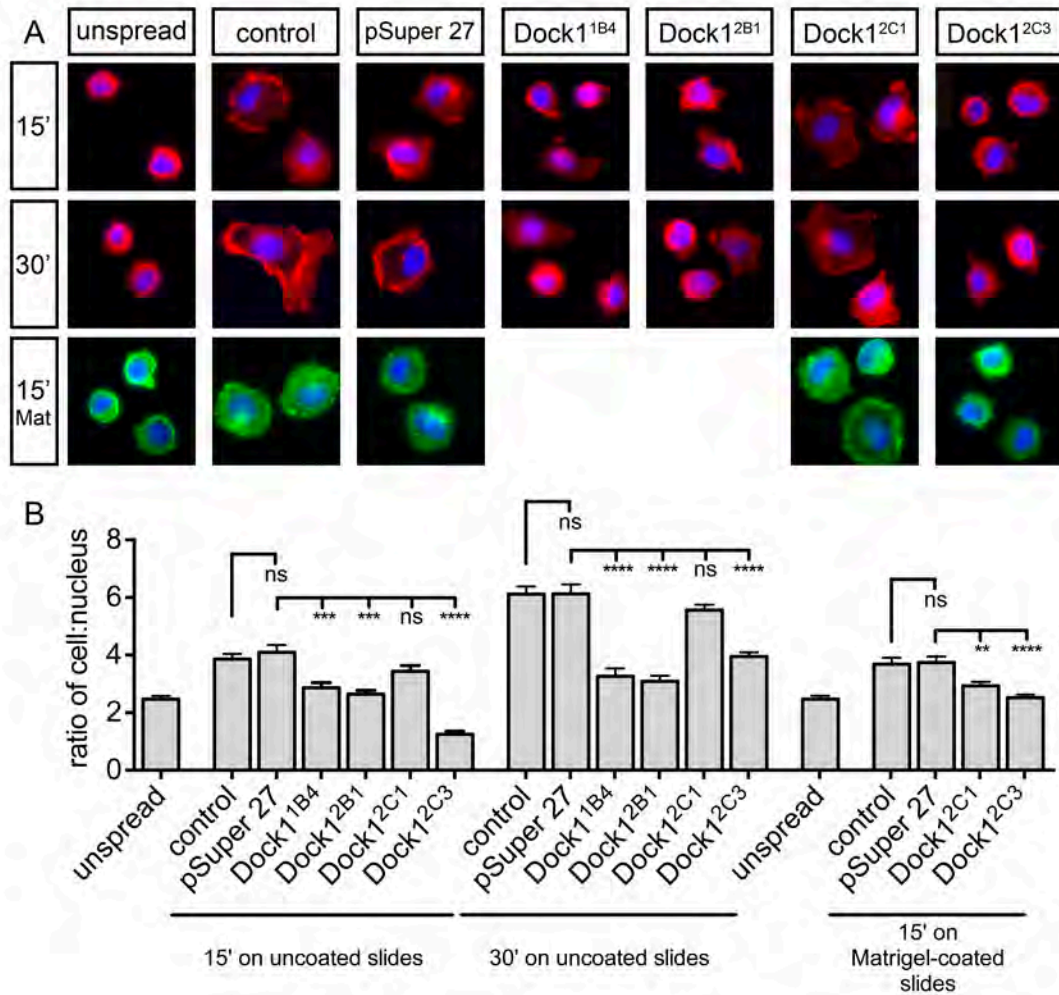


Figure 4.8. Cell spreading is affected in some Dock1 knockdown myoblasts. (A) Representative images of cells allowed to spread under the given conditions before being fixed and immunolabeled with phalloidin (actin, red or green) to highlight cell shape and DAPI (blue) to highlight nuclear area. (B) Volocity was used to determine the area of the nucleus and the cell for more than 100 cells per cell line. ** $p < 0.01$, *** $p < 0.001$, **** $p < 0.0001$.

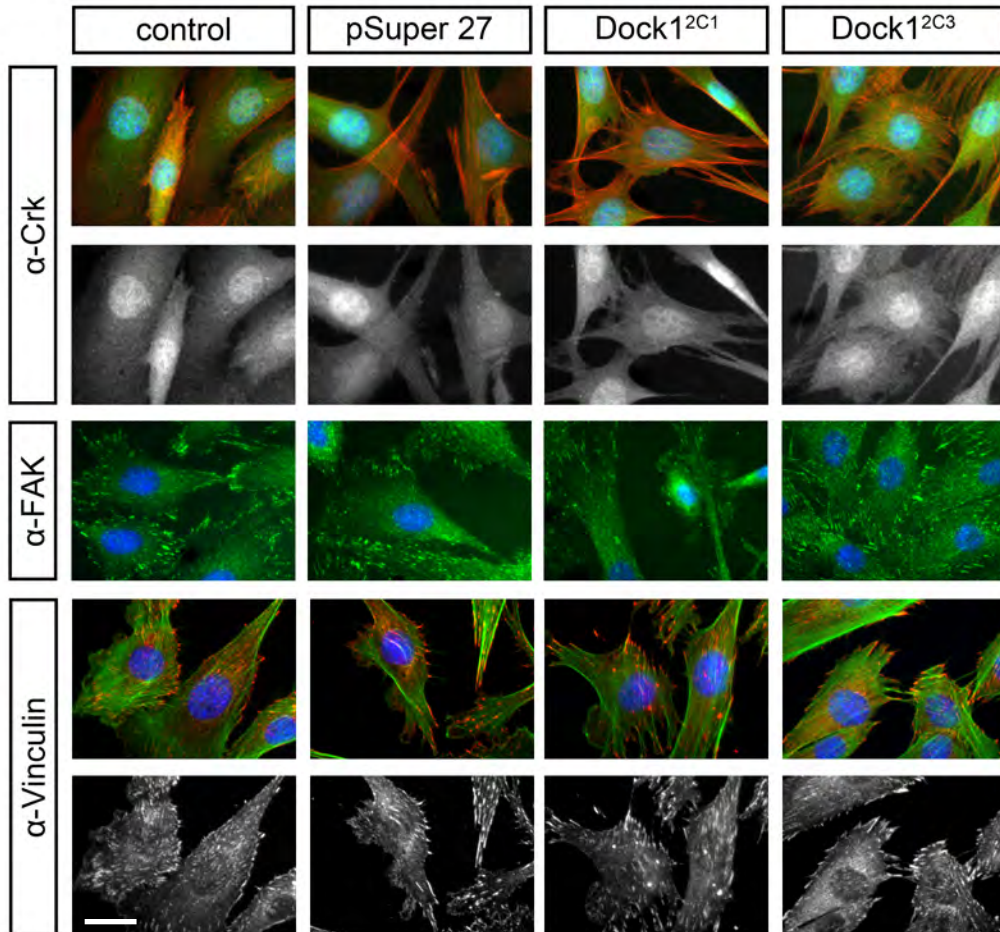


Figure 4.9. Components of focal adhesions are properly localized in Dock1 knockdown myoblasts. The indicated cell lines were plated and fixed before the shift to differentiation medium (DM) (Crk) or after one day in DM (focal adhesion kinase, FAK and Vinculin). Cells were immunolabeled with antibodies against Crk (top, green and lower panels), FAK (middle, green) and Vinculin (bottom, red and lower panels). Phalloidin (top, red and bottom, green) was used to label the actin cytoskeleton and DAPI (blue) was used to label nuclei. Bar, 25 μ m.

Depletion of Dock1 has also been shown to inhibit cell spreading (Meller, 2005). Thus, we examined the ability of Dock1 depleted myoblasts to reattach and spread (Figure 4.8). On uncoated slides, we found that Dock1^{1B4}, Dock1^{2B1} and Dock1^{2C3} myoblasts displayed a statistically significant decrease in the ratio of the cell area to the nuclear area, whereas Dock1^{2C1} myoblasts appeared similar to controls. When analyzed for their ability to spread on a glass slide coated with Matrigel, which includes a number of basement membrane components, both Dock1 knockdown myoblasts analyzed, Dock1^{2C1} and Dock1^{2C3} myoblasts did not spread normally.

Dock1 is not required for myoblast-myoblast alignment and adhesion

Contact and adhesion of myoblasts is essential for fusion (Kang, 2004). These sites can be identified by the localization of several proteins during differentiation, including N-cadherin, muscle-cadherin (M-cadherin) and β -catenin (Hollnagel et al., 2002; Nowak et al., 2009; Vasyutina et al., 2009). To test whether Dock1 is required for cell-cell contact, we differentiated control and Dock1-depleted myoblasts for one day, and fixed and stained them using antibodies against all three cell-adhesion proteins. N-cadherin, M-cadherin and β -catenin staining was observed at cell-contacts in all cell lines (Figure 4.10), indicating that Dock1 is not required for myoblasts to adhere to one another.

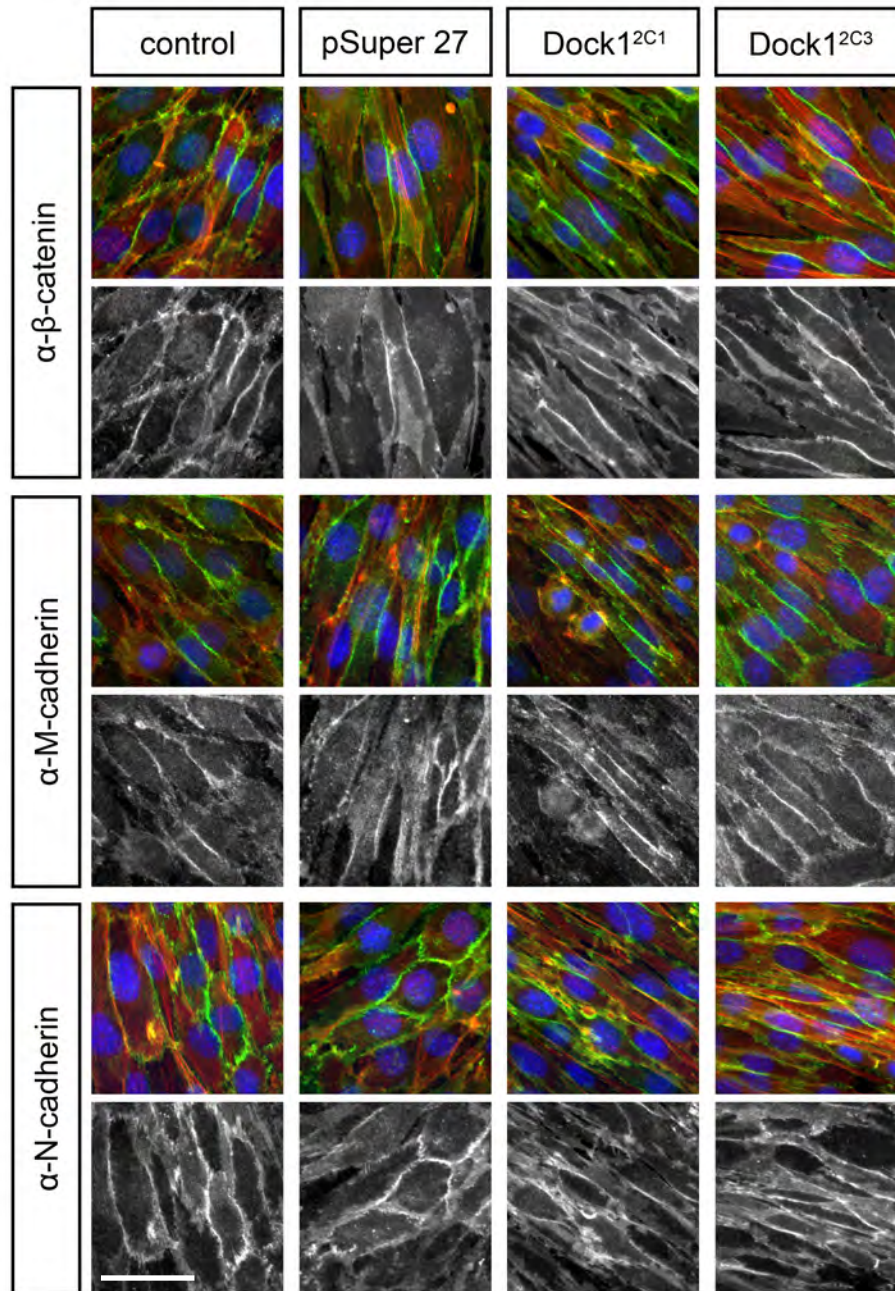


Figure 4.10. Dock1 is not required for myoblast-myoblast adhesion. Control and Dock1 knockdown myoblasts were cultured in differentiation medium for one day before being fixed and immunostained with antibodies that label cell-cell contacts (β -catenin, M-cadherin or N-cadherin, green). Actin is labeled with phalloidin (red), and nuclei are labeled using DAPI (blue). All cell-cell adhesion markers accumulate where myoblasts contact one another irrespective of Dock1 knockdown. Bar, 50 μ m.

IQSec1 is not required for myoblast migration in vitro

We were also interested in the role that IQSec1 plays during mammalian myoblast fusion. Data from *Drosophila* suggests that *loner* mutant myoblasts fail to migrate properly (Rochlin et al., 2009). To test the requirement for IQSec1 for myoblast migration, we used live imaging to track control and IQSec1-depleted myoblasts as described above. The distance and velocity of IQSec1^{2B2} knockdown myoblasts migration was not significantly different from control myoblasts over 12 hours in DM, suggesting that IQSec1 is not required for myoblast migration *in vitro* (Figure 4.11).

IQSec1 is not required for myoblast-myoblast adhesion

Previous studies in mammalian cells have suggested that IQSec1, through its activation of Arf6, is required for the endocytosis of cell adhesion molecules, including E-cadherin, a critical component of adherens junctions (AJs), and β 1-integrin (Dunphy et al., 2006; Hiroi et al., 2006). IQSec1 has also been shown to interact with α -catenin, a regulator of AJs and actin cytoskeleton remodeling and part of the E-cadherin complex, and IQSec1 knockdown myoblasts have aberrant paxillin localization and adhesion defects (Pajcini et al., 2008). Data in *Drosophila* has also hinted at this function. *Loner* is hypothesized to regulate the endocytosis of N-cadherin in FCs and FCMs and Slit in glial cells (Dottermusch-Heidel et al., 2012; Onel et al., 2004).

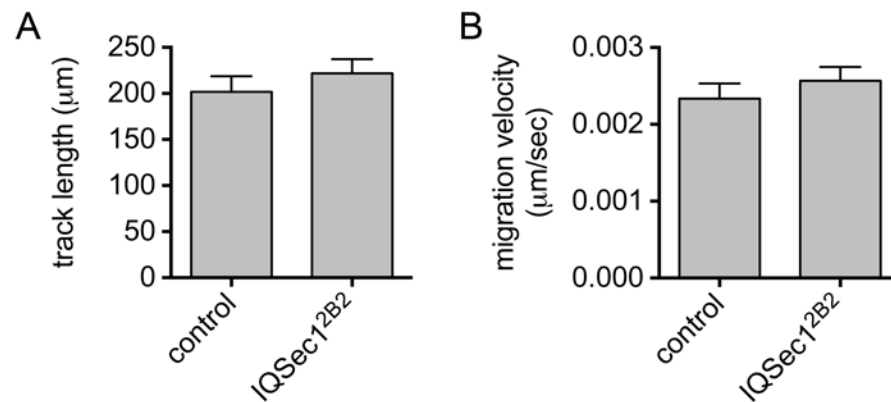


Figure 4.11. Knockdown of IQSec1 does not affect migration. (A-B) Fluorescently labeled control and IQSec1^{2B2} myoblasts were cultured in differentiation medium and imaged for 12 hours. The total track length (A) and migration velocity (B) of control and IQSec1^{2B2} myoblasts is shown.

Thus, we hypothesized that IQSec1 functions in regulating the adhesion of myoblasts by modulating the localization of cell adhesion proteins. To test this, we examined the localization of Paxillin and Vinculin, two components of focal adhesions, and M- and N-cadherin, markers of cell-cell contact (Figure 4.12). In all instances, we found that the markers appropriately accumulated at focal adhesions (Figure 4.12A) and at sites of myoblast contact (Figure 4.12B). Though we did not measure this directly, we did not find evidence for an excess of protein located at the cell surface. Together, these data suggest that IQSec1 is also not required for myoblast-myoblast adhesion in *Drosophila*.

Discussion

In this study, we have investigated the mammalian homologs of Myoblast city and Loner, two GEFs required for myoblast fusion in *Drosophila* (Chen et al., 2003; Erickson et al., 1997; Rushton et al., 1995). As has been demonstrated in this study as well as in published work, Dock1 is required for myoblast fusion *in vitro* and *in vivo*, indicating that Dock1 plays an evolutionarily conserved role in myoblast fusion (Laurin et al., 2008; Pajcini et al., 2008). However, both the function of Dock1 and at which step it acts during mammalian myoblast fusion remain unclear.

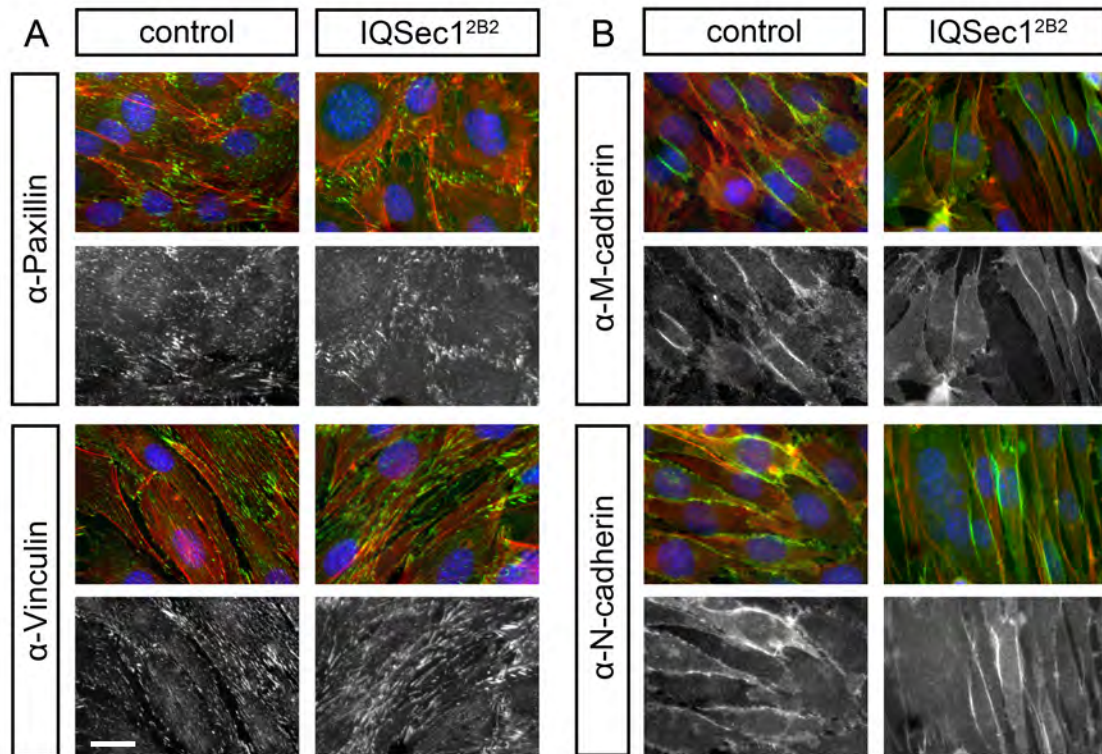


Figure 4.12. Knockdown of IQSec1 does not affect the localization of adhesion proteins. Control and IQSec1^{2B2} knockdown myoblasts were cultured for one day in differentiation medium, fixed and immunolabeled with antibodies against components of focal adhesions (A) or with antibodies against proteins that accumulate at cell-cell contacts (B). Paxillin, Vinculin, M- and N-cadherin, green and lower panels. Actin is labeled with phalloidin (red), and nuclei are labeled using DAPI (blue). Bar, 25 μ m.

Using a number of C2C12 myoblast lines in which Dock1 is depleted using shRNAs, we demonstrate here that Dock1 is not required for early steps that precede myoblast fusion, including myoblast differentiation. This is in contrast to an earlier analysis of Dock1 in C2C12 myoblasts, which concluded that Dock1 depletion delayed myogenin and MHC induction (Pajcini et al., 2008). Though the overall numbers of MHC-positive nuclei were reduced in Dock1 knockdown cell lines compared to control cell lines, we did not observe a similar delay in the onset of differentiation (data not shown). Similarly, *Dock1*-null myoblasts were not delayed in their expression of MHC *in vivo* (Laurin et al., 2008).

We also concluded that Dock1 is not required for the cell shape changes, migration or myoblast-myoblast adhesion and alignment that precede myoblast fusion. Using live imaging, we observed Dock1 knockdown myoblasts, in a manner that resembled that of control myoblasts, remodel from a fibroblast-like morphology to a spindle shape during their culture in differentiation media. At E14.5, *Dock1*-null myoblasts, though they remain mononucleated, are elongated, suggesting that they were also properly able to change their morphology. Similarly, conditional Rac1 mutant myoblasts became spindle-shaped. Thus, these data hint that Dock1 and Rac are not required for this aspect of myoblast fusion *in vitro* or *in vivo* (Laurin et al., 2008; Vasyutina et al., 2009).

We were quite surprised at the lack of a migration phenotype in the majority of our Dock1-depleted cell lines. In other mammalian cell culture systems, Dock1 is required for cellular migration (Côté et al., 2005; Kiyokawa et al., 1998a; 1998b; Meller, 2005). It is possible that residual Dock1 protein is

sufficient for driving myoblast migration, or that a redundantly acting GEF (see below) is able to compensate for Dock1 depletion. We did have one Dock1 knockdown cell line that displayed a statistically significant difference in myoblast migration compared to controls and to other Dock1 knockdown myoblast lines. We choose to think that this migration phenotype is the result of off-target effects or another underlying defect in the cells perhaps caused by the clonal selection step in spite of its depletion of Dock1 for a number of reasons.

First, in *Drosophila*, *mbc* mutant and *rac* triple mutant myoblasts remain rounded, which has been taken as evidence of a migration defect, though migration has not been assessed directly in this system (Gildor et al., 2009). However, mutation of *kette*, which is downstream of Mbc and Rac, does not affect myoblast migration *in vivo* (Rochlin et al., 2009). Thus, the contribution of Mbc and Rac to myoblast migration is unresolved. In further support of our conclusion that Dock1 is not required for myoblast migration *in vitro*, *Dock1*-null myoblasts are able to migrate from the myotome to distant sites of myogenesis, including the tongue and limb buds, *in vivo* (Birchmeier and Brohmann, 2000; Laurin et al., 2008). Similarly, analysis of a conditional Rac1 mutant mouse did not indicate that migration of mutant myoblasts was affected *in vivo* (Vasyutina et al., 2009). It is still possible that the quality of migration is affected (i.e., the proper number of myoblasts do not reach the limb bud or that myoblasts take longer to reach the limb bud) in these mouse models, and this has not been addressed. Together, these data indicate that Dock1 and Rac likely do not play a

role in myoblast migration and that other GTPases or redundantly acting GTPases must control this behavior during muscle development.

Additionally, we did not observe any defects in myoblast-myoblast adhesion and alignment when Dock1 was depleted in C2C12 myoblasts. We found that three markers of cell-cell contact, β -catenin and M- and N-cadherin, properly accumulated between adjacent myoblasts. Similarly, mononucleate myoblasts in *Dock1*-null embryos were noted to be aligned *in vivo*, though the accumulation of cell-cell contact markers was not examined (Laurin et al., 2008). Further, β -catenin also accumulated normally between cultured Rac1 mutant myoblasts, indicating that Rac is not required for the initial adhesion of myoblasts (Vasyutina et al., 2009). However, the focal adhesion proteins Vinculin and VASP, Arp2/3 and F-actin were reduced at cell-cell contact sites in Rac1 mutant myoblasts, suggesting that Rac is required for actin polymerization at sites of myoblast-myoblast contact in the mouse, as is the case in *Drosophila*.

Thus, by the process of elimination, we conclude that Dock1 is required at the site of fusion. This is supported by data from a number of other studies. For example, in *Drosophila*, Mbc localizes to the actin focus, where it is thought to activate Rac (Richardson et al., 2007). In C2C12 myoblasts, Dock1 has a similar localization and is found to colocalize with N-cadherin at sites of myoblast-myoblast contact (Nowak et al., 2009). All aspects of myoblast differentiation appeared normal in our Dock1 depleted C2C12 myoblasts and in *Rac1* conditional mutant myoblasts, which fail after the initial myoblast-myoblast adhesion step (Vasyutina et al., 2009). Finally, *Rac1* conditional mutant

myoblasts are unable to recruit and accumulate markers of actin polymerization. Thus, Dock1 plays a conserved role in mammalian myoblast fusion, and the data from both *in vitro* and *in vivo* studies suggest that it acts at the fusion site, likely regulating actin dynamics.

We failed to completely block myoblast fusion upon depletion of Dock1. This is likely due, in part, to the presence of residual Dock1 protein in our knockdown lines. Additionally, vertebrates encode a second Mbc ortholog, Dock5, which is expressed in the developing myotome of the mouse and plays a partially redundant role in myoblast fusion *in vivo* (Laurin et al., 2008). Dock1 and Dock5 are also required for myoblast fusion in zebrafish (Moore et al., 2007). Dock5 is expressed in C2C12 myoblasts, and its levels are not affected by shRNAs that target Dock1 (data not shown). Thus, Dock5 may act redundantly with Dock1 in C2C12 myoblasts during the fusion process, but this has not been experimentally tested.

Our data also suggests that IQSec1, the mammalian homolog of *Drosophila* Loner, plays a conserved role in mammalian myoblast fusion, consistent with previously published data (Pajcini et al., 2008). We hypothesized that IQSec1 may be required for myoblast migration; preliminary data from our lab suggests that this is the case for Loner (M. Baylies and B. Richardson, personal communication). However, our migration analysis does not indicate that IQSec1 is required for mammalian myoblast migration, and we did not find evidence for the mislocalization of adhesion proteins or defects in adhesion, functions that have been previously ascribed to IQSec1 depletion in other

systems (Dunphy et al., 2006; Hiroi et al., 2006). Similarly, when IQSec1 was depleted in C2C12 myoblasts, a difference in the cellular levels of β 1-integrin, E- or M-cadherin was not observed (Pajcini et al., 2008). However, in contrast to our work which did not detect mislocalization of Paxillin in our IQSec1 knockdown myoblasts, Paxillin was found to be mislocalized in another analysis of IQSec1 function in C2C12 myoblasts (Pajcini et al., 2008). Unfortunately, as we were never able to confirm IQSec1 depletion in our lines, and thus, cannot be sure that we are examining *bona fide* IQSec1 phenotypes, these discrepancies can most likely be attributed to the lack of knockdown in our cell lines.

Since its original characterization in muscle development in *Drosophila*, only one additional study has been published recently on the role of Loner in myoblast fusion, and only one study has been published on the role of its mammalian homolog during fusion. Data in *Drosophila* suggests that Loner is responsible for the trafficking of N-cadherin in muscle, which is consistent with data in the nervous system indicating that Loner is required for the proper localization of other proteins (Dottermusch-Heidel et al., 2012; Onel et al., 2004). However, neither N-cadherin or the second, closely-related N-cadherin2 is essential for myoblast fusion in *Drosophila*, indicating that Loner must traffic additional proteins that are essential for fusion or that Loner plays a second role in myoblast fusion. Thus, while Loner and IQSec1 likely have a conserved function in myoblast fusion, their role remains unclear in either system.

In summary, we have explored the roles of two GEFs, Dock1 and IQSec1 during mammalian myoblast fusion. The work presented here, as well as work

published by other labs, suggests that these proteins play a conserved role in myoblast fusion (Laurin et al., 2008; Pajcini et al., 2008). Although these studies came to the same overall conclusion that Dock1 and IQSec1 were required for mammalian myoblast fusion, there were some reported differences that can likely be attributed to *in vitro* versus *in vivo* analyses as well as differences in protein depletion between *in vitro* experiments, highlighting an important limitation of *in vitro* analyses. Finally, in *Drosophila*, mutation of *mbc* or *loner* results in the perdurance of the F-actin focus that forms at the site of fusion (Richardson et al., 2007). Though our analysis of the role of Dock1 has narrowed Dock1 function to the site of fusion, the effect of Dock1 and IQSec1 perturbation on the mammalian fusion site has not been addressed in any mammalian myoblast fusion system.

CHAPTER FIVE:

Identification of the site of myoblast fusion in mammals: PI(4,5)P₂ accumulates at the site of myoblast-myoblast adhesion and fusion *in vitro*

Chapter Overview

The site of myoblast fusion in *Drosophila* can be identified by an essential, transient accumulation of F-actin and phosphatidylinositol 4,5-bisphosphate (PIP₂) (Kim et al., 2007; Richardson et al., 2007; Bothe et al., in revision). Though regulators of the actin focus, including Myoblast city (Mbc)/Dock1 play conserved roles in myoblast fusion in *Drosophila* and mammals, the fusion site in mammalian myoblast fusion has not been as extensively characterized (Erickson et al., 1997; Laurin et al., 2008; Nolan et al., 1997; Pajcini et al., 2008; Rushton et al., 1995; this study). In fixed imaging of cultured fusing mammalian myoblasts, an accumulation of actin, termed the actin wall, has been described; however, the dynamics that underlie this structure have not been established, and thus, a defining feature of the fusion site has yet to be elucidated. In addition, recent work in C2C12 myoblasts indicates that PIP₂ accumulates at the site of myoblast contact and that PIP₂ reduction impairs the fusion process (Bach et al., 2010; Nowak et al., 2009). Together, these data hint that a structure similar to the actin focus may exist in mammals.

In this study, we identify two fluorescent reporters that directly label the actin cytoskeleton in C2C12 myoblasts and myotubes when transiently expressed. Stable expression of these reporters, however, appears toxic to myoblasts, suggesting that they compromise actin regulation. To circumvent these issues, we also use a fluorescent PIP₂ construct, which acts as an indirect reporter of the actin cytoskeleton (Tall et al., 2000). We show that

PIP₂ accumulates at the site of myoblast-myoblast contact in C2C12 myoblasts and that PIP₂ accumulations disperse prior to fusion, consistent with previously published work (Bach et al., 2010; Nowak et al., 2009). In addition, we find evidence for asymmetry at the fusion site where PIP₂ accumulates in one fusing partner and not the other, suggesting the presence of different populations of fusing myoblasts. Finally, stable, high expression of the PIP₂ reporter results in a fusion block reminiscent of the “masking” phenotype observed with PIP₂ reporter overexpression in *Drosophila* (Bothe et al., in revision). Taken together, these data indicate that PIP₂ accumulations mark the fusion site in mammals and play a conserved role in myoblast fusion.

Results

Lentivirus-mediated expression of fluorophores allows for long-term expression in C2C12 myoblasts

Previous attempts to identify the fusion site in mammalian myoblasts relied on fixed imaging, which precludes analysis of fusion site dynamics, or transfection of fluorescent reporters, which is transient and inefficient in C2C12 myoblasts (data not shown) (Bach et al., 2010; Duan and Gallagher, 2009; Nowak et al., 2009). Further, because only a subset of myoblasts are labeled and the probability of observing a fusion event during live imaging is already low, this approach is very low-throughput. Thus, we first wanted to establish a system

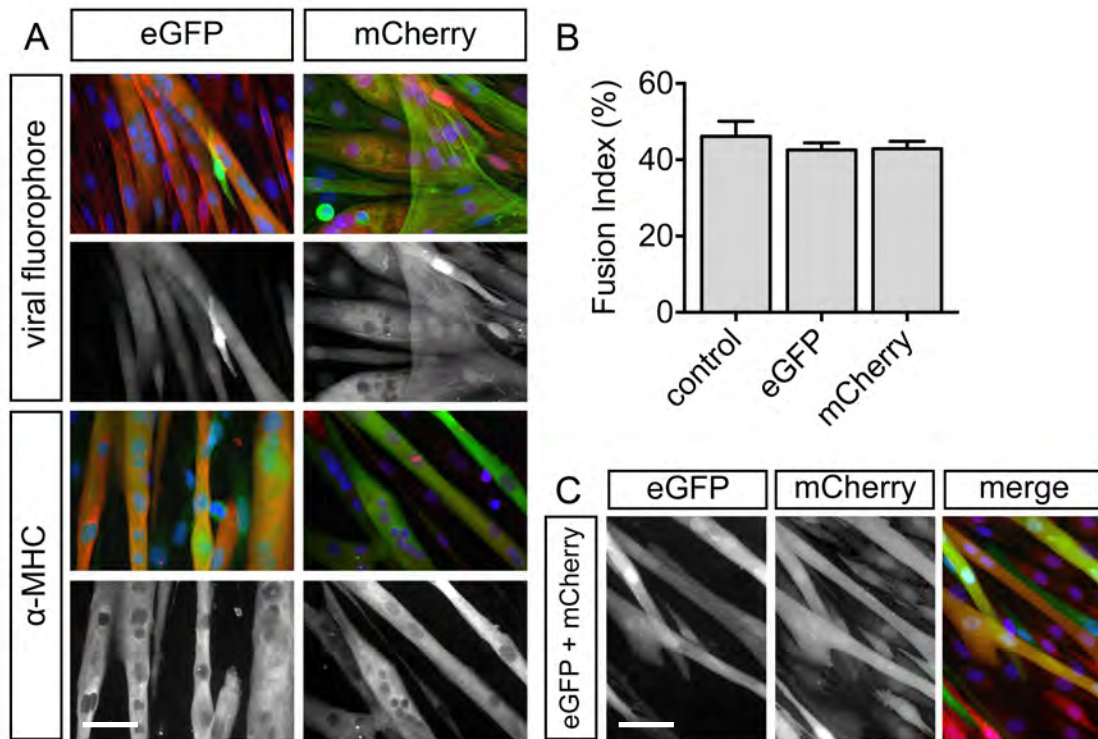


Figure 5.1. Lentivirus-mediated expression of cytoplasmic eGFP and mCherry does not affect the differentiation or fusion of C2C12 myoblasts. (A) Myoblasts expressing either cytoplasmic eGFP or mCherry were shifted to differentiation medium (DM) for 5 days after becoming confluent. (Top panels) Myotubes were fixed and immunolabeled with phalloidin to label actin (red for eGFP infected cells and green for mCherry infected cells) and DAPI to label nuclei (blue). Antibodies were not used to detect eGFP (green) and mCherry (red) expression (also in grey scale below). (Bottom panels) Myotubes were fixed and immunostained with an antibody to Myosin Heavy Chain (MHC, red for eGFP infected cells and green for mCherry infected cells; also shown in grey scale below). MHC-positive myotubes contain many nuclei and continue to express eGFP or mCherry at a high level after 5 days in DM. (B) Quantification of the fusion index for lentivirus-infected myoblasts demonstrates that fusion is not affected by lentiviral infection. Control is mock infected. (C) eGFP and mCherry myoblasts were mixed in equal numbers and shifted to DM for 5 days after becoming confluent. Myotubes were fixed and immunolabeled with DAPI (blue) to mark nuclei. The majority of myotubes form from the fusion of differentially-labeled myoblasts. Bar, 50 μ m.

Table 5.1. Summary of efficiency of lentivirus infection.

Lentivirus	Infection efficiency (%)	
	293T	C2C12
eGFP	99	>70
mCherry	95	>70
H2B::eGFP	100	>90
H2B::mCherry	100	>80
Lifeact::Ruby	85	0
GFP::UtrCH	96	10-12
BTK ^{PH} ::eGFP	-	>70
PLC δ ^{PH} ::eGFP	-	>70

that would allow us to stably and fluorescently label large populations of myoblasts for live imaging. To that end, we generated lentiviruses expressing cytoplasmic eGFP and cytoplasmic mCherry. In contrast to transfection, lentivirus infection resulted in stable, long-term reporter expression and infected C2C12 myoblasts with high efficiency (Table 5.1).

In addition, myoblasts infected with lentivirus encoding either cytoplasmic eGFP or cytoplasmic mCherry were able to differentiate and fuse normally, indicating that high expression of the fluorophore alone was not toxic and did not affect normal fusion behaviors (Figure 5.1A-B). eGFP myoblasts and mCherry myoblasts were also able to fuse with one another to generate myotubes that express both markers (Figure 5.1C). That expression of each reporter could be detected after five days highlights an important benefit of this approach over transfection.

Live imaging of fusion

We next wanted to determine whether amplifying the number of labeled myoblasts allowed us to increase the number of observed fusion events during live imaging. Unsurprisingly, we were able to easily detect a large number of fusion events, which had been impossible with transfection. With this approach, analysis of a single experiment yielded greater than 85 observable fusion events (Figure 5.2). In comparison, in over 30 imaging experiments using transient transfection, fewer than 20 fusion events have been observed.

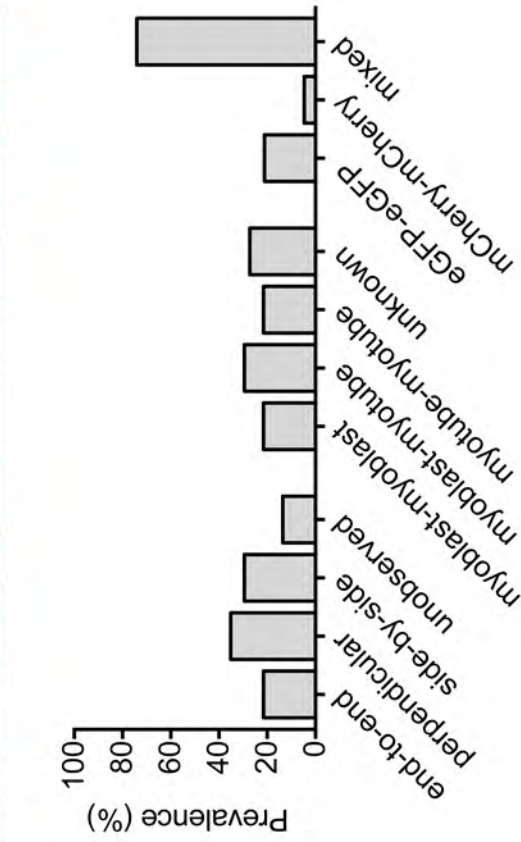
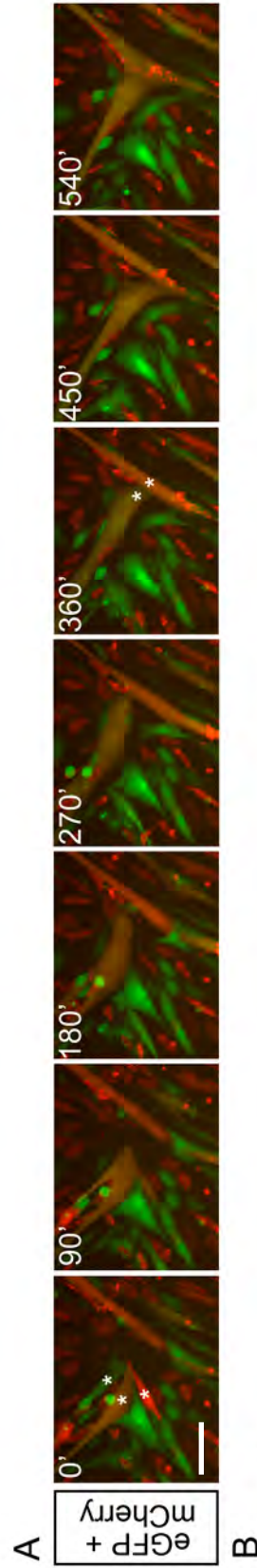


Figure 5.2. Live imaging of differentially labeled C2C12 myoblasts. (A) Myoblasts stably expressing either cytoplasmic mCherry or cytoplasmic eGFP were mixed in equal numbers and plated and treated as described above. At the start of acquisition (0'), myotubes have already formed from the fusion of myoblasts expressing either fluorophore to generate myotubes that express both fluorophores (orange). Between 0-90', a "mixed" myotube (asterisk) will fuse with an mCherry myoblast and an eGFP myoblast (asterisk). A second fusion event involving two myotubes occurs between 360-450' (asterisks). (B) Quantification of characteristics of fusion, including fusion partner choice and orientation of the fusion event. n = 85 fusion events. Bar, 50 μ m.

Thus, lentiviral-mediated expression allows for stable expression of fluorescent markers, which does not affect C2C12 myoblast differentiation or fusion and increases the throughput of this assay.

We defined each fusion event (n=85) by the orientation of the fusion event and the characteristics of the fusion partner to determine if there was any underlying bias. Over the 48 hour imaging period, we detected fusion events in each orientation: end-to-end, side-by-side or perpendicular. We also found that fusion events occurred between heterogeneous partners that could be myoblasts or myotubes and could express eGFP, mCherry or in the case of myotubes, eGFP and mCherry (Figure 5.2B). We did not observe any significant skew towards fusion of a particular kind with respect to orientation or fusion partner choice. Since we did not make note of the time at which each fusion event occurs, we therefore cannot speculate on whether particular fusion events occur more frequently at specific points in the imaging duration (for example, whether myoblast-myoblast fusions occur less frequently after 72 hours in DM compared to 48 hours in DM or compared to myotube-myotube fusions at the same time point). Additionally, as there is no read-out of contact initiation, we are not able to comment on the duration of a fusion event in mammalian muscle cell culture.

Identification of actin reporters

We next wanted to use this approach to analyze the mammalian fusion site. Previous experiments using GFP::actin caused toxicity in C2C12 myoblasts,

necessitating the identification of additional actin reporters (M. Baylies and S. Nowak, personal communication). We identified a number of available plasmids encoding fluorescently-tagged full-length actin-binding proteins, including human ACTR3 (ARP3 actin-related protein 3 homolog, also ARP3) and FBP17 (Formin-binding protein 17, also FBP1) and mouse Capzb (F-actin-capping protein subunit beta) and Dbnl (Drebin-like protein, also Abp1) (Table 5.2). ACTR3 is the ATP-binding component of the ARP2/3 complex (Welch et al., 1997). FBP17 binds to lipids such as phosphatidylinositol 4,5-bisphosphate and phosphatidylserine, promotes membrane invagination and tubulation, and enhances actin polymerization via its recruitment of N-WASP (Tsujita et al., 2006). Capzb is a member of the F-actin capping protein family and encodes the beta subunit of the WASH complex. Capzb blocks the exchange of subunits at barbed ends (Hart and Cooper, 1999; Jia et al., 2010). Dbnl is an adaptor protein that binds F-actin and dynamin, plays a role in receptor-mediated endocytosis and in the reorganization of the actin cytoskeleton, but does not promote actin polymerization on its own (Kessels et al., 2000; 2001).

In addition, we obtained plasmids encoding fluorescently-tagged small peptides or actin-binding domains, including Lifeact, a 17-amino-acid peptide which labels F-actin structures in eukaryotic cells and tissues *in vitro* and *in vivo* and UtrCH, the F-actin binding calponin homology (CH) domain of utrophin (Table 5.2) (Burkel et al., 2007; Riedl et al., 2008). All reporters are under the control of the synthetic cytomeglovirus (CMV) immediate early enhancer and chick β -actin promoter elements, which drive high levels of gene expression (Miyazaki et al., 1989).

Table 5.2. Summary of actin-binding plasmids

Reporter name	Full protein name	From?	Localization in C2C12 myoblasts	Reference
ACTR3::eGFP	ARP3 actin-related protein 3 homolog, also ARP3	human, full-length	cytoplasmic	(Welch et al., 1997)
eGFP::Capzb	F-actin-capping protein subunit beta	mouse, full-length	cytoplasmic	(Hart et al., 1999; Jia et al., 2010)
eGFP::Dbnl	Drebin-like protein, also Abp1	mouse, full-length	cytoplasmic	(Kessels et al., 2000; Kessels et al., 2001)
eGFP::FBP17	Formin-binding protein 17, also FBP1	human, full-length	puncta	(Tsujiita et al., 2006)
Lifeact::eGFP	17-amino-acid peptide	peptide	F-actin	(Riedl et al., 2008)
GFP::UtrCH	F-actin binding calponin homology (CH) domain of Utrophin (Utr)	protein domain	F-actin	(Burkel et al, 2007)
mRFP::UtrCH			F-actin	

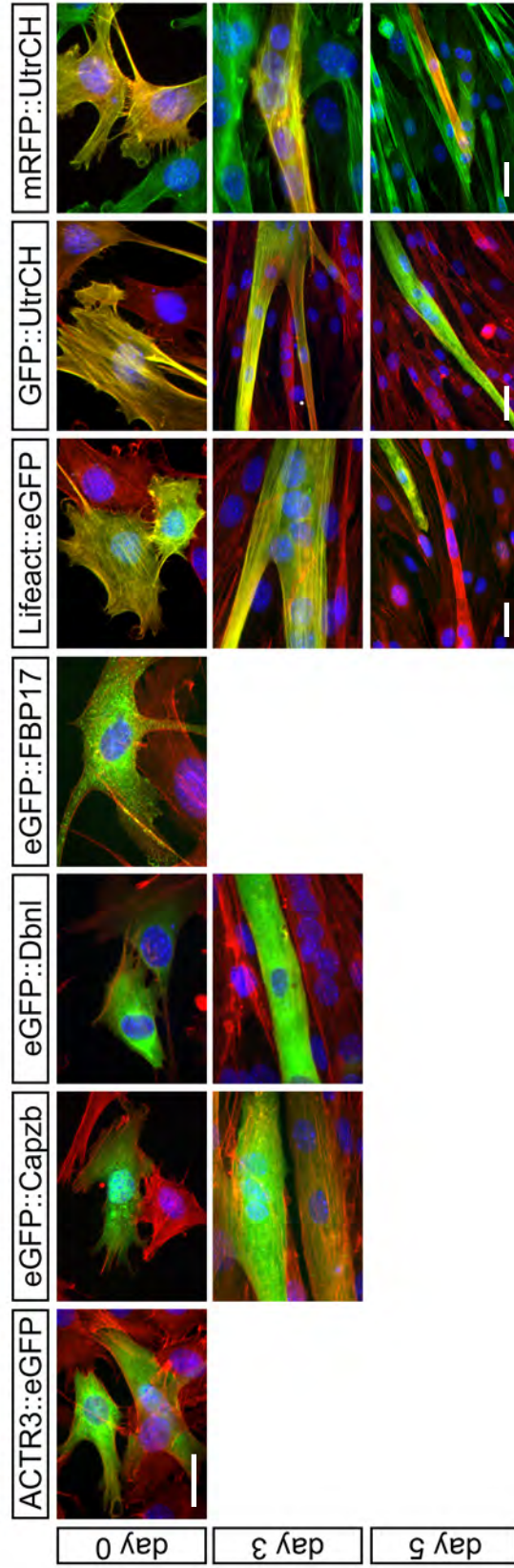


Figure 5.3. Localization of actin-binding reporters in C2C12 myoblasts during differentiation. C2C12 myoblasts were transfected with the indicated reporter construct and fixed at day 0 in growth media or at day 3 or day 5 after culturing in differentiation media. Cells were immunolabeled with DAPI (blue) to label nuclei or phalloidin to label actin (red). In the case of mRFP::UtrCH, 488-conjugated phalloidin (green) was used. Images are missing where we could no longer detect the fluorophore at the indicated time point. Bar, 30 μ m.

As a first level of analysis, we transfected C2C12 myoblasts and examined the localization of each fluorescently-tagged construct and its capacity to reflect the organization of the F-actin cytoskeleton (Figure 5.3). In proliferating myoblasts (day 0), ACTR3::eGFP, eGFP::Capzb and eGFP::Dbnl were cytoplasmic and did not appear to colocalize with phalloidin-labelled F-actin. In addition, the localization of eGFP::Capzb and eGFP::Dbnl remained cytoplasmic after three days in differentiation medium (day 3). eGFP::FBP17 was largely cytoplasmic in proliferating myoblasts but also accumulated in puncta at presumptive actin filament ends (day 0). In contrast, Lifeact::eGFP, GFP::UtrCH and mRFP::UtrCH completely or nearly completely colocalized with F-actin in proliferating and differentiating myoblasts and myotubes at all time points examined. Thus, the peptide-based reporters were the most faithful at recapitulating the actin cytoskeleton in fixed analysis.

Stable expression of Lifeact or UtrCH reporters is toxic to C2C12 myoblasts

We further explored the applicability of using tagged Lifeact and/or UtrCH to visualize the F-actin cytoskeleton during myoblast fusion. To stably label myoblasts for live imaging, we generated lentiviruses to deliver each marker. We also generated lentiviruses encoding histone H2B (H2B) fused to either eGFP or mCherry to label myonuclei. Surprisingly, upon infection with lentivirus encoding either Lifeact::Ruby or GFP::UtrCH, we recovered relatively few C2C12 myoblasts that expressed the actin reporters (Table 5.1, Figure 5.4A).

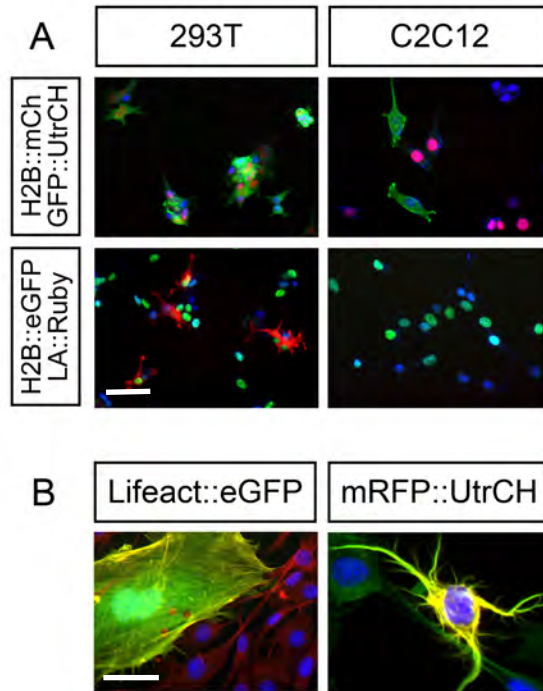


Figure 5.4. Expression of actin-binding reporters is toxic. (A) Representative images of 293T cells or C2C12 myoblasts infected with lentiviruses encoding H2B::mCherry and GFP::UtrCH or H2B::eGFP and Lifeact (LA)::Ruby. Note that few to no C2C12 myoblasts express GFP::UtrCH or LA::Ruby after infection though expression of coinfecting H2B viruses is evident. (B) Defects in the actin cytoskeleton observed in C2C12 myoblasts transfected with Lifeact::eGFP, which caused cell size defects, or mRFP::UtrCH, which caused collapse of the F-actin filaments into a few extensions, in the examples shown here. Bar, 50 μ m.

This was in contrast to H2B-fused virus, which was co-infected (Figure 5.4A) or to either control virus where efficiency was greater than 70% (Table 5.1). Further, the infection efficiency of the same viruses in 293T cells was greater than 85%, indicating that the virus was effective at infection and suggesting that overexpression of these constructs was largely toxic to C2C12 myoblasts. This is supported by data from transient transfection of the Lifeact and UtrCH reporters, which caused cell shape and size defects (Figure 5.4B), as well as previous data suggesting that GFP::actin fusions also caused toxicity in C2C12 myoblasts (M. Baylies and S. Nowak, personal communication). Thus, our efforts to stably express direct reporters of the actin cytoskeleton were unsuccessful.

Transient expression of phospholipid markers does not affect myoblast differentiation

PLC δ^{PH} ::eGFP consists of the PH domain of PLC δ fused to GFP and is a reporter of the membrane phospholipid phosphoinositol 4,5-bisphosphate (PIP₂), a known regulator of actin dynamics and activator of Arp2/3 (Miki et al., 1996; Papayannopoulos et al., 2005; Shewan et al., 2011). Because PLC δ^{PH} ::eGFP had been successfully used to observe actin dynamics indirectly, we revisited this option (Bach et al., 2010; Nowak et al., 2009; Tall et al., 2000). In C2C12 myoblasts, PLC δ^{PH} ::eGFP accumulated at sites of active actin remodeling, including lamellipodia and cleavage furrows. In contrast, we did not observe any accumulation of eGFP or BTK PH ::eGFP (the PH domain of Bruton's tyrosine

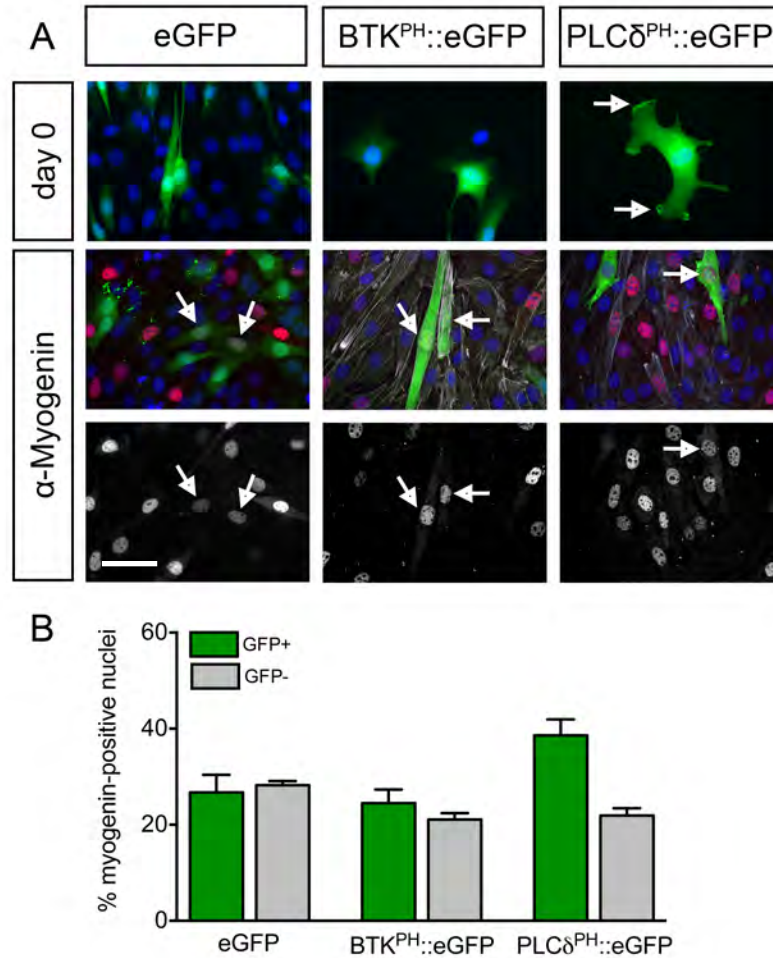


Figure 5.5. Transient expression of phospholipid reporters does not affect differentiation. (A) Localization of eGFP, BTK^{PH}::eGFP and PLC δ ^{PH}::eGFP (green) in transfected myoblasts at day 0. PLC δ ^{PH}::eGFP accumulates at sites of active actin remodeling (arrows), like lamellipodia (top). The expression of myogenin (red) in cells expressing the indicated fluorescent reporter after 36 hours in differentiation media (bottom). Myogenin is shown in lower panels, and transfected, Myogenin-positive nuclei are indicated by arrows. In all images DAPI (blue) was used to label all nuclei. (B) Quantification of percentage of Myogenin-positive nuclei by fluorescent reporter expression. Bar, 50 μ m.

kinase fused to eGFP), which binds to PIP₃ (Figure 5.5A) (Côté et al., 2005). Transient expression of either reporter did not affect myoblast differentiation (Figure 5.5A-B). Myoblasts expressing any of the constructs expressed Myogenin, a muscle-specific bHLH transcription factor and an indicator of muscle differentiation, in similar proportion to myoblasts that were not transfected (Figure 5.5B).

Live imaging of PLCδ^{PH}::eGFP reveals accumulation of PIP₂ that precedes the fusion event

Previous reports indicated that PLCδ^{PH}::eGFP accumulated at the site of myoblast-myoblast contact before fusion (Bach et al., 2010; Nowak et al., 2009). To confirm and extend these analyses, we transfected C2C12 myoblasts, shifted them to DM for 24 hours and began live imaging analysis. Strikingly, we detected a clear accumulation of PLCδ^{PH}::eGFP that dissipated prior to a labeled myoblast fusing with an unlabeled myotube (Figure 5.6A). This accumulation was reminiscent of the F-actin and PIP₂ foci observed in *Drosophila* myoblast fusion and suggested that PIP₂ accumulated at the site of mammalian myoblast fusion. The entire fusion process, measured from presumptive myoblast-myotube contact (the time point before the first evidence of accumulation is visible) to the fusion event (measured by the transfer of PLCδ^{PH}::eGFP fluorescence from the myoblast to the myotube), was completed in approximately 90 minutes but could have taken as few as 56 minutes.

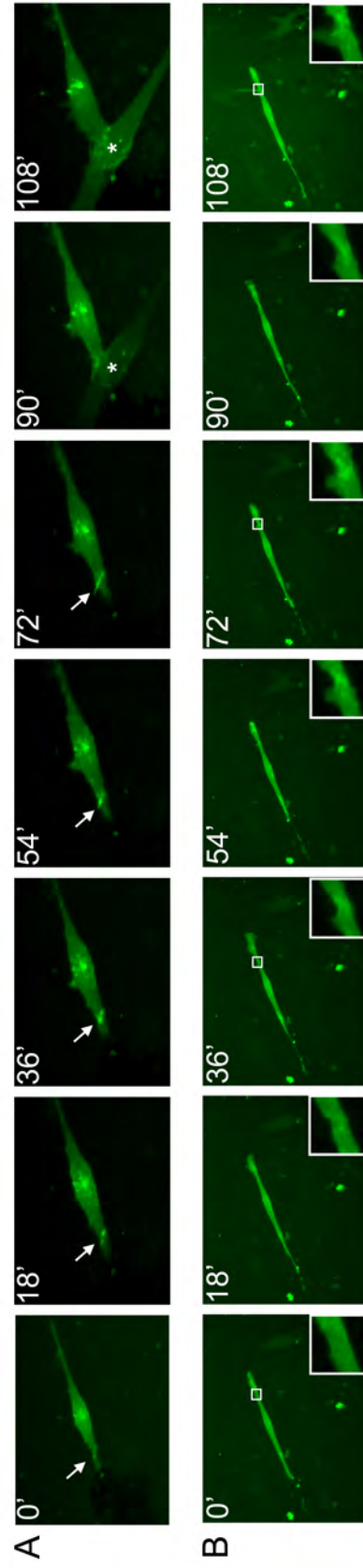


Figure 5.6. Live imaging suggests PIP_2 accumulates asymmetrically during myoblast fusion. (A-B) Live imaging of confluent field of myoblasts where a few express $\text{PLC}\delta^{\text{PH}}::\text{eGFP}$. Plates were cultured in differentiation medium for 24 hours prior to imaging and imaged for 48 hours. Frames were acquired every 18 minutes. (A) Appearance of accumulation that precedes fusion event. (B) Example of fusion event not accompanied by visible accumulation. However, deformation of membrane of fluorescent fusion partner (inset).

In additional fusion events, we failed to detect PLC $\delta^{\text{PH}}::\text{eGFP}$ accumulation prior to the fusion event (Figure 5.6B). A few possibilities, which are not mutually exclusive, could explain this. First, the fusion event may have happened quickly and between frame acquisitions. Unlike in *Drosophila* where the duration of the fusion event has been characterized, this is an unknown in mammals. Secondly, accumulation of PIP₂ may normally only occur in one fusing partner.

Interestingly, we observed a membrane deformation in the labeled myoblast prior to its fusion with an unlabeled myoblast (Figure 5.6B, inset). This is similar to the inward curvature of the founder cell (FC) membrane observed during *Drosophila* myoblast fusion, where the fusion-competent myoblast (FCM) extends an actin-rich, podosome-like structure (PLS) that invades the FC (Sens et al., 2010). As with the previous fusion event (Figure 5.6A), the duration of this event, measured from the appearance of the deformation (18') to fluorophore transfer (108') marking the completion of fusion, is 90 minutes (Figure 5.6B). Thus, mammalian myoblast fusion may be sided, both molecularly with the asymmetric accumulation of PIP₂ and behaviorally with that fusing partner being the FCM-like "aggressor."

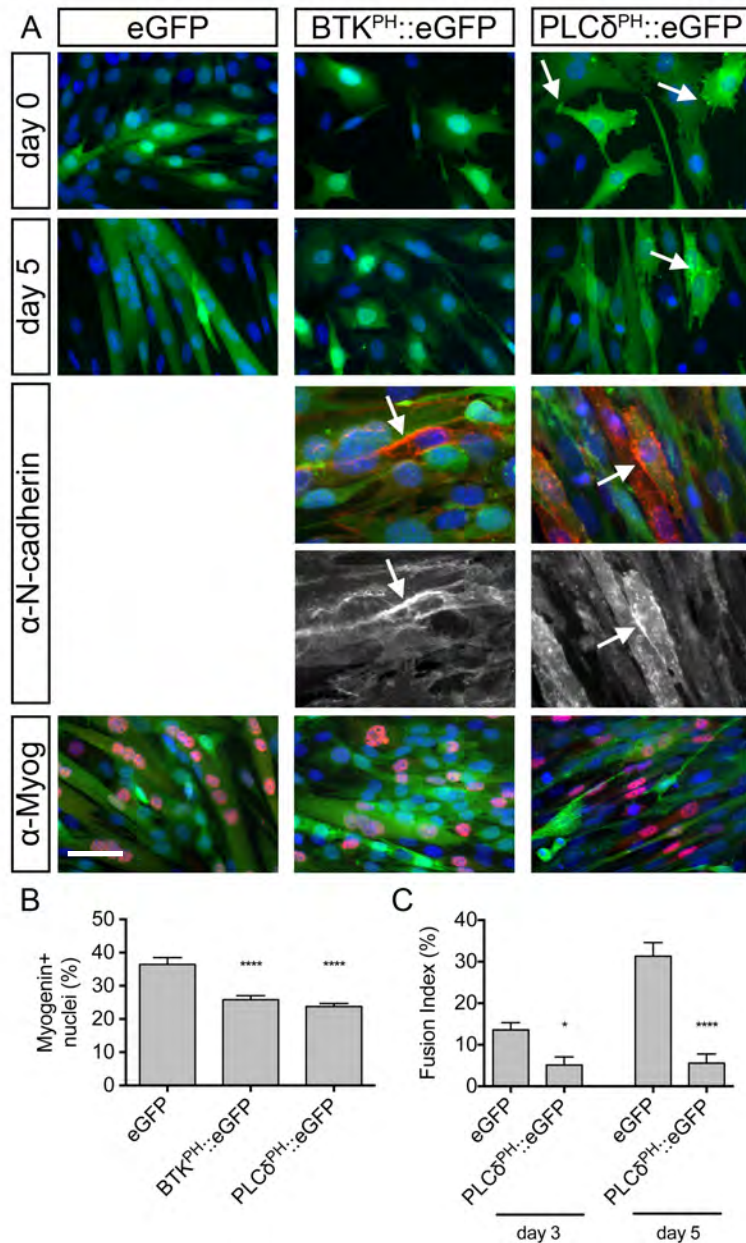


Figure 5.7. Overexpression of PH domain reporters blocks fusion but not differentiation or adhesion. (A) Localization of the indicated reporter (green, all panels) at day 0 and day 5 (top panels). Note the absence of myotubes in BTK^{PH}::eGFP and PLCδ^{PH}::eGFP at day 5. The indicated cell lines were fixed and immunostained with antibodies against N-cadherin (red, middle panels) after one day in DM and Myogenin (red, bottom panels) after three days in DM. DAPI (blue, all panels) was used to label nuclei. (B) Quantification of differentiation index at day 3 and (C) fusion index at day 3 and day 5 in DM. Bar, 50 μm. *p<0.05; ****p<0.0001.

Stable expression of phospholipid markers blocks myoblast fusion but does not affect differentiation or cell-cell adhesion

Though we were intrigued by the suggestion of fusion machinery asymmetry in mammals, we first wanted to characterize the fusion interface visualized with the PLC $\delta^{\text{PH}}::\text{eGFP}$ reporter in greater depth. Thus, we generated lentiviruses expressing PLC $\delta^{\text{PH}}::\text{eGFP}$ or BTK $^{\text{PH}}::\text{eGFP}$. In contrast to the toxicity issues that we encountered with lentiviruses that encoded more direct actin reporters, PLC $\delta^{\text{PH}}::\text{eGFP}$ and BTK $^{\text{PH}}::\text{eGFP}$ lentiviruses infected C2C12 myoblasts with efficiencies greater than 70%. These rates were similar to the infection efficiencies obtained with control cytoplasmic eGFP and mCherry lentivirus, suggesting that toxicity was not an issue with these reporters (Table 5.1).

However, we observed a severe fusion block when we differentiated these myoblasts (Figure 5.7A, C). This block in fusion is reminiscent of the block in fusion seen in *Drosophila* when the PLC $\gamma^{\text{PH}}::\text{eGFP}$ reporter is expressed at high levels, “masking” available PIP₂ moieties and suppressing downstream signaling (Bothe et al., in revision). In contrast to data in *Drosophila*, we also observed a block in fusion when the PIP₃ reporter was overexpressed (Figure 5.7A). The block in fusion was not due to an inability of myoblasts expressing either reporter to differentiate or make contacts with one another, as N-cadherin was present at contact sites (Figure 5.7A) and myogenin expression was detected in myonuclei (Figure 5.7A-B).

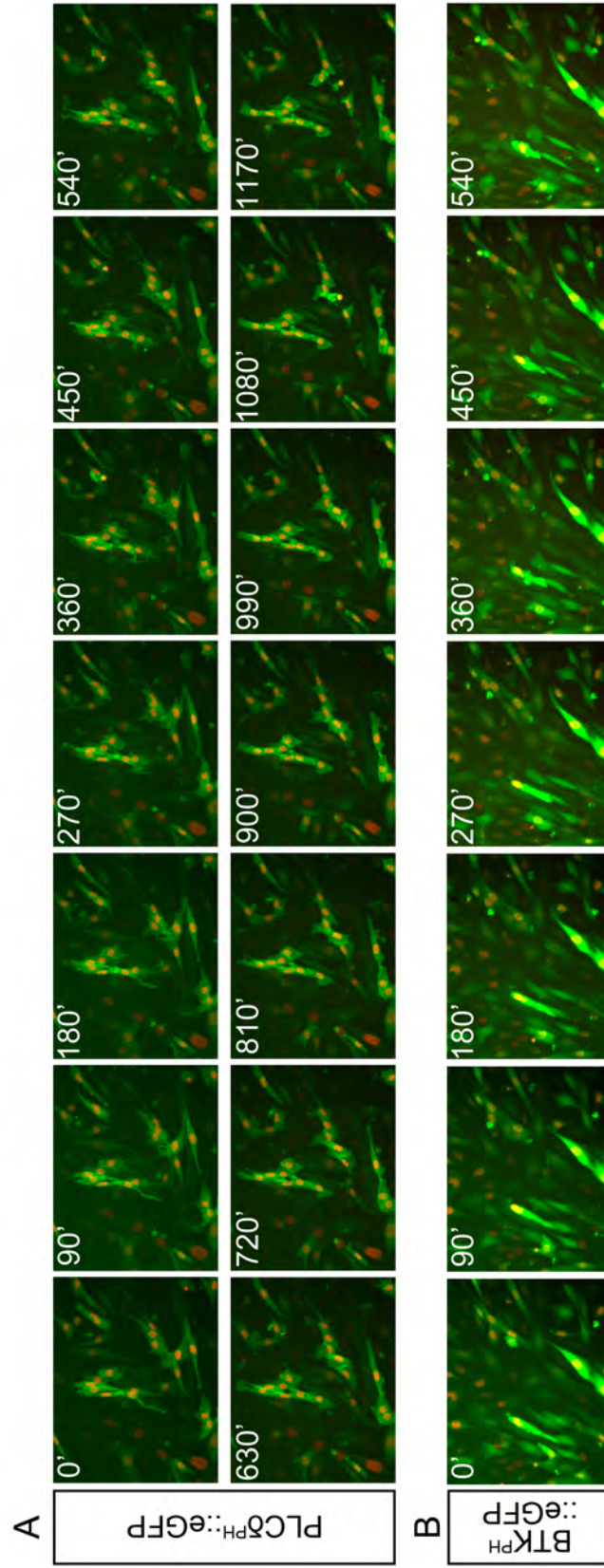


Figure 5.8. Live imaging of myoblasts overexpressing PLC δ^{PH} ::eGFP and BTK PH ::eGFP. (A-B) Confluent myoblasts were shifted to differentiation media for 48 hours before beginning live imaging. Images were acquired every 18 minutes for an additional 48 hours. (A) Myoblasts stably expressing H2B::mCherry and PLC δ^{PH} ::eGFP attach to one another and accumulate PLC δ^{PH} ::eGFP at their attachment sites. Myoblasts fail to fuse, but additional myoblasts continue to attach to other myoblasts forming myoblast aggregates. (B) Myoblasts expressing H2B::mCherry and BTK PH ::eGFP do not show evidence of BTK PH ::eGFP accumulation at sites of contact between myoblasts. Fusion also fails to occur over the imaging time frame.

Together, these data suggest that high, stable expression of the PIP₂ and PIP₃ reporters blocks fusion in mammalian myoblasts, potentially by “masking” phospholipids and disrupting downstream signaling, but does not affect myoblast differentiation or adhesion.

Live imaging of lentivirus lines shows PLCδ^{PH}::eGFP accumulations perdure and myoblasts maintain contact with one another

Though fusion was blocked when we overexpressed either reporter, we hypothesized that live imaging could still provide useful insight to myoblast fusion. In C2C12 myoblasts expressing PLCδ^{PH}::eGFP, we observed accumulation of the reporter at high levels at sites of myoblast-myoblast contact (Figure 5.8A). These accumulations were quite dynamic, and myoblasts continued to migrate and attach to one another over the imaging period, forming large aggregates of myoblasts. The formation of myoblast aggregates provides additional evidence that PLCδ^{PH}::eGFP overexpression does not affect cell-cell contact, and together with data demonstrating that overexpression does not cause a block in differentiation (Figure 5.7A, C), these experiments suggest that PLCδ^{PH}::eGFP-expressing myoblasts are actively trying to fuse. Thus, as in *Drosophila*, “masking” PIP₂ results in myoblast fusion defects, indicating that PIP₂ is required for myoblast fusion. In contrast, we failed to observe the accumulation of BTK^{PH}::eGFP in C2C12 myoblasts during live imaging, suggesting that PIP₃ does not accumulate at the fusion site (Figure 5.8B).

Discussion

Myoblast fusion is essential for myotube formation in *Drosophila* and mammals (Rochlin et al., 2009). In *Drosophila*, the F-actin and PIP₂ foci form at the myoblast fusion site (Kesper et al., 2007; Richardson et al., 2007; Bothe et al., in revision). Formation of these structures requires contact and adhesion between fusing myoblasts, and these foci resolve prior to myoblast fusion. Mutations in known fusion genes such as *kette*, *mbc* and *scar* all lead to F-actin and PIP₂ foci that fail to resolve (Richardson et al., 2007; Bothe et al., in revision).

Many of the known fusion proteins, including Mbc/Dock 1/5 and Kette/Nap1, play a conserved role in mammalian myoblast fusion (Laurin et al., 2008; Nowak et al., 2009; Pajcini et al., 2008). This conservation has been taken to suggest that the dynamic actin-based rearrangements discovered at the fusion site in *Drosophila* are conserved in mammals, but the identification and characterization of the mammalian fusion site has lagged behind. A number of factors have contributed to this, including the need for live imaging to address the outstanding questions surrounding the fusion site. Live imaging of myotube formation is not possible in the intact mouse, and thus, a cell-based approach is often used. Additionally, the identification of a suitable reagent to observe dynamic actin cytoskeleton rearrangements has been difficult.

Previous work in our lab using a GFP::actin reporter was unsuccessful as its expression was toxic (M. Baylies and S. Nowak, personal communication). We hypothesized that labeling actin monomers directly interfered with normal actin-

actin-binding protein interactions, disrupting actin regulation and causing fusion defects. Other analyses have indicated that actin fusions are somewhat functionally impaired and rely on untagged, endogenous actin to buffer the defects. GFP::actin polymerizes inefficiently, and its expression in *Dictyostelium* causes a slight cytokinesis defect (Westphal et al., 1997; Yamada et al., 2005). Additional defects in cell spreading and migration have been reported (Feng et al., 2005). Together, these data suggest that GFP::actin fusions compromise normal actin function.

Thus, we explored the utility of reporters based on actin-binding proteins. Using C1C12 myoblasts, we found that four such reporters did not faithfully recapitulate the F-actin cytoskeleton in fixed myoblasts. We hypothesized that this is likely because full-length proteins and their interactions with actin are precisely regulated to ensure that their interaction occurs within the proper cellular context.

To circumvent the issues associated with full-length actin-binding proteins, we tested two reporters that consisted of short, actin-binding domains. Lifeact, a 17-amino acid peptide, and UtrCH, the calponin homology domain of utrophin, accurately labeled the F-actin cytoskeleton in fixed imaging of C2C12 cells (Burkel et al., 2007; Riedl et al., 2008). However, we found that high expression of either reporter blocked C2C12 myoblast fusion, suggesting that their interaction with actin somehow impaired normal actin function.

Together, these data suggest that the traditional methods for labeling actin are not amenable to all studies of the actin cytoskeleton in developing myoblasts

and myotubes, especially the actin rearrangements that are critical for successful myoblast fusion. Though the reasons for this are unclear, a recent comparison of the effects of expression of eYFP::actin and eGFP::Lifeact on acto-myosin rearrangements in rat fibroblasts found significant differences in the morphology and kinetics of stress fiber reorganization between the labeling methods, with eGFP::Lifeact showing better agreement with data obtained from non-transfected fibroblasts (Deibler et al., 2011). Despite the fact that eGFP::Lifeact data appeared “silent” in this analysis, we still observed myoblast fusion defects when Lifeact::eGFP was stably expressed in C2C12 myoblasts. It is possible that Lifeact affects other aspects of actin cytoskeletal morphology and/or dynamics that were not tested. In fact, recent data from other systems report defects associated with Lifeact expression, indicating that Lifeact is also not appropriate for all analyses (Munsie et al., 2009; van der Honing et al., 2011). Another possibility is that the reporters used in this study were expressed at too high a level to allow actin to carry out its normal cellular functions. Thus, expressing lower levels of these constructs may decrease the fusion defects we observe, but this remains to be formally examined.

We used an indirect actin reporter, PLC δ^{PH} ::eGFP, which binds specifically to PIP₂ and has been previously used in C2C12 myoblasts (Bach et al., 2010; Nowak et al., 2009; Raucher et al., 2000). Earlier studies observed PLC δ^{PH} ::eGFP accumulations, which seemed to localize to contact points between myoblasts and disappear prior to myoblast fusion (Bach et al., 2010; Nowak et al., 2009). PLC δ^{PH} ::eGFP accumulations also colocalized with Dock1,

which is speculated to be localized to the mammalian fusion site similarly to its *Drosophila* homolog (Nowak et al., 2009; Richardson et al., 2007). Further, this reporter accumulated and perdured in Nap1 (the mammalian homolog of *Drosophila* Kette) knockdown myoblasts far longer than in control myoblasts, a phenotype that is reminiscent of the behavior of the F-actin and PIP₂ foci in *kette* mutant embryos (Nowak et al., 2009; Richardson et al., 2007; Bothe et al., in revision).

In our analysis, we also identified accumulations of PLC $\delta^{\text{PH}}::\text{eGFP}$ that dissolved prior to the fusion of control C2C12 myoblasts. Additionally, our results suggest that PIP₂ may be asymmetrically required at the fusion site. We find that PLC $\delta^{\text{PH}}::\text{eGFP}$ accumulation at the presumptive fusion site is associated with only some fusion events. In fusion events where PLC $\delta^{\text{PH}}::\text{eGFP}$ accumulation is absent, we see evidence for membrane deformations similar to the “dimple” observed in FCs during FCM invasion (Sens et al., 2010). Though the F-actin focus is asymmetric, analysis of the PIP₂ focus in *Drosophila* has indicated that it forms in both FCs and FCMs (Bothe et al., in revision). These differences may reflect organism-specific requirements for PIP₂ accumulation during myoblast fusion or technical limitations of our analysis.

In *Drosophila*, the current model suggests that the sequestration of PIP₂ by PLC $\delta^{\text{PH}}::\text{eGFP}$ prevents the binding of other PH domain-containing proteins, including the fusion proteins Mbc, Blow and SCAR, resulting in their failure to localize to the fusion site. Thus, downstream signaling is compromised, and fusion is blocked (Bothe et al., in revision). By expressing PLC $\delta^{\text{PH}}::\text{eGFP}$ at a

high level in C2C12 myoblasts, we were able to completely block myoblast fusion. We found that PLC $\delta^{\text{PH}}::\text{eGFP}$ accumulated at a high level at sites of myoblast-myoblast contact. These accumulations failed to resolve, and myoblasts subsequently failed to fuse. This phenotype mimicked the “sequestration” phenotype described in *Drosophila* (Bothe et al., in revision). Similarly, chemical agents that masked or reduced PIP₂ had similar effects on myoblast fusion in C2C12 myoblasts (Bach et al., 2010). Together, these data indicate that PIP₂ is required at the fusion site in mammals and that PIP₂ plays a conserved role in myoblast fusion. Data in *Drosophila* hint that the fusion machinery would be mislocalized under sequestration conditions in C2C12 myoblasts, but this has not been explored in any mammalian system to date.

PIP₂ is generated by the phosphorylation of phosphatidylinositol 4-phosphate (PI4P) by phosphatidylinositol 4-phosphate 5-kinases (PIP5K). The *Drosophila* PIP5K, Skittles, which is localized to the fusion site, is required for myoblast fusion (Bothe et al., in revision). Similarly, depletion of PIP5K in C2C12 myoblasts caused a block in fusion (Bach et al., 2010). In mammalian cell lines, an isoform of PIP5K, PIP5K γ , colocalizes with N-cadherin at sites of cell-cell contact, suggesting that PIP5K may be similarly recruited to N-cadherin accumulations found at sites of myoblast-myoblast contact (Sayegh et al., 2007). Together, these data suggest that at least some PIP₂ at the fusion site is generated from the phosphorylation of phosphatidylinositol 4-phosphate by PIP5Ks.

PIP₂ is also generated by the dephosphorylation of PIP₃. In *Drosophila*,

PIP₃ does not appear to accumulate at the fusion site during myoblast fusion (Bothe et al., in revision). Expression of a PIP₃ reporter under the same conditions that caused the PIP₂ “sequestering” phenotype in *Drosophila* also failed to cause a fusion phenotype. Further, zygotic mutants of the PIP₃ phosphatase, PTEN (Phosphatase and tensin homolog), do not show effects on fusion (M. Baylies and I. Bothe, personal communication). Together, these data suggest that PIP₃ is not required at the fusion site and may not be a precursor for PIP₂ in the context of myoblast fusion.

We also examined the role of PIP₃ during mammalian myoblast fusion. Similarly, we failed to observe PIP₃ accumulation at the site of fusion in transiently transfected myoblasts or at sites of myoblast-myoblast contact in PIP₃ reporter overexpression myoblasts. In contrast to data in *Drosophila*, however, we strongly inhibited myoblast fusion when the PIP₃ reporter was overexpressed, without affecting cellular behaviors that precede fusion, suggesting that PIP₃ may have a mammalian-specific role during myoblast fusion. The use of different PIP₃ reporters in *Drosophila* and mammals may explain the disparate phenotypes, but this has not been addressed directly. The role of PTEN in mammalian myoblast fusion has not been explored, leaving open the possibility that it too is required for myoblast fusion and that mammals may use multiple pathways to synthesize PIP₂ at the fusion site.

Finally, analysis of fusion in immortalized mouse H2k^b-tsA58 myoblasts plated on patterned arrays indicated that fusion occurs primarily end-to-end (Clark et al., 1997; 2002; Morgan et al., 1994). Though angular attachments

between myoblasts formed, these rarely culminated in a fusion event, suggesting that lateral fusion events were somehow inhibited to ensure that myotubes remained linear. In contrast, an analysis of fusion in C2C12 myoblasts on a non-patterned substrate did not detect an orientation preference for fusing partners (Nowak et al., 2009). Similarly, we did not find evidence in our analysis of a larger number of fusion events for a bias towards end-to-end fusion. In fact, we observed more perpendicular and lateral (side-by-side) fusion events than end-to-end events. These discrepancies may reflect differences between model systems or be the result of different approaches used to analyze fusion and will need to be addressed.

In summary, we have developed a system for stably labeling C2C12 myoblasts with high efficiency to increase the number of visible fusion events. Using this system, we have probed the composition of the mammalian fusion site, identifying a conserved PIP2 accumulation that precedes myoblast fusion in C2C12 myoblasts. Though our analysis was confined to the overexpression of reporter constructs, it can be modified to introduce lentiviral shRNA particles to study the role of endogenous proteins to many aspects of muscle formation *in vitro*.

CHAPTER SIX: CONCLUSIONS

Cell-cell fusion is an essential phenomenon, first identified over a hundred years ago, that occurs in diverse biological contexts, from fertilization to the formation of different cell types such as osteoclasts, giant cells, syncytiotrophoblasts and muscle (Chen, 2010). Despite its importance to the conception, development and maintenance of multicellular organisms, our understanding of the mechanisms that underlie fusion are incomplete.

We use myoblast fusion as a system to understand cell-cell fusion. Muscles in organisms from *Drosophila* to humans are multinucleated and form from the fusion of myoblasts, and many aspects and proteins in the process are shared between *Drosophila* and mammals. Both organisms specify mononucleated myoblasts from mesodermal precursors, which then undergo a conserved set of cellular behaviors required for their fusion (Chen, 2010; Rochlin et al., 2009). In addition, a fully functioning musculature is not achieved in either system until each muscle fiber constructs the contractile apparatus, makes stable contact with tendons and is innervated by the nervous system. Thus, the events that follow the generation of a multinucleated myofiber are conserved from fly to mammals, making the fly a good system for studying additional aspects of muscle development and function. We have taken advantage of the high degree of conservation in the processes and molecular players from *Drosophila* and mammals, and we have utilized both systems to address outstanding questions in the myogenesis field.

Drosophila* as a model organism for studying myogenesis *in vivo

During its development from an embryo to an adult, a process that requires only 10-12 days, *Drosophila* undergoes two periods of myogenesis, both of which utilize a conserved set of proteins and processes. Larval muscles, specific for crawling, are formed in the embryo, while the adult musculature, specific for walking, jumping and flying, is formed during metamorphosis. Importantly, the stages of *Drosophila* in which muscle is forming, namely the embryo and pupae, are amenable to live-imaging analysis, which is routinely employed.

Each microcosm of myogenesis within *Drosophila* has both its own unique benefits and drawbacks. Maternal loading in the embryo is a double-edged sword: it has likely masked roles for proteins in embryonic muscle development; however, it has also allowed for the analysis of genes that are essential for early development during later steps of myogenesis. In the adult, the proper function of the adult IFMs is not required for viability. Thus, genes essential to this process can be examined in the intact adult fly. However, some of these genes overlap with those that are required in the embryo for muscle development, making their analysis in adult muscle development less straightforward.

Genetics are often much simpler in *Drosophila* when compared to vertebrate systems. In addition to the ease of genetic manipulation in flies, there is usually only one vertebrate homolog/protein family member, circumventing issues with protein redundancy and the need to generate multiple mutant animals. Further, the genetic tools available beyond traditional alleles are more

developed in *Drosophila*. The GAL4-UAS system allows for temporal and tissue-specific expression of UAS-regulated transgenes and genome-wide RNAi libraries. Of particular relevance to the study of *Drosophila* myogenesis is the existence of mesoderm-, pan muscle- and even individual/single muscle-specific GAL4 driver lines (eg., *twist-Gal4*, *Dmef2-Gal4* and *5053-Gal4*, respectively), which allow us to describe examine muscle-autonomous gene function. As an example of this, *Dmef2-Gal4* has recently been used to express a genome-wide RNAi library to identify regulators of muscle morphogenesis in L3 larvae and adults, bypassing the requirement for these genes in other cell types (Schnorrer et al., 2010). Thus, *Drosophila* is a rapidly developing, genetically and optically tractable model for the study of muscle development. Further, the ability to examine different developmental stages and combine cell biology, developmental biology and behavioral assays is a strength of the fly.

This study has exploited the benefits of *Drosophila* as a model system to characterize Tsr and Coro function in different stages of *Drosophila* muscle morphogenesis. Briefly, our analysis of whole-animal mutants together with RNAi reduction has led to the identification of multiple novel roles for these proteins during muscle development.

The role of actin depolymerization during muscle development in *Drosophila*

This analysis is the first to show a role for the ADF/cofilin protein family in early steps of muscle development, including myoblast fusion. In *Drosophila*, myoblast fusion occurs between two myoblast cell types, founder cells (FCs) and fusion competent myoblasts (FCMs) (Rochlin et al., 2009). Four transmembrane proteins, including the FC-specific protein, Duf, function in the attraction, migration, recognition and adhesion of myoblasts (Figure 1.7) (Ruiz-Gomez et al., 2000; Strükelberg et al., 2001). Myoblast recognition and subsequent adhesion results in the organization of Duf and Sns, an FCM-specific transmembrane protein, into the FuRMAS, a signaling center that recruits the fusion machinery to the fusion site (See Introduction) (Haralalka et al., 2011; Kesper et al., 2007; Sens et al., 2010). Subsequently, the actin focus, which is surrounded by the FuRMAS, forms (Kesper et al., 2007; Sens et al., 2010). The formation and the dissolution of the actin focus directly precedes membrane breakdown and cytoplasmic continuity and depends on the Arp2/3 complex and its regulation, which nucleates branched actin polymerization (Figure 1.8) (Berger et al., 2008; Massarwa et al., 2007; Richardson et al., 2007).

We found that fusion was unaffected in *tsr* null embryos, suggesting that Tsr was not required for myoblast fusion. However, we hypothesized that maternal loading of *tsr* was masking earlier functions of *tsr*. One approach we used to further reduce *tsr* activity was to generate *tsr; ssh* double mutants. Ssh activates ADF/cofilin family proteins by removing the repressive phosphorylation at Ser3 (Bamburg, 1999). No Tsr-independent function for Ssh has been described. Thus, we reasoned that removing Ssh activity in *tsr* compromised

embryos would depress residual Tsr activity. In *tsr; ssh* double mutants, we found that myoblasts failed to fuse, and this block in fusion was associated with the absence of F-actin foci formation, despite the proper localization of Duf to sites of FC-FCM contact indicating that myoblasts are able to adhere to one another. Together, these data suggested that Tsr is required to form the focus.

How Tsr may regulate focus formation and how this is linked to the existing machinery is not clear. We observed an increased level of cortical actin in unfused *tsr; ssh* double mutant myoblasts, suggesting that one way Tsr may function at this step is to turn over cortical actin that can subsequently be used to construct the F-actin focus. More precise measurements in cortical actin and how its localization changes over time in *tsr;ssh* double mutants, as well as in mutants that are capable of building foci, will be required to examine this hypothesis. Additionally, live imaging analysis of the actin dynamics during myoblast fusion will be essential to understanding the function of Tsr here, as will the use of high resolution microscopy and photoconvertible actin probes to directly track actin localization during myoblast fusion. Further, we have not examined the localization of Tsr during muscle development *in vivo*. The available GFP::Tsr protein trap presented a number of limitations for this analysis as it was expressed ubiquitously, and at high levels, making live imaging of the mesoderm difficult; however, we have recently generated a fluorescently-tagged Tsr under *UAS* control, which will greatly simplify this analysis.

Previously, the only class of mutants known to fail to generate foci are mutants in the transmembrane proteins that mediate FC-FCM adhesion and in

an adaptor protein required to recycle Duf back to the membrane for subsequent fusion events (Richardson et al., 2007). Though the focus phenotype of *tsr; ssh* double mutants would classify Tsr with these proteins, the underlying defect that results in the failure of focus formation is not the same and suggests that additional steps after FC/myotube-FCM adhesion are required for focus formation. An important next step will be in examining the localization of the fusion machinery in *tsr; ssh* double mutants, particularly that of the actin regulators Mbc and D-WIP, which are normally recruited to the fusion site after successful FC/myotube-FCM contact, to determine if Tsr function is required for their recruitment (Haralalka et al., 2011; Kim et al., 2007; Massarwa et al., 2007; Richardson et al., 2007).

I was not the first to hypothesize that Tsr was required for myoblast fusion. Dr. Brian Richardson, a former student in the lab, postulated that Tsr may be required to remove polymerized actin from the site of fusion. He expressed *tsr* in a *kette* mutant, which has enlarged foci. Surprisingly, he found that the muscle pattern in these embryos was indistinguishable from that of *kette* mutants, and he concluded that that Tsr may not be capable of depolymerizing a large focus alone. However, in light of recent data, particularly the identification of a PIP₂ accumulation coincident with the actin focus (Bothe et al., in revision), this interpretation may not be the full picture.

ADF/cofilin family proteins are inhibited by a number of mechanisms, including phosphorylation by LIMK and TESK family kinases and by binding to PIP₂ (Bamburg, 1999). LIMK family members, in turn, are activated by Rho family

GTPases, including Rac. During normal myoblast fusion, active Rac and PIP₂ accumulate at the fusion site, and these accumulations, like the actin focus, perdure in *kette* mutants (Haralalka et al., 2011; Richardson et al., 2007; Bothe et al., in revision). These data would suggest that Tsr activity is suppressed at this site during foci formation and would remain suppressed in mutants, such as *kette*, for the duration of actin and PIP₂ foci perdurance. Inhibition of ADF/cofilin by PIP₂-binding is relieved by PIP₂ hydrolysis (Bamburg, 1999), which would then allow Tsr to resolve the actin foci. No such molecule has been described as having a role in myoblast fusion to date, but we know that PIP₂ foci must be removed from fusion sites before fusion is completed. However, this interpretation does not explain why, if Tsr is also required to resolve actin foci, overexpression of Tsr cannot overcome this inhibition. It is possible that Tsr availability is not the rate-limiting step here and that sufficient LIMK1 activity is present to inactivate even excess levels of Tsr. Thus, the signals which resolve the actin focus are still unclear, and a role for Tsr in this process cannot be ruled out. Alternatively, Tsr may play no role in focus dissolution and other proteins that promote actin depolymerization, for example the gelsolin family, may fulfill this role instead. We are actively examining the role of Gel in muscle development.

It is unclear if mammalian cofilin plays a conserved role in these early processes in mammals. Knockouts of both the ubiquitous cofilin, Cfl1, and the muscle-specific cofilin, Cfl2, have been generated in mouse, but defects in early steps in myogenesis have not been reported (Agrawal et al., 2012; Gurniak et al., 2005). *Cfl1*-null embryos developmentally arrest at E11, during early embryonic

muscle development, and the muscle was not analyzed for defects (Buckingham and Relaix, 2007; Gurniak et al., 2005). Myofibers in *Cfl2*-null mice were developmentally normal at birth, suggesting that Cfl2 is not required for muscle development in the mouse (Agrawal et al., 2012). *Cfl1* is highly expressed during early mouse development, and its expression can be detected in the myotome at E10.5 and is expressed throughout development (Gurniak et al., 2005; Vartiainen et al., 2002). *Cfl2* can also be detected in the E10.5 myotome and by E13 in the limb bud (Agrawal et al., 2007; Mohri et al., 2000). Thus, their expression overlaps in the muscle during the development of the embryonic myotubes (Buckingham and Relaix, 2007). One possibility is that Cfl1 can compensate for Cfl2 in muscle development in *Cfl2*-null mice. Alternatively, Cfl1 may be responsible for the formation of mouse skeletal muscle, and Cfl2 for the maintenance of sarcomere organization, and their functions may be non-overlapping. Whatever their relationship, our analysis has highlighted additional, earlier roles for Tsr in muscle development in *Drosophila* and would suggest that one or both mammalian cofilin proteins performs this role as well.

Though muscles appear normal at birth in *Cfl2*-null mice, they progressively deteriorate (Agrawal et al., 2012). Cfl1 is still expressed in muscle at this time, but it is not able to compensate for loss of *Cfl2*, suggesting that Cfl1 and Cfl2 have non-redundant functions in this process. We found that reducing *tsr* in *Drosophila* somatic muscle resulted in a similar phenotype as *Cfl2*-null mice, indicating that Tsr plays a conserved role later in development. Additionally,

these data suggest that Tsr fulfills both muscle roles of Cfl1 and Cfl2, consistent with it being the sole ADF/cofilin family member in *Drosophila*.

Though ADF/cofilin proteins likely play a role in regulating filament length as loss of ADF/cofilin function in *C. elegans*, mouse and *Drosophila* results in overpolymerized actin, it is not clear how they function here (Agrawal et al., 2012; Ono et al., 1999; this study). Thin filament length must be properly regulated to ensure that the thin-thick filament overlap generates optimal muscle contraction. A large number of sarcomere proteins are dedicated to stabilizing actin length, including capping proteins and other actin-stabilizing proteins, underscoring its importance to muscle function (Clark et al., 2002; Littlefield and Fowler, 1998). Thus, one would expect thin filaments to be relatively static; however, injected fluorescently-labeled G-actin readily incorporates into existing thin filaments, suggesting that thin filaments are dynamic and not capped at all times. Additionally, a “ruler” must be present to monitor the barbed and pointed ends of actin and adjust thin filament length accordingly. Further, though thin filaments do turnover, they do so at a relatively slow rate (Littlefield and Fowler, 1998), which may explain why we and others do not observe defects in sarcomere organization in the absence of cofilin until later in development.

In vertebrates, nebulin, a protein that extends from the Z-disc to the pointed end of the thin filament, has been thought to perform the function of a thin filament ruler (Clark et al., 2002). However, a more recent analysis has indicated that nebulin does not extend fully to the Tmod cap at the pointed end, and therefore cannot be responsible for measuring precise thin filament length,

but may instead specify the minimum thin filament length (Castillo et al., 2009). The giant cytoskeletal protein Titin has also been suggested to act as a thin filament ruler. Though a *Drosophila* homolog of nebulin has not been identified, *Drosophila* does encode a homolog of Titin (D-Titin). D-Titin plays an essential role in organizing the sarcomere (Machado and Andrew, 2000; Zhang et al., 2000). It is not likely that Tsr is directly sensing and responding to thin filament length: in contrast to nebulin and Titin homologs, which are giant cytoskeletal proteins and extend the length of the thin filament (Clark et al., 2002), ADF/cofilins are small proteins and as such, lack the ability to coordinate over long distances. Hence, it is unlikely that Tsr is sensing both ends of the thin filament at once. Thus, it is more appropriate to think of Tsr as the “scissors” that trim thin filaments deemed too long. However, the mechanism that coordinates the thin filament ruler and scissors is unknown.

We and others have shown that ADF/cofilin homologs are localized to the Z-disc (Papalouka et al., 2009; this study). Z-discs are the anchor site for the plus (barbed) end of the thin filament (Clark et al., 2002), but in contrast to actin polymerization in other contexts, actin polymerization in muscle predominantly occurs from the minus (pointed) end (Fischer and Fowler, 2003; Pollard et al., 2000). In other contexts, ADF/cofilin proteins regulate thin filament length from the pointed end (Bamburg, 1999). It has not been addressed whether ADF/cofilin proteins can also regulate thin filament length from the barbed end in muscle; and therefore it is unclear what the function of Tsr is here. One possibility is that Tsr is not able to depolymerize actin filaments from the barbed end (anchored at

Z-discs) and that Tsr is localized to the Z-disc to prevent it from associating with the pointed end and altering thin filament length inappropriately. However, in contrast to analysis in human skeletal muscle (Papalouka et al., 2009), we also observed Tsr localization to the H-zone, the region of non-overlap between the thick and thin filaments (Clark et al., 2002). Thus, Tsr has access to thin filament pointed ends, at least in *Drosophila*.

***Drosophila* as a model system for Nemaline myopathy**

The conservation of the late role of Tsr and Cfl2 in the maintenance of sarcomere organization coupled with the identification of two *Cfl2* mutations in patients with Nemaline myopathy (NM), motivated us to attempt to model Nemaline myopathy in *Drosophila*. In addition, the phenotypes in *tsr* depleted larvae were similar to the defects observed in patients, including the presence of nemaline rod-like accumulations, severe sarcomere organization defects and muscle weakness, suggesting that *Drosophila* would be amenable to modeling this myopathy.

Two zebrafish models of NM exist, but neither models specific mutations associated with NM, relying instead on knockdown, which may not be an accurate reflection of the activity of the disease allele (Ravenscroft et al., 2013; Telfer et al., 2012). One NM-associated mutation in *Cfl2* occurs at a conserved nucleotide (Bamburg et al., 1999; Ockeloen et al., 2012); thus, we introduced the corresponding mutation into *tsr* and examined its ability to rescue *tsr* depletion.

We found that this allele, *tsr^{G19A}*, was not able to rescue the phenotypes associated with *tsr* depletion, including defects in sarcomere organization, muscle weakness and difficulties in feeding. We did not identify any difference between the *tsr* depletion phenotype and that of *tsr^{G19A}*, suggesting that *tsr^{G19A}* (and the human disease protein) may be a functional null. However, we are able to rule out some functions: *tsr^{G19A}* is properly localized to sarcomere Z-discs and can translocate to the nucleus, indicating that the defect does not appear to be the result of mutated Tsr mislocalization.

It has been suggested that the G19A mutation, which results in a Val7Met amino acid substitution, may result in an alternatively translated protein (Ockeloen et al., 2012). Those six amino acids play essential roles in G- and F-actin binding and include the phosphoregulatory Ser3 (Bamburg et al., 1999). Thus, *tsr^{G19A}* may act similarly to the dominant negative Tsr, which also does not rescue *tsr* depletion, and this hypothesis can be tested by determining if *tsr^{G19A}* is capable of binding actin.

Our analysis suggests that *Drosophila* can be a powerful system in which to model human muscle disorders. Here, we describe a system for studying a particular disease, Nemaline myopathy. Our model for NM focuses on a conserved *Cfl2* mutation identified in patients with NM. Other genes that have been found to be mutated in patients with NM are also conserved in *Drosophila*, and these should be used to model and compare NM phenotypes generated by different disease-associated alleles. Further, *Drosophila* has been used with great success to identify therapeutics to treat certain types of cancer (Vidal et al.,

2005). Work in our own lab is similarly trying to identify compounds that treat rhabdomyosarcoma, and a similar approach can be taken to identify existing therapeutics and/or novel compounds that improve the defects we observe in our model of NM.

Coronin is required for muscle development and function

Coronin proteins coordinate the activities of Arp2/3 and ADF/cofilin in many developmental contexts (Chan et al., 2011). This analysis is the first to demonstrate a role for Coro in muscle development. We found that Coro was required for a number of steps during embryonic muscle development, including a role in establishing the full complement of muscles and proper muscle attachment. These phenotypes are similar to those observed in *tsr* mutants (this study), and Coro is a known regulator of ADF/cofilin proteins (Chan et al., 2011), suggesting that Coro and Tsr genetically interact in *Drosophila* muscle, though this has not been addressed experimentally. We have shown that Tsr genetically interacts with its other regulators, suggesting that the Tsr regulatory pathway is conserved during muscle formation.

A significant limitation of our study was the finding that putative *coro* alleles complemented deficiencies that removed *coro*, suggesting the presence of additional mutations which caused the *coro* phenotype. We were unable to resolve this over the course of this analysis, but we are actively trying to

characterize the nature of these alleles. The alternative/remaining available *coro* alleles are viable and fertile (and likely do not affect Coro function); thus, the need to develop additional alleles that can be validated molecularly and genetically is essential to the analysis of Coro function in *Drosophila*.

Still outstanding is whether Coronin has Arp2/3 and/or ADF/cofilin-independent functions in regulating actin dynamics and whether Coro activity is present/required to balance actin polymerization in all contexts. For example, Arp2/3 and Tsr are both required for myoblast fusion, but we did not find evidence for Coro being required for myoblast fusion in *Drosophila* (Rochlin et al., 2009; this study). As was the case for Tsr, maternal loading is likely masking a role for Coro in this process, but additional experiments will be required to clarify this. Further, using muscle-specific RNAi against *coro*, we and others have identified a role for Coro in sarcomere organization and larval and adult muscle function (Schnorrer et al., 2010; this study). We have shown that Tsr is involved in sarcomere maintenance in the larvae, but no role has been described for Arp2/3 in sarcomeres, where actin is predominantly linear (Clark et al., 2002). Arp2/3 does not associate with sarcomeres, though it is expressed at low levels in striated muscle (Takano et al., 2010). Arp2/3 may have a yet uncharacterized role in mature muscle. Alternatively, Coro may not exclusively function to balance the activities of actin branching and actin depolymerization and may have its own, independent functions.

Further, we observed only a modest defect in larval crawling in *coro* RNAi larvae, but analysis of larval muscle organization did not reveal any obvious

sarcomere aberrations. Data from budding yeast indicates that Crn1p (coronin) is less critical to actin dynamics than Cfl1p (cofilin) (Goode et al., 1999; Heil-Chapdelaine et al., 1998). Our data also support a more minor, but important role for Coro in muscle development. One possibility is that Coro may be required to fine-tune actin dynamics, causing subtle defects in sarcomere organization that were not apparent at our level of analysis. To examine this, we can perform high resolution microscopy paired with measurements of sarcomere length to determine if thin filament length is changed in *coro* depleted muscles. Thin filament length must be tightly regulated in order to generate the optimal muscle contraction (Clark et al., 2002). Thus, even small changes in thin filament length can affect muscle function.

Mouse as a model organism for studying myogenesis *in vivo* and *in vitro*

Amongst the model organisms, mice retain a striking similarity to human anatomy and physiology. For example, muscle in mice is composed of bundles of bundles of myofibrils, whereas embryonic muscle in *Drosophila* consists of a single fiber. Further, greater than 95% of the mouse genome is similar to our own, making the mouse currently the model of choice for the study of human disease. Consistent with this, though *Drosophila* models of muscular dystrophies are beginning to be generated and studied, the mouse remains the best model for these analyses.

The mouse is also an excellent model for the study of muscle regeneration and repair, processes which have not been documented in *Drosophila*. Many studies have indicated that the genes required for these processes overlap with those that are involved muscle development, though some differences exist.

There are, however, drawbacks to using the mouse for studying myoblast fusion. For example, many essential fusion genes are also required for earlier processes (i.e., Rac), and their mutation causes lethality prior to the onset of myogenesis, precluding the study of their function during muscle development using traditional approaches (Sugihara et al., 1998). Efforts have been taken to generate gene knockouts in every gene in mouse, but the non-traditional genetic approaches are less developed in mouse compared to *Drosophila*. Mouse geneticists routinely use the Cre-lox and FLP-FRT recombination systems to regulate gene expression in a tissue- and temporal-specific manner similar to the UAS-GAL4 system, and this system was used to bypass the requirement of Rac early in mouse development and describe its role during mammalian myoblast fusion (Vasyutina and Birchmeier, 2006). Additionally, RNAi tools in the *in vivo* setting are less developed. Lastly, the complexity of the mouse muscle architecture and the technical limitations of current microscopy methods preclude live imaging of fusion *in vivo*.

Thus, studies of mammalian myoblast fusion have largely been conducted using *in vitro* systems. Though primary *Drosophila* myoblasts can be isolated and differentiated *in vitro*, this process is more labor intensive than obtaining similar cultures from mouse. Large numbers of muscle satellite cells can be easily

obtained by injuring a muscle a few days prior to satellite cell isolation/culture, and myoblast cell lines already exist and are in wide use (Yaffe and Saxel, 1977). Importantly, satellite cells can fuse with muscle when injected into mouse making them useful for *in vivo* studies of fusion, repair and regeneration and the introduction of recombinant proteins (Barr and Leiden, 1991; Cheng et al., 2005; Dhawan et al., 1991; Pajcini et al., 2008; Yao and Kurachi, 1992).

The conservation of the actin regulators Dock1 and IQSec1 to myoblast fusion in mammals

Actin and its proper regulation is essential to both myoblast fusion model systems, and a number of actin regulators play a conserved role in *Drosophila* and mammals (Rochlin et al., 2009). We and others have demonstrated the conservation of the actin regulators Dock1 and IQSec1 to mammalian myoblast fusion (Laurin et al., 2008; Pajcini et al., 2008). In *Drosophila*, *Mbc*, the Dock1 homolog, is required at the fusion site, and mutation in *mbc* results in a strong fusion block concomitant with the perdurance of the actin and PIP₂ foci (Haralalka et al., 2011; Richardson et al., 2007; Bothe et al., in revision). The role of *Loner*, the IQSec1 homolog, is less clear, but it does not appear to be required for actin regulation at the site of fusion (Richardson et al., 2007). As in *mbc* mutants, the actin and PIP₂ foci form and fail to resolve in *mbc* and *loner* mutants (Richardson et al., 2007; Bothe et al., in revision).

The effect of Dock1 and IQSec1 depletion on the site of fusion has not been characterized in mammals. One reason for this is the lack of a defined mammalian fusion site. However, work reported here as well as the work of others has indicated that PIP₂ accumulates and disappears prior to the fusion of mammalian myoblasts, and thus, as in *Drosophila*, can be used to mark the fusion site. Thus, it will be interesting to explore whether PLCδ^{PH}::eGFP accumulations also perdure in Dock1 and IQSec1 knockdown myoblasts to determine whether this function is also conserved in mammals.

Dock1 is most well-characterized as a component of focal adhesions where it is localized by its interaction with the small adaptor protein Crk (Côté and Vuori, 2007; Meller, 2005). Data in *Drosophila* suggests that Crk is likely required for fusion though no loss of function mutants exist (Abmayr et al., 2003). Further, Elmo (which acts as a novel bipartite GEF together with Dock1) and Rac are also required for fusion in *Drosophila* (Geisbrecht et al., 2008; Hakeda-Suzuki et al., 2002; Luo et al., 1994; Meller, 2005). Rac is also required for myoblast fusion in the mouse (Vasyutina et al., 2009). Similarly, IQSec1 is suggested to regulate the localization of focal adhesion proteins, including β1 integrin and paxillin (Dunphy et al., 2006; Pajcini et al., 2008). β1 integrin regulates myoblast fusion in the mouse (Schwander et al., 2003). Though the roles of many of these proteins have only been demonstrated in only one system, an emerging theme is that focal adhesion proteins also play a role in myoblast fusion, which is likely conserved from *Drosophila* to mammals.

In addition, focal adhesion components, including B1 integrin, Talin and

ILK, have been shown to play a role in *Drosophila* myotendinous junction formation and stability as well as in sarcomere and costamere organization (Brown, 1994; Brown et al., 2002; Leptin et al., 1989; Newman and Wright, 1981; Volk et al., 1990) (Bökel and Brown, 2002; Brown, 2000; Zervas et al., 2001). This overlap in function is not surprising given that focal adhesions, like the fusion site, MTJs and costameres, are composed of large protein complexes that act as signaling centers and transmit force.

Thus, it is conceivable that Dock1 and/or IQSec1 may also have later roles after fusion in muscle development. To date, analysis of Dock1, IQSec1 and their *Drosophila* homologs has been confined to their roles in fusion since defects in fusion result in the developmental arrest of muscle differentiation. The use of alternative genetic approaches, including muscle-specific RNAi in the case of *Drosophila*, to bypass these early functions, may allow for the analysis of these later roles. In support of this approach and the possibility that Dock1/Mbc and IQSec1/Loner have roles after fusion, depletion of *Loner* using *Dmef2-Gal4* resulted in adult flies that were “weak flyers” (Schnorrer et al., 2010).

Visualizing myoblast fusion in C2C12 myoblasts

In *Drosophila*, the identification of the site of fusion precipitated a huge advancement in our understanding of the molecular mechanisms that underpin myoblast fusion, allowing us to understand the timing of myoblast fusion as well

as the types of proteins that might be important for myoblast fusion. Importantly, the identification of the actin focus distinguished between genes that caused a phenotypically similar myoblast fusion block.

This advance is lacking in any system of vertebrate mammalian myoblast fusion *in vitro* and *in vivo*. An unexpected limitation in answering this question has come in the form of technical issues. In C2C12 myoblasts, our extensive efforts to fluorescently label the actin cytoskeleton using a number of reagents and techniques have largely resulted in the almost complete block in myoblast fusion, underscoring the importance of the proper regulation of F-actin to the fusion process, but limiting our ability to investigate actin dynamics during fusion. Thus, an outstanding question in the mammalian myoblast fusion field is how can we visualize fusion?

It is likely that high levels of reporter expression contributed to some of the difficulties we had. All reporters are under the control of the synthetic cytomegalovirus (CMV) immediate early enhancer and chick β -actin promoter elements, which drive high levels of gene expression (Miyazaki et al., 1989). Thus, one approach would be to decrease the level of reporter expression by exchanging the enhancer and promoter elements. However, a critical limitation here is in achieving the optimal balance between having levels of reporter expression that are high enough to be detected during live imaging but low enough so as not to disrupt the fusion process. Microinjection of specific concentrations of reporter plasmids may make striking this balance less difficult and would add consistency from cell to cell and experiment to experiment, but

microinjection is technically challenging and time-consuming. Alternatively, a transgenic mouse that expresses the Lifeact reporter has recently been described (Riedl et al., 2010). These transgenic mice are viable, fertile, appear phenotypically normal and express Lifeact under the control of the CMV enhancer. Thus, primary myoblasts which express Lifeact could be isolated from these mice and used for live imaging experiments. This approach has the added benefit of eliminating the transfection or lentivirus generation steps, but would require isolating primary myoblasts for each experiment. Lastly, given our experience using Lifeact in C2C12 myoblasts, it is somewhat surprising that these transgenic mice are viable; however, this may highlight differences between *in vivo* and *in vitro* studies.

General fusion machinery?

A number of molecules appear to play a role in multiple fusing systems. For example, proteins that mediate myoblast adhesion during fusion, including integrins and ADAM (a disintegrin and metalloprotease) family members have been implicated in sperm-egg fusion during mammalian fertilization (Horsley and Pavlath, 2004; Wassarman and Litscher, 2010). As in mammalian myoblast fusion, however, these proteins are not essential for fusion, suggesting that additional cell adhesion molecules are required for sperm-egg fusion. ADAM-12, an ADAM family protein, also plays a role in trophoblast fusion (Huppertz and

Borges, 2010; Huppertz et al., 2006). In addition, a number of extracellular, secreted molecules play a general role in fusion. Calcium (Ca^{2+}) regulates mammalian myoblast fusion, sperm-egg fusion and yeast mating (Horsley and Pavlath, 2004; Wassarman and Litscher, 2010; Ydenberg and Rose, 2010). Interleukin-4 (Il-4), a secreted chemokine, is critical for the fusion of mammalian myoblasts and macrophages (Horsley and Pavlath, 2004; Vignery, 2010). Interestingly, however, Il-4 seems to promote giant cell formation while inhibiting osteoclast formation *in vitro* (Vignery, 2010).

Actin and its regulators also appear to play a general role in fusing systems. During yeast mating, for example, cell polarization is required for efficient cell wall degradation, and mutations in genes which affect the polarization of actin cables result in large numbers of unfused zygotes (Ydenberg and Rose, 2010). Interestingly, one such fusion mutant contains a broader fusion zone, suggesting that fusion fails because the fusion machinery is not properly localized. Additionally, Cdc42p appears to be required at multiple steps to generate proper cell polarity during yeast zygote fusion. Similarly, Cdc42 is required for mammalian myoblast fusion *in vivo*; its role during *Drosophila* myoblast fusion is less clear (Vasyutina et al., 2009). Recently, the activity of Dock1 was demonstrated to be required for both the fusion of myoblasts and the fusion of macrophages to generate multinucleated giant cells (Pajcini et al., 2008). Thus, it too appears to play a more general role in fusion. Though its role was not examined, IQSec1 mRNA can be detected in macrophages, suggesting that it may also be required for macrophage fusion. Together, these data imply

the existence of a general fusion machinery. Thus, studies in myoblast fusion may be applicable to understanding other fusing systems and vice versa.

CHAPTER SEVEN: MATERIALS AND METHODS

Drosophila

Drosophila genetics

Stocks were grown under standard conditions and crosses were performed at 25°C unless otherwise stated. *OreR* and *yw* were used as wild-type strains. Stocks used were *tsr^{N96A}* (BDSC 9108), *tsr¹* (BDSC 9107), *flr¹* (BDSC 1132), *flr^β* (BDSC 2371), *ssh¹⁻⁶³* (BDSC 9110), *ssh¹⁻¹¹* (BDSC 9111), *LIMK1^{EY08757}* (BDSC 17491), *cdi⁰⁷⁰¹³* (BDSC 11711), *409-Gal4*, *UAS-lacZ* and *coro^{ex}* alleles (Bharathi et al., 2004), *UAS-tsrt^{wt}* (gift of L. Cooley), *UAS-tsrs^{3A}* (BDSC 9236), *UAS-tsrs^{3E}* (BDSC 9238), *UAS-2XeGFP* (Halfon et al., 2002), *UAS-LIMK1::HA* (BDSC 9116 and 9117), *UAS-moesin::GFP* and *UAS-moesin::mCherry* (gifts of J. Zallen), *apME-NLS::dsRed* (Metzger et al., 2012; Richardson et al., 2007), *UAS-coro::eGFP*, *UAS-coro::mCherry*, *UAS-tsrt^{wt}::mCherry* and *UAS-tsrt^{G19A}::mCherry* (this study), *twist-Gal4* (Baylies et al., 1995), *5053-Gal4* (Ritzenthaler et al., 2000), *Dmef2-Gal4* (a gift from A. Michelson). The Transgenic RNAi Project (TRiP) stocks, *UAS-tsrt RNAi* (HMS00534), *UAS-LIMK1 RNAi* (JF02063), *UAS-coro RNAi* (HMS02007), *UAS-flr RNAi* (JF01620) were obtained from the *Drosophila* RNAi Screening Center (DRSC). *UAS-tsrt-IR* (110599) and *UAS-flr-IR* (108442) were obtained from the Vienna *Drosophila* RNAi Center (VDRC) (Dietzl et al., 2007). *UAS-coro-IR* (VDRC 109644) and *UAS-ssh-IR* (VDRC 107998) were gifts of E. Schejter. Protein traps were obtained from FlyTrap (Buszczak et al., 2007; Kelso et al., 2004; Morin et al., 2001; Quiñones-Coello et al., 2007):

ZCL0663 (*Zasp66*), *CC00578* (*Tm1*), *ZCL0613*, *ZCL1537* and *ZCL2393* (*Tsr*). Deficiencies were obtained from the Bloomington Stock Center: *Df(2R)BSC261* and *Df(2R)Exel6050* [deficiencies removing *coro*].

Germline transformation and constructs

UAS-coro::eGFP and *UAS-coro::mCherry* DNA were constructed by PCR amplifying the full length cDNA from the *coro RA* transcript (LD37992, Drosophila Genomics Resource Center, DGRC) with primers to introduce BglIII restriction sites. Primers used were: 5' CACC AGA TCT ATG TCA TTT CGC GTA GTG CGC 3' and 5' AGA TCT GTC CTC GTC CTT TGA CGT TCC 3'. Amplified cDNA was introduced into the pUAST vector containing eGFP or mCherry cloned into the BglIII and NotI restriction sites to generate C-terminal fluorophore tags on *Coro*.

UAS-tsr^{wt}::mCherry and *UAS-tsr^{G19A}::mCherry* were constructed by PCR amplifying the full length cDNA from the *tsr RA* transcript (LD06785, DGRC) with primers to introduce EcoRI and BglIII restriction sites. Additionally, primers were used to introduce a G19A mutation via PCR resulting in a Val-to-Met amino acid change. Forward primers used were: 5' CACC GAA TTC ATG GCT TCT GGT GTA ACT GTG TCT 3' (wild-type) and 5' CACC GAA TTC ATG GCT TCT GGT GTA ACT **ATG** TCT GAT GTC TGC AAG ACT ACA T 3' (G19A). The bolded nucleotide indicates the introduced mutation. The reverse primer 5' AGA TCT TTG GCG GTC GGT GGC CCG GAG TTT 3' was used for both constructs. Amplified cDNA was introduced into the pUAST vector containing mCherry cloned

into the BglIII and NotI restriction sites to generate C-terminal fluorophore tags on Tsr. Constructs were injected via random P-element insertion into embryos by Genetic Services (Cambridge, MA).

Immunohistochemistry

Embryos were collected at 25°C (unless indicated otherwise) on apple juice agar plates and were fixed in 4% paraformaldehyde/heptane. Embryos were mounted in Prolong Gold (Molecular Probes). Larvae were dissected in relaxing buffer as previously described (Bai et al., 2007; Brent et al., 2009) and fixed in formalin for 20 minutes. Antibodies were used at the indicated final dilutions. Antibodies used were rat anti-tropomyosin (1:1000, Abcam), mouse anti-myosin heavy chain (1:500, gift from S. Abmayr), chicken anti- β -galactosidase (1:1000, Abcam), rabbit anti-dsRed (1:400, Clontech), mouse anti-GFP (1:200; PA; Clontech), rabbit anti-Zasp (1:200, gift from F. Schöck), rat anti-StripeA (1:200, in low-Triton buffer) and guinea pig anti-StripeB (1:200) (gifts from T. Volk) and mouse anti-BPS-integrin (1:50, DSHB CF.6G11). Alexa Fluor 488-, Alexa Fluor 555-, and Alexa Fluor 647-conjugated secondary antibodies were used at 1:400, Alexa Fluor 546-, and Alexa Fluor 647- conjugated phalloidin were used at 1:200 for staining of embryos and 1:100 for larvae (Invitrogen). Hoechst 33342 (1:10,000) was used to label nuclei in larval muscle.

For imaging of protein traps, embryos were collected and dechorionated as above and mounted in Halocarbon 700 Oil (Halocarbon Products) on a glass

slide and covered with a coverslip. Larvae were isolated from yeast paste, rinsed briefly in water to remove all traces of yeast and mounted as above. Slides were kept overnight and imaged the following day.

Fluorescent confocal images were acquired on a Leica SP5 laser scanning confocal microscope using the LAS AF 2.2 software (objectives used: 20x 0.70 NA HC PL APO multi-immersion, 40x 1.25 NA, 63x 1.4 NA, or 100x 1.43 NA HCX PL APO oil). Images were analyzed and processed using Volocity (Improvision) and Photoshop CS5 (Adobe).

Live imaging

Embryos were collected, dechorionated, mounted on stage outfitted with an air permeable membrane, immersed in Halocarbon 700 Oil (Halocarbon Products) and covered with a coverslip. Time-lapse sequences were acquired using the same confocal system as described above. GFP was excited at 488nm. All time-lapse sequences were taken as a series of Z-stacks over time (4D imaging), with 0.5 μ m sections captured every 30-45 seconds. Movies were created from image sequences using Volocity (Improvision).

Viability

Embryos were collected, dechorionated and Stage 15-17 embryos of the appropriate genotype were hand-selected and placed on apple juice agar plates.

Embryos were allowed to hatch into larvae and larvae were transferred into vials to continue development. Viability was analyzed by counting the number of unhatched embryos and hatched first-instar larvae, pupae and the number of adult flies emerging after pupation.

Cuticle preparations

Embryos were aged when possible, collected and dechorionated as above. Embryos were transferred to an Eppendorf containing 0.5 mL heptane, devitellinized in 1:1 heptane:methanol and rinsed several times with methanol. Methanol was replaced with 1:4 glycerol:HAc and incubated overnight at 65°C. The following day, fix was removed and embryos were mounted on a slide in 150uL of Hoyer's medium. Slides were weighted down and allowed to harden at 65°C overnight. Images were acquired on a Zeiss Axiophot microscope.

Larval behavior

Larval behavior was assessed as previously described with minor modifications (Louis et al., 2008a; 2008b). Briefly, embryos (stage 16 and 17) were hand-selected as described above. Embryos were placed on a yeast-coated apple juice plate overnight at 25°C. The following day, first-instar larvae were transferred into vials of standard food containing bromophenol blue (Fischer Scientific). Third-instar larvae were isolated from the vial 3 days later (prior to

becoming wandering third-instar larvae). Larvae were tracked individually as they migrated towards an odor source (0.25M ethyl butyrate, Sigma) and recorded with a CCD camera for 5 minutes until they reached the odorant or contacted any of the walls of the apparatus. Images were processed by Ethovision software (Noldus).

Adult histology

Analysis of adult muscle patterning using hematoxylin and eosin-stained paraffin sections was performed as previously described with minor modifications (Morriss et al., 2012). Briefly, adult flies were anesthetized using CO₂. Heads, wings and legs were removed using scissors to isolate the thorax and abdomen. Specimens were fixed overnight in 4% paraformaldehyde at 4°C. The following day, thoraces were washed in PBS and dehydrated in an ethanol series. Ethanol was displaced by xylene and then paraffin. Specimens were mounted in an embedding mold and 8-10um sections were cut using a microtome. Sections were deparaffinized in xylene, rehydrated using an ethanol series, stained with Hematoxylin Stain Gill 2 (Thermo Scientific) and Eosin Y (Fisher) and mounted in Cytoseal-XYL (VWR).

Statistics

Statistical analysis were performed using Prism (GraphPad Software Inc.). Pairwise comparisons were made using a Student's t test and group comparisons were made by ANOVA followed by Tukey's posthoc analysis.

Satellite cell-derived C2C12 myoblasts

Plasmid constructs

Plasmids pCX::PH-GFP, pCX::myr-Ven and pCX::myr-RFP have been described previously (Nowak et al., 2009; Rhee et al., 2006; Tall et al., 2000). Constructs expressing shRNA oligos against Dock180 and Iqsec1 were designed by S. Nowak. Plasmids encoding fluorescently-tagged actin-binding proteins, including ACTR3::eGFP (8462), eGFP::Capzb (13298), eGFP::Dbn1 (26719), eGFP::FBP17 (22229), GFP::UtrCH (26737) and mRFP::UtrCH (26739), were obtained from Addgene. Lentiviral plasmids were a gift of L. Studer.

Cell culture

C2C12 myoblasts (ATCC) were passaged and proliferated in growth medium (GM; Dulbecco's Modified Eagle Medium [DMEM, Mediatech] containing 15%

fetal bovine serum [Sigma] supplemented with 1% glutamine [Mediatech], 1% penicillin/streptomycin [Mediatech], 0.1% gentamycin sulfate [Mediatech] and 0.5% chick embryo extract [Sera Laboratory]). Cells were cultured at 37°C in 5% CO₂ in culture dishes coated with 10% Matrigel (BD Biosciences). For differentiation and fusion, cells were rinsed with PBS and cultured in differentiation medium (DM; DMEM containing 5% normal horse serum, supplemented with 1% penicillin/streptomycin, 1% glutamine and 0.1% gentamycin sulfate) for the times indicated.

Production of stable cell lines

C2C12 myoblasts were transfected using the Lipofectamine/Plus system (Invitrogen). Stable cell lines were generated by transfection with either empty vectors or vectors expressing Dock1- or IQSec1-specific shRNA oligos and selected in GM containing 1 µg/ml puromycin. To prevent differences in fusion rates between each population due to variations in cell-passage number, cells from the same passage were used for transfection with control and knockdown vectors, and were passaged at the same time to ensure similar 'age' of both control and experimental myoblasts. Clonal cell lines were isolated following 1 week of selection in puromycin, and evaluated for fusion phenotype and knockdown of target protein by western blotting when possible. Lentivirus production and generation of stable lines was performed as described (Papapetrou et al., 2009). The full length protocol is included in Appendix A.

Immunofluorescence and immunoblotting

Myoblasts were grown in 6-cm culture dishes, fixed in 4% paraformaldehyde, permeabilized in PBS + 0.1% Triton X-100 and blocked in PBS containing 1% bovine serum albumin (BSA). Cells were incubated overnight with primary antibodies at 4°C. Primary antibodies used were: anti-sarcomeric Mhc (MF20; 1:10 DSHB), anti-Dock180 (1:100, Santa Cruz Biotechnology), anti-N-cadherin (1:100, BD Biosciences), anti-M-cadherin (1:100, BD Transduction), anti-Vinculin (1:50, Sigma) and anti-Paxillin (1:100, BD Transduction). Alexa Fluor 488-, and Alexa Fluor 555-conjugated secondary antibodies were used at 1:400, Alexa Fluor 488-, and Alexa Fluor 546-conjugated phalloidin were used at 1:200. Cells were counterstained with DAPI and mounted in Prolong Gold (Molecular Probes). Wide-field images were acquired on a Zeiss Axiophot microscope and processed using Photoshop CS5 (Adobe). Immunoblotting was performed as described (Nowak et al., 2009). Anti- α -tubulin (1:2000, Accurate Chemical) was used as a loading control.

Fusion index calculation

The fusion index was defined as the percentage of nuclei contained in myosin heavy chain-positive structures ($n > \text{three nuclei total}$), compared to the total number of nuclei contained within the field. For each experimental condition and

time point, a minimum of ten fields were randomly imaged at identical magnification from immunofluorescently labeled samples at the indicated time point.

Live imaging and migration tracking

For standard imaging, C2C12 myoblasts were transfected as described above and grown to confluence prior to imaging. For imaging in which two differentially fluorescent populations were used, C2C12 myoblasts were transfected separately, trypsinized, mixed together and grown to confluence prior to imaging. Confluent plates were switched to DM and incubated for the indicated time at 37°C. HEPES was added to a final concentration of 50 μ M just prior to imaging. Cells were imaged on an Olympus inverted microscope equipped with an environmental chamber set at 37°C. Time-lapse sequences were acquired using MetaMorph software and image sequences were assembled using Volocity (Improvision). Myoblast tracking was performed using Volocity.

Cell spreading

Slides were coated with indicated ECM components for 1 hour at 37°C. Fibronectin (Sigma-Aldrich) was used at 1-5 μ g/cm² or 0.5-50 μ g/ml. Laminin (Sigma-Aldrich) was used at 1-2 μ g/cm². Excess ECM was removed by three PBS washes. PBS was used to store plates until use. For the cell spreading

assay, cells were trypsinized, collected and centrifuged. Cell pellets were resuspended in chilled PBS and re-centrifuged. Cell pellets were resuspended in chilled serum-free media and cells were counted using a hemacytometer. Cell suspensions were adjusted to $1-2 \times 10^5$ cells/mL and incubated for 40 minutes in suspension at 37°C. Cells were seeded in triplicate at a density of $2-4 \times 10^5$ cells per 2 mL and incubated for the indicated time. Slides were fixed and processed for immunofluorescence as described above. Usually, only phalloidin and DAPI were used. Cell size was determined using ImageJ software.

Statistics

Average fusion indices and standard error were calculated using Microsoft Excel. Statistical analysis were performed using Prism (GraphPad Software Inc.). Pairwise comparisons were made using a Student's t test and group comparisons were made by ANOVA followed by Tukey's posthoc analysis.

APPENDIX

Lentiviral production

Reagents:

1. 1% gelatin: Fisher, type A, #G8-500; 1 g in 100 mL 1 x PBS
2. poly-L-lysine: Sigma, 50 mL bottle, #P4832
3. coating buffer: 20 mL 1% gelatin solution
180 mL 1 x PBS
50 mL poly-L-lysine

Mix well. Filter through 0.22 μm . Store at 4°C.

To coat 10 cm tissue culture plates: Pipet 5 mL into plate. Swirl to cover entire plate; reuse for 4 additional plates. Discard. Can use coated plates immediately or next day.

4. 10% Fetal Bovine Serum in DMEM containing no antibiotics or antifungals
5. 2x HBS (HEPES-buffered saline); for 1 L: 281 mM NaCl = 16.42g
100 mM HEPES = 23.82g
1.5 mM Na₂HPO₄ = 0.21g
1 L ddH₂O

Filter through 0.22 μm . pH 7.12 using 5 M NaOH. Filter again.

6. 293T cells of no more than 2-3 weeks passage. 293T cells are loosely adherent so use care when changing media and always pipet down the sides of the plate.
7. Beckman centrifuge liner tubes: 1x 3.5 UC tube MFG 98374, part# 344058
8. Ultracentrifuge tubes and caps
9. Shaking apparatus borrowed from Studer lab
10. large number of 10 cm tissue culture plates

NOTE: Bleach everything that comes into contact with virus before throwing away.

General timeline for generating proper number of plates (1 virus, 1 round of centrifugation = 27 plates):

day -4 - Thaw and plate vial of 293T cells at 1:3

day -3 - Split 1:6

day -1 (day prior to transfection) - passage 1:3 or 1:4 depending on confluence in late afternoon/early evening. Want 90% confluence in 16-20 hrs.

day 0 - change media ~1 hr (7 mL) before transfection

day 1 - change media 16-18 hours after transfection

day 2 - virus collection

day 3 - freeze virus

Day 0 - Transfection

1. Discard media and add 7 mL of fresh 10% FBS in DMEM 1 hr prior to transfection. Ideally, 293Ts are at 90% confluence for highest titer.

2. Ready DNA Mastermix in 50 mL conical tube- see example Excel workbook:

(A) ug/ul	(B) Name of plasmid	(C) ug	(D) ul	(E) (ul)	(F) number of plates
1.66	viral plasmid	10	6.02	108.30	18
1.72	CMVdR8.91	7.5	4.37	78.67	
1.647	pUCMDG	2.5	1.52	27.32	
	2.5M CaCl ₂		50.00	900.00	
	H ₂ O		438.09	7885.70	
	Total			9000.00	

(A) concentration of plasmids listed in B

(B) CMVdR8.91 and pUCMDG are co-transfected

(C) value in this column does not change

(D) = column C/column A; **NOTE:** ul of 2.5M CaCl₂ does not change here and volume of water is 500 - sum of other volumes in column.

(E) = column D x column F

(F) = number of plates collecting virus from; **NOTE:** use 27 x 10 cm plates for one round of virus production and one round of centrifugation. If making multiple viruses, use any multiple of 27 (ie, if making two viruses, use 54 plates and at the centrifugation step detailed below, use positions 1-3 for virus 1 and positions 4-6 for virus 2 and repeat the centrifugation step)

3. When ready to transfect: Use one pipet to bubble DNA Mastermix. Slowly (drop-wise) add an equal volume of 2x HBS with a pipet in the other hand. Vortex the DNA:HBS mixture briefly.
4. Add 1 mL drop-wise - and from as high as the hood will allow - to each plate. Gently move the plate forward and back and side-to-side to evenly distribute mixture. Repeat for all plates. When placing the plates in the incubator, be sure to re-shake the plates as above.
5. In 1 hr, calcium crystals should be visible under a light microscope. These should be distributed evenly and there should be many.
6. The following day: discard and change media 16-18 hrs post-transfection.

Day 1 - change media

1. Change and discard media. Add 10 mL 10% FBS in DMEM. Virus is now alive and actively produced. Be sure to soak all tips and pipets in bleach.
2. Ready Beckman centrifuge tubes, caps and liner tube:
for centrifuge tubes: spray generously with 70% EtOH
dry upside down overnight on paper towels
keep plastic liners in closed container

Day 2 - Virus Collection

1. Prepare centrifuge tubes: Place tubes and lids and liners open side-up in a styrofoam holder for 50 mL conical vials. Wrap completely with plastic wrap. UV-sterilize - Place plastic wrap-wrapped rack in without hitting the back of the machine. Sterilize for 20'. At this time, also pre-chill the ultracentrifuge. First, ensure the appropriate rotor is installed and the settings are correct (20K rpm, 4°C, 90 minutes and 9, 7). Close the lid and press the vacuum button. (Later, to load the centrifuge tubes, press the vacuum button again and the door should unlock.)
2. Match up centrifuge tubes with their caps - both are numbered 1-6 - and a liner.
3. Insert liner into centrifuge tube.
4. Pipet viral media from 293Ts into 250 or 500 mL sterile filter. You can replace the media on one plate to look for presence of fluorescence marker.

*If collecting a second day, replace the media with 10 mL of warm media and

invert over paper towels to dry
return to tube rack

Day 3 - Freezing virus

1. Retrieve liner/conicals from cold room on ice.
2. Spin liner and conical at 2000 rpm (~4.5 setting) at 4°C for 2 minutes. (You must pre-cool the centrifuge. Remember to return it to 37°C when finished.) During this time, also chill cryovials on dry ice. You need one cryovial per centrifuge tube.
3. Using 150 L of COLD media, transfer viral media to cryovial. Return to dry ice.
4. Repeat with remaining liner/conicals and cryovials.
5. Store at -80°C for at least 72 hr before infecting/titrating: virus titer will drop when you freeze; thus, waiting allows everything to stabilize and you to have reproducible experiments.

Generating lentivirus vector

A fluorophore (to mark virus-producing cells during production and infection) is cloned upstream of a P2A sequence and the DNA of interest. Importantly, this does not generate a tagged protein, but could be modified to do so. AgeI and Sall restriction sites are used to introduce the DNA into the lentivirus vector to generate:

-----AgeI-FLUOROPHORE-P2A-YOUR LENTIVIRUS-Sall-----

Primers for cloning into lentivirus vector, including the P2A sequence:

Fluorophore:

AgeI_for: CCGGTT*accggt***ATG**...
overhang AgeI start

P2A_rev: agggccgggattctcctccacgtcacctgctgttgagtagtgagaagttgttgctccagatcc...

Your lentivirus:

P2A_for:
ggatctggagcaacaaacttctcactactcaaacaagcaggtgacgtggaggagaatcccggccct**ATG**
start

Sall_rev: CCGGTT*gtcgac*...
overhang Sall

BIBLIOGRAPHY

- Abe, H., and Obinata, T. (1989). An actin-depolymerizing protein in embryonic chicken skeletal muscle: purification and characterization. *Journal of Biochemistry* *106*, 172–180.
- Abe, H., Endo, T., Yamamoto, K., and Obinata, T. (1990). Sequence of cDNAs encoding actin depolymerizing factor and cofilin of embryonic chicken skeletal muscle: two functionally distinct actin-regulatory proteins exhibit high structural homology. *Biochemistry* *29*, 7420–7425.
- Abe, H., Ohshima, S., and Obinata, T. (1989). A cofilin-like protein is involved in the regulation of actin assembly in developing skeletal muscle. *Journal of Biochemistry* *106*, 696–702.
- Abmayr, S.M., and Pavlath, G.K. (2012). Myoblast fusion: lessons from flies and mice. *Development* *139*, 641–656.
- Abmayr, S.M., Balagopalan, L., Galletta, B.J., and Hong, S.-J. (2003). Cell and molecular biology of myoblast fusion. *Int. Rev. Cytol.* *225*, 33–89.
- Agnew, B.J., Minamide, L.S., and Bamburg, J.R. (1995). Reactivation of phosphorylated actin depolymerizing factor and identification of the regulatory site. *J. Biol. Chem.* *270*, 17582–17587.
- Agrawal, P.B., Greenleaf, R.S., Tomczak, K.K., Lehtokari, V.-L., Wallgren-Pettersson, C., Wallefeld, W., Laing, N.G., Darras, B.T., Maciver, S.K., Dormitzer, P.R., et al. (2007). Nemaline myopathy with minicores caused by mutation of the CFL2 gene encoding the skeletal muscle actin-binding protein, cofilin-2. *Am. J. Hum. Genet.* *80*, 162–167.
- Agrawal, P.B., Joshi, M., Savic, T., Chen, Z., and Beggs, A.H. (2012). Normal myofibrillar development followed by progressive sarcomeric disruption with actin accumulations in a mouse Cfl2 knockout demonstrates requirement of cofilin-2 for muscle maintenance. *Human Molecular Genetics* *21*, 2341–2356.
- Akkila, W.M., Chambers, R.L., Ornatsky, O.I., and McDermott, J.C. (1997). Molecular cloning of up-regulated cytoskeletal genes from regenerating skeletal muscle: potential role of myocyte enhancer factor 2 proteins in the activation of muscle-regeneration-associated genes. *Biochem. J.* *325 (Pt 1)*, 87–93.
- Alberts, A.S. (2000). Identification of a Carboxyl-terminal Diaphanous-related Formin Homology Protein Autoregulatory Domain. *Journal of Biological Chemistry* *276*, 2824–2830.

- Amberg, D.C., Basart, E., and Botstein, D. (1995). Defining protein interactions with yeast actin in vivo. *Nat. Struct. Biol.* *2*, 28–35.
- Appleton, B.A., Wu, P., and Wiesmann, C. (2006). The crystal structure of murine coronin-1: a regulator of actin cytoskeletal dynamics in lymphocytes. *Structure* *14*, 87–96.
- Armand, P., Knapp, A.C., Hirsch, A.J., Wieschaus, E.F., and Cole, M.D. (1994). A novel basic helix-loop-helix protein is expressed in muscle attachment sites of the *Drosophila* epidermis. *Molecular and Cellular Biology* *14*, 4145–4154.
- Artero, R. (2003). Notch and Ras signaling pathway effector genes expressed in fusion competent and founder cells during *Drosophila* myogenesis. *Development* *130*, 6257–6272.
- Artero, R.D., Castanon, I., and Baylies, M.K. (2001). The immunoglobulin-like protein Hibris functions as a dose-dependent regulator of myoblast fusion and is differentially controlled by Ras and Notch signaling. *Development* *128*, 4251–4264.
- Avirneni-Vadlamudi, U., Galindo, K.A., Endicott, T.R., Paulson, V., Cameron, S., and Galindo, R.L. (2012). *Drosophila* and mammalian models uncover a role for the myoblast fusion gene TANC1 in rhabdomyosarcoma. *J. Clin. Invest.* *122*, 403–407.
- Bach, A.-S., Enjalbert, S., Comunale, F., Bodin, S., Vitale, N., Charrasse, S., and Gauthier-Rouvière, C. (2010). ADP-ribosylation factor 6 regulates mammalian myoblast fusion through phospholipase D1 and phosphatidylinositol 4,5-bisphosphate signaling pathways. *Mol. Biol. Cell* *21*, 2412–2424.
- Bai, J., Hartwig, J.H., and Perrimon, N. (2007). SALS, a WH2-Domain-Containing Protein, Promotes Sarcomeric Actin Filament Elongation from Pointed Ends during *Drosophila* Muscle Growth. *Developmental Cell* *13*, 828–842.
- Balagopalan, L., Chen, M.H., Geisbrecht, E.R., and Abmayr, S.M. (2006). The CDM Superfamily Protein MBC Directs Myoblast Fusion through a Mechanism That Requires Phosphatidylinositol 3,4,5-Triphosphate Binding but Is Independent of Direct Interaction with DCrk. *Molecular and Cellular Biology* *26*, 9442–9455.
- Ball, E., Ball, S.P., and Sparrow, J.C. (1985). A mutation affecting larval muscle development in *Drosophila melanogaster*. *Dev. Genet.* *6*, 77–92.
- Bamburg, J.R. (1999). Proteins of the ADF/cofilin family: essential regulators of actin dynamics. *Annu. Rev. Cell Dev. Biol.* *15*, 185–230.

- Bamburg, J.R., and Bray, D. (1987). Distribution and cellular localization of actin depolymerizing factor. *The Journal of Cell Biology* *105*, 2817–2825.
- Bamburg, J.R., Harris, H.E., and Weeds, A.G. (1980). Partial purification and characterization of an actin depolymerizing factor from brain. *FEBS Letters* *121*, 178–182.
- Bamburg, J.R., McGough, A., and Ono, S. (1999). Putting a new twist on actin: ADF/cofilins modulate actin dynamics. *Trends in Cell Biology* *9*, 364–370.
- Barletta, G.M. (2003). Nephrin and Neph1 Co-localize at the Podocyte Foot Process Intercellular Junction and Form cis Hetero-oligomers. *Journal of Biological Chemistry* *278*, 19266–19271.
- Barr, E., and Leiden, J.M. (1991). Systemic delivery of recombinant proteins by genetically modified myoblasts. *Science* *254*, 1507–1509.
- Bate, M. (1990). The embryonic development of larval muscles in *Drosophila*. *Development* *110*, 791–804.
- Bate, M., Rushton, E., and Currie, D.A. (1991). Cells with persistent twist expression are the embryonic precursors of adult muscles in *Drosophila*. *Development* *113*, 79–89.
- Baylies, M.K., and Bate, M. (1996). twist: a myogenic switch in *Drosophila*. *Science* *272*, 1481–1484.
- Baylies, M.K., Bate, M., and Ruiz-Gomez, M. (1998). Myogenesis: a view from *Drosophila*. *Cell* *93*, 921–927.
- Beall, C.J., and Fyrberg, E. (1991). Muscle abnormalities in *Drosophila melanogaster* heldup mutants are caused by missing or aberrant troponin-I isoforms. *The Journal of Cell Biology* *114*, 941–951.
- Becker, S., Pasca, G., Strumpf, D., Min, L., and Volk, T. (1997). Reciprocal signaling between *Drosophila* epidermal muscle attachment cells and their corresponding muscles. *Development* *124*, 2615–2622.
- Beckett, K., and Baylies, M.K. (2007). 3D analysis of founder cell and fusion competent myoblast arrangements outlines a new model of myoblast fusion. *Dev. Biol.* *309*, 113–125.
- Berger, S., Schafer, G., Kesper, D.A., Holz, A., Eriksson, T., Palmer, R.H., Beck, L., Klambt, C., Renkawitz-Pohl, R., and Onel, S.F. (2008). WASP and SCAR have distinct roles in activating the Arp2/3 complex during myoblast fusion. *J. Cell. Sci.* *121*, 1303–1313.

- Bharathi, V., Pallavi, S.K., Bajpai, R., Emerald, B.S., and Shashidhara, L.S. (2004). Genetic characterization of the *Drosophila* homologue of coronin. *J. Cell. Sci.* *117*, 1911–1922.
- Birchmeier, C., and Brohmann, H. (2000). Genes that control the development of migrating muscle precursor cells. *Curr. Opin. Cell Biol.* *12*, 725–730.
- Blair, A., Tomlinson, A., Pham, H., Gunsalus, K.C., Goldberg, M.L., and Laski, F.A. (2006). Twinstar, the *Drosophila* homolog of cofilin/ADF, is required for planar cell polarity patterning. *Development* *133*, 1789–1797.
- Bober, E., Franz, T., Arnold, H.H., Gruss, P., and Tremblay, P. (1994). Pax-3 is required for the development of limb muscles: a possible role for the migration of dermomyotomal muscle progenitor cells. *Development* *120*, 603–612.
- Bodenstein, D. (1950). The postembryonic development of *Drosophila*. In *Biology of Drosophila*, M. Demerec, ed. (New York: John Wiley & Sons Incorporated), pp. 275–367.
- Bökel, C., and Brown, N.H. (2002). Integrins in development: moving on, responding to, and sticking to the extracellular matrix. *Developmental Cell* *3*, 311–321.
- Bondesen, B.A., Jones, K.A., Glasgow, W.C., and Pavlath, G.K. (2007). Inhibition of myoblast migration by prostacyclin is associated with enhanced cell fusion. *The FASEB Journal* *21*, 3338–3345.
- Borycki, A.G., Li, J., Jin, F., Emerson, C.P., and Epstein, J.A. (1999). Pax3 functions in cell survival and in pax7 regulation. *Development* *126*, 1665–1674.
- Bosch, M., Le, K.H.D., Bugyi, B., Correia, J.J., Renault, L., and Carlier, M.-F. (2007). Analysis of the function of Spire in actin assembly and its synergy with formin and profilin. *Mol. Cell* *28*, 555–568.
- Bour, B.A., Chakravarti, M., West, J.M., and Abmayr, S.M. (2000). *Drosophila* SNS, a member of the immunoglobulin superfamily that is essential for myoblast fusion. *Genes Dev.* *14*, 1498–1511.
- Bourgouin, C., Lundgren, S.E., and Thomas, J.B. (1992). *apterous* is a *drosophila* LIM domain gene required for the development of a subset of embryonic muscles. *Neuron* *9*, 549–561.
- Bravo-Cordero, J.J., Magalhaes, M.A.O., Eddy, R.J., Hodgson, L., and Condeelis, J. (2013). Functions of cofilin in cell locomotion and invasion. *Nat Rev Mol Cell Biol* *14*, 405–417.

- Bravo-Cordero, J.J., Oser, M., Chen, X., Eddy, R., Hodgson, L., and Condeelis, J. (2011). A Novel Spatiotemporal RhoC Activation Pathway Locally Regulates Cofilin Activity at Invadopodia. *Current Biology* *21*, 635–644.
- Brieher, W.M., Kueh, H.Y., Ballif, B.A., and Mitchison, T.J. (2006). Rapid actin monomer-insensitive depolymerization of *Listeria* actin comet tails by cofilin, coronin, and Aip1. *The Journal of Cell Biology* *175*, 315–324.
- Brown, F.D. (2001). Phosphatidylinositol 4,5-bisphosphate and Arf6-regulated membrane traffic. *The Journal of Cell Biology* *154*, 1007–1018.
- Brown, N.H. (1994). Null mutations in the alpha PS2 and beta PS integrin subunit genes have distinct phenotypes. *Development* *120*, 1221–1231.
- Brown, N.H. (2000). Cell-cell adhesion via the ECM: integrin genetics in fly and worm. *Matrix Biol.* *19*, 191–201.
- Brown, N.H., Gregory, S.L., Rickoll, W.L., Fessler, L.I., Prout, M., White, R.A.H., and Fristrom, J.W. (2002). Talin is essential for integrin function in *Drosophila*. *Developmental Cell* *3*, 569–579.
- Brugnera, E., Haney, L., Grimsley, C., Lu, M., Walk, S.F., Tosello-Tramont, A.-C., Macara, I.G., Madhani, H., Fink, G.R., and Ravichandran, K.S. (2002). Unconventional Rac-GEF activity is mediated through the Dock180–ELMO complex. *Nat. Cell Biol.*
- Buckingham, M., and Relaix, F. (2007). The Role of Pax Genes in the Development of Tissues and Organs: Pax3 and Pax7 Regulate Muscle Progenitor Cell Functions. *Annu. Rev. Cell Dev. Biol.* *23*, 645–673.
- Bulchand, S., Menon, S.D., George, S.E., and Chia, W. (2010). The intracellular domain of Dumbfounded affects myoblast fusion efficiency and interacts with Rolling pebbles and Loner. *PLoS ONE* *5*, e9374.
- Burkart, C., Qiu, F., Brendel, S., Benes, V., Hååg, P., Labeit, S., Leonard, K., and Bullard, B. (2007). Modular proteins from the *Drosophila* sallimus (sis) gene and their expression in muscles with different extensibility. *Journal of Molecular Biology* *367*, 953–969.
- Burkel, B.M., Dassow, von, G., and Bement, W.M. (2007). Versatile fluorescent probes for actin filaments based on the actin-binding domain of utrophin. *Cell Motil. Cytoskeleton* *64*, 822–832.
- Burtnick, L.D., Koepf, E.K., Grimes, J., Jones, E.Y., Stuart, D.I., McLaughlin, P.J., and Robinson, R.C. (1997). The crystal structure of plasma gelsolin: implications for actin severing, capping, and nucleation. *Cell* *90*, 661–670.

- Burtnick, L.D., Urosev, D., Irobi, E., Narayan, K., and Robinson, R.C. (2004). Structure of the N-terminal half of gelsolin bound to actin: roles in severing, apoptosis and FAF. *Embo J.* *23*, 2713–2722.
- Buttgereit, D. (1996). Transcription of the beta 1 tubulin (beta Tub56D) gene in apodemes is strictly dependent on muscle insertion during embryogenesis in *Drosophila melanogaster*. *Eur. J. Cell Biol.* *71*, 183–191.
- Buszczak, M., Paterno, S., Lighthouse, D., Bachman, J., Planck, J., Owen, S., Skora, A.D., Nystul, T.G., Ohlstein, B., Allen, A., et al. (2007). The carnegie protein trap library: a versatile tool for *Drosophila* developmental studies. *Genetics* *175*, 1505–1531.
- Cai, L., Holoweckyj, N., Schaller, M.D., and Bear, J.E. (2005). Phosphorylation of coronin 1B by protein kinase C regulates interaction with Arp2/3 and cell motility. *J. Biol. Chem.* *280*, 31913–31923.
- Cai, L., Makhov, A.M., and Bear, J.E. (2007a). F-actin binding is essential for coronin 1B function in vivo. *J. Cell. Sci.* *120*, 1779–1790.
- Cai, L., Marshall, T.W., Uetrecht, A.C., Schafer, D.A., and Bear, J.E. (2007b). Coronin 1B coordinates Arp2/3 complex and cofilin activities at the leading edge. *Cell* *128*, 915–929.
- Callahan, C.A., Bonkovsky, J.L., Scully, A.L., and Thomas, J.B. (1996). derailed is required for muscle attachment site selection in *Drosophila*. *Development* *122*, 2761–2767.
- Campellone, K.G., and Welch, M.D. (2010). A nucleator arms race: cellular control of actin assembly. *Nat Rev Mol Cell Biol* *11*, 237–251.
- Campellone, K.G., Webb, N.J., Znameroski, E.A., and Welch, M.D. (2008). WHAMM is an Arp2/3 complex activator that binds microtubules and functions in ER to Golgi transport. *Cell* *134*, 148–161.
- Campion, D.R. (1984). The muscle satellite cell: a review. *Int. Rev. Cytol.* *87*, 225–251.
- Carlier, M.F., Laurent, V., Santolini, J., Melki, R., Didry, D., Xia, G.X., Hong, Y., Chua, N.H., and Pantaloni, D. (1997). Actin depolymerizing factor (ADF/cofilin) enhances the rate of filament turnover: implication in actin-based motility. *The Journal of Cell Biology* *136*, 1307–1322.
- Carmena, A., Bate, M., and Jiménez, F. (1995). Lethal of scute, a proneural gene, participates in the specification of muscle progenitors during *Drosophila* embryogenesis. *Genes Dev.* *9*, 2373–2383.

- Carmena, A., Murugasu-Oei, B., Menon, D., Jiménez, F., and Chia, W. (1998). Inscuteable and numb mediate asymmetric muscle progenitor cell divisions during *Drosophila* myogenesis. *Genes Dev.* *12*, 304–315.
- Castanon, I., and Baylies, M.K. (2002). A Twist in fate: evolutionary comparison of Twist structure and function. *Gene* *287*, 11–22.
- Castillo, A., Nowak, R., Littlefield, K.P., Fowler, V.M., and Littlefield, R.S. (2009). A nebulin ruler does not dictate thin filament lengths. *Biophysical Journal* *96*, 1856–1865.
- Castrillon, D.H., and Wasserman, S.A. (1994). Diaphanous is required for cytokinesis in *Drosophila* and shares domains of similarity with the products of the limb deformity gene. *Development* *120*, 3367–3377.
- Chan, K.T., Creed, S.J., and Bear, J.E. (2011). Unraveling the enigma: progress towards understanding the coronin family of actin regulators. *Trends in Cell Biology* *21*, 481–488.
- Chanana, B., Graf, R., Koledachkina, T., Pflanz, R., and Vorbrüggen, G. (2007). AlphaPS2 integrin-mediated muscle attachment in *Drosophila* requires the ECM protein Thrombospondin. *Mech. Dev.* *124*, 463–475.
- Chanana, B., Steigemann, P., Jäckle, H., and Vorbrüggen, G. (2009). Reception of Slit requires only the chondroitin-sulphate-modified extracellular domain of Syndecan at the target cell surface. *Proceedings of the National Academy of Sciences* *106*, 11984–11988.
- Charrasse, S., Comunale, F., Fortier, M., Portales-Casamar, E., Debant, A., and Gauthier-Rouvière, C. (2007). M-cadherin activates Rac1 GTPase through the Rho-GEF trio during myoblast fusion. *Mol. Biol. Cell* *18*, 1734–1743.
- Chen, A., Leikina, E., Melikov, K., Podbilewicz, B., Kozlov, M.M., and Chernomordik, L.V. (2008). Fusion-pore expansion during syncytium formation is restricted by an actin network. *J. Cell. Sci.* *121*, 3619–3628.
- Chen, E.H. (2010). *Cell Fusion: Overviews and Methods* (Humana Press).
- Chen, E.H., and Olson, E.N. (2001). Antisocial, an intracellular adaptor protein, is required for myoblast fusion in *Drosophila*. *Developmental Cell* *1*, 705–715.
- Chen, E.H., Grote, E., Mohler, W., and Vignery, A. (2007). Cell–cell fusion. *FEBS Letters* *581*, 2181–2193.
- Chen, E.H., Pryce, B.A., Tzeng, J.A., Gonzalez, G.A., and Olson, E.N. (2003). Control of myoblast fusion by a guanine nucleotide exchange factor, loner, and its effector ARF6. *Cell* *114*, 751–762.

- Chen, J., Godt, D., Gunsalus, K., Kiss, I., Goldberg, M., and Laski, F.A. (2001). Cofilin/ADF is required for cell motility during *Drosophila* ovary development and oogenesis. *Nat. Cell Biol.* *3*, 204–209.
- Chen, Z.F., and Behringer, R.R. (1995). *twist* is required in head mesenchyme for cranial neural tube morphogenesis. *Genes Dev.* *9*, 686–699.
- Cheng, L., Lai, M.D., Sanderson, J.E., Yu, C.M., and Li, M. (2005). Enhanced fusion of myoblasts with myofibers for efficient gene delivery induced by a partially purified protein fraction from rat muscle extract. *Archives of Biochemistry and Biophysics* *441*, 141–150.
- Chereau, D., Boczkowska, M., Skwarek-Maruszewska, A., Fujiwara, I., Hayes, D.B., Rebowski, G., Lappalainen, P., Pollard, T.D., and Dominguez, R. (2008). Leiomodin is an actin filament nucleator in muscle cells. *Science* *320*, 239–243.
- Chereau, D., Kerff, F., Graceffa, P., Grabarek, Z., Langsetmo, K., and Dominguez, R. (2005). Actin-bound structures of Wiskott-Aldrich syndrome protein (WASP)-homology domain 2 and the implications for filament assembly. *Proc. Natl. Acad. Sci. U.S.A.* *102*, 16644–16649.
- Chhabra, E.S., and Higgs, H.N. (2007). The many faces of actin: matching assembly factors with cellular structures. *Nat. Cell Biol.* *9*, 1110–1121.
- Chintapalli, V.R., Wang, J., and Dow, J.A.T. (2007). Using FlyAtlas to identify better *Drosophila melanogaster* models of human disease. *Nat. Genet.* *39*, 715–720.
- Choe, H., Burtnick, L.D., Mejillano, M., Yin, H.L., Robinson, R.C., and Choe, S. (2002). The calcium activation of gelsolin: insights from the 3A structure of the G4-G6/actin complex. *Journal of Molecular Biology* *324*, 691–702.
- Clark, K.A., Bland, J.M., and Beckerle, M.C. (2007). The *Drosophila* muscle LIM protein, Mlp84B, cooperates with D-titin to maintain muscle structural integrity. *J. Cell. Sci.* *120*, 2066–2077.
- Clark, K.A., McElhinny, A.S., Beckerle, M.C., and Gregorio, C.C. (2002). Striated Muscle Cytoarchitecture: An Intricate Web of Form and Function. *Annu. Rev. Cell Dev. Biol.* *18*, 637–706.
- Clark, K.A., McGrail, M., and Beckerle, M.C. (2003). Analysis of PINCH function in *Drosophila* demonstrates its requirement in integrin-dependent cellular processes. *Development* *130*, 2611–2621.
- Clark, P., Coles, D., and Peckham, M. (1997). Preferential adhesion to and survival on patterned laminin organizes myogenesis in vitro. *Experimental Cell Research* *230*, 275–283.

- Clark, P., Dunn, G.A., Knibbs, A., and Peckham, M. (2002). Alignment of myoblasts on ultrafine gratings inhibits fusion in vitro. *Int. J. Biochem. Cell Biol.* *34*, 816–825.
- Clemen, C.S., Rybakin, V., and Eichinger, L. (2008). The coronin family of proteins. *Subcell. Biochem.* *48*, 1–5.
- Cole, F., Zhang, W., Geyra, A., Kang, J.-S., and Krauss, R.S. (2004). Positive regulation of myogenic bHLH factors and skeletal muscle development by the cell surface receptor CDO. *Developmental Cell* *7*, 843–854.
- Conley, C.A., Fritz-Six, K.L., Almenar-Queralt, A., and Fowler, V.M. (2001). Leiomodins: larger members of the tropomodulin (Tmod) gene family. *Genomics* *73*, 127–139.
- Constantin, B., Imbert, N., Besse, C., Cognard, C., and Raymond, G. (1995). Cultured rat skeletal muscle cells treated with cytochalasin exhibit normal dystrophin expression and intracellular free calcium control. *Biol. Cell* *85*, 125–135.
- Cooper, R.N., Tajbakhsh, S., Mouly, V., Cossu, G., Buckingham, M., and Butler-Browne, G.S. (1999). In vivo satellite cell activation via Myf5 and MyoD in regenerating mouse skeletal muscle. *J. Cell. Sci.* *112 (Pt 17)*, 2895–2901.
- Corbin, V., Michelson, A.M., Abmayr, S.M., Neel, V., Alcamo, E., Maniatis, T., and Young, M.W. (1991). A role for the *Drosophila* neurogenic genes in mesoderm differentiation. *Cell* *67*, 311–323.
- Cornelison, D.D., and Wold, B.J. (1997). Single-cell analysis of regulatory gene expression in quiescent and activated mouse skeletal muscle satellite cells. *Dev. Biol.* *191*, 270–283.
- Cornelison, D.D.W., Olwin, B.B., Rudnicki, M.A., and Wold, B.J. (2000). MyoD^{-/-} Satellite Cells in Single-Fiber Culture Are Differentiation Defective and MRF4 Deficient. *Dev. Biol.* *224*, 122–137.
- Côté, J.F. (2002). Identification of an evolutionarily conserved superfamily of DOCK180-related proteins with guanine nucleotide exchange activity. *J. Cell. Sci.* *115*, 4901–4913.
- Côté, J.-F., and Vuori, K. (2007). GEF what? Dock180 and related proteins help Rac to polarize cells in new ways. *Trends in Cell Biology* *17*, 383–393.
- Côté, J.-F., Motoyama, A.B., Bush, J.A., and Vuori, K. (2005). A novel and evolutionarily conserved PtdIns(3,4,5)P₃-binding domain is necessary for DOCK180 signalling. *Nat. Cell Biol.* *7*, 797–807.

- Coué, M., Brenner, S.L., Spector, I., and Korn, E.D. (2001). Inhibition of actin polymerization by latrunculin A. *FEBS Letters* *213*, 316–318.
- Crossley, A.C. (1978). The Morphology and Development of the *Drosophila* Muscular System. In *The Genetics and Biology of Drosophila*, M. Ashburner, and T.R.F. Wright, eds. (London: Academic Press), pp. 499–560.
- Crozatier, M., and Vincent, A. (1999). Requirement for the *Drosophila* COE transcription factor Collier in formation of an embryonic muscle: transcriptional response to notch signalling. *Development* *126*, 1495–1504.
- Currie, D.A., and Bate, M. (1991). The development of adult abdominal muscles in *Drosophila*: myoblasts express twist and are associated with nerves. *Development* *113*, 91–102.
- Deibler, M., Spatz, J.P., and Kemkemer, R. (2011). Actin fusion proteins alter the dynamics of mechanically induced cytoskeleton rearrangement. *PLoS ONE* *6*, e22941.
- D'Souza-Schorey, C., and Chavrier, P. (2006). ARF proteins: roles in membrane traffic and beyond. *Nat Rev Mol Cell Biol* *7*, 347–358.
- Danowski, B.A., Imanaka-Yoshida, K., Sanger, J.M., and Sanger, J.W. (1992). Costameres are sites of force transmission to the substratum in adult rat cardiomyocytes. *The Journal of Cell Biology* *118*, 1411–1420.
- de Hostos, E.L., Bradtke, B., Lottspeich, F., Guggenheim, R., and Gerisch, G. (1991). Coronin, an actin binding protein of *Dictyostelium discoideum* localized to cell surface projections, has sequence similarities to G protein beta subunits. *Embo J.* *10*, 4097–4104.
- de Hostos, E.L., Rehfuess, C., Bradtke, B., Waddell, D.R., Albrecht, R., Murphy, J., and Gerisch, G. (1993). *Dictyostelium* mutants lacking the cytoskeletal protein coronin are defective in cytokinesis and cell motility. *The Journal of Cell Biology* *120*, 163–173.
- de Hostos, E.L. (2008). A brief history of the coronin family. *Subcell. Biochem.* *48*, 31–40.
- Demontis, F., and Perrimon, N. (2009). Integration of Insulin receptor/Foxo signaling and dMyc activity during muscle growth regulates body size in *Drosophila*. *Development* *136*, 983–993.
- Derivery, E., and Gautreau, A. (2010). Generation of branched actin networks: assembly and regulation of the N-WASP and WAVE molecular machines. *Bioessays* *32*, 119–131.

- Dhawan, J. (2004). Modulation of acto-myosin contractility in skeletal muscle myoblasts uncouples growth arrest from differentiation. *J. Cell. Sci.* *117*, 3735–3748.
- Dhawan, J., Pan, L.C., Pavlath, G.K., Travis, M.A., Lanctot, A.M., and Blau, H.M. (1991). Systemic delivery of human growth hormone by injection of genetically engineered myoblasts. *Science* *254*, 1509–1512.
- Dickson, B.J., and Gilestro, G.F. (2006). Regulation of commissural axon pathfinding by slit and its Robo receptors. *Annu. Rev. Cell Dev. Biol.* *22*, 651–675.
- Doberstein, S.K., Fetter, R.D., Mehta, A.Y., and Goodman, C.S. (1997). Genetic analysis of myoblast fusion: blown fuse is required for progression beyond the prefusion complex. *The Journal of Cell Biology* *136*, 1249–1261.
- Dohrmann, C., Azpiazu, N., and Frasch, M. (1990). A new *Drosophila* homeo box gene is expressed in mesodermal precursor cells of distinct muscles during embryogenesis. *Genes Dev.* *4*, 2098–2111.
- Donaldson, J.G., and Jackson, C.L. (2000). Regulators and effectors of the ARF GTPases. *Curr. Opin. Cell Biol.* *12*, 475–482.
- Donaldson, J.G. (2003). Multiple Roles for Arf6: Sorting, Structuring, and Signaling at the Plasma Membrane. *Journal of Biological Chemistry* *278*, 41573–41576.
- Donaldson, J.G. (2008). Arfs and membrane lipids: sensing, generating and responding to membrane curvature. *Biochem. J.* *414*, e1–e2.
- Donalies, M., Cramer, M., Ringwald, M., and Starzinski-Powitz, A. (2009). Expression of M-cadherin, a member of the cadherin multigene family, correlates with differentiation of skeletal muscle cells. *Proc. Natl. Acad. Sci. U.S.a.* *88*, 8024–8028.
- Donoviel, D.B., Freed, D.D., Vogel, H., Potter, D.G., Hawkins, E., Barrish, J.P., Mathur, B.N., Turner, C.A., Geske, R., Montgomery, C.A., et al. (2001). Proteinuria and perinatal lethality in mice lacking NEPH1, a novel protein with homology to NEPHRIN. *Molecular and Cellular Biology* *21*, 4829–4836.
- Dottermusch-Heidel, C., Groth, V., Beck, L., and Önel, S.-F. (2012). The Arf-GEF Schizo/Loner regulates N-cadherin to induce fusion competence of *Drosophila* myoblasts. *Dev. Biol.* *368*, 18–27.
- Duan, H., Skeath, J.B., and Nguyen, H.T. (2001). *Drosophila* *Lame duck*, a novel member of the Gli superfamily, acts as a key regulator of myogenesis by

- controlling fusion-competent myoblast development. *Development* 128, 4489–4500.
- Duan, R., and Gallagher, P.J. (2009). Dependence of myoblast fusion on a cortical actin wall and nonmuscle myosin IIA. *Dev. Biol.* 325, 374–385.
- Dubreuil, R.R., and Wang, P. (2000). Genetic analysis of the requirements for alpha-actinin function. *J. Muscle Res. Cell. Motil.* 21, 705–713.
- Duchek, P., Somogyi, K., Jékely, G., Beccari, S., and Rørth, P. (2001). Guidance of cell migration by the *Drosophila* PDGF/VEGF receptor. *Cell* 107, 17–26.
- Duncan, I.W. (2002). Transvection Effects in *Drosophila*. *Annu. Rev. Genet.* 36, 521–556.
- Dunphy, J.L., Moravec, R., Ly, K., Lasell, T.K., Melancon, P., and Casanova, J.E. (2006). The Arf6 GEF GEP100/BRAG2 Regulates Cell Adhesion by Controlling Endocytosis of β 1 Integrins. *Current Biology* 16, 315–320.
- Dunphy, J.L., Ye, K., and Casanova, J.E. (2007). Nuclear Functions of the Arf Guanine Nucleotide Exchange Factor BRAG2. *Traffic* 8, 661–672.
- Dworak, H.A., Charles, M.A., Pellerano, L.B., and Sink, H. (2001). Characterization of *Drosophila* hibris, a gene related to human nephrin. *Development* 128, 4265–4276.
- Dyer, N., Rebollo, E., Dominguez, P., Elkhatib, N., Chavrier, P., Daviet, L., Gonzalez, C., and Gonzalez-Gaitan, M. (2007). Spermatocyte cytokinesis requires rapid membrane addition mediated by ARF6 on central spindle recycling endosomes. *Development* 134, 4437–4447.
- Eden, S., Rohatgi, R., Podtelejnikov, A.V., Mann, M., and Kirschner, M.W. (2002). Mechanism of regulation of WAVE1-induced actin nucleation by Rac1 and Nck. *Nature* 418, 790–793.
- Edwards, K.A., Montague, R.A., Shepard, S., Edgar, B.A., Erikson, R.L., and Kiehart, D.P. (1994). Identification of *Drosophila* cytoskeletal proteins by induction of abnormal cell shape in fission yeast. *Proc. Natl. Acad. Sci. U.S.A.* 91, 4589–4593.
- Erickson, M.R., Galletta, B.J., and Abmayr, S.M. (1997). *Drosophila* myoblast city encodes a conserved protein that is essential for myoblast fusion, dorsal closure, and cytoskeletal organization. *The Journal of Cell Biology* 138, 589–603.
- Estrada, B., Choe, S.E., Gisselbrecht, S.S., Michaud, S., Raj, L., Busser, B.W., Halfon, M.S., Church, G.M., and Michelson, A.M. (2006). An integrated strategy for analyzing the unique developmental programs of different myoblast subtypes. *PLoS Genet* 2, e16.

- Estrada, B., Gisselbrecht, S.S., and Michelson, A.M. (2007). The transmembrane protein Perdido interacts with Grip and integrins to mediate myotube projection and attachment in the *Drosophila* embryo. *Development* *134*, 4469–4478.
- Evangelista, M., Pruyne, D., Amberg, D.C., Boone, C., and Bretscher, A. (2002). Formins direct Arp2/3-independent actin filament assembly to polarize cell growth in yeast. *Nat. Cell Biol.* *4*, 32–41.
- Farrell, E.R., Fernandes, J., and Keshishian, H. (1996). Muscle organizers in *Drosophila*: the role of persistent larval fibers in adult flight muscle development. *Dev. Biol.* *176*, 220–229.
- Faulkner, G., Pallavicini, A., Formentin, E., Comelli, A., Ievolella, C., Trevisan, S., Bortoletto, G., Scannapieco, P., Salamon, M., Mouly, V., et al. (1999). ZASP: a new Z-band alternatively spliced PDZ-motif protein. *The Journal of Cell Biology* *146*, 465–475.
- Fernandes, J.J., and Keshishian, H. (1996). Patterning the dorsal longitudinal flight muscles (DLM) of *Drosophila*: insights from the ablation of larval scaffolds. *Development* *122*, 3755–3763.
- Fernandes, J., Bate, M., and VijayRaghavan, K. (1991). Development of the indirect flight muscles of *Drosophila*. *Development* *113*, 67–77.
- Fischer, R.S., and Fowler, V.M. (2003). Tropomodulins: life at the slow end. *Trends in Cell Biology* *13*, 593–601.
- Föger, N., Rangell, L., Danilenko, D.M., and Chan, A.C. (2006). Requirement for coronin 1 in T lymphocyte trafficking and cellular homeostasis. *Science* *313*, 839–842.
- Föger, N., Jenckel, A., Orinska, Z., Lee, K.H., Chan, A.C., and Bulfone-Paus, S. (2011). Differential regulation of mast cell degranulation versus cytokine secretion by the actin regulatory proteins Coronin1a and Coronin1b. *Trends in Cell Biology* *208*, 1777–1787.
- Fogerty, F.J., Fessler, L.I., Bunch, T.A., Yaron, Y., Parker, C.G., Nelson, R.E., Brower, D.L., Gullberg, D., and Fessler, J.H. (1994). Tiggrin, a novel *Drosophila* extracellular matrix protein that functions as a ligand for *Drosophila* alpha PS2 beta PS integrins. *Development* *120*, 1747–1758.
- Folker, E.S., Schulman, V.K., and Baylies, M.K. (2012). Muscle length and myonuclear position are independently regulated by distinct Dynein pathways. *Development* *139*, 3827–3837.

- Fradkin, L.G., Dura, J.-M., and Noordermeer, J.N. (2010). Ryks: new partners for Wnts in the developing and regenerating nervous system. *Trends Neurosci.* *33*, 84–92.
- Fradkin, L.G., van Schie, M., Wouda, R.R., de Jong, A., Kamphorst, J.T., Radjkoemar-Bansraj, M., and Noordermeer, J.N. (2004). The *Drosophila* Wnt5 protein mediates selective axon fasciculation in the embryonic central nervous system. *Dev. Biol.* *272*, 362–375.
- Fraenkel, G., and Rudall, K.M. (1940). A study of the physical and chemical properties of the insect cuticle. *Proc. Roy. Soc. Lond. B* *129*, 1–35.
- Frasch, M., Hoey, T., Rushlow, C., Doyle, H., and Levine, M. (1987). Characterization and localization of the even-skipped protein of *Drosophila*. *Embo J.* *6*, 749–759.
- Frasch, M. (1999). Controls in patterning and diversification of somatic muscles during *Drosophila* embryogenesis. *Current Opinion in Genetics & Development* *9*, 522–529.
- Fristrom, J.W. (1965). Development of the morphological mutant *cryptocephal* of *Drosophila melanogaster*. *Genetics* 297–318.
- Frommer, G., Vorbrüggen, G., Pasca, G., Jäckle, H., and Volk, T. (1996). Epidermal *egr*-like zinc finger protein of *Drosophila* participates in myotube guidance. *Embo J.* *15*, 1642–1649.
- Furlong, E.E., Andersen, E.C., Null, B., White, K.P., and Scott, M.P. (2001). Patterns of gene expression during *Drosophila* mesoderm development. *Science* *293*, 1629–1633.
- Füchtbauer, E.M., and Westphal, H. (2004). MyoD and myogenin are coexpressed in regenerating skeletal muscle of the mouse. *Dev. Dyn.* *193*, 34–39.
- Fyrberg, C., Ketchum, A., Ball, E., and Fyrberg, E. (1998). Characterization of lethal *Drosophila melanogaster* alpha-actinin mutants. *Biochem. Genet.* *36*, 299–310.
- Galbiati, F., Volonte, D., Engelman, J.A., Scherer, P.E., and Lisanti, M.P. (1999). Targeted down-regulation of caveolin-3 is sufficient to inhibit myotube formation in differentiating C2C12 myoblasts. Transient activation of p38 mitogen-activated protein kinase is required for induction of caveolin-3 expression and subsequent myotube formation. *J. Biol. Chem.* *274*, 30315–30321.
- Galkin, V.E., Orlova, A., Briehar, W., Kueh, H.Y., Mitchison, T.J., and Egelman, E.H. (2008). Coronin-1A stabilizes F-actin by bridging adjacent actin protomers

and stapling opposite strands of the actin filament. *Journal of Molecular Biology* *376*, 607–613.

Galkin, V.E., Orlova, A., Kudryashov, D.S., Solodukhin, A., Reisler, E., Schröder, G.F., and Egelman, E.H. (2011). Remodeling of actin filaments by ADF/cofilin proteins. *Proceedings of the National Academy of Sciences* *108*, 20568–20572.

Galletta, B.J., Chakravarti, M., Banerjee, R., and Abmayr, S.M. (2004). SNS: Adhesive properties, localization requirements and ectodomain dependence in S2 cells and embryonic myoblasts. *Mech. Dev.* *121*, 1455–1468.

Gallup, B., and Dubowitz, V. (1973). Failure of “dystrophic” neurones to support functional regeneration of normal or dystrophic muscle in culture. *Nature* *243*, 287–289.

Gammie, A.E., Brizzio, V., and Rose, M.D. (1998). Distinct morphological phenotypes of cell fusion mutants. *Mol. Biol. Cell* *9*, 1395–1410.

Gandhi, M., Achard, V., Blanchoin, L., and Goode, B.L. (2009). Coronin switches roles in actin disassembly depending on the nucleotide state of actin. *Mol. Cell* *34*, 364–374.

Gandhi, M., Jangi, M., and Goode, B.L. (2010). Functional surfaces on the actin-binding protein coronin revealed by systematic mutagenesis. *Journal of Biological Chemistry* *285*, 34899–34908.

Gatfield, J., Albrecht, I., Zanolari, B., Steinmetz, M.O., and Pieters, J. (2005). Association of the leukocyte plasma membrane with the actin cytoskeleton through coiled coil-mediated trimeric coronin 1 molecules. *Mol. Biol. Cell* *16*, 2786–2798.

Gaul, U., Seifert, E., Schuh, R., and Jäckle, H. (1987). Analysis of Krüppel protein distribution during early *Drosophila* development reveals posttranscriptional regulation. *Cell* *50*, 639–647.

Geisbrecht, E.R., Haralalka, S., Swanson, S.K., Florens, L., Washburn, M.P., and Abmayr, S.M. (2008). *Drosophila* ELMO/CED-12 interacts with Myoblast city to direct myoblast fusion and ommatidial organization. *Dev. Biol.* *314*, 137–149.

Gelbart, W.M., and Emmert, D.B. (2010). FlyBase High Throughput Expression Pattern Data Beta Version.

George-Weinstein, M., Gerhart, J., Blitz, J., Simak, E., and Knudsen, K.A. (1997). N-cadherin promotes the commitment and differentiation of skeletal muscle precursor cells. *Dev. Biol.* *185*, 14–24.

- Gerke, P. (2003). Homodimerization and Heterodimerization of the Glomerular Podocyte Proteins Nephrin and NEPH1. *Journal of the American Society of Nephrology* 14, 918–926.
- Gildor, B., Massarwa, R., Shilo, B.-Z., and Schejter, E.D. (2009). The SCAR and WASp nucleation-promoting factors act sequentially to mediate *Drosophila* myoblast fusion. *EMBO Rep.* 10, 1043–1050.
- Gillingham, A.K., and Munro, S. (2007). The Small G Proteins of the Arf Family and Their Regulators. *Annu. Rev. Cell Dev. Biol.* 23, 579–611.
- Gilsohn, E., and Volk, T. (2010). Slowdown promotes muscle integrity by modulating integrin-mediated adhesion at the myotendinous junction. *Development* 137, 785–794.
- Goley, E.D., and Welch, M.D. (2006). The ARP2/3 complex: an actin nucleator comes of age. *Nat Rev Mol Cell Biol* 7, 713–726.
- Goode, B.L., Wong, J.J., Butty, A.C., Peter, M., McCormack, A.L., Yates, J.R., Drubin, D.G., and Barnes, G. (1999). Coronin promotes the rapid assembly and cross-linking of actin filaments and may link the actin and microtubule cytoskeletons in yeast. *The Journal of Cell Biology* 144, 83–98.
- Goode, B.L., and Eck, M.J. (2007). Mechanism and Function of Formins in the Control of Actin Assembly. *Annu. Rev. Biochem.* 76, 593–627.
- Gotwals, P.J., Fessler, L.I., Wehrli, M., and Hynes, R.O. (1994). *Drosophila* PS1 integrin is a laminin receptor and differs in ligand specificity from PS2. *Proc. Natl. Acad. Sci. U.S.A.* 91, 11447–11451.
- Graveley, B.R., Brooks, A.N., Carlson, J.W., Cherbas, L., Choi, J., Davis, C.A., Dobin, A., Duff, M., Eads, B., Hansen, K.D., et al. (2010). The *D. melanogaster* transcriptome: modENCODE RNA-Seq data.
- Gregory, S.L., and Brown, N.H. (1998). kakapo, a gene required for adhesion between and within cell layers in *Drosophila*, encodes a large cytoskeletal linker protein related to plectin and dystrophin. *The Journal of Cell Biology* 143, 1271–1282.
- Griffin, C.A., Kafadar, K.A., and Pavlath, G.K. (2009). MOR23 Promotes Muscle Regeneration and Regulates Cell Adhesion and Migration. *Developmental Cell* 17, 649–661.
- Griffin, C.A., Apponi, L.H., Long, K.K., and Pavlath, G.K. (2010). Chemokine expression and control of muscle cell migration during myogenesis. *J. Cell. Sci.* 123, 3052–3060.

Gros, J., Manceau, M., Thomé, V., and Marcelle, C. (2005). A common somitic origin for embryonic muscle progenitors and satellite cells. *Nature Publishing Group* 435, 954–958.

Grounds, M.D., White, J.D., Rosenthal, N., and Bogoyevitch, M.A. (2002). The role of stem cells in skeletal and cardiac muscle repair. *Journal of Histochemistry and Cytochemistry* 50, 589–610.

Gumienny, T.L., Brugnera, E., Tosello-Trampont, A.C., Kinchen, J.M., Haney, L.B., Nishiwaki, K., Walk, S.F., Nemergut, M.E., Macara, I.G., Francis, R., et al. (2001). CED-12/ELMO, a novel member of the CrkII/Dock180/Rac pathway, is required for phagocytosis and cell migration. *Cell* 107, 27–41.

Gunsalus, K.C., Bonaccorsi, S., Williams, E., Verni, F., Gatti, M., and Goldberg, M.L. (1995). Mutations in twinstar, a Drosophila gene encoding a cofilin/ADF homologue, result in defects in centrosome migration and cytokinesis. *The Journal of Cell Biology* 131, 1243–1259.

Guo, M., Jan, L.Y., and Jan, Y.N. (1996). Control of daughter cell fates during asymmetric division: interaction of Numb and Notch. *Neuron* 17, 27–41.

Gurniak, C.B., Perlas, E., and Witke, W. (2005). The actin depolymerizing factor n-cofilin is essential for neural tube morphogenesis and neural crest cell migration. *Dev. Biol.* 278, 231–241.

Haas, J.N. (1950). Cytoplasmic growth in the muscle fibers of larvae of *Drosophila melanogaster*. *Growth* 14, 277–294.

Hakeda-Suzuki, S., Ng, J., Tzu, J., Dietzl, G., Sun, Y., Harms, M., Nardine, T., Luo, L., and Dickson, B.J. (2002). Rac function and regulation during *Drosophila* development. *Nature* 416, 438–442.

Han, S., Nam, J., Li, Y., Kim, S., Cho, S.-H., Cho, Y.S., Choi, S.-Y., Choi, J., Han, K., Kim, Y., et al. (2010). Regulation of dendritic spines, spatial memory, and embryonic development by the TANC family of PSD-95-interacting proteins. *J. Neurosci.* 30, 15102–15112.

Haralalka, S., Shelton, C., Cartwright, H.N., Katzfey, E., Janzen, E., and Abmayr, S.M. (2011). Asymmetric Mbc, active Rac1 and F-actin foci in the fusion-competent myoblasts during myoblast fusion in *Drosophila*. *Development* 138, 1551–1562.

Hart, M.C., and Cooper, J.A. (1999). Vertebrate isoforms of actin capping protein beta have distinct functions *In vivo*. *The Journal of Cell Biology* 147, 1287–1298.

Hasegawa, H., Kiyokawa, E., Tanaka, S., Nagashima, K., Gotoh, N., Shibuya, M., Kurata, T., and Matsuda, M. (1996). DOCK180, a major CRK-binding protein,

alters cell morphology upon translocation to the cell membrane. *Molecular and Cellular Biology* 16, 1770–1776.

Hasty, P., Bradley, A., Morris, J.H., Edmondson, D.G., Venuti, J.M., Olson, E.N., and Klein, W.H. (1993). Muscle deficiency and neonatal death in mice with a targeted mutation in the myogenin gene. *Nature* 364, 501–506.

Hatanaka, H., Ogura, K., Moriyama, K., Ichikawa, S., Yahara, I., and Inagaki, F. (1996). Tertiary structure of destrin and structural similarity between two actin-regulating protein families. *Cell* 85, 1047–1055.

Hatini, V., and DiNardo, S. (2001). Divide and conquer: pattern formation in *Drosophila* embryonic epidermis. *Trends Genet.* 17, 574–579.

Hawke, T.J., and Garry, D.J. (2001). Myogenic satellite cells: physiology to molecular biology. *J. Appl. Physiol.* 91, 534–551.

Hayakawa, K., Minami, N., Ono, S., Ogasawara, Y., Totsuka, T., Abe, H., Tanaka, T., and Obinata, T. (1993). Increased expression of cofilin in dystrophic chicken and mouse skeletal muscles. *Journal of Biochemistry* 114, 582–587.

Heil-Chapdelaine, R.A., Tran, N.K., and Cooper, J.A. (1998). The role of *Saccharomyces cerevisiae* coronin in the actin and microtubule cytoskeletons. *Curr. Biol.* 8, 1281–1284.

Higgs, H.N., and Peterson, K.J. (2005). Phylogenetic analysis of the formin homology 2 domain. *Mol. Biol. Cell* 16, 1–13.

Hiroi, T., Someya, A., Thompson, W., Moss, J., and Vaughan, M. (2006). GEP100/BRAG2: activator of ADP-ribosylation factor 6 for regulation of cell adhesion and actin cytoskeleton via E-cadherin and alpha-catenin. *Proc. Natl. Acad. Sci. U.S.A.* 103, 10672–10677.

Hollnagel, A., Grund, C., Franke, W.W., and Arnold, H.-H. (2002). The cell adhesion molecule M-cadherin is not essential for muscle development and regeneration. *Molecular and Cellular Biology* 22, 4760–4770.

Horsley, V. (2003). Prostaglandin F2alpha stimulates growth of skeletal muscle cells via an NFATC2-dependent pathway. *The Journal of Cell Biology* 161, 111–118.

Horsley, V., Friday, B.B., Matteson, S., Kegley, K.M., Gephart, J., and Pavlath, G.K. (2001). Regulation of the growth of multinucleated muscle cells by an NFATC2-dependent pathway. *The Journal of Cell Biology* 153, 329–338.

Horsley, V., and Pavlath, G.K. (2004). Forming a Multinucleated Cell: Molecules That Regulate Myoblast Fusion. *Cells Tissues Organs* 176, 67–78.

- Horsley, V., Jansen, K.M., Mills, S.T., and Pavlath, G.K. (2003). IL-4 acts as a myoblast recruitment factor during mammalian muscle growth. *Cell* *113*, 483–494.
- Hovens, C.M., Stacker, S.A., Andres, A.C., Harpur, A.G., Ziemiecki, A., and Wilks, A.F. (1992). RYK, a receptor tyrosine kinase-related molecule with unusual kinase domain motifs. *Proc. Natl. Acad. Sci. U.S.A.* *89*, 11818–11822.
- Humphries, C.L., Balcer, H.I., D'Agostino, J.L., Winsor, B., Drubin, D.G., Barnes, G., Andrews, B.J., and Goode, B.L. (2002). Direct regulation of Arp2/3 complex activity and function by the actin binding protein coronin. *The Journal of Cell Biology* *159*, 993–1004.
- Huppertz, B., Bartz, C., and Kokozidou, M. (2006). Trophoblast fusion: fusogenic proteins, syncytins and ADAMs, and other prerequisites for syncytial fusion. *Micron* *37*, 509–517.
- Huppertz, B., and Borges, M. (2010). Placenta Trophoblast Fusion. In *Cell Fusion: Overviews and Methods*, E.H. Chen, ed. (Humana Press), pp. 135–147.
- Ibarra, N., Pollitt, A., and Insall, R.H. (2005). Regulation of actin assembly by SCAR/WAVE proteins. *Biochem. Soc. Trans.* *33*, 1243–1246.
- Iida, K., Moriyama, K., Matsumoto, S., Kawasaki, H., Nishida, E., and Yahara, I. (1993). Isolation of a yeast essential gene, COF1, that encodes a homologue of mammalian cofilin, a low-M(r) actin-binding and depolymerizing protein. *Gene* *124*, 115–120.
- Ikeda, K. (1981). Neuromuscular physiology. In *Genetics and Biology of Drosophila*, M. Ashburner, and T.R.F. Wright, eds. (Academic Press).
- Irintchev, A., Zeschnigk, M., Starzinski-Powitz, A., and Wernig, A. (2004). Expression pattern of M-cadherin in normal, denervated, and regenerating mouse muscles. *Dev. Dyn.* *199*, 326–337.
- Iwai, Y., Usui, T., Hirano, S., Steward, R., Takeichi, M., and Uemura, T. (1997). Axon patterning requires DN-cadherin, a novel neuronal adhesion receptor, in the *Drosophila* embryonic CNS. *Neuron* *19*, 77–89.
- Jackson, C.L., and Casanova, J.E. (2000). Turning on ARF: the Sec7 family of guanine-nucleotide-exchange factors. *Trends in Cell Biology* *10*, 60–67.
- Jagla, T., Bellard, F., Lutz, Y., Dretzen, G., Bellard, M., and Jagla, K. (1998). ladybird determines cell fate decisions during diversification of *Drosophila* somatic muscles. *Development* *125*, 3699–3708.
- Jani, K., and Schöck, F. (2007). Zasp is required for the assembly of functional integrin adhesion sites. *The Journal of Cell Biology* *179*, 1583–1597.

Jansen, K.M. (2006). Mannose receptor regulates myoblast motility and muscle growth. *The Journal of Cell Biology* 174, 403–413.

Jia, D., Gomez, T.S., Metlagel, Z., Umetani, J., Otwinowski, Z., Rosen, M.K., and Billadeau, D.D. (2010). WASH and WAVE actin regulators of the Wiskott-Aldrich syndrome protein (WASP) family are controlled by analogous structurally related complexes. *Proceedings of the National Academy of Sciences* 107, 10442–10447.

Jin, P., Duan, R., Luo, F., Zhang, G., Hong, S.N., and Chen, E.H. (2011). Competition between Blown Fuse and WASP for WIP Binding Regulates the Dynamics of WASP-Dependent Actin Polymerization *In Vivo*. *Developmental Cell* 20, 623–638.

Kaipa, B.R., Shao, H., Schafer, G., Trinkewitz, T., Groth, V., Liu, J., Beck, L., Bogdan, S., Abmayr, S.M., and Onel, S.F. (2013). Dock mediates Scar- and WASp-dependent actin polymerization through interaction with cell adhesion molecules in founder cells and fusion-competent myoblasts. *J. Cell. Sci.* 126, 360–372.

Kang, J.S. (2004). Netrins and neogenin promote myotube formation. *The Journal of Cell Biology* 167, 493–504.

Katzemich, A., Liao, K.A., Czerniecki, S., and Schöck, F. (2013). Alp/Enigma family proteins cooperate in Z-disc formation and myofibril assembly. *PLoS Genet* 9, e1003342.

Katzemich, A., Long, J.Y., Jani, K., Lee, B.R., and Schöck, F. (2011). Muscle type-specific expression of Zasp52 isoforms in *Drosophila*. *Gene Expr. Patterns* 11, 484–490.

Kawamura, K. (2004). N-WASP and WAVE2 Acting Downstream of Phosphatidylinositol 3-Kinase Are Required for Myogenic Cell Migration Induced by Hepatocyte Growth Factor. *Journal of Biological Chemistry* 279, 54862–54871.

Kelso, R.J., Buszczak, M., Quiñones, A.T., Castiblanco, C., Mazzalupo, S., and Cooley, L. (2004). Flytrap, a database documenting a GFP protein-trap insertion screen in *Drosophila melanogaster*. *Nucleic Acids Research* 32, D418–D420.

Kesper, D.A., Stute, C., Buttgerit, D., Kreisköther, N., Vishnu, S., Fischbach, K.-F., and Renkawitz-Pohl, R. (2007). Myoblast fusion in *Drosophila melanogaster* is mediated through a fusion-restricted myogenic-adhesive structure (FuRMAS). *Dev. Dyn.* 236, 404–415.

Kessels, M.M., Engqvist-Goldstein, A.E., and Drubin, D.G. (2000). Association of mouse actin-binding protein 1 (mAbp1/SH3P7), an Src kinase target, with

dynamic regions of the cortical actin cytoskeleton in response to Rac1 activation. *Mol. Biol. Cell* *11*, 393–412.

Kessels, M.M., Engqvist-Goldstein, A.E., Drubin, D.G., and Qualmann, B. (2001). Mammalian Abp1, a signal-responsive F-actin-binding protein, links the actin cytoskeleton to endocytosis via the GTPase dynamin. *The Journal of Cell Biology* *153*, 351–366.

Khoshnoodi, J., Sigmundsson, K., Ofverstedt, L.-G., Skoglund, U., Obrink, B., Wartiovaara, J., and Tryggvason, K. (2003). Nephrin promotes cell-cell adhesion through homophilic interactions. *Am. J. Pathol.* *163*, 2337–2346.

Kidd, T., Bland, K.S., and Goodman, C.S. (1999). Slit is the midline repellent for the robo receptor in *Drosophila*. *Cell* *96*, 785–794.

Kim, S., Shilagardi, K., Zhang, S., Hong, S.N., Sens, K.L., Bo, J., Gonzalez, G.A., and Chen, E.H. (2007). A critical function for the actin cytoskeleton in targeted exocytosis of prefusion vesicles during myoblast fusion. *Developmental Cell* *12*, 571–586.

Kimura, T., Taniguchi, S., and Niki, I. (2010). Actin assembly controlled by GDP-Rab27a is essential for endocytosis of the insulin secretory membrane. *Archives of Biochemistry and Biophysics* *496*, 33–37.

Kiyokawa, E., Hashimoto, Y., Kobayashi, S., Sugimura, H., Kurata, T., and Matsuda, M. (1998a). Activation of Rac1 by a Crk SH3-binding protein, DOCK180. *Genes Dev.* *12*, 3331–3336.

Kiyokawa, E., Hashimoto, Y., Kurata, T., Sugimura, H., and Matsuda, M. (1998b). Evidence that DOCK180 up-regulates signals from the CrkII-p130(Cas) complex. *J. Biol. Chem.* *273*, 24479–24484.

Knirr, S., Azpiazu, N., and Frasch, M. (1999). The role of the NK-homeobox gene *slouch* (S59) in somatic muscle patterning. *Development* *126*, 4525–4535.

Knudsen, K.A., and Horwitz, A.F. (1977). Tandem events in myoblast fusion. *Dev. Biol.* *58*, 328–338.

Kocherlakota, K.S., Wu, J.M., McDermott, J., and Abmayr, S.M. (2008). Analysis of the Cell Adhesion Molecule Sticks-and-Stones Reveals Multiple Redundant Functional Domains, Protein-Interaction Motifs and Phosphorylated Tyrosines That Direct Myoblast Fusion in *Drosophila melanogaster*. *Genetics* *178*, 1371–1383.

Kramer, S.G., Kidd, T., Simpson, J.H., and Goodman, C.S. (2001). Switching repulsion to attraction: changing responses to slit during transition in mesoderm migration. *Science* *292*, 737–740.

- Krauss, R.S., Cole, F., Gaio, U., Takaesu, G., Zhang, W., and Kang, J.-S. (2005). Close encounters: regulation of vertebrate skeletal myogenesis by cell-cell contact. *J. Cell. Sci.* *118*, 2355–2362.
- Kraut, R., and Campos-Ortega, J.A. (1996). *inscuteable*, a neural precursor gene of *Drosophila*, encodes a candidate for a cytoskeleton adaptor protein. *Dev. Biol.* *174*, 65–81.
- Kreuz, A.J., Simcox, A., and Maughan, D. (1996). Alterations in flight muscle ultrastructure and function in *Drosophila* tropomyosin mutants. *The Journal of Cell Biology* *135*, 673–687.
- Kueh, H.Y., Charras, G.T., Mitchison, T.J., and Briehner, W.M. (2008). Actin disassembly by cofilin, coronin, and Aip1 occurs in bursts and is inhibited by barbed-end cappers. *The Journal of Cell Biology* *182*, 341–353.
- LaBeau-DiMenna, E.M., Clark, K.A., Bauman, K.D., Parker, D.S., Cripps, R.M., and Geisbrecht, E.R. (2012). Thin, a Trim32 ortholog, is essential for myofibril stability and is required for the integrity of the costamere in *Drosophila*. *Proceedings of the National Academy of Sciences* *109*, 17983–17988.
- Lahaye, L.L., Wouda, R.R., de Jong, A.W.M., Fradkin, L.G., and Noordermeer, J.N. (2012). WNT5 Interacts with the Ryk Receptors Doughnut and Derailed to Mediate Muscle Attachment Site Selection in *Drosophila melanogaster*. *PLoS ONE* *7*, e32297.
- Lappalainen, P., Fedorov, E.V., Fedorov, A.A., Almo, S.C., and Drubin, D.G. (1997). Essential functions and actin-binding surfaces of yeast cofilin revealed by systematic mutagenesis. *Embo J.* *16*, 5520–5530.
- Lappalainen, P., Kessels, M.M., Cope, M.J., and Drubin, D.G. (1998). The ADF homology (ADF-H) domain: a highly exploited actin-binding module. *Mol. Biol. Cell* *9*, 1951–1959.
- Laurin, M., Fradet, N., Blangy, A., Hall, A., Vuori, K., and Côté, J.-F. (2008). The atypical Rac activator Dock180 (Dock1) regulates myoblast fusion in vivo. *Proceedings of the National Academy of Sciences* *105*, 15446–15451.
- Lemmon, M.A. (2008). Membrane recognition by phospholipid-binding domains. *Nat Rev Mol Cell Biol* *9*, 99–111.
- Leonard, S.A., Gittis, A.G., Petrella, E.C., Pollard, T.D., and Lattman, E.E. (1997). Crystal structure of the actin-binding protein actophorin from *Acanthamoeba*. *Nat. Struct. Biol.* *4*, 369–373.
- Leptin, M., Bogaert, T., Lehmann, R., and Wilcox, M. (1989). The function of PS integrins during *Drosophila* embryogenesis. *Cell* *56*, 401–408.

- Li, Z., Mericskay, M., Agbulut, O., Butler-Browne, G., Carlsson, L., Thornell, L.E., Babinet, C., and Paulin, D. (1997). Desmin is essential for the tensile strength and integrity of myofibrils but not for myogenic commitment, differentiation, and fusion of skeletal muscle. *The Journal of Cell Biology* *139*, 129–144.
- Lin, M.-C., Galletta, B.J., Sept, D., and Cooper, J.A. (2010). Overlapping and distinct functions for cofilin, coronin and Aip1 in actin dynamics in vivo. *J. Cell. Sci.* *123*, 1329–1342.
- Linardopoulou, E.V., Parghi, S.S., Friedman, C., Osborn, G.E., Parkhurst, S.M., and Trask, B.J. (2007). Human subtelomeric WASH genes encode a new subclass of the WASP family. *PLoS Genet* *3*, e237.
- Littlefield, R., and Fowler, V.M. (1998). Defining actin filament length in striated muscle: rulers and caps or dynamic stability? *Annu. Rev. Cell Dev. Biol.* *14*, 487–525.
- Liu, C.Z., Chen, Y., and Sui, S.F. (2006). The identification of a new actin-binding region in p57. *Cell Res.* *16*, 106–112.
- Liu, S.-L., Needham, K.M., May, J.R., and Nolen, B.J. (2011). Mechanism of a concentration-dependent switch between activation and inhibition of Arp2/3 complex by coronin. *Journal of Biological Chemistry* *286*, 17039–17046.
- Louis, M., Huber, T., Benton, R., Sakmar, T.P., and Vosshall, L.B. (2008a). Bilateral olfactory sensory input enhances chemotaxis behavior. *Nat. Neurosci.* *11*, 187–199.
- Louis, M., Piccinotti, S., and Vosshall, L.B. (2008b). High-resolution measurement of odor-driven behavior in *Drosophila* larvae. *J Vis Exp*.
- Luo, L., Liao, Y.J., Jan, L.Y., and Jan, Y.N. (1994). Distinct morphogenetic functions of similar small GTPases: *Drosophila* Drac1 is involved in axonal outgrowth and myoblast fusion. *Genes Dev.* *8*, 1787–1802.
- Machado, C., and Andrew, D.J. (2000). D-Titin: a giant protein with dual roles in chromosomes and muscles. *The Journal of Cell Biology* *151*, 639–652.
- MackKrell, A.J., Blumberg, B., Haynes, S.R., and Fessler, J.H. (1988). The lethal myospheroid gene of *Drosophila* encodes a membrane protein homologous to vertebrate integrin beta subunits. *Proc. Natl. Acad. Sci. U.S.a.* *85*, 2633–2637.
- Mahaffey, J.P., Grego-Bessa, J., Liem, K.F., and Anderson, K.V. (2013). Cofilin and Vangl2 cooperate in the initiation of planar cell polarity in the mouse embryo. *Development* *140*, 1262–1271.

- Maley, M.A., Fan, Y., Beilharz, M.W., and Grounds, M.D. (1994). Intrinsic differences in MyoD and myogenin expression between primary cultures of SJL/J and BALB/C skeletal muscle. *Experimental Cell Research* *211*, 99–107.
- Maniak, M., Rauchenberger, R., Albrecht, R., Murphy, J., and Gerisch, G. (1995). Coronin involved in phagocytosis: dynamics of particle-induced relocalization visualized by a green fluorescent protein Tag. *Cell* *83*, 915–924.
- Marchand, J.B., Kaiser, D.A., Pollard, T.D., and Higgs, H.N. (2001). Interaction of WASP/Scar proteins with actin and vertebrate Arp2/3 complex. *Nat. Cell Biol.* *3*, 76–82.
- Mardahl-Dumesnil, M., and Fowler, V.M. (2001). Thin filaments elongate from their pointed ends during myofibril assembly in *Drosophila* indirect flight muscle. *The Journal of Cell Biology* *155*, 1043–1053.
- Marín, M.-C., Rodríguez, J.-R., and Ferrús, A. (2004). Transcription of *Drosophila* troponin I gene is regulated by two conserved, functionally identical, synergistic elements. *Mol. Biol. Cell* *15*, 1185–1196.
- Massarwa, R., Carmon, S., Shilo, B.-Z., and Schejter, E.D. (2007). WIP/WASp-Based Actin-Polymerization Machinery Is Essential for Myoblast Fusion in *Drosophila*. *Developmental Cell* *12*, 557–569.
- Matsuda, M., Ota, S., Tanimura, R., Nakamura, H., Matuoka, K., Takenawa, T., Nagashima, K., and Kurata, T. (1996). Interaction between the amino-terminal SH3 domain of CRK and its natural target proteins. *J. Biol. Chem.* *271*, 14468–14472.
- McGough, A. (1998). F-actin-binding proteins. *Current Opinion in Structural Biology* *8*, 166–176.
- McGough, A., Pope, B., Chiu, W., and Weeds, A. (1997). Cofilin changes the twist of F-actin: implications for actin filament dynamics and cellular function. *The Journal of Cell Biology* *138*, 771–781.
- McKim, K.S., Matheson, C., Marra, M.A., Wakarchuk, M.F., and Baillie, D.L. (1994). The *Caenorhabditis elegans* unc-60 gene encodes proteins homologous to a family of actin-binding proteins. *Mol. Gen. Genet.* *242*, 346–357.
- Meller, N. (2005). CZH proteins: a new family of Rho-GEFs. *J. Cell. Sci.* *118*, 4937–4946.
- Menon, S.D. (2005). A positive feedback loop between Dumbfounded and Rolling pebbles leads to myotube enlargement in *Drosophila*. *The Journal of Cell Biology* *169*, 909–920.

- Menon, S.D., and Chia, W. (2001). *Drosophila* rolling pebbles: a multidomain protein required for myoblast fusion that recruits D-Titin in response to the myoblast attractant Dumbfounded. *Developmental Cell* *1*, 691–703.
- Metzger, T., Gache, V., Xu, M., Cadot, B., Folker, E.S., Richardson, B.E., Gomes, E.R., and Baylies, M.K. (2012). MAP and kinesin-dependent nuclear positioning is required for skeletal muscle function. *Nature* *484*, 120–124.
- Miki, H., Miura, K., and Takenawa, T. (1996). N-WASP, a novel actin-depolymerizing protein, regulates the cortical cytoskeletal rearrangement in a PIP2-dependent manner downstream of tyrosine kinases. *Embo J.* *15*, 5326–5335.
- Miyauchi-Nomura, S., Obinata, T., and Sato, N. (2012). Cofilin is required for organization of sarcomeric actin filaments in chicken skeletal muscle cells. *Cytoskeleton (Hoboken)* *69*, 290–302.
- Miyazaki, J., Takaki, S., Araki, K., Tashiro, F., Tominaga, A., Takatsu, K., and Yamamura, K. (1989). Expression vector system based on the chicken beta-actin promoter directs efficient production of interleukin-5. *Gene* *79*, 269–277.
- Mohler, W.A., Simske, J.S., Williams-Masson, E.M., Hardin, J.D., and White, J.G. (1998). Dynamics and ultrastructure of developmental cell fusions in the *Caenorhabditis elegans* hypodermis. *Curr. Biol.* *8*, 1087–1090.
- Mohri, K., Takano-Ohmuro, H., Nakashima, H., Hayakawa, K., Endo, T., Hanaoka, K., and Obinata, T. (2000). Expression of cofilin isoforms during development of mouse striated muscles. *J. Muscle Res. Cell. Motil.* *21*, 49–57.
- Moon, A.L., Janmey, P.A., Louie, K.A., and Drubin, D.G. (1993). Cofilin is an essential component of the yeast cortical cytoskeleton. *The Journal of Cell Biology* *120*, 421–435.
- Moore, C.A., Parkin, C.A., Bidet, Y., and Ingham, P.W. (2007). A role for the Myoblast city homologues Dock1 and Dock5 and the adaptor proteins Crk and Crk-like in zebrafish myoblast fusion. *Development* *134*, 3145–3153.
- Moore, R., and Walsh, F.S. (1993). The cell adhesion molecule M-cadherin is specifically expressed in developing and regenerating, but not denervated skeletal muscle. *Development* *117*, 1409–1420.
- Morgan, J.E., Beauchamp, J.R., Pagel, C.N., Peckham, M., Ataliotis, P., Jat, P.S., Noble, M.D., Farmer, K., and Partridge, T.A. (1994). Myogenic cell lines derived from transgenic mice carrying a thermolabile T antigen: a model system for the derivation of tissue-specific and mutation-specific cell lines. *Dev. Biol.* *162*, 486–498.

- Morgan, T.E., Lockerbie, R.O., Minamide, L.S., Browning, M.D., and Bamburg, J.R. (1993). Isolation and characterization of a regulated form of actin depolymerizing factor. *The Journal of Cell Biology* 122, 623–633.
- Morin, X., Daneman, R., Zavortink, M., and Chia, W. (2001). A protein trap strategy to detect GFP-tagged proteins expressed from their endogenous loci in *Drosophila*. *Proc. Natl. Acad. Sci. U.S.a.* 98, 15050–15055.
- Morishige, M., Hashimoto, S., Ogawa, E., Toda, Y., Kotani, H., Hirose, M., Wei, S., Hashimoto, A., Yamada, A., Yano, H., et al. (2007). GEP100 links epidermal growth factor receptor signalling to Arf6 activation to induce breast cancer invasion. *Nature Publishing Group* 10, 85–92.
- Morriss, G.R., Bryantsev, A.L., Chechenova, M., LaBeau, E.M., Lovato, T.L., Ryan, K.M., and Cripps, R.M. (2012). Analysis of skeletal muscle development in *Drosophila*. *Methods Mol. Biol.* 798, 127–152.
- Mukherjee, P., Gildor, B., Shilo, B.Z., VijayRaghavan, K., and Schejter, E.D. (2011). The actin nucleator WASp is required for myoblast fusion during adult *Drosophila* myogenesis. *Development* 138, 2347–2357.
- Muneyuki, E., Nishida, E., Sutoh, K., and Sakai, H. (1985). Purification of cofilin, a 21,000 molecular weight actin-binding protein, from porcine kidney and identification of the cofilin-binding site in the actin sequence. *Journal of Biochemistry* 97, 563–568.
- Munsie, L.N., Caron, N., Desmond, C.R., and Truant, R. (2009). Lifeact cannot visualize some forms of stress-induced twisted F-actin. *Nat Meth* 6, 317.
- Nabel-Rosen, H., Dorevitch, N., Reuveny, A., and Volk, T. (1999). The balance between two isoforms of the *Drosophila* RNA-binding protein how controls tendon cell differentiation. *Mol. Cell* 4, 573–584.
- Nabel-Rosen, H., Volohonsky, G., Reuveny, A., Zaidel-Bar, R., and Volk, T. (2002). Two isoforms of the *Drosophila* RNA binding protein, how, act in opposing directions to regulate tendon cell differentiation. *Developmental Cell* 2, 183–193.
- Nabeshima, Y., Hanaoka, K., Hayasaka, M., Esumi, E., Li, S., Nonaka, I., and Nabeshima, Y. (1993). Myogenin gene disruption results in perinatal lethality because of severe muscle defect. *Nature* 364, 532–535.
- Nag, S., Larsson, M., Robinson, R.C., and Burtnick, L.D. (2013). Gelsolin: The tail of a molecular gymnast. *Cytoskeleton (Hoboken)* 70, 360–384.
- Nagaoka, R., Abe, H., and Obinata, T. (1996a). Site-directed mutagenesis of the phosphorylation site of cofilin: its role in cofilin-actin interaction and cytoplasmic localization. *Cell Motil. Cytoskeleton* 35, 200–209.

- Nagaoka, R., Minami, N., Hayakawa, K., Abe, H., and Obinata, T. (1996b). Quantitative analysis of low molecular weight G-actin-binding proteins, cofilin, ADF and profilin, expressed in developing and degenerating chicken skeletal muscles. *J. Muscle Res. Cell. Motil.* *17*, 463–473.
- Newman, S.M., and Wright, T.R. (1981). A histological and ultrastructural analysis of developmental defects produced by the mutation, lethal(1)mysospheroid, in *Drosophila melanogaster*. *Dev. Biol.* *86*, 393–402.
- Ng, J., and Luo, L. (2004). Rho GTPases regulate axon growth through convergent and divergent signaling pathways. *Neuron* *44*, 779–793.
- Nguyen, H.T., Bodmer, R., Abmayr, S.M., McDermott, J.C., and Spoerel, N.A. (1994). D-mef2: a *Drosophila* mesoderm-specific MADS box-containing gene with a biphasic expression profile during embryogenesis. *Proc. Natl. Acad. Sci. U.S.A.* *91*, 7520–7524.
- Nishida, E., Maekawa, S., and Sakai, H. (1984). Cofilin, a protein in porcine brain that binds to actin filaments and inhibits their interactions with myosin and tropomyosin. *Biochemistry* *23*, 5307–5313.
- Niwa, R., Nagata-Ohashi, K., Takeichi, M., Mizuno, K., and Uemura, T. (2002). Control of actin reorganization by Slingshot, a family of phosphatases that dephosphorylate ADF/cofilin. *Cell* *108*, 233–246.
- Noble, M., Lewis, S.A., and Cowan, N.J. (1989). The microtubule binding domain of microtubule-associated protein MAP1B contains a repeated sequence motif unrelated to that of MAP2 and tau. *The Journal of Cell Biology* *109*, 3367–3376.
- Nolan, K.M., Barrett, K., Lu, Y., Hu, K.Q., Vincent, S., and Settleman, J. (1997). Myoblast city, the *Drosophila* homolog of DOCK180/CED-5, is required in a Rac signaling pathway utilized for multiple developmental processes. *Genes Dev.* *138*, 3337–3342.
- Nolen, B.J., Littlefield, R.S., and Pollard, T.D. (2004). Crystal structures of actin-related protein 2/3 complex with bound ATP or ADP. *Proc. Natl. Acad. Sci. U.S.A.* *101*, 15627–15632.
- Nongthomba, U., Ansari, M., Thimmaiya, D., Stark, M., and Sparrow, J. (2007). Aberrant Splicing of an Alternative Exon in the *Drosophila* Troponin-T Gene Affects Flight Muscle Development. *Genetics* *177*, 295–306.
- Nose, A., Isshiki, T., and Takeichi, M. (1998). Regional specification of muscle progenitors in *Drosophila*: the role of the msh homeobox gene. *Development* *125*, 215–223.

- Nowak, S.J., Nahirney, P.C., Hadjantonakis, A.-K., and Baylies, M.K. (2009). Nap1-mediated actin remodeling is essential for mammalian myoblast fusion. *J. Cell. Sci.* *122*, 3282–3293.
- O'Brien, S.P., Seipel, K., Medley, Q.G., Bronson, R., Segal, R., and Streuli, M. (2000). Skeletal muscle deformity and neuronal disorder in Trio exchange factor-deficient mouse embryos. *Proc. Natl. Acad. Sci. U.S.A.* *97*, 12074–12078.
- Ockeloen, C.W., Gilhuis, H.J., Pfundt, R., Kamsteeg, E.J., Agrawal, P.B., Beggs, A.H., Dara Hama-Amin, A., Diekstra, A., Knoers, N.V.A.M., Lammens, M., et al. (2012). Congenital myopathy caused by a novel missense mutation in the CFL2 gene. *Neuromuscular Disorders* *22*, 632–639.
- Oda, T., Iwasa, M., Aihara, T., Maéda, Y., and Narita, A. (2009). The nature of the globular- to fibrous-actin transition. *Nature* *457*, 441–445.
- Ohashi, K., Hosoya, T., Takahashi, K., Hing, H., and Mizuno, K. (2000). A *Drosophila* homolog of LIM-kinase phosphorylates cofilin and induces actin cytoskeletal reorganization. *Biochemical and Biophysical Research Communications* *276*, 1178–1185.
- Ohtake, Y. (2006). Multifunctional roles of MT1-MMP in myofiber formation and morphostatic maintenance of skeletal muscle. *J. Cell. Sci.* *119*, 3822–3832.
- Oku, T., Itoh, S., Ishii, R., Suzuki, K., Nauseef, W.M., Toyoshima, S., and Tsuji, T. (2005). Homotypic dimerization of the actin-binding protein p57/coronin-1 mediated by a leucine zipper motif in the C-terminal region. *Biochem. J.* *387*, 325–331.
- Oku, T., Itoh, S., Okano, M., Suzuki, A., Suzuki, K., Nakajin, S., Tsuji, T., Nauseef, W.M., and Toyoshima, S. (2003). Two regions responsible for the actin binding of p57, a mammalian coronin family actin-binding protein. *Biol. Pharm. Bull.* *26*, 409–416.
- Onel, S., Bolke, L., and Klämbt, C. (2004). The *Drosophila* ARF6-GEF Schizo controls commissure formation by regulating Slit. *Development* *131*, 2587–2594.
- Ono, S., and Benian, G.M. (1998). Two *Caenorhabditis elegans* actin depolymerizing factor/cofilin proteins, encoded by the unc-60 gene, differentially regulate actin filament dynamics. *J. Biol. Chem.* *273*, 3778–3783.
- Ono, S., Baillie, D.L., and Benian, G.M. (1999). UNC-60B, an ADF/cofilin family protein, is required for proper assembly of actin into myofibrils in *Caenorhabditis elegans* body wall muscle. *The Journal of Cell Biology* *145*, 491–502.

- Ono, S., Minami, N., Abe, H., and Obinata, T. (1994). Characterization of a novel cofilin isoform that is predominantly expressed in mammalian skeletal muscle. *J. Biol. Chem.* *269*, 15280–15286.
- Ono, S. (2001). The *Caenorhabditis elegans* unc-78 gene encodes a homologue of actin-interacting protein 1 required for organized assembly of muscle actin filaments. *The Journal of Cell Biology* *152*, 1313–1319.
- Otomo, T., Tomchick, D.R., Otomo, C., Panchal, S.C., Machius, M., and Rosen, M.K. (2005). Structural basis of actin filament nucleation and processive capping by a formin homology 2 domain. *Nature* *433*, 488–494.
- Pajcini, K.V., Pomerantz, J.H., Alkan, O., Doyonnas, R., and Blau, H.M. (2008). Myoblasts and macrophages share molecular components that contribute to cell-cell fusion. *The Journal of Cell Biology* *180*, 1005–1019.
- Palamidessi, A., Frittoli, E., Garré, M., Faretta, M., Mione, M., Testa, I., Diaspro, A., Lanzetti, L., Scita, G., and Di Fiore, P.P. (2008). Endocytic Trafficking of Rac Is Required for the Spatial Restriction of Signaling in Cell Migration. *Cell* *134*, 135–147.
- Papalouka, V., Arvanitis, D.A., Vafiadaki, E., Mavroidis, M., Papadodima, S.A., Spiliopoulou, C.A., Kremastinos, D.T., Kranias, E.G., and Sanoudou, D. (2009). Muscle Lim Protein Interacts with Cofilin 2 and Regulates F-Actin Dynamics in Cardiac and Skeletal Muscle. *Molecular and Cellular Biology* *29*, 6046–6058.
- Papapetrou, E.P., Tomishima, M.J., Chambers, S.M., Mica, Y., Reed, E., Menon, J., Tabar, V., Mo, Q., Studer, L., and Sadelain, M. (2009). Stoichiometric and temporal requirements of Oct4, Sox2, Klf4, and c-Myc expression for efficient human iPSC induction and differentiation. *Proceedings of the National Academy of Sciences* *106*, 12759–12764.
- Papayannopoulos, V., Co, C., Prehoda, K.E., Snapper, S., Taunton, J., and Lim, W.A. (2005). A polybasic motif allows N-WASP to act as a sensor of PIP(2) density. *Mol. Cell* *17*, 181–191.
- Parsons, R. (1974). Expression of the dystrophin muscularis (dy) recessive gene in mice. *Nature* *251*, 621–622.
- Pätäri Sampo, A., Ihalmo, P., and Holthöfer, H. (2006). Molecular basis of the glomerular filtration: Nephrin and the emerging protein complex at the podocyte slit diaphragm. *Ann Med* *38*, 483–492.
- Petersen, J., Nielsen, O., Egel, R., and Hagan, I.M. (1998). FH3, a domain found in formins, targets the fission yeast formin Fus1 to the projection tip during conjugation. *The Journal of Cell Biology* *141*, 1217–1228.

- Piepenburg, O., Vorbrüggen, G., and Jäckle, H. (2000). *Drosophila* segment borders result from unilateral repression of hedgehog activity by wingless signaling. *Mol. Cell* *6*, 203–209.
- Pollard, T.D. (1986). Rate constants for the reactions of ATP- and ADP-actin with the ends of actin filaments. *The Journal of Cell Biology* *103*, 2747–2754.
- Pollard, T.D., and Cooper, J.A. (1986). Actin and actin-binding proteins. A critical evaluation of mechanisms and functions. *Annu. Rev. Biochem.* *55*, 987–1035.
- Pollard, T.D., Blanchoin, L., and Mullins, R.D. (2000). Molecular mechanisms controlling actin filament dynamics in nonmuscle cells. *Annu Rev Biophys Biomol Struct* *29*, 545–576.
- Pollard, T.D. (2007). Regulation of actin filament assembly by Arp2/3 complex and formins. *Annu Rev Biophys Biomol Struct* *36*, 451–477.
- Pomiès, P., Macalma, T., and Beckerle, M.C. (1999). Purification and characterization of an alpha-actinin-binding PDZ-LIM protein that is up-regulated during muscle differentiation. *J. Biol. Chem.* *274*, 29242–29250.
- Powell, J.A. (1973). Development of normal and genetically dystrophic mouse muscle in tissue culture. I. Prefusion and fusion activities of muscle cells: phase contrast and time lapse study. *Experimental Cell Research* *80*, 251–264.
- Pownall, M.E., Gustafsson, M.K., and Emerson, C.P., Jr. (2002). Myogenic Regulatory Factors and the Specification of Muscle Progenitors in Vertebrate Embryos. *Annu. Rev. Cell Dev. Biol.* *18*, 747–783.
- Prakash, S., Caldwell, J.C., Eberl, D.F., and Clandinin, T.R. (2005). *Drosophila* N-cadherin mediates an attractive interaction between photoreceptor axons and their targets. *Nat. Neurosci.* *8*, 443–450.
- Pring, M., Evangelista, M., Boone, C., Yang, C., and Zigmond, S.H. (2003). Mechanism of Formin-Induced Nucleation of Actin Filaments. *Biochemistry* *42*, 486–496.
- Prokop, A., Martín-Bermudo, M.D., Bate, M., and Brown, N.H. (1998a). Absence of PS integrins or laminin A affects extracellular adhesion, but not intracellular assembly, of hemiadherens and neuromuscular junctions in *Drosophila* embryos. *Dev. Biol.* *196*, 58–76.
- Prokop, A., Uhler, J., Roote, J., and Bate, M. (1998b). The kakapo mutation affects terminal arborization and central dendritic sprouting of *Drosophila* motorneurons. *The Journal of Cell Biology* *143*, 1283–1294.

- Pruyne, D., Evangelista, M., Yang, C., Bi, E., Zigmond, S., Bretscher, A., and Boone, C. (2002). Role of formins in actin assembly: nucleation and barbed-end association. *Science* 297, 612–615.
- Puius, Y.A., Mahoney, N.M., and Almo, S.C. (1998). The modular structure of actin-regulatory proteins. *Curr. Opin. Cell Biol.* 10, 23–34.
- Quinlan, M.E., Heuser, J.E., Kerkhoff, E., and Mullins, R.D. (2005). *Drosophila* Spire is an actin nucleation factor. *Nature* 433, 382–388.
- Quiñones-Coello, A.T., Petrella, L.N., Ayers, K., Melillo, A., Mazzalupo, S., Hudson, A.M., Wang, S., Castiblanco, C., Buszczak, M., Hoskins, R.A., et al. (2007). Exploring strategies for protein trapping in *Drosophila*. *Genetics* 175, 1089–1104.
- Radhakrishna, H., and Donaldson, J.G. (1997). ADP-ribosylation factor 6 regulates a novel plasma membrane recycling pathway. *The Journal of Cell Biology* 139, 49–61.
- Radhakrishna, H., Al-Awar, O., Khachikian, Z., and Donaldson, J.G. (1999). ARF6 requirement for Rac ruffling suggests a role for membrane trafficking in cortical actin rearrangements. *J. Cell. Sci.* 112 (Pt 6), 855–866.
- Radice, G.L., Rayburn, H., Matsunami, H., Knudsen, K.A., Takeichi, M., and Hynes, R.O. (1997). Developmental defects in mouse embryos lacking N-cadherin. *Dev. Biol.* 181, 64–78.
- Rappleye, C.A., Paredes, A.R., Smith, C.W., McDonald, K.L., and Aroian, R.V. (1999). The coronin-like protein POD-1 is required for anterior-posterior axis formation and cellular architecture in the nematode *Caenorhabditis elegans*. *Genes Dev.* 13, 2838–2851.
- Rau, A., Buttgerit, D., Holz, A., Fetter, R., Doberstein, S.K., Paululat, A., Staudt, N., Skeath, J., Michelson, A.M., and Renkawitz-Pohl, R. (2001). rolling pebbles (rols) is required in *Drosophila* muscle precursors for recruitment of myoblasts for fusion. *Development* 128, 5061–5073.
- Raucher, D., Stauffer, T., Chen, W., Shen, K., Guo, S., York, J.D., Sheetz, M.P., and Meyer, T. (2000). Phosphatidylinositol 4,5-bisphosphate functions as a second messenger that regulates cytoskeleton-plasma membrane adhesion. *Cell* 100, 221–228.
- Ravenscroft, G., Miyatake, S., Lehtokari, V.-L., Todd, E.J., Vornanen, P., Yau, K.S., Hayashi, Y.K., Miyake, N., Tsurusaki, Y., Doi, H., et al. (2013). Mutations in KLHL40 are a frequent cause of severe autosomal-recessive nemaline myopathy. *Am. J. Hum. Genet.* 93, 6–18.

- Rearden, A. (1994). A new LIM protein containing an autoepitope homologous to "senescent cell antigen". *Biochemical and Biophysical Research Communications* 201, 1124–1131.
- Relaix, F. (2006). Skeletal muscle progenitor cells: from embryo to adult. *Cell. Mol. Life Sci.* 63, 1221–1225.
- Relaix, F., Rocancourt, D., Mansouri, A., and Buckingham, M. (2004). Divergent functions of murine Pax3 and Pax7 in limb muscle development. *Genes Dev.* 18, 1088–1105.
- Relaix, F., Rocancourt, D., Mansouri, A., and Buckingham, M. (2005). A Pax3/Pax7-dependent population of skeletal muscle progenitor cells. *Nature Publishing Group* 435, 948–953.
- Remedios, dos, C.G., Chhabra, D., Kekic, M., Dedova, I.V., Tsubakihara, M., Berry, D.A., and Nosworthy, N.J. (2003). Actin binding proteins: regulation of cytoskeletal microfilaments. *Physiological Reviews* 83, 433–473.
- Rhee, J.M., Purity, M.K., Lackan, C.S., Long, J.Z., Kondoh, G., Takeda, J., and Hadjantonakis, A.-K. (2006). In vivo imaging and differential localization of lipid-modified GFP-variant fusions in embryonic stem cells and mice. *Genesis* 44, 202–218.
- Richardson, B.E., Beckett, K., Nowak, S.J., and Baylies, M.K. (2007). SCAR/WAVE and Arp2/3 are crucial for cytoskeletal remodeling at the site of myoblast fusion. *Development* 134, 4357–4367.
- Riedl, J., Crevenna, A.H., Kessenbrock, K., Yu, J.H., Neukirchen, D., Bista, M., Bradke, F., Jenne, D., Holak, T.A., Werb, Z., et al. (2008). Lifeact: a versatile marker to visualize F-actin. *Nat Meth* 5, 605–607.
- Ritzenthaler, S., Suzuki, E., and Chiba, A. (2000). Postsynaptic filopodia in muscle cells interact with innervating motoneuron axons. *Nat. Neurosci.* 3, 1012–1017.
- Rivero, F., Muramoto, T., Meyer, A.-K., Urushihara, H., Uyeda, T.Q.P., and Kitayama, C. (2005). A comparative sequence analysis reveals a common GBD/FH3-FH1-FH2-DAD architecture in formins from Dictyostelium, fungi and metazoa. *BMC Genomics* 6, 28.
- Robertson, C.W. (1936). Metamorphosis of *Drosophila melanogaster* including an accurately timed account of the principal morphological changes. *J. Morph.* 59, 351–399.

- Robinson, R.C., Turbedsky, K., Kaiser, D.A., Marchand, J.B., Higgs, H.N., Choe, S., and Pollard, T.D. (2001). Crystal structure of Arp2/3 complex. *Science* *294*, 1679–1684.
- Rochlin, K., Yu, S., Roy, S., and Baylies, M.K. (2009). Myoblast fusion: when it takes more to make one. *Dev. Biol.* *341*, 66–83.
- Rodal, A.A., Tetreault, J.W., Lappalainen, P., Drubin, D.G., and Amberg, D.C. (1999). Aip1p interacts with cofilin to disassemble actin filaments. *The Journal of Cell Biology* *145*, 1251–1264.
- Rodal, A.A., Sokolova, O., Robins, D.B., Daugherty, K.M., Hippenmeyer, S., Riezman, H., Grigorieff, N., and Goode, B.L. (2005). Conformational changes in the Arp2/3 complex leading to actin nucleation. *Nat Struct Mol Biol* *12*, 26–31.
- Roote, C.E., and Zusman, S. (1995). Functions for PS integrins in tissue adhesion, migration, and shape changes during early embryonic development in *Drosophila*. *Dev. Biol.* *169*, 322–336.
- Rosen, G.D., Sanes, J.R., LaChance, R., Cunningham, J.M., Roman, J., and Dean, D.C. (1992). Roles for the integrin VLA-4 and its counter receptor VCAM-1 in myogenesis. *Cell* *69*, 1107–1119.
- Rothenberg, M.E., Rogers, S.L., Vale, R.D., Jan, L.Y., and Jan, Y.-N. (2003). *Drosophila* pod-1 crosslinks both actin and microtubules and controls the targeting of axons. *Neuron* *39*, 779–791.
- Rouiller, I., Xu, X.-P., Amann, K.J., Egile, C., Nickell, S., Nicastro, D., Li, R., Pollard, T.D., Volkman, N., and Hanein, D. (2008). The structural basis of actin filament branching by the Arp2/3 complex. *The Journal of Cell Biology* *180*, 887–895.
- Rudnicki, M.A., Schnegelsberg, P.N., Stead, R.H., Braun, T., Arnold, H.H., and Jaenisch, R. (1993). MyoD or Myf-5 is required for the formation of skeletal muscle. *Cell* *75*, 1351–1359.
- Rui, Y., Bai, J., and Perrimon, N. (2010). Sarcomere formation occurs by the assembly of multiple latent protein complexes. *PLoS Genet* *6*, e1001208.
- Ruiz-Gomez, M., and Bate, M. (1997). Segregation of myogenic lineages in *Drosophila* requires numb. *Development* *124*, 4857–4866.
- Ruiz-Gomez, M., Coutts, N., Price, A., Taylor, M.V., and Bate, M. (2000). *Drosophila* dumbfounded: a myoblast attractant essential for fusion. *Cell* *102*, 189–198.

- Ruiz-Gomez, M., Romani, S., Hartmann, C., Jäckle, H., and Bate, M. (1997). Specific muscle identities are regulated by Krüppel during *Drosophila* embryogenesis. *Development* *124*, 3407–3414.
- Ruiz-Gómez, M., Coutts, N., Suster, M.L., Landgraf, M., and Bate, M. (2002). *myoblasts incompetent* encodes a zinc finger transcription factor required to specify fusion-competent myoblasts in *Drosophila*. *Development* *129*, 133–141.
- Rushton, E., Drysdale, R., Abmayr, S.M., Michelson, A.M., and Bate, M. (1995). Mutations in a novel gene, *myoblast city*, provide evidence in support of the founder cell hypothesis for *Drosophila* muscle development. *Development* *121*, 1979–1988.
- Rybakin, V., and Clemen, C.S. (2005). Coronin proteins as multifunctional regulators of the cytoskeleton and membrane trafficking. *Bioessays* *27*, 625–632.
- Rybakin, V., Stumpf, M., Schulze, A., Majoul, I.V., Noegel, A.A., and Hasse, A. (2004). Coronin 7, the mammalian POD-1 homologue, localizes to the Golgi apparatus. *FEBS Letters* *573*, 161–167.
- Sagot, I., Rodal, A.A., Moseley, J., Goode, B.L., and Pellman, D. (2002). An actin nucleation mechanism mediated by Bni1 and profilin. *Nat. Cell Biol.* *4*, 626–631.
- Sanger, J.W., and Holtzer, H. (1972). Cytochalasin B: effects on cell morphology, cell adhesion, and mucopolysaccharide synthesis (cultured cells-contractile microfilaments-glycoproteins-embryonic cells-sorting-out). *Proc. Natl. Acad. Sci. U.S.a.* *69*, 253–257.
- Sanoudou, D., and Beggs, A.H. (2001a). Clinical and genetic heterogeneity in nemaline myopathy--a disease of skeletal muscle thin filaments. *Trends Mol Med* *7*, 362–368.
- Sayegh, El, T.Y., Arora, P.D., Ling, K., Laschinger, C., Janmey, P.A., Anderson, R.A., and McCulloch, C.A. (2007). Phosphatidylinositol-4,5 biphosphate produced by PIP5K γ regulates gelsolin, actin assembly, and adhesion strength of N-cadherin junctions. *Mol. Biol. Cell* *18*, 3026–3038.
- Schäfer, G., Weber, S., Holz, A., Bogdan, S., Schumacher, S., Müller, A., Renkawitz-Pohl, R., and Önel, S.-F. (2007). The Wiskott-Aldrich syndrome protein (WASP) is essential for myoblast fusion in *Drosophila*. *Dev. Biol.* *304*, 664–674.
- Schnorrer, F., and Dickson, B.J. (2004). Muscle building; mechanisms of myotube guidance and attachment site selection. *Developmental Cell* *7*, 9–20.

- Schnorrer, F., Kalchhauser, I., and Dickson, B.J. (2007). The transmembrane protein Kon-tiki couples to Dgrip to mediate myotube targeting in *Drosophila*. *Developmental Cell* *12*, 751–766.
- Schnorrer, F., Schönbauer, C., Langer, C.C.H., Dietzl, G., Novatchkova, M., Schernhuber, K., Fellner, M., Azaryan, A., Radolf, M., Stark, A., et al. (2010). Systematic genetic analysis of muscle morphogenesis and function in *Drosophila*. *Nature* *464*, 287–291.
- Schroter, R.H. (2004). kette and blown fuse interact genetically during the second fusion step of myogenesis in *Drosophila*. *Development* *131*, 4501–4509.
- Schwander, M., Leu, M., Stumm, M., Dorchies, O.M., Rugg, U.T., Schittny, J., and Müller, U. (2003). Beta1 integrins regulate myoblast fusion and sarcomere assembly. *Developmental Cell* *4*, 673–685.
- Seale, P., Sabourin, L.A., Girgis-Gabardo, A., Mansouri, A., Gruss, P., and Rudnicki, M.A. (2000). Pax7 is required for the specification of myogenic satellite cells. *Cell* *102*, 777–786.
- Sellin, L. (2002). NEPH1 defines a novel family of podocin-interacting proteins. *The FASEB Journal*.
- Sens, K.L., Zhang, S., Jin, P., Duan, R., Zhang, G., Luo, F., Parachini, L., and Chen, E.H. (2010). An invasive podosome-like structure promotes fusion pore formation during myoblast fusion. *The Journal of Cell Biology* *191*, 1013–1027.
- Sesé, M., Corominas, M., Stocker, H., Heino, T.I., Hafen, E., and Serras, F. (2006). The Cdi/TESK1 kinase is required for Sevenless signaling and epithelial organization in the *Drosophila* eye. *J. Cell. Sci.* *119*, 5047–5056.
- Shelton, C., Kocherlakota, K.S., Zhuang, S., and Abmayr, S.M. (2009). The immunoglobulin superfamily member Hbs functions redundantly with Sns in interactions between founder and fusion-competent myoblasts. *Development* *136*, 1159–1168.
- Shemesh, T., Otomo, T., Rosen, M.K., Bershadsky, A.D., and Kozlov, M.M. (2005). A novel mechanism of actin filament processive capping by formin: solution of the rotation paradox. *The Journal of Cell Biology* *170*, 889–893.
- Shewan, A., Eastburn, D.J., and Mostov, K. (2011). Phosphoinositides in cell architecture. *Cold Spring Harb Perspect Biol* *3*, a004796.
- Shimada, A., Nyitrai, M., Vetter, I.R., Kühlmann, D., Bugyi, B., Narumiya, S., Geeves, M.A., and Wittinghofer, A. (2004). The core FH2 domain of diaphanous-related formins is an elongated actin binding protein that inhibits polymerization. *Mol. Cell* *13*, 511–522.

- Shina, M.C., Müller-Taubenberger, A., Unal, C., Schleicher, M., Steinert, M., Eichinger, L., Müller, R., Blau-Wasser, R., Glöckner, G., and Noegel, A.A. (2011). Redundant and unique roles of coronin proteins in *Dictyostelium*. *Cell. Mol. Life Sci.* *68*, 303–313.
- Shina, M.C., Unal, C., Eichinger, L., Müller-Taubenberger, A., Schleicher, M., Steinert, M., and Noegel, A.A. (2010). A Coronin7 homolog with functions in actin-driven processes. *Journal of Biological Chemistry* *285*, 9249–9261.
- Smythe, G.M., Davies, M.J., Paulin, D., and Grounds, M.D. (2001). Absence of desmin slightly prolongs myoblast proliferation and delays fusion *in vivo* in regenerating grafts of skeletal muscle. *Cell Tissue Res.* *304*, 287–294.
- Sohn, R.L., Huang, P., Kawahara, G., Mitchell, M., Guyon, J., Kalluri, R., Kunkel, L.M., and Gussoni, E. (2009). A role for nephrin, a renal protein, in vertebrate skeletal muscle cell fusion. *Proceedings of the National Academy of Sciences* *106*, 9274–9279.
- Someya, A., Sata, M., Takeda, K., Pacheco-Rodriguez, G., Ferrans, V.J., Moss, J., and Vaughan, M. (2001). ARF-GEP(100), a guanine nucleotide-exchange protein for ADP-ribosylation factor 6. *Proc. Natl. Acad. Sci. U.S.a.* *98*, 2413–2418.
- Someya, A. (2006). Involvement of a guanine nucleotide-exchange protein, ARF-GEP100/BRAG2a, in the apoptotic cell death of monocytic phagocytes. *Journal of Leukocyte Biology* *80*, 915–921.
- Sparrow, J.C., and Schöck, F. (2009). The initial steps of myofibril assembly: integrins pave the way. *Nat Rev Mol Cell Biol* *10*, 293–298.
- Spoerl, Z., Stumpf, M., Noegel, A.A., and Hasse, A. (2002). Oligomerization, F-actin interaction, and membrane association of the ubiquitous mammalian coronin 3 are mediated by its carboxyl terminus. *J. Biol. Chem.* *277*, 48858–48867.
- Spradling, A.C., Stern, D., Beaton, A., Rhem, E.J., Laverly, T., Mozden, N., Misra, S., and Rubin, G.M. (1999). The Berkeley *Drosophila* Genome Project gene disruption project: Single P-element insertions mutating 25% of vital *Drosophila* genes. *Genetics* *153*, 135–177.
- Srinivas, B.P., Woo, J., Leong, W.Y., and Roy, S. (2007). A conserved molecular pathway mediates myoblast fusion in insects and vertebrates. *Nat. Genet.* *39*, 781–786.
- Stacker, S.A., Hovens, C.M., Vitali, A., Pritchard, M.A., Baker, E., Sutherland, G.R., and Wilks, A.F. (1993). Molecular cloning and chromosomal localisation of

the human homologue of a receptor related to tyrosine kinases (RYK). *Oncogene* **8**, 1347–1356.

Steffen, A., Faix, J., Resch, G.P., Linkner, J., Wehland, J., Small, J.V., Rottner, K., and Stradal, T.E.B. (2006). Filopodia formation in the absence of functional WAVE- and Arp2/3-complexes. *Mol. Biol. Cell* **17**, 2581–2591.

Steffen, A., Rottner, K., Ehinger, J., Innocenti, M., Scita, G., Wehland, J., and Stradal, T.E.B. (2004). Sra-1 and Nap1 link Rac to actin assembly driving lamellipodia formation. *Embo J.* **23**, 749–759.

Strumpf, D., and Volk, T. (1998). Kakapo, a novel cytoskeletal-associated protein is essential for the restricted localization of the neuregulin-like factor, vein, at the muscle-tendon junction site. *The Journal of Cell Biology* **143**, 1259–1270.

Strünkelberg, M., Bonengel, B., Moda, L.M., Hertenstein, A., de Couet, H.G., Ramos, R.G., and Fischbach, K.F. (2001). *rst* and its paralogue *kirre* act redundantly during embryonic muscle development in *Drosophila*. *Development* **128**, 4229–4239.

Subramanian, A., Prokop, A., Yamamoto, M., Sugimura, K., Uemura, T., Betschinger, J., Knoblich, J.A., and Volk, T. (2003). Shortstop recruits EB1/APC1 and promotes microtubule assembly at the muscle-tendon junction. *Curr. Biol.* **13**, 1086–1095.

Subramanian, A., Wayburn, B., Bunch, T., and Volk, T. (2007). Thrombospondin-mediated adhesion is essential for the formation of the myotendinous junction in *Drosophila*. *Development* **134**, 1269–1278.

Sugihara, K., Nakatsuji, N., Nakamura, K., Nakao, K., Hashimoto, R., Otani, H., Sakagami, H., Kondo, H., Nozawa, S., Aiba, A., et al. (1998). Rac1 is required for the formation of three germ layers during gastrulation. *Oncogene* **17**, 3427–3433.

Sun, C., Kilburn, D., Lukashin, A., Crowell, T., Gardner, H., Brundiars, R., Diefenbach, B., and Carulli, J.P. (2003). Kirrel2, a novel immunoglobulin superfamily gene expressed primarily in β cells of the pancreatic islets☆. *Genomics* **82**, 130–142.

Sutoh, K., and Mabuchi, I. (1989). End-label fingerprintings show that an N-terminal segment of depactin participates in interaction with actin. *Biochemistry* **28**, 102–106.

Suzuki, T., Li, W., Zhang, J.-P., Tian, Q.-B., Sakagami, H., Usuda, N., Usuda, N., Kondo, H., Fujii, T., and Endo, S. (2005). A novel scaffold protein, TANC, possibly a rat homolog of *Drosophila* rolling pebbles (*rols*), forms a multiprotein complex with various postsynaptic density proteins. *Eur. J. Neurosci.* **21**, 339–350.

- Swan, L.E., Schmidt, M., Schwarz, T., Ponimaskin, E., Prange, U., Boeckers, T., Thomas, U., and Sigrist, S.J. (2006). Complex interaction of Drosophila GRIP PDZ domains and Echinoid during muscle morphogenesis. *Embo J.* *25*, 3640–3651.
- Swan, L.E., Wichmann, C., Prange, U., Schmid, A., Schmidt, M., Schwarz, T., Ponimaskin, E., Madeo, F., Vorbrüggen, G., and Sigrist, S.J. (2004). A glutamate receptor-interacting protein homolog organizes muscle guidance in Drosophila. *Genes Dev.* *18*, 223–237.
- Swank, D.M., Wells, L., Kronert, W.A., Morrill, G.E., and Bernstein, S.I. (2000). Determining structure/function relationships for sarcomeric myosin heavy chain by genetic and transgenic manipulation of Drosophila. *Microsc. Res. Tech.* *50*, 430–442.
- Tagawa, A., Rappleye, C.A., and Aroian, R.V. (2001). pod-2, along with pod-1, Defines a New Class of Genes Required for Polarity in the Early Caenorhabditis elegans Embryo. *Dev. Biol.* *233*, 412–424.
- Tajbakhsh, S., and Buckingham, M. (2000). The birth of muscle progenitor cells in the mouse: spatiotemporal considerations. *Curr. Top. Dev. Biol.* *48*, 225–268.
- Tajbakhsh, S., and Cossu, G. (1997). Establishing myogenic identity during somitogenesis. *Current Opinion in Genetics & Development* *7*, 634–641.
- Tajbakhsh, S., Rocancourt, D., and Buckingham, M. (1996). Muscle progenitor cells failing to respond to positional cues adopt non-myogenic fates in myf-5 null mice. *Nature* *384*, 266–270.
- Takano, K., Watanabe-Takano, H., Suetsugu, S., Kurita, S., Tsujita, K., Kimura, S., Karatsu, T., Takenawa, T., and Endo, T. (2010). Nebulin and N-WASP cooperate to cause IGF-1-induced sarcomeric actin filament formation. *Science* *330*, 1536–1540.
- Tall, E.G., Spector, I., Pentylala, S.N., Bitter, I., and Rebecchi, M.J. (2000). Dynamics of phosphatidylinositol 4,5-bisphosphate in actin-rich structures. *Curr. Biol.* *10*, 743–746.
- Telfer, W.R., Nelson, D.D., Waugh, T., Brooks, S.V., and Dowling, J.J. (2012). Neb: a zebrafish model of nemaline myopathy due to nebulin mutation. *Dis Model Mech* *5*, 389–396.
- Theriot, J.A., and Mitchison, T.J. (1991). Actin microfilament dynamics in locomoting cells. *Nature* *352*, 126–131.
- Thirion, C., Stucka, R., Mendel, B., Gruhler, A., Jaksch, M., Nowak, K.J., Binz, N., Laing, N.G., and Lochmüller, H. (2001). Characterization of human muscle type

cofilin (CFL2) in normal and regenerating muscle. *Eur. J. Biochem.* *268*, 3473–3482.

Thisse, B., Messal, el, M., and Perrin-Schmitt, F. (1987). The twist gene: isolation of a *Drosophila* zygotic gene necessary for the establishment of dorsoventral pattern. *Nucleic Acids Research* *15*, 3439–3453.

Thisse, B., Stoetzel, C., Gorostiza-Thisse, C., and Perrin-Schmitt, F. (1988). Sequence of the twist gene and nuclear localization of its protein in endomesodermal cells of early *Drosophila* embryos. *Embo J.* *7*, 2175–2183.

Tiegs, O.W. (1955). The flight muscles of insects. *Phil. Trans. Roy. Soc. Lond. B.* *238*, 221–348.

Tomancak, P., Beaton, A., Weizmann, R., Kwan, E., Shu, S., Lewis, S.E., Richards, S., Ashburner, M., Hartenstein, V., Celniker, S.E., et al. (2002). Systematic determination of patterns of gene expression during *Drosophila* embryogenesis. *Genome Biol.* *3*, RESEARCH0088.

Tomancak, P., Berman, B.P., Beaton, A., Weizmann, R., Kwan, E., Hartenstein, V., Celniker, S.E., and Rubin, G.M. (2007). Global analysis of patterns of gene expression during *Drosophila* embryogenesis. *Genome Biol.* *8*, R145.

Tryggvason, K., and Wartiovaara, J. (2001). Molecular basis of glomerular permselectivity. *Curr. Opin. Nephrol. Hypertens.* *10*, 543–549.

Tsujita, K., Itoh, T., Kondo, A., Oyama, M., Kozuka-Hata, H., Irino, Y., Hasegawa, J., and Takenawa, T. (2010). Proteome of acidic phospholipid-binding proteins: spatial and temporal regulation of Coronin 1A by phosphoinositides. *Journal of Biological Chemistry* *285*, 6781–6789.

Ueno, H., Sakita-Ishikawa, M., Morikawa, Y., Nakano, T., Kitamura, T., and Saito, M. (2003). A stromal cell-derived membrane protein that supports hematopoietic stem cells. *Nat Immunol* *4*, 457–463.

van der Honing, H.S., van Bezouwen, L.S., Emons, A.M.C., and Ketelaar, T. (2011). High expression of Lifeact in *Arabidopsis thaliana* reduces dynamic reorganization of actin filaments but does not affect plant development. *Cytoskeleton (Hoboken)* *68*, 578–587.

Vartiainen, M.K., Mustonen, T., Mattila, P.K., Ojala, P.J., Thesleff, I., Partanen, J., and Lappalainen, P. (2002). The three mouse actin-depolymerizing factor/cofilins evolved to fulfill cell-type-specific requirements for actin dynamics. *Mol. Biol. Cell* *13*, 183–194.

Vasyutina, E., and Birchmeier, C. (2006). The development of migrating muscle precursor cells. *Brain Struct Funct* *211*, 37–41.

- Vasyutina, E., Martarelli, B., Brakebusch, C., Wende, H., and Birchmeier, C. (2009). The small G-proteins Rac1 and Cdc42 are essential for myoblast fusion in the mouse. *Proceedings of the National Academy of Sciences* *106*, 8935–8940.
- Vidal, M., Wells, S., Ryan, A., and Cagan, R. (2005). ZD6474 suppresses oncogenic RET isoforms in a *Drosophila* model for type 2 multiple endocrine neoplasia syndromes and papillary thyroid carcinoma. *Cancer Research* *65*, 3538–3541.
- Vignery, A. (2010). Macrophage Fusion. In *Cell Fusion: Overviews and Methods*, E.H. Chen, ed. (Humana Press), pp. 149–161.
- Volk, T. (1999). Singling out *Drosophila* tendon cells: a dialogue between two distinct cell types. *Trends Genet.* *15*, 448–453.
- Volk, T., and VijayRaghavan, K. (1994). A central role for epidermal segment border cells in the induction of muscle patterning in the *Drosophila* embryo. *Development* *120*, 59–70.
- Volk, T., Fessler, L.I., and Fessler, J.H. (1990). A role for integrin in the formation of sarcomeric cytoarchitecture. *Cell* *63*, 525–536.
- Volohonsky, G., Edenfeld, G., Klämbt, C., and Volk, T. (2007). Muscle-dependent maturation of tendon cells is induced by post-transcriptional regulation of stripeA. *Development* *134*, 347–356.
- Vorbrüggen, G., and Jäckle, H. (1997). Epidermal muscle attachment site-specific target gene expression and interference with myotube guidance in response to ectopic stripe expression in the developing *Drosophila* epidermis. *Proc. Natl. Acad. Sci. U.S.A.* *94*, 8606–8611.
- Wakelam, M.J. (2005). The fusion of myoblasts. *Biochem. J.* *228*, 1–12.
- Wang, X. (2003). Cell Corpse Engulfment Mediated by *C. elegans* Phosphatidylserine Receptor Through CED-5 and CED-12. *Science* *302*, 1563–1566.
- Wang, J., Sanger, J.M., and Sanger, J.W. (2005). Differential effects of Latrunculin-A on myofibrils in cultures of skeletal muscle cells: insights into mechanisms of myofibrillogenesis. *Cell Motil. Cytoskeleton* *62*, 35–47.
- Wang, W., Eddy, R., and Condeelis, J. (2007). The cofilin pathway in breast cancer invasion and metastasis. *Nat. Rev. Cancer* *7*, 429–440.
- Wassarman, P.M., and Litscher, E.S. (2010). Mammalian Fertilization Is Dependent on Multiple Membrane Fusion Events. In *Cell Fusion: Overviews and Methods*, E.H. Chen, ed. (Humana Press), pp. 99–113.

- Wayburn, B., and Volk, T. (2009). LRT, a tendon-specific leucine-rich repeat protein, promotes muscle-tendon targeting through its interaction with Robo. *Development* *136*, 3607–3615.
- Weaver, A.M., Heuser, J.E., Karginov, A.V., Lee, W.-L., Parsons, J.T., and Cooper, J.A. (2002). Interaction of cortactin and N-WASp with Arp2/3 complex. *Curr. Biol.* *12*, 1270–1278.
- Wegorzewska, M., Krauss, R.S., and Kang, J.-S. (2003). Overexpression of the immunoglobulin superfamily members CDO and BOC enhances differentiation of the human rhabdomyosarcoma cell line RD. *Mol. Carcinog.* *37*, 1–4.
- Welch, M.D., DePace, A.H., Verma, S., Iwamatsu, A., and Mitchison, T.J. (1997). The human Arp2/3 complex is composed of evolutionarily conserved subunits and is localized to cellular regions of dynamic actin filament assembly. *The Journal of Cell Biology* *138*, 375–384.
- Westphal, M., Jungbluth, A., Heidecker, M., Mühlbauer, B., Heizer, C., Schwartz, J.M., Marriott, G., and Gerisch, G. (1997). Microfilament dynamics during cell movement and chemotaxis monitored using a GFP-actin fusion protein. *Curr. Biol.* *7*, 176–183.
- Williams, B.A., and Ordahl, C.P. (1994). Pax-3 expression in segmental mesoderm marks early stages in myogenic cell specification. *Development* *120*, 785–796.
- Williams, J.A., Bell, J.B., and Carroll, S.B. (1991). Control of *Drosophila* wing and haltere development by the nuclear vestigial gene product. *Genes Dev.* *5*, 2481–2495.
- Wriggers, W., Tang, J.X., Azuma, T., Marks, P.W., and Janmey, P.A. (1998). Cofilin and gelsolin segment-1: molecular dynamics simulation and biochemical analysis predict a similar actin binding mode. *Journal of Molecular Biology* *282*, 921–932.
- Wu, Y.-C., Cheng, T.-W., Lee, M.-C., and Weng, N.-Y. (2002). Distinct Rac Activation Pathways Control *Caenorhabditis elegans* Cell Migration and Axon Outgrowth. *Dev. Biol.* *250*, 145–155.
- Xavier, C.-P., Eichinger, L., Fernandez, M.P., Morgan, R.O., and Clemen, C.S. (2008). Evolutionary and functional diversity of coronin proteins. *Subcell. Biochem.* *48*, 98–109.
- Xia, H., Winokur, S.T., Kuo, W.L., Altherr, M.R., and Bretz, D.S. (1997). Actinin-associated LIM protein: identification of a domain interaction between PDZ and spectrin-like repeat motifs. *The Journal of Cell Biology* *139*, 507–515.

- Yablonka-Reuveni, Z., and Rivera, A.J. (1994). Temporal expression of regulatory and structural muscle proteins during myogenesis of satellite cells on isolated adult rat fibers. *Dev. Biol.* *164*, 588–603.
- Yaffe, D., and Saxel, O. (1977). Serial passaging and differentiation of myogenic cells isolated from dystrophic mouse muscle. *Nature* *270*, 725–727.
- Yamada, S., Pokutta, S., Drees, F., Weis, W.I., and Nelson, W.J. (2005). Deconstructing the cadherin-catenin-actin complex. *Cell* *123*, 889–901.
- Yao, S.N., and Kurachi, K. (1992). Expression of human factor IX in mice after injection of genetically modified myoblasts. *Proc. Natl. Acad. Sci. U.S.a.* *89*, 3357–3361.
- Yarnitzky, T., Min, L., and Volk, T. (1997). The *Drosophila* neuregulin homolog Vein mediates inductive interactions between myotubes and their epidermal attachment cells. *Genes Dev.* *11*, 2691–2700.
- Ydenberg, C.A., and Rose, M.D. (2010). Yeast Mating. In *Cell Fusion: Overviews and Methods*, E.H. Chen, ed. (Humana Press), pp. 3–20.
- Yonezawa, N., Homma, Y., Yahara, I., Sakai, H., and Nishida, E. (1991). A short sequence responsible for both phosphoinositide binding and actin binding activities of cofilin. *J. Biol. Chem.* *266*, 17218–17221.
- Yonezawa, N., Nishida, E., Iida, K., Yahara, I., and Sakai, H. (1990). Inhibition of the interactions of cofilin, destrin, and deoxyribonuclease I with actin by phosphoinositides. *J. Biol. Chem.* *265*, 8382–8386.
- Zammit, P. (2002). Kinetics of Myoblast Proliferation Show That Resident Satellite Cells Are Competent to Fully Regenerate Skeletal Muscle Fibers. *Experimental Cell Research* *281*, 39–49.
- Zervas, C.G., Gregory, S.L., and Brown, N.H. (2001). *Drosophila* integrin-linked kinase is required at sites of integrin adhesion to link the cytoskeleton to the plasma membrane. *The Journal of Cell Biology* *152*, 1007–1018.
- Zhang, L., Luo, J., Wan, P., Wu, J., Laski, F., and Chen, J. (2011). Regulation of cofilin phosphorylation and asymmetry in collective cell migration during morphogenesis. *Development* *138*, 455–464.
- Zhang, Y., Featherstone, D., Davis, W., Rushton, E., and Broadie, K. (2000). *Drosophila* D-titin is required for myoblast fusion and skeletal muscle striation. *J. Cell. Sci.* *113* (Pt 17), 3103–3115.
- Zigmond, S.H. (1993). Recent quantitative studies of actin filament turnover during cell locomotion. *Cell Motil. Cytoskeleton* *25*, 309–316.

Zigmond, S.H., Evangelista, M., Boone, C., Yang, C., Dar, A.C., Sicheri, F., Forkey, J., and Pring, M. (2003). Formin leaky cap allows elongation in the presence of tight capping proteins. *Curr. Biol.* *13*, 1820–1823.

Zinzen, R.P., Girardot, C., Gagneur, J., Braun, M., and Furlong, E.E.M. (2009). Combinatorial binding predicts spatio-temporal cis-regulatory activity. *Nature* *462*, 65–70.

Zuchero, J.B., Coutts, A.S., Quinlan, M.E., Thangue, N.B.L., and Mullins, R.D. (2009). p53-cofactor JMY is a multifunctional actin nucleation factor. *Nature Publishing Group* *11*, 451–459.

Zusman, S., Grinblat, Y., Yee, G., Kafatos, F.C., and Hynes, R.O. (1993). Analyses of PS integrin functions during *Drosophila* development. *Development* *118*, 737–750.